

Contents

Interactions Between Metal Ions and Living Organisms in Sea Water

Kenneth Kustin and Guy C. McLeod 1

Inorganic Metabolic Gas Exchange in Biochemistry

Gernot Renger 39

Complex Formation of Monovalent Cations with Biofunctional Ligands

Wolfgang Burgermeister and Ruthild Winkler-Oswatitsch 91

Author Index Volumes 26–69 197

Interactions Between Metal Ions and Living Organisms in Sea Water

Kenneth Kustin

Department of Chemistry, Brandeis University, Waltham, Massachusetts 02154, U.S.A.

Guy C. McLeod

New England Aquarium, Central Wharf, Boston, Massachusetts 02110, U.S.A.

Table of Contents

I. Introduction	2
II. Metal Ions Added by Man to the Marine Environment	2
A. Survey of Metals	3
B. Bioavailability of Metal Ions	8
III. Organism-Environment Interactions	10
A. Phytoplankton as a Basic Source of Metal Ions	10
B. Concentration of Metal Ions in Phytoplankton	11
IV. Entry of Metal Ions into Living Systems	12
A. Molecular Models of Metal Binding	12
1. Complex Formation	12
2. Ion Exchange	17
B. Assimilation of Metal Ions: Regulated Removal and Transport	18
V. Impact of Metal Ions on Selected Organisms	19
A. Speciation and Algae	20
1. Chemoreception, Uptake and Response	21
2. Copper Transport	24
B. Accumulation of Metal Ions by Bivalve Mollusks	25
1. Bivalve Feeding Selectivity	26
2. Metal Ion Uptake	27
C. Dynamics of Vanadium Uptake by Tunicates	28
VI. References	34

I. Introduction

We intend to review the progress that has been made in understanding the impact of heavy metal ions introduced into the marine environment. We focus on the ions, V, Cr, Fe, Cu, Pb and Hg. Exotic elements, such as Hf or Ta, or elements for which sensitive, reliable measurement techniques have not been extensively developed, such as W, will be excluded from consideration. The elements selected fall into two categories. Vanadium, chromium, iron and copper are essential elements in human and animal nutrition¹⁾. Lead and mercury, while not essential, are nevertheless accumulated by marine organisms, and pass along the food chain, coming ultimately to large predators and mankind. At some point in the chain the relative degree of physiological disturbance produced by accumulation of these ions in the tissues increases, and they become toxic. The effect experienced depends on the organism involved.

Although the biological effects of metal ions vary considerably from one species to another, the mode of interaction at the sea water/organism interface is essentially the same. Thus, studies with phytoplankton will receive considerable emphasis here. These microorganisms are excellent subjects: the relative ease in maintenance and analysis conferred by their small size, large numbers and convenient growing conditions has led to the most extensive experimentation. Larger organisms, especially animals, are more difficult subjects to treat experimentally. Nevertheless, considerable progress has been made with tunicates, which accumulate and integrate vanadium, and with bivalves. Results with these selected living systems will be discussed.

II. Metal Ions Added by Man to the Marine Environment

As a chemical medium, the ocean is far from ideal from the standpoints of homogeneity and constancy of composition, temperature, and pressure. It can be either stirred or unstirred, depending on location and the time available for observation. Thus, the concept of establishing a "baseline" concentration level of a particular element may be illusory not because of interference from man, but because of intrinsic differences encountered within the oceanic medium.

Reliable information on the oceanic concentrations of many scarce elements can now be routinely supplied, as a result of improvements in sampling and analysis techniques. Differences in concentrations between estuarine, slope, and deep waters can be determined. Concentration differences between the surface microlayer and subsurface have been measured for mercury²⁾. In view of the greater degree of subtlety that is now possible in describing the chemical composition of sea water, we will sketch in the broad composition of sea water in order to define average "natural" metal ion abundances. We shall also indicate where to expect significant differences from these values. With these values serving as references, we shall consider the concentrations of contaminating metal ions in detail.

The most complete study of elemental sea water composition has been provided by Goldberg and colleagues³⁾. From this data we can sort the metal ions into three convenient groups. Major metal ions are present at mid-oceanic concentration levels in excess of 10^{-3} M. Included in this class are sodium, magnesium, calcium, and potassium. Less abundant are the metals with average concentrations in the range $10^{-6} - 10^{-3}$ M; namely, strontium, lithium, aluminum, and rubidium. The third grouping, metal ions with average concentrations less than 10^{-6} M, constitutes the trace metals. The six elements to be considered in detail fall into this last category.

A. Survey of Metals

The avenues of transport of trace metals to the oceans may be:

- a) atmospheric paths,
- b) streams,
- c) direct injections from outfalls,
- d) introduction by ships.

The problem is to assess the flux of trace metals at critical points in the marine realm ascribable to each of the pathways.

Alterations in trace metal concentrations in the marine environment due to man's activities are difficult to establish, since natural levels are often poorly known, or when known show variations. At present, measurement of concentration gradients (both vertical and horizontal) from known pollution sources is the primary method to assess trace metal contamination of the marine environment. High trace metal inputs into estuarine or coastal areas from industrial effluents as well as from river run-off have been measured. Without knowledge of the make-up of these source materials, distinguishing between a natural and an anthropogenic origin for increased metal concentrations is an insoluble problem.

Estimates of potential trace metal oceanic input based on atmospheric washout, mining productivity figures, and relative river transport are given in Tables 1 and 2. Of the ions selected for discussion in this article, lead and copper offer the potentially greatest inputs to oceanic systems. More detailed information on mercury movement is shown in Table 3⁴⁾. The principal transfer of mercury from the continents to the oceans probably takes place through the atmosphere. The quantity of mercury carried by rivers to the ocean is an order of magnitude less than the amount volatilized from the earth to the atmosphere. Man-made flows are less than this natural outgassing. However, despite the high natural background, Weiss *et al.* were able to detect increasing trends in mercury levels associated with snow deposition in the Greenland glacier for the period 1952 to 1965.

Estimates have been prepared for mercury and other metals for atmospheric inputs to oceanic systems. Table 1 gives these estimates for oceanic waters based on ratios of current urban air values to average crustal material values. Both lead and cadmium have higher enhancement ratios (2,300 and 1,900) than mercury (1,100). When percent increase estimates are made for ocean concentrations, the concentration range for cadmium is 0.02 to 8 $\mu\text{g/l}$, and for mercury 0.1 to 0.8 $\mu\text{g/l}$. No probable percent increase is given for lead.

Table 1. Possible impact of atmospheric pollutants on the marine environment⁴⁾

Element	Concentration				Estimated % increase of trace elements in upper 200 m of ocean ³⁾	
	Open ocean (μg/l)	U.S. urban air (μg/m ³) ¹⁾	Enhancement ratio in air ²⁾	Ratio air/ocean	High	Most probable
Pb	0.02	1,000	2,300	50,000	—	—
Al	1	1,500	0.5	1,000	200	30
Cd	0.02	20	1,900	1,000	400	20
Sc	0.001	1	1	1,000	80	20
Sn	0.02	20	280	1,000	—	20
Mn	0.3	200	6	700	60	15
Fe	5	2,000	1.0	400	80	8
La	0.01	3	3	300	—	6
V	1	200	42	200	40	4
Zn	3	700	270	200	25	4
Cu	2	200	83	100	100	2
Ag	0.01	2	830	200	—	4
Cr	0.3	40	11	130	20	3
Be	0.005	1	10	200	—	4
Sb	0.2	20	2,800	100	10	2
In	0.001	0.1	29	100	—	2
Ti	1	100	0.5	100	4	2
Co	0.03	2	2	70	4	1
Se	0.1	4	2,500	40	5	0.8
Hg	0.1	3	1,100	30	8	0.6
W	0.1	5	93	50	—	1
Ga	0.02	1	2	50	—	1
Ni	2	30	12	15	4	0.3
Ca	0.3	4	37	10	—	0.3
Ta	0.02	0.2	3	10	—	0.3
As	2	20	310	10	0.8	0.2
Mo	10	10	190	1	—	0.02
U	3	0.1	1	0.03	—	Negligible

1) Urban air values are approximations taken from the compilation of Roberts and Perkins (personal communication, 1972).

2) The ratio of the concentration in urban particulates of a specific element to iron, divided by the ratio of the same elements in average crustal material.

3) The % increase represents the magnitude by which these trace elements could have been increased in the upper 200 meters of the ocean based on the anthropogenic lead concentrations in this layer. The high estimates are those which might be expected in oceanic regions adjacent to certain large urban areas (Robertson & Perkins, pers. comm., 1972).

4) Source: Baseline Studies of Pollutants in the Marine Environment and Research Recommendations, Deliberations of the IDOE Baseline Conference, May 24 to 26, 1971, N.Y., 1972.

Interactions Between Metal Ions and Living Organisms in Sea Water

Table 2. World heavy metal production and potential ocean inputs⁵⁾

Substance	Mining production ¹⁾ (million tons/yr)	Transport by river to oceans ²⁾ (million tons/yr)	Atmospheric washout ³⁾ (million tons/yr)
Pb	3	0.1	0.3
Cu	6	0.25	0.2
V	0.02	0.03	0.02
Ni	0.5	0.01	0.03
Cr	2	0.04	0.02
Sn	0.2	0.002	0.02
Cd	0.01	0.0005	0.01
As	0.06	0.07	
Hg	0.009	0.003	0.08 ⁴⁾
Zn	5	0.7	
Se	0.002	0.007	
Ag	0.01	0.01	
Mo		0.03	
Sb	0.07	0.01	

1) U.S. Department of Interior (1970a and b).

2) Bertine and Goldberg (1971).

3) Estimated from aerosol data of Egorov, *et al.* (1970) and Hoffman (1971).

4) Goldberg, unpublished data.

5) Source: Marine Environmental Quality: Suggested Research Programs for Understanding Man's Effect on the Oceans, NAS-NRC Ocean Affairs Board, Aug 9 to 13, 1971.

Table 3. Environmental Mercury Fluxes¹⁾

	Tons/yr
<i>Natural Flows</i>	
Continents to atmosphere (by degassing of the earth's crust)	
Based on precipitation with rain	8.4×10^4
Based on atmospheric content	15.0×10^4
Based on content in Greenland Glacier	2.5×10^4
River transport to oceans	3.8×10^3
<i>Flows Involving Man</i>	
World production (1968)	8.8×10^3
Entry to atmosphere from fossil fuel combustion	1.6×10^3
Entry to atmosphere during cement manufacture	1.0×10^2
Losses in industrial and agricultural usage	4.0×10^3

1) Source: Weiss, *et al.* (1971)⁴⁾.

These values may be compared with currently recorded ranges for these metals. A summary of most complete information is available on mercury⁵⁾. A summary of the historical analytical record provides a range of 0.003 to 0.364 $\mu\text{g/l}$. Measurements of levels in Long Island Sound varied from 0.045 to 0.078 $\mu\text{g/l}$, but as much as 50 to 60% of the mercury present existed in association with organic compounds. Since many earlier measurements were concerned only with total mercury measurements and provision was not made for recovery of organic forms, the reported ranges may still be low. The range of 0.003 to 0.364 $\mu\text{g/l}$ appears to be somewhat lower than the percent estimated increase indicated by the International Decade of Ocean Exploration baseline estimates.

Anomalous high concentrations of copper are found in marine areas adjacent to known sources such as sewage outfalls and waste disposal sites. Near shore values of 20 $\mu\text{g/l}$ have been recorded⁶⁾, for example, whereas open ocean concentrations initially determined by Fabricand, *et al.* were reports at less than 3.0 $\mu\text{g/l}$ ⁷⁾.

Lead inputs to oceanic systems have been measured⁸⁾. Using isotope correlation, they identified the prime aerosol source as leaded gasoline. Profiles of lead concentrations in ocean water cluster between 0.02 $\mu\text{g/l}$ and 0.04 $\mu\text{g/l}$ for water below 500 m; shallow water coastal concentrations may range from 0.07 to 0.35 $\mu\text{g Pb/l}$ ⁹⁾. While values as high as 10 $\mu\text{g Pb/l}$ have been reported, it is possible that some of these higher values reflect shipboard contamination⁹⁾.

As in the case of mercury, a long-term trend in increasing lead concentration is apparent from an examination of lead aerosols associated with Greenland snow¹⁰⁾. The data indicate a slow increase in lead content from 1,750 to 1,940 (25 times), then a rapid rise (500 times) above natural levels.

Due to the high insolubility of the most stable oxidation state of iron in sea water, Fe(III), the concentration of iron in the ocean as a whole has remained relatively unaltered despite the appreciable man-made inputs^{11, 12)}. In estuarine and coastal waters, especially near large cities, increases have been noted¹³⁾. The iron found in sea water is mainly in the form of suspended material, the concentration of which varies with depth¹⁴⁾. For iron concentrations in sea waters near the surface, we estimate a present day value in excess of the value quoted in Table 1 of 5 $\mu\text{g/l}$.

The chemistry of chromium confers a unique character to studies of the concentration levels of this element in sea water not encountered with the other metals. Chromium is present in natural waters in two stable, chemically quite different oxidation states: chromium(III) and chromium(VI). Thus, if the total concentration level of 0.3 $\mu\text{g/l}$ is accepted, the interesting question is how is this amount distributed between the two oxidation states.

In a study of the distribution of Cr-51 in the Columbia River and Oregon (USA) coastal water, it was found that the metal was in the hexavalent state when introduced into the river¹⁵⁾. A portion of the metal was reduced to the trivalent state in flowing to the sea, but once in the Pacific Ocean, no further reduction took place¹⁶⁾. Both forms of the metal have been reported in Japanese coastal waters¹⁷⁾. A study of samples from the Irish Sea indicated a predominance of Cr(III)¹⁸⁾. In general, studies yield figures indicating substantial amounts of both valence states in a given sample of sea water¹⁹⁾.

This interesting stationary state may arise from a balance between two competing tendencies. Oxidation favors the hexavalent state, even though the rate of air oxidation of Cr(III) may be relatively slow. However, despite the decrease in oxidizing potential of the Cr(VI)/Cr(III) couple in going from standard conditions ($1 \text{ M}[\text{H}^+]$) to the pH 8 of sea water, chromium(VI) is still a powerful oxidizing agent, and would be expected to oxidize the organic material present in sea water. The tendency of the chromium(III) thus produced to form complexes with the natural chelators present would then stabilize this state.

Extensive measurements on the concentration of vanadium in Boston Harbor waters have been reported²⁰. An average value of $3.2 \pm 0.7 \text{ } \mu\text{g/l}$ has been reported for filtered sea water. The data for Massachusetts coastal water is within agreement of other coastal areas: North West Pacific Ocean, 2.6–3.5; Plymouth, England, in-shore, 5–7; Plymouth, England, offshore, 2.4–2.7; Wakayama Prefecture, Japan, 3.4–3.6; and Kagoshima Bay, Japan, 1.6–1.7 $\mu\text{g/l}$ ²⁰. These values are higher than the earliest determinations which were less than $1 \text{ } \mu\text{g/l}$, probably due to analytic errors and inherent inaccuracies. The amount of vanadium in the particulate phase is clearly much lower. A range of values has been reported; the best estimate is $0.3 \text{ } \mu\text{g/l}$. The sediments in Boston Harbor are rich in vanadium, the average concentration is $56 \pm 26 \text{ } \mu\text{g/g}$ for the upper five cm. Despite this potential source of contamination of the coastal waters, little change in vanadium level has been observed²⁰.

If one assumes that other elements are transported by the atmosphere from urban centers in a manner similar to that of lead, and are subsequently deposited on the ocean surface and mixed vertically at a rate similar to that of lead, then the expected increase in ocean water concentrations of other elements can be calculated (Table 4). The most probable values show increases of 30% (Table 1) for several of the elements, although higher concentrations may exist. The values of the most probable increases suggest that trace elements in the surface layers bear little relationship to the concentration of elements found in organisms. The uptake of trace elements by the marine biota, however, does depend upon the chemical state of the elements, and we shall discuss this further in the later sections.

In addition to atmospheric transport, the principal flowpath materials carried to the ocean are indicated in Fig. 1. It can be argued that what is important in estimating the increases in metal ion inputs to sea water is their *bioavailability*. To estimate that quality, account must be taken of the form of the metal ion, the input of organic material, and the fraction of that material active as chelating agents. Certainly, the

Table 4. Mid-range metal concentrations in the oceans

Metal	$\mu\text{g/Liter}$
Copper	3.00
Chromium	0.30
Iron	10.00
Lead (estimated natural)	0.03
Mercury	0.10
Vanadium	3.00

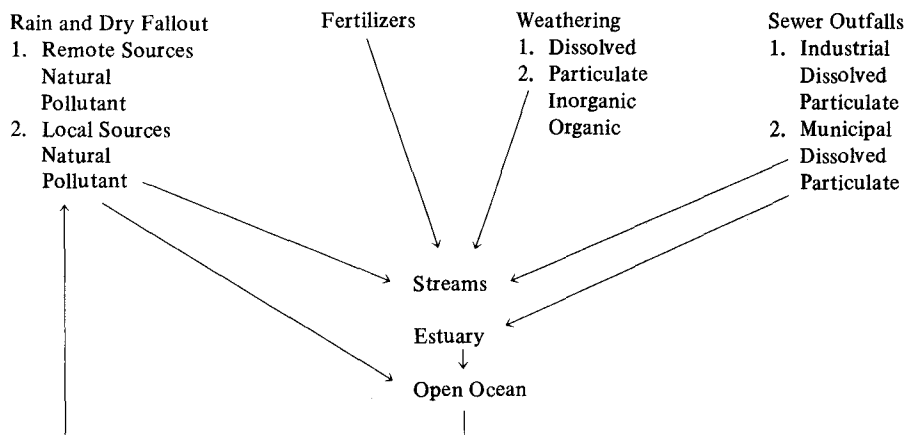


Fig. 1. Principal paths of materials to the ocean environment

fertilizer and sewage outfalls will deliver strongly chelated metal ions to oceanic waters.

B. Bioavailability of Metal Ions

While ranges of total concentration serve to set bounds for experimentally determining effects on marine populations, the actual species of metal ion available to the biological population is of importance. Sillén, in a classic paper, has computed the stable species of many metals in sea water²¹. He concluded, for example, that Hg^{+2} , Cd^{+2} , and Pb^{+2} exist primarily as chloride complexes. pH determines the availability of the hydroxide ion and thereby the solubility of metal hydroxides. Sillén assumed a pH of 8.1 ± 0.2 as representative. Significant variations could occur, however, in estuarine waters. When concentrations of trace elements were compared with calculations of their solubility products and stability constants, the observed values were considerably less than the calculated values. The implication is that the heavy metals are not in equilibrium with solid phases of their salts, but that other processes, such as chelation and adsorption, control their concentration.

The control processes of chelation and adsorption are in turn partially dependent on the route of entry of the trace metal into the ocean system. Transport via stream or river is a complex process which varies from metal to metal. For example, analysis of trace metal transport for Fe, Cu, Co, and Mn, with respect to five possible processes was carried out²². These processes included:

1. a) dissolving of ionic species and inorganic associations,
b) complexing with organic molecules;
2. absorption on solids;
3. precipitation on solids (metallic coatings);
4. incorporation in solid biological materials; and
5. incorporation in crystalline structures.

Incorporation in the crystalline structure is the major mechanism for transporting Cu and Cr. Mn is carried in coatings, and Fe, Ni, and Co are distributed equally between coatings and crystalline solids.

Another suggestion is that the natural removal cycle for Pb via river transport is an exchange between a dissolved chelated form and an insoluble precipitated form⁹⁾. Exchange may occur with the precipitated form settling out on the continental shelves. Hence, while river transport mechanisms may be known in detail, removal mechanisms for oceanic systems are only known in more general terms. These removal mechanisms are:

1. adsorption into sediments, and
2. incorporation into biological materials.

The latter removal mechanism may or may not be favored by speciation of metals into organic chelated complexes. In some coastal regions the principal particulate pollutant is primary sewage sludge, containing substantial levels of heavy metals that are especially concentrated in the digested sludge, as indicated by data supplied by analyses at the treatment facility (Table 5).

Table 5. Heavy metals from a metropolitan primary treatment facility¹⁾

Metal	Concentration Range Observed in 1973	
	In digested sludge ($\mu\text{g/g}$ wet weight)	Effluent (mg/l)
Zinc	20.0–260.0	0.20–1.60
Cadmium	0.9– 1.5	0.01–0.04
Lead	5.0– 34.0	0.01–0.16
Copper	10.0– 60.0	0.10–0.80

¹⁾ Data supplied by J. Kooch of the Metropolitan District Commission sewage treatment facility, Deer Island, Massachusetts.

When the sewage solids mix with saline harbor waters, that part of the metal load which is reversibly adsorbed on the particles may be released to the aqueous phase by exchange with magnesium and calcium ions. The same phenomenon may also occur when the suspended solid load of the region's rivers flow into a harbor estuary. However, a number of studies have shown that only a small portion of the particulate metal load is desorbed in this way. For example, silver(I), which was adsorbed on natural particulates and then desorbed on contact with sea water, made up only a few percent of the total soluble load transported by six major rivers²³⁾. The radioactive chromium (^{51}Cr) found in Columbia River sediments contaminated with effluent from a nuclear reactor facility was not released by the major cations of sea water or by 0.05 M CuSO_4 ²⁴⁾. The results of previous work in this laboratory (New England Aquarium) showed that of the silver(I) and cadmium(II) adsorbed on the clay minerals kaolin and montmorillonite, in essentially deionized water, less than half was desorbed on mixing with sea water²⁵⁾. One may postulate from results such as these that most of the heavy metals occluded within a complex organic

matrix such as sewage sludge would not be released through simple displacement reactions.

An understanding of the pathways and rates of trace metal movement through the marine ecosystem, the areas of accumulation and time constants of accumulation, and the ultimate fate of trace metals in the ecosystem is important to an understanding of where, for how long, at what concentration level, and in what form organisms will be exposed to trace metals from various sources that we have listed in the previous pages. Prior studies show that there is already some low level trace metal pollution in many areas of the continental shelf, slope, and open ocean. As we have stated, this contamination is from atmospheric fallout, both dry and precipitation, from air masses of the industrial northeast U.S.A., from ships ejecting wastes or carrying dredge spoils to areas of the continental shelf, from fishing boats, from the transport of water and/or suspended matter from areas of past and present high levels of trace metal contamination, and from the relentless movement of trace metal concentrations by ocean currents.

One of the problems we face in an adequate assessment of the effects of metal ion contamination is to distinguish between natural and anthropogenic trace metal inputs. There may be, for example, several sources for the trace metals found in marine samples. The bioavailability of these metal ions depends strongly on the nature of the metallic species present: whether they are in dissolved or particulate form, what the oxidation state is, to what extent chelated, to what extent hydrolyzed, etc. Even in the dilute sea waters, a source yielding a strongly chelated, or metal-organic form of an ion yields a potentially more bioactive species than a source delivering free metal ions rapidly exchanged by particulates. One clearly bioavailable source would be in a metal ion enriched nutrient. Phytoplankton may well be such a source.

III. Organism-Environment Interactions

A. Phytoplankton as a Basic Source of Metal Ions

Marine phytoplankton may be a substantial source of trace metals. A number of studies have documented the ability of algae to adsorb and concentrate heavy metals²⁶⁾. The dissolved levels of cadmium, copper, manganese, lead and zinc generally decreased during periods of high productivity in the waters of Monterrey Bay, California. A substantial loss of dissolved manganese was observed during a *Phaeocystis* bloom²⁷⁾. Determining concentration factors under these conditions is uncertain since during bloom conditions high growth rates appear to dilute metal levels within the algal mass. As has been pointed out²⁸⁾, such lower metal levels may also be due to the chelation of metals by extracellular products that should be at high concentration during a bloom. By lowering the metal's chemical activity these natural complexing agents should decrease metal uptake by phytoplankton. Recent work at the New England Aquarium has shown that two species of freshwater algae, *Chlorella vulgaris* and *Anabaena constricta*, can significantly reduce dissolved levels

of Ag, Cd and Cr(III) in dense cultures, *i.e.*, 10^5 – 10^6 cells/ml. On a dry weight basis these algae appear to accumulate such metals up to 5×10^4 times their dissolved concentration at equilibrium²⁹). Even greater uptake of chromium by the marine diatom, *Skeletonema costatum*, has been reported⁷). Diatoms, which are the dominant class of phytoplankton in Boston Harbor and Massachusetts Bay, may generally be more efficient metal scavengers because of adsorption on their siliceous cell membrane.

B. Concentration of Metal Ions in Phytoplankton

Concentration of trace metals in phytoplankton is of importance in considering the biological contribution to the transport and removal of these elements in geochemical cycles. Construction of budgets associated with geochemical cycles has proved useful in differentiating areas in which biological components are significant to the geochemical cycle. A prototype study is that of Kuntzler for ^{55}Fe in the Pacific³⁰). By considering phytoplankton uptake, transfers to other trophic levels, and downward detrital rain, physical and biological removal processes were differentiated. Based on residence time, biological removal of Fe was estimated at 7.8 yr and was insignificant compared with physical processes of 2.7 yr. Only in areas of upwelling was biological removal considered significant with an estimated residence time of 0.3 yr. Similar estimates of 0.3 yr have been made for biological removal of lead in upwelling areas⁹).

While such general estimates are useful, attempts to relate trace metal levels directly with phytoplankton activity, particularly seasonal activity, have offered conflicting results³¹). It was not possible, for example, to demonstrate any seasonal cycle in the concentration of soluble and particulate iron in the Sargasso Sea. This was in spite of the fact that experimental evidence was available indicating that iron was a limiting factor to phytoplankton growth for the area.

An attempt has been made to follow seasonal variations in the distribution of particulate copper and chlorophyll *a* in the Straits of Florida⁶). No consistent correlation was found between particulate copper and chlorophyll *a*. The difficulties associated with these types of measurements are discussed by Spencer and Brewer³²), who sought to show seasonal variation of copper, zinc, and nickel levels in the Gulf of Maine and the Sargasso Sea. For the Gulf of Maine, they estimated the total amount of copper available to be the order of 150 mg/m^2 for the period March to October, whereas the estimated uptake by phytoplankton based on a Cu/P ratio of 0.0065 was 28 mg/m^2 for the same period. Their results clearly show the need for synoptic data to document any seasonal variations due to uptake.

The difficulty of acquiring field data to relate trace metal concentrations to primary productivity, even at the gross uptake level, points to a formidable task posed for trying to relate trace metal levels quantitatively with effects on phytoplankton populations *in situ* in open water situations. In more complex regions, such as estuaries, there are added complications such as turbid mixing, deposition, and possible exchange reactions between sediments, bottom dwelling organisms, and the water column. In the near term, we are likely to be faced with having to establish

toxicity effects in laboratory-based studies except in situations of extreme pollution where clear concentration gradients may be established.

Though metal ions and marine phytoplankton are simple themselves, the total interaction between metal ions in their various forms, with phytoplankton throughout the cyclic seasons is complex and difficult to describe quantitatively. The main point is clear, however, marine phytoplankton remove a significant fraction of the metal ions available in sea water. To higher organisms there are thus three sources of metal ions: the aqueous phase of sea water, non-living particulate matter, and marine phytoplankton. In the following sections we discuss the mechanism of assimilation of metal ions from all sources by selected organisms.

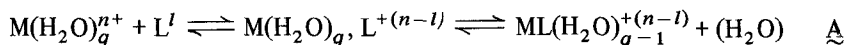
IV. Entry of Metal Ions into Living Systems

A. Molecular Models of Metal Binding

The molecular models of metal binding are either chelation or ion exchange. Actually, both models share many of the same features. They differ in only one essential regard: chelation occurs in homogeneous solution, but ion exchange is a heterogeneous, two-phase process. Clearly, entry of a metal ion into a biological system involves attachment of the metal ion to a binding group. However, the metal ion, if cationic, will already be strongly coordinated to the solvent. If anionic, as in the case of vanadium, present as vanadate ion, the metal ion is in the center of a tetrahedral array of oxo (O^{2-}) ligands. Therefore, the first step in ion uptake involves *substitution*: the replacement of one or more groups coordinated to the metal ion by the incoming binding group.

1. Complex Formation

Consider first the chelation of a solvated cation, $M(S)_q^{n+}$. Here, S is a solvent molecule (water); n is the positive, l the negative charge; and q , the solvation number, also represents the maximum coordination number of the metal ion. With no significant loss in generality, let the incoming group, or ligand, have only one binding site. Then, the binding process, in aqueous solution, may be represented by the following reaction scheme³³.



The first step represents formation of an ion-pair ($M(H_2O)_q, L^{+(n-l)}$). This process equilibrates very rapidly; the formation rate constant is generally diffusion controlled. The second step shows the real substitution process. The relaxation time for this first order process is controlled by the rate of release of a water molecule from the metal ion's inner coordination shell.

The advent of fast reaction techniques permitted a thorough investigation of this important reaction for almost all known stable metal ions with a wide variety

of ligands. The subject has been extensively reviewed in the past³⁴⁻³⁸; more recently with emphasis on metal ions in biological solutions³⁹⁻⁴¹. In this review we summarize the results for the selected metal ions, beginning with the metals present in sea water as cations.

The mechanism of the substitution step can show two types of limiting behavior⁴². The decision as to which type prevails depends on carrying out activation studies (temperature-dependence of the rate constant), solvent exchange rate determinations, and complex formation rate constant determinations with several ligands. For several metal ions like Ni^{2+} , the exchange rate constant's entropy of activation is positive, and ligand properties do not appreciably affect the rate of substitution; then, the solvent exchange rate is a characteristic of the metal ion, and the mechanism is dissociative (D). In contrast, associative (A) mechanisms have negative entropies of activation; the substitution rate constants vary with ligand, and a characteristic substitution rate constant is not a meaningful concept.

Another way of expressing these mechanistic distinctions is through a description of the activated complex. For the (D) mechanism, the activated complex has a reduced coordination number, while for the (A) mechanism the coordination number increases upon forming the activated complex. In the most commonly encountered case, the ground state reactant ion has an inner coordination shell with six binding sites. In the (D) mechanism the activated complex has fivefold and in the (A) mechanism sevenfold coordination. Obviously, real systems will not fit perfectly into the rather tidy picture presented by these limiting cases. For example, a concerted movement of solvent molecule out of the coordination shell with simultaneous penetration of the incoming ligand is a very likely process intermediate between (A) and (D). For a clear discussion of these mechanisms and their refinements the excellent monograph by Langford and Gray is recommended⁴².

A cationic metal ion thermodynamically stable in more than one valence state can undergo substitution via both mechanisms. For V^{2+} , the (D) mechanism prevails, with a characteristic rate constant approximately 10^2 s^{-1} . For most trivalent metal ions, a range of rates is found when different ligands are studied³⁴. However, for V^{3+} , not enough systems have been studied in aqueous solution to allow firm conclusions to be drawn. The negative entropy of activation suggests the (A) mechanism^{43, 44}, although results in other media cast some doubt on these conclusions³⁶. Upon being oxidized still further, a simple cationic species is no longer observed; vanadium(IV) is present in aqueous solution as the VO^{2+} ion. Substitution is dissociative; the characteristic rate constant is 500 s^{-1} ^{45, 46}. Further oxidation of vanadium to the +5 state leads to VO_2^+ , which is only stable in aqueous solution below pH 1⁴⁷.

Of considerable importance is the kinetics of this oxidative process. It is known that the air oxidation of vanadium(IV) is moderately rapid⁴⁸. Therefore, vanadium entering sea water from natural waters or from pollutants will be present as monomeric and aggregated vanadate anions⁴⁹. At the high dilution present in the oceans, $\sim 5 \times 10^{-8} \text{ M}$, and the typical pH's around 8, the equilibria would be shifted towards monomers of different degrees of protonation. Thus, substitution now occurs on an oxyanion, and will be discussed later.

Two widely separated oxidation states of chromium are both found in sea water – chromium(III) and chromium(VI). Considerable disagreement exists, however, on

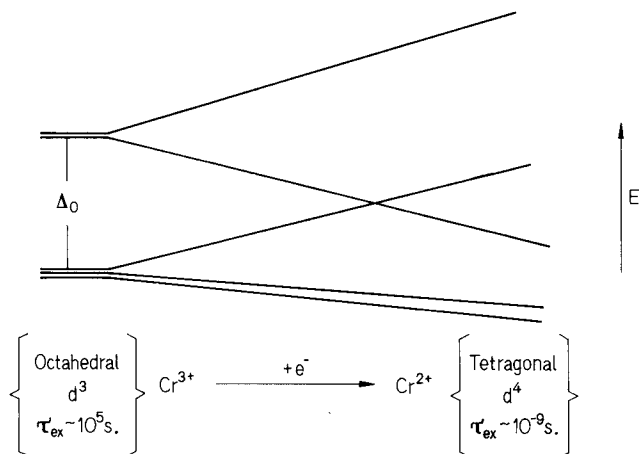


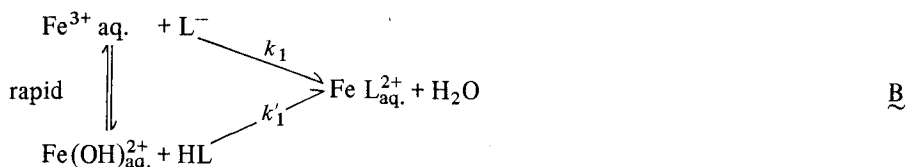
Fig. 2. Energy-level diagrams giving the d -orbital splittings as an octahedral complex undergoes increasing tetragonal distortion. Here E is energy, Δ_0 is the splitting between the e_g (upper) and t_{2g} (lower) orbitals in an octahedral field, and τ_{ex} is the lifetime of a water molecule in the inner coordination sphere

which state is favored in open ocean waters at pH 8. The experimental evidence indicates that both forms must be considered¹⁵⁻¹⁹. Since chromium(VI) is an oxyanion, we consider cationic chromium(III), first.

Although thermodynamically unstable in neutral media, it is instructive to begin with chromous ion (Cr^{2+}), and then make a comparison with chromium(III). The lifetime of a water molecule in the inner coordination shell of Cr^{2+} is $\sim 10^{-9}$ s; in contrast, the lifetime of a water molecule in the Cr^{3+} inner coordination shell is $\sim 10^5$ s⁵⁰. How can the removal of one electron produce such a profound effect, making chromium(II) complexes extremely labile, and chromium(III) complexes extremely inert? A reasonable explanation is shown below in Fig. 2. The Jahn-Teller distortion characteristic of a d^4 ion lowers the activation energy for the attainment of either the (A) or (D) activated complex for chromous substitution. For chromium(III), (d^3) in full octahedral symmetry, the crystal field splitting between the occupied and unoccupied d -orbitals confers exceptional stability on the ground state. Hence, the electrostatic effect, which causes an ion of higher charge to hold its inner coordination shell more tightly, is augmented by the crystal field effect, in a far more pronounced way than for the V^{2+} vs V^{3+} case discussed above, or Fe^{2+} vs Fe^{3+} , to be considered next.

There is no ambiguity concerning the predominant oxidation state of iron in sea water; it is +3. The oxidation of iron(II) by atmospheric oxygen is relatively rapid⁵¹. Ferrous ion is labile, with a water exchange rate of $3.2 \times 10^6 \text{ s}^{-1}$ at 25°C ³⁴. The few complexation studies completed with this ion show relatively little variation with ligand, and the (D) mechanism seems to prevail³⁶. Considerably more studies have been carried out with iron(III), with considerably less mechanistic certainty. In keeping with the simple electrostatic effect, the lifetime of a water molecule in the iron(III) inner coordination shell is longer compared with ferrous. For $\text{Fe}(\text{H}_2\text{O})_6^{3+}$,

the water exchange rate constant is $8.2 \times 10^3 \text{ s}^{-1}$ ³⁴). The rate law governing the interaction between iron(III) and a given ligand can be ambiguous due to the existence of indistinguishable pathways. Thus, if the ligand is a weak acid HL, complexing in L^- form, the two complex formation steps



in B are indistinguishable because their activated complexes have equivalent stoichiometries. The conclusion that has been reached is that OH^- in the inner coordination shell labilizes the remaining waters³⁶); i.e., $k'_1 \gg k_1$. However, unlike the classically accessible chromium(III) system, which is clearly (A)⁵², the much more labile iron(III) system appears to follow a (D) mechanism^{36, 53}.

The most interesting feature of the iron(III) studies is the labilization produced by a strongly coordinated group³⁴); in the above case, OH^- . The effect of this ligand on activation energy is twofold. The lowering of symmetry raises the energy level of the ground state with respect to that of the activated complex. The repulsion of a negative, or neutral, but strong field binding group like $-\text{NH}_2$ repels the remaining inner sphere water molecules, thereby weakening the $\text{M}-\text{OH}_2$ bond. One important consequence of this effect is that, in the absence of kinetically impeded ring closure, the entry of a multidentate chelating reagent into the inner coordination shell will be controlled by the rate constant for release of the *first* water molecule. For copper(II), however, another effect appears.

Like Cr^{2+} , the $d^9 \text{ Cu}^{2+}$ ion has a Jahn-Teller distortion. Although ultimately showing sixfold coordination, the structure of the complex is distorted, with four equatorial water molecules, and two less tightly bound axial water molecules. The water exchange rate constant, never accurately measured by NMR line-broadening techniques, could nevertheless be established by chemical relaxation at $1-2 \times 10^9 \text{ s}^{-1}$ ⁵⁴). When the incoming ligand is monodentate, inversion — a more rapid process than substitution — brings the ligand into an equatorial position. A coordinated bidentate ligand would block this mechanism. Hence, in the absence of other effects, the formation of the second, or bis-complex, is slower than the formation of the first, or mono-complex, for chelating ligands⁵⁵.

Unlike the metal ions just under consideration, mercury and lead do not have vacant or partially filled d -orbitals, nor do they normally assume a high charge. Thus, their aqueous chemistries resemble those of other divalent d^0 and, especially, d^{10} ions³³). Both ions substitute extremely rapidly, and have only been studied with a few non-classical techniques. For Pb^{2+} , a survey of results shows substitution rate constants in the range $10^8 - 2 \times 10^9 \text{ M}^{-1} \text{ s}^{-1}$ ⁵⁶).

Reactions with Hg^{2+} are virtually diffusion controlled^{56, 57}). Organomercury bonds, however, are kinetically inert. Reactions of, for example, $\text{H}_3\text{C}-\text{Hg}-\text{OH}$ (methylmercuric hydroxide) in aqueous media occur with replacement of hydroxide

rather than methyl. These reactions are still quite rapid, and the temperature-jump method was used to study



where $\text{X}^{q-} = \text{Cl}^-$, Br^- , I^- , SCN^- , and SO_3^{2-} ⁵⁸). The forward rate constants for these ligands vary from $1.1 \times 10^4 \text{ M}^{-1} \text{ s}^{-1}$ for Cl^- to 7.0×10^6 for I^- ; less variation is exhibited by the reverse rate constants, which cover the range $4.1 \times 10^7 \text{ M}^{-1} \text{ s}^{-1}$ (I^-) to $5.0 \times 10^8 \text{ M}^{-1} \text{ s}^{-1}$ (Cl^-) for the mononegative ions⁵⁸). The strong ligand dependence of the forward step is consistent with an (A) mechanism. Any trends in the reverse reaction with OH^- may be due to steric blocking by increasingly larger X groups.

The kinetics of oxoanion chelation show reactivity patterns different from the analogous cationic reactions. Although emphasizing chromate and vanadate in this review, the results for all transition metal-containing oxoanions will be summarized to gain a better understanding of the mechanism involved. In fact, as shall be shown, chromate stands apart from oxoanions like vanadate, molybdate and tungstate.

Upon mixing together solutions of tungstate and catechol at pH 8, a yellow color appears to form "instantaneously". The reaction actually has about a 0.3 sec half-life at 25 °C and pH 8 when $[\text{WO}_4^{2-}] = 2 \times 10^{-2} \text{ M}$ and $[\text{catechol}] = 1.0 \times 10^{-4} \text{ M}$. Crystal structures of tungstate, vanadate, and molybdate complexes with ligands like catechol, 8-hydroxyquinoline and EDTA (ethylenediaminetetraacetate) show octahedral coordination around the central metal ion; whereas the uncomplexed oxoanions are tetrahedral in solid and solution⁴⁷). Chromate does not expand its coordination number. The reaction of chromate with, for example, thiocyanate leads to replacement of one oxo ligand on chromium(VI) by thiocyanate. Thus, reactions of chromate with ligands may be viewed as esterifications; the reactions of vanadate with ligands are more properly thought of as complexation reactions.

The dynamics of substitution on tetrahedral chromium(VI) has been studied by temperature-jump and rapid mixing^{59, 60}). The mechanistic interpretation of these results has to account for the acid catalysis. The most satisfactory mechanism involves the rapid protonation of HCrO_4^- , followed by rate-determining water elimination and attachment of the incoming ligand on the threefold coordinated activated complex⁶¹). Therefore, the substrate is, at best, weakly coordinated to the metal center in the transition state; variations in the observed rate constants are due to ratios of rate constants for the elementary steps in this mechanism.

A considerably different picture has been developed for molybdate and tungstate^{62, 63}), and vanadate⁶⁴). The reactivity patterns found in these studies are several; the most important is that the rate of formation of mono-complex increases with increasing acidity. For the formation of the bis-complex, the hydrogen ion dependence is weaker, but varies in the opposite sense — the rate goes down with increasing acidity. Furthermore, the complex formation rate constants increase with increasing ligand basicity. Clearly, an (A) mechanism is indicated; yet, differences exist on the exact details^{62a, 63d}).

Evidence gathered on sodium molybdate solution by ultrasonics and NMR suggest that although MoO_4^{2-} is tetrahedral, the protonated species HMoO_4^- is sixfold

(probably octahedrally) coordinated^{65, 66}. (It is possible that octahedral coordination does not occur until further protonation to H_2MoO_4 occurs⁶⁷). This conclusion rests on indirect evidence, however.) If HMoO_4^- and MoO_4^{2-} are structurally similar, then the chelation reaction is addition, not substitution. If HMoO_4^- is more properly represented by the formula $\text{Mo}(\text{O})_2(\text{OH})_3\text{H}_2\text{O}^-$, inferred from the NMR study⁶⁶, then chelation is a substitution process.

Both the addition⁶², and substitution⁶³ mechanisms have been thoroughly discussed. In either case it is clear that the protonated oxoanion is more reactive in forming the mono-complex. Further complexation involves a species already in sixfold coordination; hence, further protonation does not affect the oxoanion. Instead, the ligand is protonated, which makes it less reactive, thereby accounting for the opposite trend in the $[\text{H}^+]$ dependence of higher order substitution. These conclusions apply to molybdate and tungstate, and most likely to vanadate, on which further research is being carried out.

2. Ion Exchange

In the previous discussion of chelation, little mention was made of the relative stabilities of metal-ligand complexes. From the kinetics standpoint, however, the trends in stability can be readily understood as arising from differences in the complex dissociation rate constant. Very little variation in association rate constant is observed for metal ions substituting via the (D) mechanism. The ligand variation in the (A) mechanism, though detectable, is nevertheless modest in comparison with the range of values encountered in the dissociation rate constants of a given metal ion with a series of ligands³⁴. These rate constants are for the second step in scheme A, which also serves to illustrate another facet of metal-ligand binding.

Reaction scheme A helps to distinguish between purely electrostatic interactions and other types of bonding effects such as orbital overlap and symmetry. As depicted in A, the ion-pair is held together by coulombic forces. Factors determining the rate of release of a water molecule from the metal ion's inner coordination shell, and the strength of the ligand-metal attachment certainly include aspects of simple electrostatic metal-ion and metal-dipole bonding. These considerations alone cannot account for the trends in the relative kinetics and bonding; crystal field theory plays a decisive role in explaining these phenomena³³.

Both electrostatic and ligand field effects are important in understanding ion exchange, the process which dominates the uptake of metal ions from sea water by living systems. Since ion exchange can be regarded as an equilibrium process, the experimental evidence is more readily treated by theory than is the kinetics of complexation. A successful theoretical model of ion exchange has to account for the selectivity of the process. Of course, other features of metal ion binding interactions such as order of magnitude equilibrium constants and saturation curves should also be correctly predicted.

The various attempts to describe ion exchange quantitatively have been summarized by Kunin⁶⁸. One of the earliest efforts at interpreting ion exchange utilized the Freundlich isotherm; namely, $x/m = a C^b$, where x/m is the amount of solute

taken up per gram of adsorbent, C is the equilibrium concentration of solute, and a and b are adjustable parameters for a specific system at a constant temperature. This equation has been widely applied in metal ion uptake studies⁶⁹). Yet, from a theoretical standpoint it is unsatisfactory, and its apparent success leads to misunderstanding. The Freundlich isotherm, an empirical relation, does not account for the finite capacity of the exchanger. Moreover, since the two parameters are adjusted to make the data fit, the physical or chemical significance of their final values, *viz.*, specificity, is not immediately apparent, if at all present.

A theory of equilibrium ion exchange has been presented by Rice and Nagasawa which agrees with experiment⁷⁰). The model upon which the theory is based locates the binding sites on a crosslinked polyelectrolyte gel. These sites bind the exchanging group through electrostatic ion-pair equilibria. This interaction is solely responsible for the selectivity; *i.e.*, the relative strength of the binding, as shown by the equilibrium quotient. In the model, allowance is made for interactions between neighboring sites. As the binding sites and exchangeable groups are usually oppositely charged, it is clear that exchange properties will depend on the charges on the binding sites, the distance between sites and the nature of the medium between those sites.

B. Assimilation of Metal Ions: Regulated Removal and Transport

From the complexation and ion exchange models we can immediately obtain some important conclusions about the biological effects of metal ion contamination. The list of essential elements shows that living systems have already discriminated amongst the available metallic elements. Very light elements with high charge to ionic radius ratios and a strong tendency to hydrolyze like beryllium and aluminum have been largely bypassed. Heavy metals with low charge to radius ratios have not been incorporated by living systems for physiological purposes. We can thus distinguish two types of pollutants and their effects. Pollution of sea water by essential elements will not usually have immediate toxic effects. Vanadium, chromium, manganese, iron, cobalt, nickel, copper and zinc are *preferentially* adsorbed; increases in their concentration level may affect growth, size, reproductive rate, etc., but toxicity will not be expected unless the concentration level is massively increased, and free metal ions appear within the affected organism. Cadmium, mercury and lead are present in natural waters, but do not compete favorably with essential trace elements for binding sites. Increases in the concentration levels of these elements sufficient to compensate for their less efficient binding ability can result in their assimilation by living systems.

The uptake of metal ions by living systems need not be due to a single mechanism. In fact, evidence has been gathered showing that at least two mechanisms may be simultaneously operative⁷¹). At low dose rates iron uptake in mice, rats, and dogs shows saturation; the uptake rate data actually follow a Lineweaver-Burk plot usually used for the Michaelis-Menten enzyme catalysis equation. At high dose the amount of iron adsorbed is proportional to the amount administered. Presumably, at higher doses a physical process such as diffusion accounts for the transfer of iron out of

the lumen of the gut into the mucosal cells. The Lineweaver-Burk plot does not imply enzyme activity in the uptake process. Any "steady-state" process involving a single intermediate, or "non-interacting" binding site is identical with the Langmuir adsorption isotherm⁷²⁾, of which the Michaelis-Menten mechanism is one example.

The term "non-interacting" has a different meaning from that previously used to describe the model of ion-exchange. The active sites in enzymes can, and do⁷³⁾, change conformation and position with respect to solvent in the course of catalysis. More significant change has been observed, however, in which the binding of substrate changes the equilibrium quotient for binding further substrate; this process is cooperativity, of course⁷⁴⁾. This effect has not, to our knowledge, been observed in metal ion uptake. The success of the Rice-Nagasawa model for ion exchange does not imply that binding sites of similar composition and mechanism of action occur exclusively in marine organisms. Other types of binding may well occur, for proteins are present in cell membranes, and may present strong-field binding sites, especially potent in the uptake of transition metal ions.

However, it may well be that the initial step of metal ion uptake does involve simple electrostatic ion exchange. The selection and absorption could come as a result of transport through the membrane separating environment and organism, or at a point further along the metabolic pathway for a given metal ion. Such a selection process has been indicated for iron in mammals⁷¹⁾. Ion specific carriers are known to exist; their kinetic and equilibrium properties would be consistent with this type of uptake⁷⁵⁾. Pore formation, another mechanism for ion transport across membranes, may also play a role in uptake, especially where higher doses are concerned⁷⁶⁾.

V. Impact of Metal Ions on Selected Organisms

What is the availability of trace metals in recent sediments to the benthic flora and fauna dwelling upon and within those sediments? Metals locked in solid phases as mineral grains, rock fragments and shell fragments are removed from the ecosystem. Metals absorbed on settling particulates such as hydrous manganese and iron oxides, clay mineral and detrital materials, may have lost much, but not all, of their bio-availability. Notable exceptions may be mercury, arsenic and possibly selenium, in that microbial activity within the sediments may convert the inorganic metal to volatile organo-metallic compounds and hydrides which can redissolve into the waters above. The availability of transition metals to benthic fauna and to the aquatic food chain will depend on their behavior at the sediment (interstitial) water interface which, in turn, will depend on the processes controlling the uptake and release of metals at the solid surfaces.

Theoretical generalization is not enough to evaluate the availability of metals to benthic fauna. In actual fact, the rate of uptake of any element and the extent of its retention in an organism are dependent on a number of ill-defined factors. As the data in Table 6 indicate, the extent of biological enrichment varies considerably between species. It is likely governed by:

- 1) the particular metal involved and its physiological importance to the organism,
- 2) the physical and chemical state of the element and its availability to a specific organism,
- 3) the concentration of the elements in the environment and the presence of other elements that may inhibit or enhance its uptake. The accumulation of one heavy metal by an organism may be altered by the relative abundance of another in the environment in one of three ways:
 - (a) metals of similar properties may substitute for one another;
 - (b) some metals may have an inhibitory effect on others;
 - (c) one element may have a synergistic effect with another.
- 4) the morphology of the organism, its life history, its condition and age, and its particular role in the food chain. Closely related species may behave differently and organisms of the same species may concentrate metals at different rates, depending on environmental conditions. Generally, young and active organisms tend to accumulate heavy metal ions most rapidly.

As a result of the interaction of these many factors, it is difficult to forecast the extent to which any heavy metal may be concentrated in a given organism. This section will therefore treat three widely differing examples: the copper-algae interaction, metal ions and bivalves, and vanadium uptake by tunicates.

Table 6. Concentration Factors for the Trace Element Composition of Shellfish Compared with the Marine Environment

Element	Enrichment Factors		
	Scallop	Oyster	Mussel
Silver	2,300	18,700	330
Cadmium	2,260,000	318,000	100,000
Chromium	200,000	60,000	320,000
Copper	3,000	13,700	3,000
Iron	291,500	68,200	196,000
Manganese	55,500	4,000	13,500
Molybdenum	90	30	60
Nickel	12,000	4,000	14,000
Lead	5,300	3,300	4,000
Vanadium	4,500	1,500	2,500
Zinc	28,000	110,300	9,100

Source: B. Ketchum (Ed.), *The Water's Edge*, M.I.T. Press, 1972.

A. Speciation and Algae

Attempts to relate plankton activity with trace metal distribution in natural waters have proven difficult. Some researchers have hypothesized that iron, copper, or naturally occurring ligands are controlling factors for outbreaks of toxic dinoflagel-

late blooms^{77, 78}). These hypotheses remain unproven. In the laboratory, trace metals and ligands have replaced the undefined "soil extracts" and have been used to supplement natural sea water or synthetic media to grow algae⁷⁹). There is also evidence that the addition of strong complexing agents to recently upwelled sea water can immediately increase productivity⁸⁰). Smayda⁸¹) has found that the second most important factor (after nitrogen limitation) limiting the growth potential of water from Narragansett Bay is a property of the water which could be eliminated by the addition of EDTA. Thus, it is not unlikely that trace metal – organic interactions in ocean water do indeed affect productivity.

For a number of reasons, both biological and chemical, copper is the metal which would be most likely to control metal mediated productivity. It typically forms complexes with organic ligands that are stronger than those formed by most other transition metals. A major potential competitor in sea water, ferric iron, is extensively hydrolyzed at pH 8, and in fact does not compete effectively. Copper is found in coastal waters at the moderately high 1 to 10 ppb range, which enables it to out-compete the less abundant metals such as Ni^{2+} , Pb^{2+} , and Co^{2+} that form complexes of comparable stability. If a strong ligand is added to a ligand-poor sea water system, copper will be completely titrated before the ligand interacts significantly with any other metal. In a system where the metals are already associated with moderately strong ligands, a strong ligand will primarily affect the speciation of the copper. In addition, divalent copper is a potent photosensitizing agent for many organic acids and could be responsible, in part, for aging phenomena in sea water⁸²). If copper is present without strong chelating agents or if it is present in excess of the strong complexing capacity, it is toxic to most algae^{83–85}), although toxicity varies widely⁸⁶). Extraordinarily high levels of copper can be tolerated in many cases if the medium is over-chelated. Nonetheless, copper is an essential nutrient for algae⁸⁷).

1. Chemoreception, Uptake and Response

A full understanding of the mechanisms of uptake and biological utilization of copper requires that chemical, biological, and biochemical investigations be integrated in a unified approach. An examination of the response of the physical, chemical, and biological systems of the organism is a vital area of research. A clear-cut differentiation of modes of metal uptake must be established. Non-biological processes such as ion exchange should be recognized as potentially independent of metabolically mediated uptake. Active rejection of metals must also be considered.

Initial bioavailability of the metal is determined by its chemical speciation in the medium. The importance of production of extracellular metal binding organic materials extends to both natural water and research considerations. Plankton response to metals in natural waters is not mediated simply by the total metal concentration. In the laboratory situation, accurate calculation of uncomplexed metal concentration requires the knowledge of the nature of the ligand and its concentration.

The sensitivity and response of plankton to copper varies widely. *Dunaliella tertiolecta* showed visible growth in the presence of 3 ppm of inorganically complexed copper, whereas *Cyclotella nana* and *Chaetoceros* sp would not grow visible in the presence of 50 ppb inorganically complexed copper⁸⁶). It has been demon-

strated that reproduction of the green algae *Chlorella pyrenoidosa* and the photosynthetic rate of the diatom *Nitzschia palea* are depressed by copper to a greater extent than the *photosynthetic* rate of *Chlorella* and the reproductive rate of *Nitzschia*⁸⁵). The release of metal binding organics by the diatom, but not by *Chlorella*, is implicated. It is also possible that the use of synchronous cultures of the diatom and the sampling time within the cell cycle were responsible for a lesser effect of copper on the growth rate of *Nitzschia*.

Response of the organism to copper stress is dependent on the status of the culture. In the absence of synchrony, effects can be masked by the presence of only a fraction of the cells being in a sensitive phase of their development. Application of copper in the dark often elicits responses that are different in intensity or type than those observed in the light⁸⁸⁻⁹¹). Anaerobic conditions exacerbate the deleterious effects of Cu⁹²). Critical evaluation of these data and data generated in our own work has led us to some hypotheses regarding the systems affected by copper.

In particular, there are two related questions:

- 1) Are the changes that allow *Skeletonema* to grow after a few days of lag phase due to changes in the chemistry of the medium and/or changes in the biochemistry of the cells?
- 2) If there is a change in the physiology of the cells, can one conclude that there are biochemical events, pathways, which are more sensitive than others to the influence of copper, *i.e.*, is a cell in a non-proliferating (lag phase) stage more susceptible to copper stress than exponentially growing cells?

Changes in both medium and cellular chemistry are not mutually exclusive. Chemostat experiments have clearly demonstrated that the complexing capacity of the medium increases when the cells are stressed with high levels of copper, although we do not know if this increase is the result of exudates or of release of organic material due to cell lysis. The changes in the chemistry of the medium may have a "non-biological" origin (*i.e.*, not due to exudates). Artificial media present problems of aging, particularly with respect to precipitate formation. A specific medium, Aquil, was designed to avoid this pitfall. The concentrations of nutrients and trace metals are theoretically low enough to avoid precipitate formation. In spite of these precautions it is not unlikely that small changes may occur with time due to adsorption of trace metals on the wall of the container or on very small colloids of hydrous ferric oxide which may form. Indeed, in f/2 medium without EDTA, ferric iron has been shown to protect a *Pyraminomas* sp. against copper toxicity⁹³). Such a phenomenon may occur on a smaller scale in a less enriched medium like Aquil.

Silica, which also has a very complex chemistry and can form colloids, could possibly remove some free copper by scavenging. These possibilities of non-biological or biological changes in the medium need to be clarified. It is most probable that changes in cellular physiology may be partially responsible for insensitivity to copper at certain stages of the life cycle of a cell.

Indeed it is most intriguing to observe the wide variations in sensitivity in a single species. Steeman-Neilson and coworkers found that the influence of copper depended on the stage of the cell cycle of *Chlorella*⁸⁵). If the initial steps of cell division had taken place, the cell continued to divide. They made the same observation with *Nitzschia palea*⁸⁹): the photosynthetic rate is most drastically reduced when the

cells are taken just prior to cell division. It was also found that reduction in respiration of *Chlorella* was much larger with older cells⁹⁴. Our own experiments indicate that Cu may interfere particularly with cellular division during the lag phase and silicone metabolism.

Other studies of sensitivity to specific chemicals have shown that it is crucial to correlate a given response of a cell to its "physiological" status, *i.e.*, its stage in its cell cycle⁹⁵. In work at the New England Aquarium with batch cultures of *Skeletonema* we have observed that a lag phase develops when stationary phase cells are used as an inoculum for Aquil containing 6 or 7 μM copper. J. Reuter (personal communication) at MIT has performed analogous experiments using exponential phase cells as the inoculum. He did not observe either a lag phase or change in growth curve when compared to controls. Because the experiments were performed in different labs with slightly different conditions, they were not identical and work is now underway to perform the complete set of experiments. The evidence does point to a differential sensitivity of stationary phase cells and exponential phase cells to copper effects on division.

In an attempt to localize the action of copper on the cellular metabolism and biochemical pathways one has to narrow the immense number of possibilities to a few most probable ones. It is known that copper, which is found in plastocyanin, is an essential component of the electron transport system of the chloroplast. It also inhibits photosynthesis of isolated chloroplasts⁹⁶ and in high concentrations it reduces the concentration of pigments in whole cells⁹¹. Although light is required to observe inhibition by copper, the photosystems are not necessarily directly involved. Experiments performed at a variety of light intensities with isolated chloroplasts⁹⁶ as well as with whole cells⁹⁰ demonstrate that copper affects a dark reaction and not the photoact *per se*.

From the difference in response between different algal species it appears that copper may be acting at a variety of loci. *Chlorella* does not show inhibition for a few hours except at saturating light intensity. The action of copper in that organism may be one that requires a time dependent penetration inside the cell to reach specific sites such as the chloroplast. Conditions which may favor the penetration of copper, such as those found in anaerobic cultures, are followed by a rapid decoloration in pigment material and a rapid inhibition, even with *Chlorella*⁹⁷. On the contrary, *Nitzschia palea* and possibly other diatoms may be affected as soon as copper is present at the level of the cellular membrane. The rapid response of diatoms may occur because silicon metabolism is directly connected to membrane function and membrane function is rapidly affected by materials in the aqueous phase. Indeed, we have visual evidence from our experiments that the silica shells are altered in the presence of copper and that cell division, which also depends on silicon uptake, is also affected.

Experiments done on isolated chloroplasts showed that all the chloroplast reactions tested are inhibited by copper and that manganese reduced this effect⁹⁶. The lack of influence of light in these experiments implies that the photoact *per se* is not involved. The authors suggested that a manganese activated enzyme was involved. Another possible mechanism is that copper and manganese both influence membrane permeability, but in opposite directions.

Conclusions reached with isolated chloroplasts cannot be directly generalized to the intact cells. In the intact cells copper will be confronted with the cell wall, cell membrane, and various compartments of the cytoplasm before reaching the chloroplasts. One can therefore expect that action on the chloroplast will follow action on the cellular membrane and perhaps on various cytoplasmic metabolic pathways. Copper may inhibit biochemical pathways at the periphery of the cell, with a greater number of organelles being reached as the concentration increases.

Finally there is evidence of interaction between sulfur metabolism, silicon metabolism, copper, and cell division. Copper is known to interfere with the formation of disulfide bonds and it can also denature proteins. Sulfur is generally involved in nuclear and cellular division. One possible effect of copper may be the disruption of disulfide bridges in proteins. Another is through general disruption of other pathways involving covalently bonded sulfur. In addition, silicon is a required compound in division of diatoms. Following

- a) the pathways of sulfur incorporation using radiotracer techniques, and
- b) silicon incorporation by direct analysis as a function of copper stress will clarify the role of copper in the metabolic pathways controlling utilization of these elements by the algae.

2. Copper Transport

Recognition of copper by the organism's biochemical apparatus once the metal is within the cell membrane can be expected because copper is an essential micro-nutrient. However, cellular recognition of the copper in its various forms outside the cells has not been investigated in any detail. It is not known at this time whether initial uptake at the cell-water interface is aided by the production of organic material by an active metabolic pathway in the cell by active "shuttle" through the membrane, or simply due to physical/chemical processes such as ion exchange. In a situation of copper starvation, the organism could respond by activating a metabolic pathway to aid in scavenging copper from solution. An analogous situation exists for the production of deferrisiderochromes by bacteria, fungi, and some plant species where conditions of iron deficiency exist⁹³). Predictions of production of extracellular metal-bound organic material in response to metal stress have been borne out experimentally. Evidence of metabolically mediated uptake is lacking. However, non-metabolic uptake of metals by the cell wall, presumably by ion exchange, has been documented^{98, 99}). The importance, then, of metabolic control of metal uptake is as yet unknown.

The elucidation of mechanisms by which materials are transported from the extracellular fluid through the cellular membrane and into the cell is currently an active area of research. Work on the effects of cadmium on *Naviculla pelliculosa* demonstrated that the metal did not have to penetrate into the cytoplasm to affect silicon uptake¹⁰⁰). Other systems, such as those involved in photosynthesis, will be affected primarily by metal ions that are able to pass through the cell wall. Copper uptake in *Skeletonema* has been measured, but not its distribution on the cell (adsorbed) and within the cell (transported through the cell wall). Knowledge of

the distribution would enable us to eliminate certain areas of cellular biochemistry from consideration as important sites of copper activity.

Experimental evidence points to numerous ways in which copper can adversely affect the cell. Cell wall permeability is certainly changed, at least for non-growing *Chlorella* cells⁹²). A variety of effects on the photosynthetic system has been observed^{85, 88, 90, 91}). Growth rate and/or final cell densities can be reduced^{85, 88, 101}). Distribution of phosphorus within the cell has been altered by the addition of copper⁹⁴). These results imply that a multitude of biochemical pathways can be deleteriously affected by copper, depending on the organism and the experimental conditions.

One cannot neglect the fact that algae do have a copper requirement. As early as 1953, Walker showed that *Chlorella* requires copper¹⁰²). More recently, in an elegant series of experiments, Manahan and Smith demonstrated quantitatively the minimum level of uncomplexed copper necessary for optimal growth of *Chlorella vulgaris* and *Oocystic marssonii*¹⁰³). Copper is present in various enzymes¹⁰⁴) and in plastocyanin¹⁰⁵), an intermediate redox catalyst in the electron path from photosystem II to photosystem I. Presumably, the minimum requirement fulfills the synthetic needs to produce these compounds.

One can consider that plankton have regulatory means by which copper at moderate concentrations is shunted mainly to the copper requiring systems and does not interfere with copper sensitive systems. At higher levels, a rejection mechanism presumably operates. At toxic levels of copper, this mechanism can no longer keep up with the input of metal due to the large external driving force.

B. Accumulation of Metal Ions by Bivalve Mollusks

Bivalve mollusks have been shown to accumulate a variety of heavy metals directly from solution and from their food supply. Therefore, it has often been suggested that the mollusks may serve as indicator organisms for the level of heavy metals in the local environment, once the seasonal changes in metal concentration are accounted for^{28, 106, 107}). Whether the main source of metal contamination comes from the food or from solution is not entirely clear, and may in part be dependent upon the metal itself or the species of animal. For example, Preston and Jeffries have shown that the European oyster, *Ostrea edulis*, probably absorbs metals such as zinc and cobalt from ingested particles rather than from solution¹⁰⁸). On the other hand, Schulz-Baldes found that mussels, *Mytilus edulis*, took up lead equally from solution and from algae containing a high lead count¹⁰⁷). Using chromium-51 and the American oyster, *Crassostrea virginica*, it was found that the metal uptake was more rapid from solution than from a labelled algal suspension of *Chlamydomonas*¹⁰⁹). However, it was suggested that in the natural environment the food supply could be a more important source of ⁵¹Cr. Absorption by direct uptake from solution approached a maximum asymptotically that could not account for the high levels of radioactivity found in some mollusks. Nevertheless, because there are relatively little data available and since all of the above mentioned studies have shown that food contributes a significant part to the concentration of heavy metals, the question arises as to the availability of the metals from the food supply.

The concept of bioavailability of particulate heavy metals has been of concern to many investigators. The approach taken by chemists to distinguish the available metal component from the total particulate concentration has usually been to extract the solid phase with concentrated salt solutions that are neutral or weakly acidic or basic, that impose small redox potential changes, or that provide a chelating ligand known to form stable transition metal complexes. These approaches have resulted in a variety of methods in the literature for the determination of heavy metal availability, most of which are sufficiently different from one another to make the comparison of results difficult.

1. Bivalve Feeding Selectivity

In bivalve mollusks there are two sites for the selection of particulate matter: the gills/labial palps, and the stomach. Studies on selectivity by the gills have generally shown that there is a size limit below which the animal does not retain particles efficiently¹¹⁰. Bernard has outlined a mechanism for the selection of particulate matter which is based on the specific gravity of the particles such that the more dense material does not reach the gills and is rejected as pseudofeces¹¹¹. Based on Bernard's data the particulate matter passed into the stomach would not be selected on food value.

Despite the fact that particle selection on the gills may not depend upon the nutritive value of the material, bivalves have a chemosensory mechanism which will influence the filtration/pumping rate and consequently the total size of the ingested ration. Dissolved food and metabolic substances stimulate ciliary activity in isolated gill tissue of *Mytilus edulis*¹¹², and the same substances stimulate the pumping rate in intact animals¹¹³. The filtration rate can be stimulated by a solution of glucose or various other compounds¹¹⁴; the metabolic rate is also increased by the addition of a glucose solution¹¹⁵. Filtrates of algal cultures and non-particulate cell extracts may either stimulate the filtration rate or depress the pumping rate^{116, 117}. The mechanism behind this chemosensitivity is unknown, but mussels possess two pallial sense organs, the osphradium and the abdominal organ, which could test the inhalent water, although there may also be receptors on the mantle edge¹¹⁸. The sensitivity of these organs to metals is unknown. To date the only metal which has been shown to influence the pumping rate is copper, and it is thought that this is due to a direct influence of the metal on the intact cilia¹¹⁹. LaRoche, *et al.*, have shown that copper affects the gill cilia in lamellibranchs. If bivalves can detect metals which are incorporated in algal cells or metals adsorbed onto particulate matter this may affect the filtration/pumping rate and consequently influence the total amount of food ingested or the ratio of contaminated to uncontaminated food in the stomach¹²⁰. If bivalves show metal ion selectivity in feeding, then the stomach contents would not reflect the metal concentration in the environment. For example, if the animals were in an area where there was a periodic flush of sewage sludge and this cation caused a reduction in the feeding rate, then the stomach contents would not reflect the actual environmental conditions surrounding the mussels.

Provided that the particulate matter is accepted by the gills it will then undergo selection in the stomach. Selection is a function of the ciliary tracts of the various

sorting areas found in the stomach¹²¹). It is generally assumed that the heavier (larger) particles bypass the digestive gland by way of rejection tracts and the intestinal groove, while the lighter (smaller) particles are maintained in the gastric circulation until they are taken into the digestive gland. In the snail *Lymnaea stagnalis*¹²², and the slug *Agriolimax reticulatus*¹²³, particle selection in the stomach has been demonstrated using X-ray opaque markers. In both cases particle selection was based on size; the smaller particles passed into the digestive gland. Using bivalves, Foster-Smith compared the fate of alumina and the diatom *Phaeodactylum* in a mixed suspension¹²⁴. Once the mixture was present in the gut the alumina was treated independently of the algal cells. The first feces expelled contained a predominance of alumina, indicating that it was selectively eliminated. However, further experiments using labeled algae suggested that food could be retained in the gut, and mixed with further additions of particulates, for 15–18 hours. The differential rate at which particulate matter is passed through the gut may have an influence on the accumulation of heavy metals. If metals are bound to particles which are selectively absorbed, then the metal may not be released from the sediment and adsorbed by the bivalve. On the other hand, if metals are bound to small particles they may be selectively digested, causing an increased accumulation of metal in the animal above that found in the surrounding environment.

2. Metal Ion Uptake

The total absence of comparative data on the feeding and biodeposition rate of bivalves when fed metal contaminated and uncontaminated algae makes analysis of the results difficult. It is possible that there will be no immediate selection against any of the metals in comparison with the controls. Schulz-Baldes maintained mussels in the laboratory on lead contaminated algae for a period of six weeks¹⁰⁷, but, as he pointed out, the ration fed was hardly adequate. Therefore, his data cannot, a priori, be used as an indication of the results. One of the few studies on the metabolic effect of heavy metals on bivalves, by Brown and Newell¹¹⁹, demonstrated that copper but not zinc inhibited the ciliary activity of the gills in whole mussels or gill preparations. Although extrapolation to the natural environment may not be totally warranted on such limited results, if the feeding and biodeposition rate were to be artificially reduced this could cause a shift in the food chain dynamics.

The effect of sewage sludge or suspended sediment on feeding and biodeposition is also difficult to predict. There are little data available on the influence of suspended matter or silt on feeding in bivalves. A recent paper by Winter indicated that a small quantity of silt in suspension would enhance the filtration rate¹²⁵. If this holds true for sewage sludge and for silt with a high concentration of metals, then we may find an even greater accumulation of metals in these animals than when fed only contaminated algae.

The influence of heavy metals on assimilation is, again, impossible to predict. For the mussel, Thompson and Bayne have shown that assimilation efficiency and the total assimilated ratio is a function of cell concentration¹¹⁵. If metal contaminated and uncontaminated algae are consumed at the same rate, then there may be no detectable difference in assimilation. On the other hand, when the animals

are also fed a suspension of sewage sludge and silt, if the filtration rate is stimulated then assimilation efficiency may drop¹²⁵⁾, although the total assimilated ration may actually increase with a corresponding increase in metal concentration. However, if the silt is rejected as pseudofeces or selectively rejected in the stomach, then there would be a decrease in assimilation efficiency but not necessarily in the total amount of uncontaminated algae consumed with a corresponding decrease in the metal accumulation.

C. Dynamics of Vanadium Uptake by Tunicates

Vanadium is an essential trace element to humans; it is also essential to tunicates. However, these marine organisms concentrate vanadium within their blood cells, where the element is present in *molar* concentrations and the term "trace element" is no longer appropriate.

Although feeding on microorganisms and detritus which may contain vanadium, tunicates can extract and thrive on the vanadium present in the aqueous phase of sea water⁴⁹⁾. The oxidation state of the element thus extracted is +5; the form is less well known. In sea water at pH 8 an anionic, monomeric vanadate species is present in some partially protonated form. The representations HVO_4^{2-} and H_2VO_4^- are convenient formalisms; they may or may not accurately represent the stoichiometric composition.

Other oxyanionic species are present in sea water, such as SO_4^{2-} , CrO_4^{2-} , and, especially, H_2PO_4^- and HPO_4^{2-} . All these anions are taken up by tunicates¹²⁶⁾. They are not assimilated, however, but are rapidly turned over. Laboratory attempts to measure vanadate uptake in the presence of phosphate generally show inhibition of uptake of the essential element. This observation can be explained by the formation of vanadate-phosphate complexes which are not bound at the uptake sites⁴⁹⁾. At the high levels of phosphate used, the equilibria would be shifted away from monomeric vanadate, whereas in sea water these moderately stable complexes would remain virtually fully dissociated.

Critical to achieving an understanding of the molecular mechanism of vanadium uptake is the rate of water transport produced by the tunicate. Knowing the water transport, or pumping, rate is useful in several biological applications¹²⁷⁾; it is, however, strictly unnecessary in evaluating uptake data. A knowledge of the transport rate is nevertheless required to ensure that analysis of vanadium uptake by tracer techniques measures assimilation and not an experimental artifact. A consideration of the dynamics of vanadium uptake begins, therefore, with water transport.

The processes of respiration and feeding depend on the transport of sea water through the tunicate body. Pumping need not be continuous, however, and has, in fact, been observed to be intermittent¹²⁸⁾. The values reported are therefore averages; the instantaneous value may be expected to be somewhat higher. The measurement technique may also affect the final value, and careful precautions have to be taken to avoid unrealistic, erroneous values^{129, 130)}. Larger transport rates will be produced by larger specimens. On a normalized, per gram wet weight basis, however, the average value is approximately 80 ml/hr/g wet weight for solitary, sessile

tunicates of gross weights in the range 1 to 100 g. To effect comparison with radio-vanadium uptake data for the widely distributed and studied species *Ciona intestinalis*, a member of the class Ascideacea, we shall use the value 50 ml/hr/g wet weight for this tunicate¹³¹).

The problem of how and where vanadium is recognized, adsorbed and assimilated is interesting and challenging. Of the several studies previously carried out, we cite in particular the investigations of Bielig, Rummel and coworkers for their extensiveness and thoroughness^{49, 132}). In this review we shall concentrate on a study of *Ciona* employing a more detailed data analysis in order to relate the uptake data to the molecular mechanisms of vanadate chelation¹³³).

For a small organism possessing a translucent outer skin and immersed in sea water, it is natural to question whether direct adsorption on this outer covering, or test, is possible. Partitioning experiments designed to answer this question systematically show that uptake occurs through the inhaled current and not through the test¹³³). The technique of radioisotope exchange can then be used to measure the rate of vanadium uptake by "tagging" the element with minute concentrations of a radioisotope, namely ⁴⁸V or ⁴⁹V.

It is well known, however, that the exchange of a radioisotope between two compartments always follows a first-order rate law *regardless of mechanism*¹³⁴). Thus, if we let V_A and V_A^* be vanadium and radiovanadium, respectively, in sea water; and V_B and V_B^* be vanadium and radiovanadium in the tunicate, then the exchange reaction can be represented by the reaction



The rate of exchange R (moles vanadium $l^{-1} h^{-1}$) and the total vanadium in each compartment, namely, $[V_A^*] + [V_A] = a$ and $[V_B^*] + [V_B] = b$ are constant during each experiment. Let the radiovanadium concentration in sea water at the end of a run when no further change is observable be denoted $[V_A^*]_\infty$, then the net rate is

$$-d[V_A^*]/dt = \beta_2([V_A^*] - [V_A^*]_\infty) \quad (1)$$

where $\beta_2 = R(a + b)/ab$. Upon integration, evaluation of the boundary conditions and rearrangement the following equation is obtained

$$y = \beta_1 e^{-\beta_2 t} + \beta_3 \quad (2)$$

where y is the relative activity of the radiovanadium remaining in solution ($y = \text{radioactivity at time, } t = t / \text{radioactivity at time, } t = 0$). The data and fit to Eq. (2) are shown in Fig. 3.

The meaning of each experimental parameter is now clear: β_2 (h^{-1}) is the apparent rate constant; $\beta_3 = y_\infty$, where y_∞ is relative radioactivity at infinite time; and $\beta_1 = 1 - y_\infty$. The apparent rate constant obtained from these data shows a variation reflecting the different masses of tunicates used in the experiments. This difference from experiment to experiment results in a variation of the ratio of absorption sites to volume of sea water. Constancy is exhibited when β_2 is divided by a

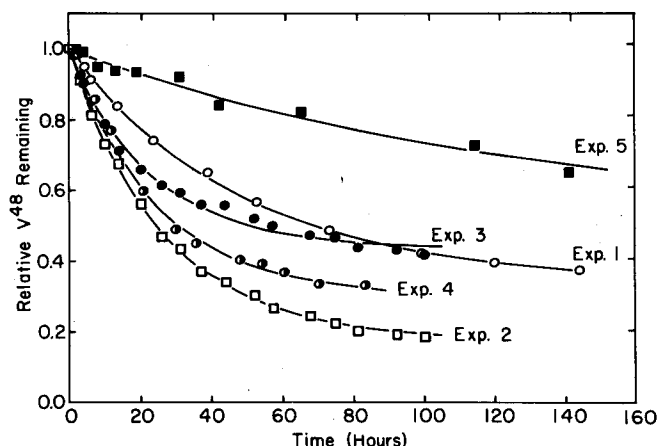


Fig. 3. Relative radioactivity remaining in solution vs. time for *Ciona intestinalis*. The smooth curves are drawn by a Cal Comp plotter to fit the expression $y = \beta_1 e^{-\beta_2 t} + \beta_3$. Experiment 1: 100-ml volume, four tunicates total wet mass 3.6 g, initial radioactive vanadium 0.835 μCi ; initial non-radioactive vanadium 3.4 ± 0.5 ppb. Experiment 2: 100-ml volume, four tunicates total wet mass 6.1 g, initial radioactive vanadium 0.042 μCi ; initial nonradioactive vanadium 4.1 ± 0.5 ppb. Experiment 3: 500-ml volume, four tunicates total wet mass 28.6 g, initial radioactive vanadium 0.170 μCi ; initial nonradioactive vanadium 4.1 ± 0.5 ppb. Experiment 4: 500-ml volume, two tunicates total wet mass 31.0 g, initial radioactive vanadium 1.142 μCi ; initial nonradioactive vanadium 3.4 ± 0.4 ppb. Experiment 5: 1,500-ml volume; 10 tunicates total wet mass 17.0 g, initial radioactive vanadium 2.12 μCi ; initial nonradioactive vanadium 2.8 ± 0.9 ppb

correction factor, f , derived below. The resultant value is $\beta_2/f = (6.5 \pm 0.7) \times 10^{-2} \text{ kg h}^{-1} \text{ kg}^{-1}$.

A lower limit of $\sim 0.1 \text{ h}^{-1}$ can be set for the intrinsic water transport rate constant¹³¹). This value is higher than any value of β_2 , for which the range in these studies was $0.007 < \beta_2 < 0.06 \text{ h}^{-1}$. Mixing of reagents (*viz.*, the passage of inhaled sea water over the vanadium binding sites) is therefore the more rapid of the two sequential processes, mixing and uptake. The radiovanadium studies can therefore be used to draw conclusions on the mechanism of uptake as β_2/f is determined by chemical factors.

The effect of vanadium concentration on uptake cannot be determined in natural sea water. Specimens of *Ciona* were therefore equilibrated for one week in sea water solutions of elevated vanadate concentrations. No deleterious effects were observed; no experimentally significant increase of vanadium in the tissues was observed, either. A $\ln\text{-}\ln$ plot of R/f vs $[V_A]$ is linear with slope 1. Therefore, under a thousandfold increase in vanadium concentration above the natural level in sea water, the uptake is first-order in vanadate concentration, showing no saturation.

A reaction scheme leading to exchange and consistent with these observations is



where L represents a binding site and $V_B L$ replaces V_B in the exchange reaction \underline{D} . In this simplified representation, vanadate is removed from sea water by attachment to a site, L, within the tunicate. Scheme \underline{E} does not, yet, represent the mechanism. First the general rate law for \underline{E}

$$R = k_1[V_A]^n[L]^q - k_{-1}[V_B L]^p \quad (3)$$

has to be evaluated.

Addition of tunicates to a closed sea water system represents addition of a "stock solution" of binding sites with concentration $[L]_0$. The actual concentration of binding sites available, $[L]$, can be thought of as a dilution of the total number of binding sites, $[L]_0 m_t$ (m_t is the tunicate mass) by the mass of sea water, m_s , in the experiment; *i.e.*, $[L] = [L]_0 m_t / m_s$, where both m_t and m_s are in kg units. Substitution into Eq. (3) yields.

$$R = k_1[V_A]^n([L]_0 f)^q - k_{-1}[V_B L]^p \quad (4)$$

where $f = m_t / m_s$. Under the conditions of these experiments, $[V_A^*] < [V_B^* L] \ll \ll [V_A] \ll [V_B L]$, and

$$R \cong \beta_2 [V_A] \quad (5)$$

Equating Eqs. (4) and (5) yields

$$\beta_2 [V_A] = k_1[V_A]^n([L]_0 f)^q - k_{-1}[V_B L]^p \quad (6)$$

We next eliminate $[V_B L]$ from Eq. (6). Conservation in the exchange reaction leads to the relation

$$[V_A^*]_\infty / [V_B L^*]_\infty = [V_A] / [V_B L] \quad (7)$$

From (7) and the definitions of f , β_1 and β_3 , we obtain the desired expression for $[V_B L]$; namely,

$$[V_B L] = \beta_1 [V_A] / \beta_3 f \quad (8)$$

Substitution of (8) into (6) yields

$$\beta_2 [V_A] = k_1[V_A]^n([L]_0 f)^q - k_{-1}(\beta_1 [V_A] / \beta_3 f)^p \quad (9)$$

As a working hypothesis we let $k_1[V_A]^n([L]_0 f)^q \gg k_{-1}(\beta_1 [V_A] / \beta_3 f)^p$. The experiments in natural abundance sea water ($[V_A] = \text{constant}$) show that β_2 is linearly proportional to f ; hence $q = 1$. If, then, $[V_A]$ is allowed to vary and $q = 1$, we have

$$R/f \cong \beta_2 [V_A] / f \cong k_1[V_A]^n [L]_0 \quad (10)$$

As mentioned above, the plot of $\ln(R/f)$ vs. $\ln[V_A]$ is linear¹³³, establishing that $n = 1$. These procedures justify the working hypothesis, and allow p to be determined.

Rearrangement of (9), with $n = 1$ and $q = 1$, leads to

$$\ln[V_A]f = c + p \ln(\beta_1[V_A]/\beta_3f) \quad (11)$$

where $c = \ln k_1 - \ln(k_1[L]_0 - \beta_2/f)$. A plot of equation (11) is linear with slope $p = 1$. Therefore, scheme D represents the mechanism of the reaction, and equation (6) becomes

$$\beta_2/f = k_1[L]_0 - k_{-1}\beta_1/\beta_3f^2 \quad (12)$$

Least squares analysis of (12) yields¹³⁴

$$k_1[L]_0 = 1.00 \pm 0.09 \text{ h}^{-1}$$

$$k_{-1} = (2.8 \pm 1.5) \times 10^{-4} \text{ h}^{-1}$$

The vanadium turnover time, T_V , in the experiment is given by $1/k_{-1}$; therefore, $T_V = 1/k_{-1} \sim 5 \text{ mo.}$

To assure internal consistency, an experiment was carried out with a "hot" tunicate. A specimen which had assimilated ^{48}V was transferred to unlabelled sea water, and the rate of radiovanadium exchange determined. The value $\beta_2/f = 0.33 \text{ kg h}^{-1} \text{ kg}^{-1}$ is in reasonably good agreement with the uptake value.

The physiology of ascidians has recently been reviewed¹³⁵, and no firm conclusion can yet be drawn for the function of the assimilated vanadium. From the uptake studies, however, we have a clearer picture of the initial stages of vanadium assimilation. A typical ascidian such as *Ciona* abstracts vanadate anion from sea water. The site of assimilation lies in the alimentary tract. Specimens dosed with sodium vanadate added to sea water extract vanadium according to mechanism D. As the vanadate concentration increases $\beta_3 \rightarrow 1$; consequently, the percentage of radiovanadium remaining in solution approaches unity, although the rate has not leveled off. The directly determined vanadium concentration in *Ciona* is $1 \times 10^{-4} \text{ mol/kg wet weight tunicate}$ ¹³³. From the kinetics study $[V_B L] = \beta_1[V_A]/\beta_3f \cong 4 \times 10^{-6} \text{ mol/kg wet weight tunicate}$ at the natural vanadium concentration level. Thus, only a small fraction of the accumulated vanadium is involved in the exchange process. The regulated uptake of vanadium displayed by *Ciona* can therefore be understood in terms of chelation or ion exchange at the assimilation site.

If assimilation occurs through chelation followed by membrane transport, model system rate constants may be applied to the uptake results. Some vanadate complex formation rate constants are known¹³⁶. For EDTA at pH 8.1 $k_1 = 133 \text{ M}^{-1} \text{ s}^{-1}$; for alizarin (1,2-dihydroxyanthraquinone) $k_1 = 1.0 \times 10^4 \text{ M}^{-1} \text{ s}^{-1}$. From the experimentally determined values of $k_1[L]_0$, we calculate $[L]_0 \sim 2.8 \times 10^{-8} \text{ M}$ for an alizarin-like chelating agent and $[L]_0 \sim 2.1 \times 10^{-6} \text{ M}$ for an EDTA-like chelating agent at pH 8. If generation of binding sites is a limiting factor in assimilation, then

mechanism E favors strongly basic chelating agents (perhaps derivatives of catechol, as is alizarin), for which fewer binding sites are necessary.

Ions added to sea water by natural processes exceed man's input, with few exceptions. Harbor and estuarine waters, however, are sites potentially capable of sustaining significant increases in many metal ion concentrations due to pollution. The effect of non-essential ions on living systems will be to select against those individuals in a population which are incapable of handling the stress caused by the increased concentration perturbation. If the conditions persist, the — usually — toxic metal ion will be passed upwards in the food chain at higher concentrations than before. Toleration by individuals of this increased dose will vary; the effects on man will probably range from uncomfortable to hazardous.

Pollution by essential metal ions poses a different problem. Not yet understood are the effects of greater availability of nutrient metal ions on development, growth, size, reproductive rates, etc. Since the chances for appreciable change in the levels of essential metal ion concentrations increase each year — for example, with vanadium, which is abundant in many petroleum oils — the often subtle interactions between metal ions and living organisms deserve further careful study.

Acknowledgments. The authors wish to acknowledge the unpublished work of Drs. T. Gilbert and R. Langton (New England Aquarium) on bivalve molluscs, and of Drs. R. Stolzberg and N. Morel (New England Aquarium) on copper-ligand algae interactions, which are used as examples in the text. The example of tunicate incorporation and assimilation of vanadium is from the work of the authors (National Science Foundation Grant No GB 3361 J) with the collaboration of Drs. K. V. Ladd and D. Toppen.

VI. References

- 1) Underwood, E. J.: Trace elements in human and animal nutrition. 3rd edit. New York: Academic Press 1971.
- 2) Fitzgerald, W. F., Hunt, C. D.: *J. Rech. Atmos.* 1974, 629.
- 3) Goldberg, E.: Minor elements in sea water. In: Riley, Chemical oceanography. Riley, J. P., Skirrow, G. (eds.). London: Academic Press, 1965; vide for earlier references.
- 4) Weiss, H., Koide, M., Goldberg, E. D.: *Science* 175, 962 (1971).
- 5) Fitzgerald, W. F., Lyons, W. B.: *Nature* 242, 452 (1973).
- 6) Alexander, J. E., Corcoran, E. F.: *Limnol. Oceanogr.* 12, 236 (1967).
- 7) Fabricand, B. P., Sawyer, R. R., Ungar, S. G., Adler, S.: *Geochim. Cosmochim. Acta* 26, 1023 (1962).
- 8) Chow, T. J., Earl, J. L.: *Science* 169, 577 (1970).
- 9) Chow, T. J., Patterson, C. C.: *Earth Planet. Sci. Lett.* 1, 397 (1966).
- 10) Murozumi, M., Chow, T. J., Patterson, C. C.: *Geochim. Cosmochim. Acta* 33, 1247 (1969).
- 11) Horne, R. A.: *Marine chemistry*. New York: Wiley-Interscience 1969.
- 12) Brewer, P. G., Spencer, D. W., Robertson, D. E.: *Earth Planet. Sci. Lett.* 16, 111 (1972).
- 13) Vaccaro, R. F., Grice, G. D., Rowe, G. T., Wiebe, P. H.: *Water Research* 6, 231 (1972).
- 14) Spencer, D. W., Sachs, P. L.: *Marine Geology* 9, 117 (1970).
- 15) Curl, Jr., H., Cutshall, N., Osterberg, C.: *Nature* 205, 275 (1965).
- 16) Cutshall, N., Johnson, V., Osterberg, C.: *Science* 152, 202 (1966).
- 17) Fukai, R.: *Nature* 213, 901 (1967).
- 18) Chuecas, L., Riley, J. P.: *Anal. Chim. Acta* 35, 240 (1966).
- 19) Elderfield, H.: *Earth Planet. Sci. Lett.* 9, 10 (1970).
- 20) Ladd, K. V.: Ph. D. Thesis, Brandeis University, Waltham, Massachusetts 02154, U.S.A.
- 21) Sillén, D. L.: *Chemical equilibrium in analytical chemistry*. New York: Wiley-Interscience 1962.
- 22) Gibbs, R. J.: *Science* 180, 71 (1973).
- 23) Kharkar, D. P., Turekian, K. K., Bertine, K. K.: *Geochim. Cosmochim. Acta* 32, 285 (1968).
- 24) Johnson, V., Cutshall, N., Osterberg, C.: *Water Resources Res.* 3, 99 (1967).
- 25) Gilbert, T. R., Clay, A. M.: New england aquarium, unpublished results.
- 26) Knauer, G. A., Martin, J. H.: *Limnol. Oceanogr.* 18, 597 (1973).
- 27) Morris, A. W.: *Nature* 233, 427 (1971).
- 28) Bryan, G. W.: *J. Mar. Biol. Ass. U. K.* 53, 145 (1973).
- 29) Gilbert, T. R., Leighty, D. A.: New england aquarium, unpublished results.
- 30) Radioactivity in the Marine Environment. N.A.S. Publications, Washington, D.C., 1971.
- 31) Menzel, D. W., Spaeth, J. P.: *Limnol. Oceanogr.* 7, 155 (1962).
- 32) Spencer, D. W., Brewer, P. G.: *Geochim. Cosmochim. Acta* 33, 325 (1969).
- 33) Eigen, M.: *Ber. Bunsenges. Physik. Chem.* 67, 753 (1963).
- 34) Kustin, K., Swinehart, J.: *Progr. Inorg. Chem.* 13, 107, (1970).
- 35) Wilkins, R. G.: The study of kinetics and mechanism of reactions of transition metal complexes. Boston: Allyn and Bacon, Inc. 1974.
- 36) Langford, C. H., Sastri, V. S.: *Reaction mechanisms in inorganic chemistry*, London: Butterworths 1972, p. 203–267.
- 37) Dasgupta, T. P.: *Reaction mechanisms in inorganic chemistry*. London: Butterworths 1974, p. 63–91.
- 38) Hague, D. N.: *Inorganic reaction mechanisms*, Vol. 3. London: Specialist Periodical Report, The Chemical Society 1974, p. 261–296.
- 39) Hughes, M. N.: *Reaction mechanisms in inorganic chemistry*. London: Butterworths 1974, p. 327–364.
- 40) Sigel, H.: *Metal ions in biological systems*, Vol. 1,5. New York: M. Dekker 1974.
- 41) Eichhorn, G. L.: *Inorganic biochemistry*. Elsevier: Amsterdam 1973.
- 42) Langford, C. H., Gray, H. B.: *Ligand substitution processes*. New York: Benjamin 1965.
- 43) Kruse, W., Thusius, D.: *Inorg. Chem.* 7, 250 (1968).
- 44) Baker, B. K., Orhanovic, M., Sutin, N.: *J. Amer. Chem. Soc.* 89, 722 (1967).

- 45) Wütrich, K., Connick, R. E.: *Inorg. Chem.* 6, 583 (1967); *Inorg. Chem.* 7, 1377 (1968).
- 46) Tomiyasu, H., Gordon, G.: *Inorg. Chem.* 15, 870 (1976).
- 47) Cotton, F. A., Wilkinson, G.: *Advanced inorganic chemistry*. 3rd edit. New York: Interscience 1972, p. 821.
- 48) Dean, G. A., Herringshaw, J. F.: *Talanta* 10, 793 (1963).
- 49) McLeod, G. C., Ladd, K. V., Kustin, K., Toppen, D. L.: *Limnol. Oceanogr.* 20, 491 (1975).
- 50) Ref. 47): p. 836 for Cr(III); p. 657 for Cr(II).
- 51) Stumm, W., Morgan, J. J.: *Aquatic chemistry*. New York: Wiley 1970, p. 534–538.
- 52) Stranks, D. R., Swaddle, T. W.: *J. Amer. Chem. Soc.* 93, 2783 (1971).
- 53) Koren, R., Perlmutter-Hayman, B.: *Inorg. Chem.* 11, 3055 (1972).
- 54) Kustin, K., Kirschenbaum, L. K.: *J. Chem. Soc. (A)*, 1970, 684.
- 55) Feltch, S. M., Stuehr, J. E., Tin, G. W.: *Inorg. Chem.* 14, 2175 (1975).
- 56) Eigen, M., Wilkins, R. G.: *Mechanisms of inorganic reactions*. In: *Advances in chemistry*, Vol. 49. Gould, R. F. (ed.). Washington, D. C.: American Chemical Society 1955, p. 55.
- 57) Eigen, M., Eyring, E. M.: *Inorg. Chem.* 2, 636 (1963).
- 58) Eigen, M., Geier, G., Kruse, W.: *Essays in coordination chemistry*. Schneider, W., Anderegg, G., Gut, R. (eds.). Basel: Birkhauser 1964, p. 164.
- 59) Muirhead, K. A., Haight, Jr., G. P., Beattie, J. K.: *J. Amer. Chem. Soc.* 94, 3006 (1972).
- 60) Lin, C.-t., Beattie, J. K.: *J. Amer. Chem. Soc.* 94, 3011 (1972).
- 61) Haim, A.: *Inorg. Chem.* 11, 3147 (1972).
- 62) Knowles, P. F., Diebler, H.: *Trans. Faraday Soc.* 84, 977 (1968);
Diebler, H., Timms, R. E.: *J. Chem. Soc. (A)*, 1971, 273.
- 63) Kustin, K., Liu, S.-t.: *J. Amer. Chem. Soc.* 95, 2487 (1973);
Honig, D. S., Kustin, K.: *J. Amer. Chem. Soc.* 95, 5525 (1973);
Kustin, K., Liu, S.-t.: *Inorg. Chem.* 12, 2362 (1973);
Gilbert, K., Kustin, K.: *J. Amer. Chem. Soc.* 98, 5502 (1976).
- 64) Kustin, K., Toppen, D. L.: *J. Amer. Chem. Soc.* 95, 3564 (1973).
- 65) Honig, D. S., Kustin, K.: *J. Phys. Chem.* 76, 1575 (1972).
- 66) Vold, R. R., Vold, R. L.: *J. Magn. Reson.* 19, 365 (1975).
- 67) Cruywagen, J. J., Rohwer, E. F. C. H.: *Inorg. Chem.* 14, 3136 (1975).
- 68) Kunin, R.: *Ion exchange resins*. 2nd edit. New York: John Wiley 1958, p. 17–24.
- 69) Jones, R. F.: *Limnol. Oceanogr.* 5, 312 (1960).
- 70) Rice, S. A., Nagasawa, M.: *Polyelectrolyte solutions*. New York: Academic Press 1961, p. 461–486.
- 71) Forth, W., Rummel, W.: *Physiol. Rev.* 53, 724 (1973).
- 72) Amdur, I., Hammes, G. G.: *Chemical kinetics*. New York: McGraw-Hill 1966, p. 170.
- 73) Lipscomb, W. N.: *Tetrahedron* 30, 1725 (1974).
- 74) Weber, G.: *Adv. Prot. Chem.* 29, 1 (1975).
- 75) Grell, E., Funck, T., *J. Supramolec. Str.* 1, 3076 (1973).
- 76) Hlodky, S. B., Gordon, L. G. M., Haydon, D. A.: *Ann. Rev. Phys. Chem.* 25, 11 (1974).
- 77) Martin, D.: *Equilibrium concepts in natural water systems*. In: *Advances in chemistry*, Vol. 67. R. F. Gould (ed.). Washington, D. C.: American Chemical Society 1967, p. 255.
- 78) Yentsch, C. M., Cole, E. J., Salvaggio, M. G.: *Proc. 1st Internatl. Conf. Toxic Dinoflagellate Blooms*, V. R. LoCicero, (ed.). Boston: Mass. Sci. and Tech. Found 1975, p. 164.
- 79) Provasoli, L., McLaughlin, J., Droup, M.: *Archiv. für Mikrobiologie* 25, 392 (1957).
- 80) Barber, R. T.: *Trace metals and metal-organic interactions in natural waters*. P. C. Singer (Ed.). Ann Arbor: Sci. Publ. 1973, p. 321.
- 81) Smayda, T. J.: *Limnol. Oceanogr.* 19, 889 (1976).
- 82) Barber, R. T., Ryther, J. H.: *J. Exper. Mar. Bio. Ecol.* 3, 191 (1969).
- 83) Davey, E. W., Morgan, M. J., Erickson, S. J.: *Limnol. Oceanogr.* 18, 993 (1973).
- 84) Horne, A. J., Goldman, C. R.: *Science* 183, 409 (1974).
- 85) Steemann Nielsen, E., Wium-Andersen, S.: *Mar. Biol.* 6, 93 (1970).
- 86) Erickson, S. J., Lackie, N., Maloney, T. E.: *J. Water Pollut. Contr. Fed.* 42, R271 (1970).
- 87) Manahan, S. E., Smith, M. J.: *Environ. Technol.* 7, 829 (1973).
- 88) Steemann Nielsen, E., Wium-Andersen, S.: *Physiol. Plant.* 24, 480 (1971).
- 89) Steemann Nielsen, E., Wium-Andersen, S.: *Verh. Internat. Verein. Limnol.* 18, 78 (1972).

- 90) Steemann Nielsen, E., Kamp-Nielsen, L., Wium-Andersen, S.: *Physiol. Plant.* 22, 1121 (1969).
- 91) Gross, R. E., Pungno, P., Dugger, W.: *Plant Physiol.* 46, 183 (1970).
- 92) McBrien, D. C. H., Hassal, K. A. *Physiol. Plant.* 18, 1059 (1967).
- 93) Neilands, J. B.: *Science* 156, 1443 (1967).
- 94) Hassal, K.: *Physiol. Plant.* 16, 323 (1963).
- 95) Gutknecht, J.: Ph. D. Thesis, p. 29–35 and p. 67–72, University of North Carolina, Chapel Hill, North Carolina, U.S.A. 1964.
- 96) Clark, J. S., Turner, R. C.: *Soil Sci.* 107, 4 (1969).
- 97) Davies, C., Hartley, R. D., Lawson, G. J.: *J. Chromatogr.* 18, 47 (1965).
- 98) Smith, R. G.: *Anal. Chem.* 48, 74 (1967).
- 99) Rossotti, H.: *Talanta* 21, 809 (1974).
- 100) Lewin, J. C.: *J. Gen. Physiol.* 37, 589 (1954).
- 101) Steemann Nielsen, E., Kamp-Nielsen, L.: *Physiol. Plant.* 23, 828 (1970).
- 102) Walker, J.: *Arch. Biochem. Biophys.* 46, 1 (1953).
- 103) Manahan, S., Smith, M.: *Anal. Chem.*, 7, 829 (1973).
- 104) Eyster, C.: *Algae and man.* D. F. Jackson (Ed.). New York: Plenum Press 1964, p. 86.
- 105) Rabinowitch, E., Govindjee: *Photosynthesis.* New York: John Wiley 1964, p. 193–194.
- 106) Geltsoff, P. S.: U. S. Fish and Wildlife service, *Fishery Bulletin* 64, 1964.
- 107) Schulz-Baldes, M.: *Mar. Biol.* 25, 177 (1974).
- 108) Preston, A., Jefferies, D. F.: *Environmental contamination by radioactive materials.* Vienna: International Atomic Energy Agency 1969, p. 183–211.
- 109) Preston, E. M.: *J. Exp. Mar. Biol. Ecol.* 6, 47 (1971).
- 110) Brown, B. F., Newell, R. C.: *Mar. Biol.* 16, 108 (1972).
- 111) Bernard, F. R.: *Biol. Bull.* 146, 1 (1974).
- 112) Schlieper, C., Kowalski, R.: *Kieler Meeresforsch.* 14, 114 (1958).
- 113) Flugel, H., Schlieper, C.: *Kieler Meeresforsch.* 18, 51 (1962).
- 114) Theede, H.: *Kieler Meeresforsch.* 19, 20 (1963).
- 115) Thompson, R. J., Bayne, B. L.: *J. Exp. Mar. Biol. Ecol.* 9, 111 (1972).
- 116) Davidr, C.: *Neth. J. Sea Res.* 2, 233 (1964).
- 117) Bayne, B. L.: *Proc. 9th Europ. Mar. Biol. Symp.*, H. Barnes (ed.). Aberdeen University Press. 1975, p. 213–238.
- 118) White, R. J. Jr.: M. A. Thesis, Northeastern University, Boston, Massachusetts, U.S.A. 1972.
- 119) Brown, B. F., Newell, R. C.: *Mar. Biol.* 16, 108 (1972).
- 120) LaRoche, G., Gardner, G. R., Eisler, R., Jackim, E. H., Yevich, P. P., Zaroogian, G. E.: *Bioassay Tech. Environ. Chem.* 1973, p. 199–216.
- 121) Reid, R. G. B.: *Proc. Zool. Soc. Lond.* 142, 156 (1965).
- 122) Veldhuijzen, J. P.: *Neth. J. Zool.* 24, 10 (1974).
- 123) Walker, G.: *Proc. Malac. Soc. Lond.* 40, 33 (1972).
- 124) Foster-Smith, R. L.: *J. Mar. Biol. Ass. U. K.* 55, 411 (1975).
- 125) Thompson, R. J., Bayne, B. L.: *Mar. Biol.* 27, 317 (1974).
- 126) Bielig, H.-J., Jost, E., Pflieger, K., Rummel, W.: *Hoppe-Seyler's physiol. Chemie* 325, 132 (1961);
Bielig, H.-J., Pflieger, K., Rummel, W., Seifen, E.: *Hoppe-Seyler's physiol. Chemie* 327, 35 (1961);
Rummel, W., Bielig, H.-J., Forth, W., Pflieger, K., Rudiger, W., Seifen, E.: *Protides of the Biological Fluids* 14, 205 (1966).
- 127) Jørgensen, C. B.: *Biol. Rev.* 30, 391 (1955).
- 128) Mangum, C., Van Winkle, W.: *Amer. Zool.* 13, 529 (1973).
- 129) Hamevi, H., Haskins, H. H.: *Science* 163, 823 (1969).
- 130) Holmes, N.: *J. Exp. Mar. Biol. Ecol.* 11, 1 (1973).
- 131) Kustin, K., Ladd, K. V., McLeod, G. C., Toppen, D. L.: *Biol. Bull.* 147, 608 (1974).
- 132) Bielig, H.-J., Jost, E., Pflieger, K., Rummel, W., Seifen, E.: *Hoppe-Seyler's Zeitschrift f. physiol. Chemie* 325, 122 (1961);
Bielig, H.-J., Pflieger, K., Rummel, W., Seifen, E.: *Hoppe-Seyler's Zeitschrift f. physiol. Chemie* 326, 249 (1961).
- 133) Kustin, K., Ladd, K. V., McLeod, G. C.: *J. Gen. Physiol.* 65, 315 (1975).

- 134) Frost, A. A., Pearson, R. G.: Kinetics and mechanism. 2nd edit. New York: John Wiley 1961, p. 192–193.
- 135) Goodbody, I.: *Adv. Mar. Biol.* 12, 1 (1974).
- 136) Kustin, K., Toppen, D. L.: *J. Amer. Chem. Soc.* 95, 3564 (1973).

Received August 17, 1976

Inorganic Metabolic Gas Exchange in Biochemistry

Priv. Doz. Dr. Gernot Renger

Max Volmer Institut für Physikalische Chemie und Molekularbiologie der Technischen Universität Berlin, D-1000 Berlin 12, Germany

Table of Contents

1.	Introduction	41
2.	The Overall Counterbalance Reaction of Autotrophic and Heterotrophic Organisms	42
3.	The Role of Ozone as Atmospheric UV-Shield	44
4.	Metabolic Processes in Autotrophic Organisms Involving Gaseous Compounds	46
4.1.	The Carbon Dioxide Reduction in the Stroma Region	46
4.1.1.	Carbon Dioxide Transport to the Biocatalysts Responsible for CO ₂ -Fixation	48
4.1.2.	The Chemical Reactions at the Biocatalysts Leading to CO ₂ -Fixation	50
4.2.	The Oxygen Evolution in the Thylakoid Region	51
4.2.1.	The Photoelectric Generators of Photosynthesis	52
4.2.2.	The Watersplitting Enzyme System	56
4.2.3.	The Reduction of NADP ⁺ and the Possibility of the Evolution of Molecular Hydrogen	64
4.2.4.	Properties of the Electron Transport Chain of the Primary Processes of Photosynthesis	66
4.2.5.	The ATP-Synthesizing System	67
4.3.	Non-oxygen Evolving Autotrophic Organisms	68
5.	Nitrogen Fixation	69
6.	Metabolic Processes in Heterotrophic Organisms Involving Gaseous Compounds	73
6.1.	Thermodynamic and Kinetic Properties of Molecular Oxygen	74
6.2.	The Protection of Biosystems to Toxic Attack by Oxygen	76

In memoriam to my parents († 28. 8. and 20. 9. 1975)

6.3.	Oxygen Transport Systems	77
6.4.	The Metabolic Chemical Reactions of O ₂	80
6.4.1.	The Decarboxylations Leading to the Formation of Metabolically Bound Hydrogen	80
6.4.2.	The Oxidation of Metabolically Bound Hydrogen to Water.. . . .	81
7.	Conclusions	83
8.	References	85

1. Introduction

In a rough simplification terrestrial life can be considered as the chemistry of proteins, existing either in an aqueous phase (globular proteins) or in a membrane bound form with a lipidic surrounding. Proteins are composed mainly of 5 elements: carbon, hydrogen, oxygen, nitrogen and to a minor degree of sulfur. The ultimate substrates for the synthesis of proteins in the biosphere are rather simple molecules like water, carbon dioxide, molecular oxygen and nitrogen and minerals. Accordingly gas exchange reactions play a fundamental role in the chemistry of the biological world. Gaseous compounds either enter as substrates into the complex reaction sequences of metabolic processes or release them as terminal products. The metabolism of a biological organism is the interconnection of a huge number of elementary reactions under highly controlled conditions.

Biological organisms are thermodynamically unstable systems^{a)}. Their formation and growing represents an increase of order and thus a local entropy decrease arises. Hence, biological systems must necessarily be open systems requiring an external source of free energy for their development and sustenance. According to the realization of this fundamental free energy requirement all biological systems can be subdivided into two categories:

- a) *Autotrophic* organisms which are able to use extraterrestrial solar radiation energy via the process of photosynthesis.
- b) *Heterotrophic* organisms using exclusively terrestrial free energy sources via oxidative processes of food "combustion".

Since food consumed by heterotrophic organisms originates from autotrophs, photosynthesis is the prerequisite for the existence of the terrestrial biosphere, as already pointed out by Boltzmann in 1886²⁾.

Energetics and kinetics of gaseous reactions are determined by parameters like temperature and pressure. Proteins are sensitive to thermal degradation and to high pressure gradients. Therefore, in contrast to the well-known technical processes (e.g. nitrogen fixation by Haber-Bosch-method, see Ref.⁶⁾, biological reactions can be realized only in a narrow range of reaction parameters (temperature, pressure gradients). The unique tool available to biological systems for the performance of different reactions under controlled conditions is the application of highly advanced catalytic techniques.

Accordingly, two different types of events have to be distinguished:

- a) the transport of the reactants to the catalytic sites occurring mainly via diffusion processes and
- b) the chemical reaction mechanism at the catalytic sites itself.

It must be emphasized that according to Darwins theory evolution leads – by the process of mutation and selection – to the "survival of the fittest". Hence, biological systems and their functional elements can be expected to be extremely highly specialized and optimized for the problems they have to solve. It is therefore a very interesting task to search for the "ingenueous solutions" which nature has

a) According to Morowitz¹⁾ the free energy of nonaqueous cell constituents is on average 0.27 eV per atom above the thermodynamic equilibrium.

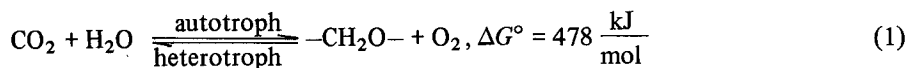
“found” by trial and error for the realization of a special problem. In this sense, this article will not only give a description of some biochemical reaction schemes and biological principles, but in addition it will try to evoke an interest for the extraordinary elaboration and interdigitation of complex reaction sequences in the biological world, leading to dynamic quasi equilibrium states^{b)}.

The above mentioned considerations indicate that for an understanding of metabolic gas exchange reactions a thorough knowledge is required for both, the chemistry of the process and the function and structure of the special “reaction vessel” developed for its realization.

It is not possible to provide here a complete survey of all metabolic processes including gaseous molecules. Thus, a few examples will be selected for a broader description of the functional principles of biological systems including gaseous compounds either as substrates or as products. As photosynthesis appears to be the indispensable prerequisite for the evolution and sustenance of the present stage of life this process will represent the main part of the following paper.

2. The Overall Counterbalance Reaction of Autotrophic and Heterotrophic Organisms

In a first order approximation the earth can be envisaged to be a nearly isolated system in regard to material fluxes, but an open system for energy fluxes. Therefore, any netto increase of the biomass has to be counterbalanced by a decrease in the mass of nonbiological components. However, the netto increase is negligibly small^{c)}. Hence, with respect to the materials of the biosphere there exists practically a dynamic terrestrial equilibrium state (see Fig. 1), whereas, the processes occurring in the biosphere are energetically driven ultimately by extraterrestrial solar radiation. The dynamic equilibrium-like state of materials is the result of a long evolutionary process. At the present stage nearly all of the photoautotrophic organisms are oxygen evolving and carbon dioxide consuming systems (for exceptions see 4.3.), whereas the heterotrophic organisms are oxygen consuming and carbon dioxide evolving systems (for exceptions see 6.4.2). Hence, the fundamental overall reaction of the autotrophic organisms is the photosensitized formation of carbohydrates from CO₂ and H₂O:



b) Because of significant changes during geological periods there does not exist a true dynamic equilibrium. However, neglecting small range oscillatory changes, in a first approximation quasi equilibrium states can be assumed to exist for comparatively short times of some thousand years.

c) It has been estimated that the total mass of all fossil fuels generated by photosynthesis during mega years corresponds to the total amount of reaction products produced by all present photosynthetic organisms in only about 100 years³⁾.

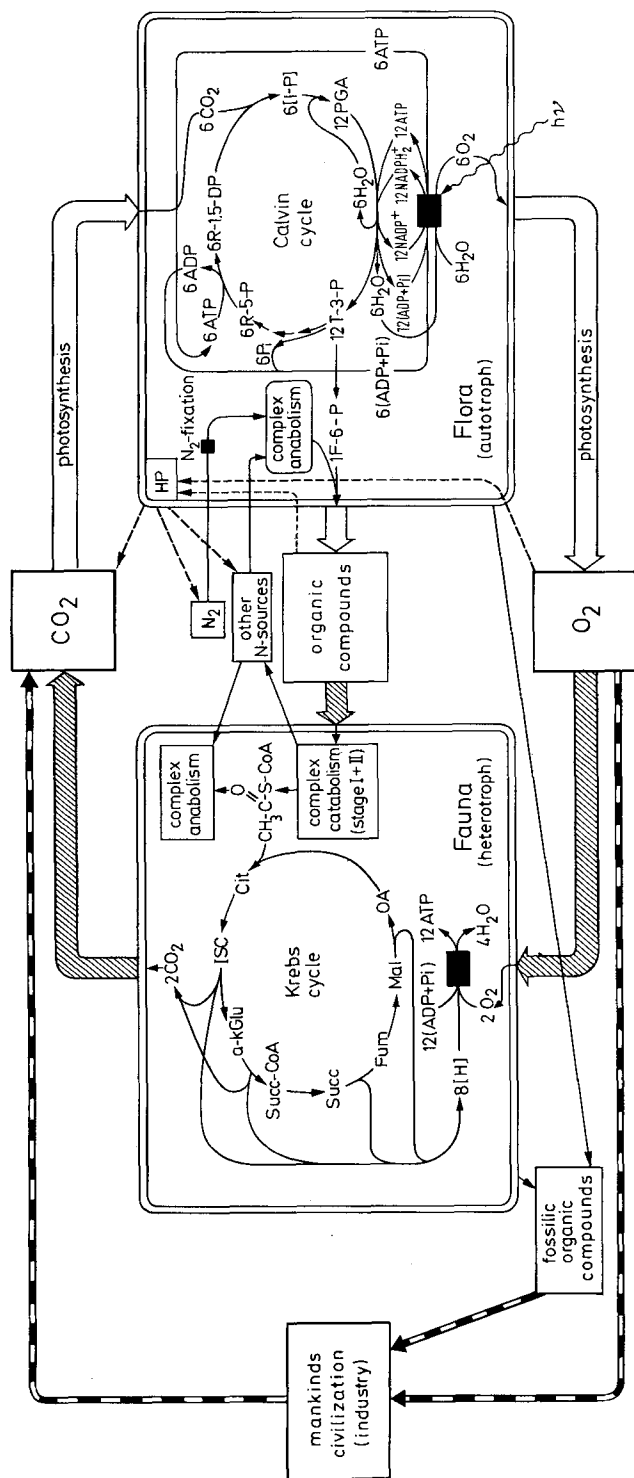


Fig. 1. Scheme of the main biological processes including gaseous compounds. The thickness of the arrows represents roughly the quantitative turnover of the corresponding processes (except mankind activity being overrepresented). The big black boxes symbolize the membrane systems containing the centers of biotrophic organisms in higher autotrophic (thylakoid system) and heterotrophic (mitochondrial inner membrane system) organisms, respectively. Some activities of primitive organisms have been omitted for the sake of clarity. The following abbreviations are used: ADP = adenosine diphosphate, ATP = adenosine triphosphate, P_i = inorganic phosphate.

Flora: F-6-P = fructose-6-phosphat, $\text{NADP}^+/\text{NADPH}_2$ = nicotinamide adenosindinucleotide phosphate in oxidized and reduced form (under physiological conditions NADPH_2 is deprotonized into $\text{NADP} + \text{H}^+$), PGA = phosphoglyceric acid, R-5-P = ribulose-5-phosphate, R-1,5-DP = ribulose-1,5-diphosphate, T-3-P = triose-3-phosphate, I-P = primary intermediary product of CO_2 bonding. HP symbolizes heterotrophic processes (e.g. respiratory activity) occurring in autotrophic organisms.

Fauna: α -Kglu = α -ketoglutarate, Cit = citrate, Fum = fumarate, [H] = metabolically bound hydrogen, ISC = isocitrate, Mal = malate, OA = oxaloacetate, Succ = succinate, Suco-CoA = succinate Bound to coenzyme A

where $-\text{CH}_2\text{O}-$ represents a stoichiometric unit of carbohydrates. On the other hand, the fundamental overall reaction of the heterotrophic organisms is the "cold combustion" (see Chapter 6) of carbohydrates, *i.e.* the reversal of reaction (1).

Therefore, the most important overall processes of the biological systems include the gases CO_2 and O_2 (see Fig. 1). The overall turnover rate of these processes is of the order of 300–500 giga-tons CO_2 per annum^{4, 5)}. It should be noted that now a point could be reached where the natural dynamic equilibrium-like state becomes slowly shifted towards CO_2 by the work of man. Beyond the main CO_2 – O_2 -cycle there exist further metabolic reactions including other gaseous molecules like N_2 or H_2S . The overall turnover rate of these processes is small in comparison to that of the CO_2 – O_2 -reactions (see 4.3. and 5.).

In addition to the gaseous compounds directly participating in the metabolic processes there exists one gaseous species which plays a unique role for the existence of biological organisms on the earth surface: ozone. This molecule provides an indispensable atmospheric shield to ultraviolet radiation. Hence, it seems to be worthwhile first of all to discuss briefly the protective role of ozone before going into details about the metabolic processes involving gaseous compounds and the biological apparatus, by which these reactions are performed.

3. The Role of Ozone as Atmospheric UV-Shield

Ozone is one of the strongest oxidizing compounds (the system $\text{O}_2 + \text{H}_2\text{O} \rightleftharpoons \text{O}_3 + 2 \text{H}^+ + 2e$ has a normal redox potential of + 2.07 V⁶⁾) and therefore acts as a poison for biological systems⁷⁾. Hence, ozone is not included into the metabolic processes of the biosphere. On the other hand, ozone is an indispensable prerequisite for the existence of biological systems on the earth surface. The solar irradiation impinging on the gaseous terrestrial atmosphere contains a significant part of UV-irradiation, see Fig. 2, left⁸⁾. Biological macromolecules (DNA, proteins) are quite sensitive to UV-irradiation^{d)} of the wavelength range of 200–300 nm^{8a)}. Hence, for the viability of biological systems – especially under aerobic conditions – the existence of a suitable UV-shield is required. Since water absorbs UV-irradiation and because the atmosphere was rather anaerobic^{e)} a specific UV-shield was not necessary for the first primitive biological organisms developed in the urocean. Hence, the phylogenetic evolution could begin in the oceans without a specific atmospheric UV-shield. However, for the population of the earth surface with biological systems in an aerobic environment the development of a suitable UV-shield in the atmosphere was an indispensable prerequisite.

d) UV is especially harmful under aerobic conditions, because it catalyzes harmful biological oxidations in the presence of oxygen.

e) The steady state concentration of O_2 due to nonbiological processes of O_2 -formation and consumption giving rise to "Urey point" was estimated to have been rather low^{9, 10)}.

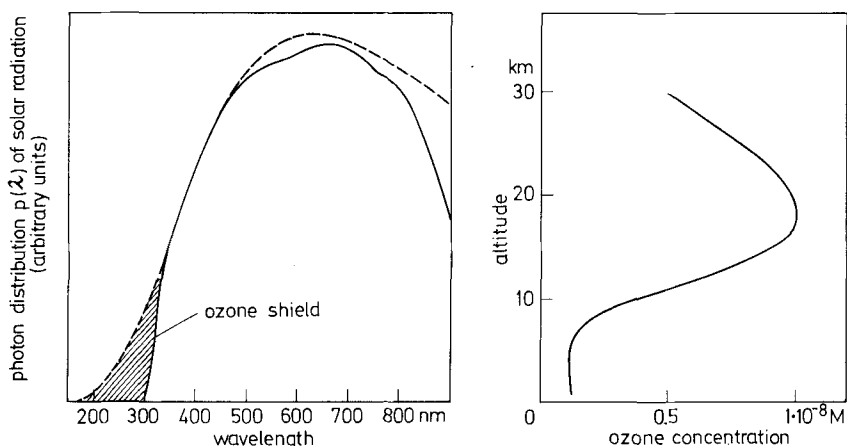


Fig. 2. Ozone effect on solar radiation (left) and dependence of ozone concentration on atmospheric altitude (right). In the left part the dotted curve represents the photon distribution of solar energy outside the atmosphere (based on the assumption of black body radiation at $T = 5773$ K). The full curve gives the photon distribution of solar radiation reaching earth surface (see Ref.⁸). The ozone effect is shown by shadowed area, the decline above 800 nm is mainly due to absorption by water vapour. On the right side the full curve represents qualitatively a typical ozone profile, the real ozone distribution significantly depends on the local situation (geography), see Ref.¹⁵

With the development of oxygen evolving bluegreen algae about two to three gigayears ago^{11, 12}) the practically oxygen free atmosphere became more and more oxygenic until the present concentration has been reached (see 4.2.). However, at the same time photoreactions of atmospheric oxygen led to the formation of ozone which acts now as the unique protective shield to solar UV-irradiation. This effect is shown in Fig. 2 (left side).

The ozone content of the atmosphere is held nearly constant by a dynamic equilibrium determined by the rates of formation and destruction, respectively.

The ozone formation occurs nearly exclusively via the photo-induced generation of oxygen atoms and a subsequent triple impact process:



M represents a particle which is required for the energy uptake liberated by the reaction between O and O_2 ($\Delta H^\circ = -144 \text{ kJ/mole}^\text{f}$) in order to prevent the instantaneous dissociation of the just synthesized ozone molecule⁶).

The ozone destruction is mainly caused by its own photolysis (Chapman-mechanism,¹³):

^f) It is now stipulated to use the "Joule" (abbrev. J) as energy unit instead of calorie (1 cal $\hat{=}$ 4.184 J). Hence, in the following the unit J will be used.



But, in addition traces of water, of different nitrogen oxides and of organic components catalyze the destruction of ozone via a radical mechanism (for rev. see Ref.¹⁴⁾).

The parameters which influence the ozone formation and destruction (e.g. UV-radiation intensity, oxygen partial pressure and total pressure) are not constant throughout the atmosphere. Therefore, the ozone density varies with the altitude of the atmospheric level in a characteristic pattern with a significant maximum in the range of 15–25 km above the earth surface (see Fig. 2 right).

Because of the catalytic effect of some impurities, the atmospheric ozone equilibrium is very sensitive to pollution of the atmosphere. Therefore, taking into account the role of ozone as a protective shield to UV-damaging, air pollution could become a serious danger for all biological systems living on the earth¹⁶⁾.

4. Metabolic Processes in Autotrophic Organisms Involving Gaseous Compounds

Photosynthesis of most algae and higher plants occurs within the cells in highly specialized organelles, the chloroplasts. In Fig. 3 the principal hierarchy of structural and functional organization of photosynthesis in a mature plant leaf is shown. It is apparent that the chloroplasts are structurally subdivided into two main regions: a) *stroma* region and b) *thylakoid* region. The pioneering work of Blackman¹⁷⁾, of van Niel¹⁸⁾ and of R. Hill¹⁹⁾ led to the conclusion that generally two different types of processes take place: a) reactions (resp. reaction sequences) requiring light as indispensable driving force and b) dark reactions (resp. reaction sequences). It has been shown that the structural compartmentation of the chloroplasts also includes the functional separation of the overall reaction described by Eq. (1) into two different main reaction sequences, namely, the so-called “*primary processes*”,^{g)} requiring light which are located in the thylakoid system and the so-called “*secondary processes*”, being independent of light, occurring in the stroma region (see Fig. 3).

4.1. The Carbon Dioxide Reduction in the Stroma Region

In the stroma region, a liquid aqueous phase containing water soluble globular enzymes, the carbon dioxide is reduced to carbohydrates. The reduction needs an ap-

^{g)} It should be emphasized that the term “primary processes”, widely used in the literature for the reaction sequence leading to the light induced electron transport from water to NADP^+ (see 4.2.), not only includes pure photochemical reactions, but also a number of dark electron transfer reactions.

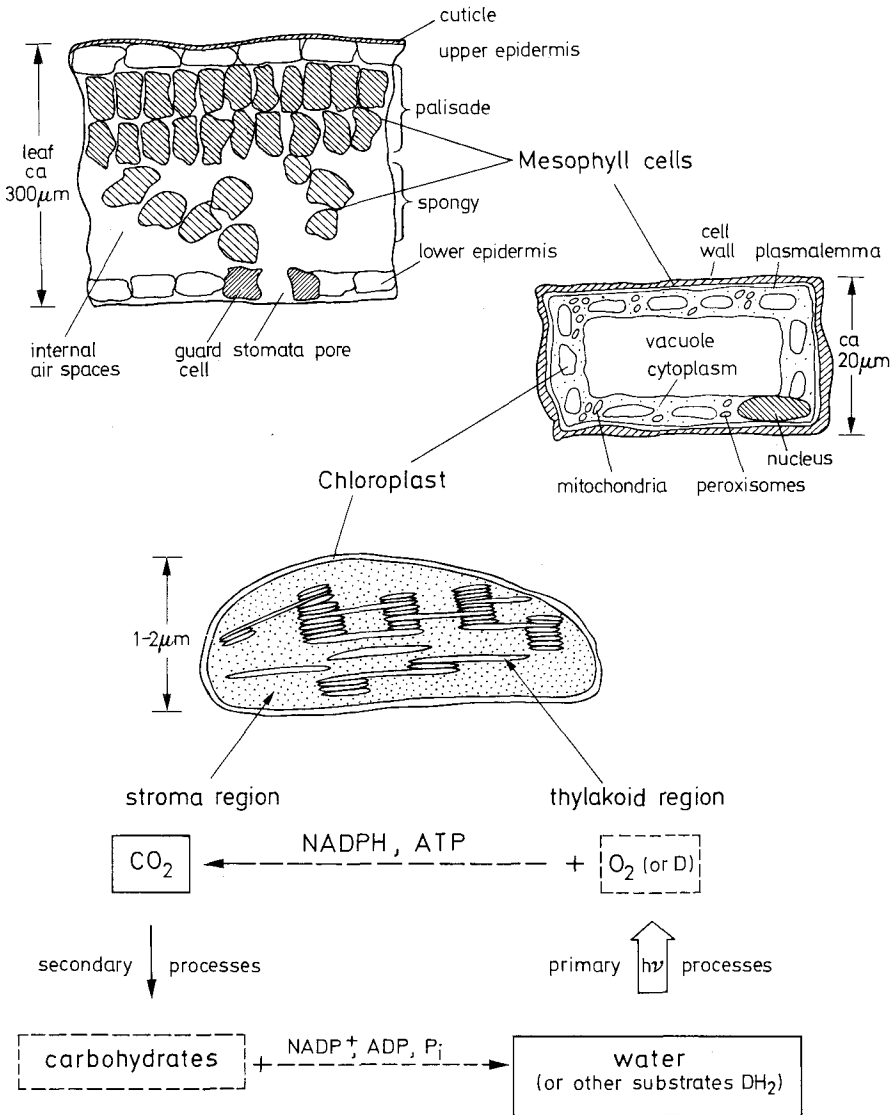
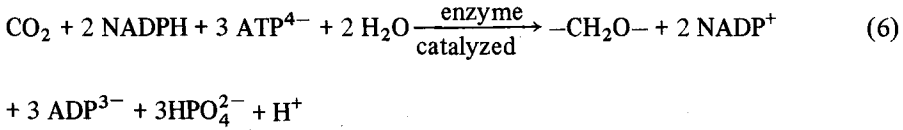


Fig. 3. Principal organization scheme of photosynthesis in plant leaves (Schematic representation of plant organelles according to Ref. 134)

appropriate hydrogen donor which is supported in the form of NADPH . As the reduction of CO_2 by NADPH is an endergonic process^{h)}, an additional free energy supply is required. This energy is provided by the hydrolysis of ATP , known to be as a nearly universal free energy source in all metabolic processes (see 4.2.5.).

^{h)} Metabolic processes with positive free energy change are referred to as endergonic, with a negative one as exergonic, respectively.

Hence, taking into account physiological pH conditions ($\text{pH} \approx 8$, see Ref.²⁰⁾), the overall reaction of CO_2 -fixation can be written in the form:



The overall turnover rate of CO_2 incorporation is determined by the properties of the catalytic enzyme system and by the local concentration of substrates and products, respectively.

4.1.1. Carbon Dioxide Transport to the Biocatalysts Responsible for CO_2 -Fixation

Whereas NADPH and ATP are produced as internal substrates in a light dependent reaction sequence in the thylakoid region (see 4.2.), the supply of CO_2 as external substrate is mainly governed by diffusion processes from the outer environment, surrounding the organism, to the enzyme system. The diffusion flux j_m of a component m along a time independent concentration gradient is given by the first Fick's law:

$$\vec{j}_m = -D_m \cdot \text{grad } c_m \quad (7)$$

If one approximately regards the total diffusion of CO_2 to be a predominantly 1-dimensional process perpendicular to the plane of the leaf surface and if furthermore the concentration difference $\Delta c_{\text{CO}_2}^{(i)}$ across a diffusion barrier i divided by barrier thickness δ_i is used instead of the concentration gradient, then Eq. (7) gives:

$$\vec{j}_{\text{CO}_2}^{(i)} = -\frac{D_{\text{CO}_2}^{(i)}}{\delta_i} \cdot \Delta c_{\text{CO}_2}^{(i)} \quad (8a)$$

where $D_{\text{CO}_2}^{(i)}/\delta_i$ is a permeability and the reciprocal value represents a resistance R_i against diffusion. Hence, Eq. (8a) can be written in the form:

$$\vec{j}_{\text{CO}_2}^{(i)} = -\frac{\Delta c_{\text{CO}_2}^{(i)}}{R_i} \quad (8b)$$

The description of CO_2 -diffusion in leaves by Fick's law in the form of Eq. (8b) is convenient because it allows the use of electrical analogue models. In this way the process of CO_2 diffusion can be described by a series of resistances. However, the external CO_2 is not the only CO_2 source for the CO_2 fixing enzyme system because within the plant cells CO_2 is produced by respiratory processes (see 6.4.). Thus one obtains the circuit analogue pattern for CO_2 fluxes depicted in Fig. 4. Then, the net CO_2 flux from environment into leaves is given by:

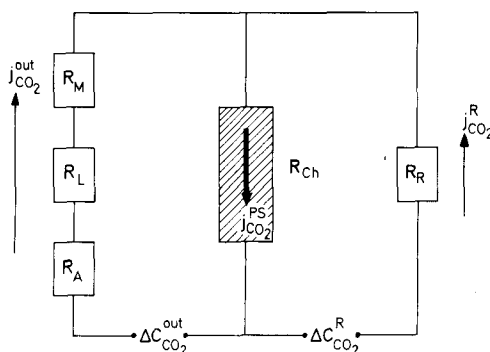


Fig. 4. Simplified electric analog model of CO_2 fluxes in plants.

$\Delta C_{\text{CO}_2}^{\text{out}}$ = difference of CO_2 concentration in the outer turbulent air (or of the outer bulk water for water plants) and the CO_2 concentration at the enzyme catalyzing CO_2 -binding.

$\Delta C_{\text{CO}_2}^{\text{R}}$ = difference of CO_2 concentration between the site of respiration and the CO_2 concentration at the enzyme catalyzing CO_2 binding.

R_A = resistance of the unstirred air layer on the surface of the leaves (or of a thin unstirred water layer surrounding water plants).

R_L = resistance of the leaf containing mainly two components (compare Fig. 3): R_{St} = stomata and R_{A_i} = inner air spaces $R_L = R_{\text{St}} + R_{A_i}$.

R_M = resistance of mesophyll cells containing mainly 3 components (compare Fig. 3): R_{CW} = cell wall, R_{Pl} = plasmalemma and R_{Cyt} = cytoplasm. $R_M = R_{\text{CW}} + R_{\text{Pl}} + R_{\text{Cyt}}$.

R_{Ch} = resistance of chloroplasts containing 2 components: R_{CE} = chloroplast envelope and R_{Str} = stroma including the photosynthetic apparatus of CO_2 incorporation.

R_R = respiratory resistance.

$j_{\text{CO}_2}^{\text{out}}$ = CO_2 flux from the outside into the leaf (or vice versa).

$j_{\text{CO}_2}^{\text{R}}$ = rate of CO_2 generation within cells by respiration.

$j_{\text{CO}_2}^{\text{PS}}$ = rate of total photosynthetic CO_2 incorporation

$$j_{\text{CO}_2}^{\text{out}} = \frac{\Delta c_{\text{CO}_2}^{\text{out}} - \Delta c_{\text{CO}_2}^{\text{R}} + j^{\text{R}} \cdot R_R}{R_A + R_L + R_M} \quad (9)$$

Hence, a net CO_2 uptake, and therefore a net CO_2 -incorporation into carbohydrates by photosynthesis versus CO_2 -release by respiration, is only possible above a critical external CO_2 concentration $c_{\text{CO}_2}^{\text{out}}$ referred to as the compensation point (c.p.). Evidently, according to Eq. (9) the compensation point in photorespiringⁱ⁾ plants is considerably higher than in other plants.

Typical values at 23 °C for the compensation point are 5–10 ppm CO_2 for non-photorespiring plants (e.g. sugarcane, maize, sorghum) and 40–100 ppm CO_2 for photorespiring plants (e.g. wheat, tomato, tobacco)²¹⁾ as compared with normal CO_2 concentration in air of 320 ppm. The numerical values of the types of resistances of Eq. (9) vary considerably for different plants and environmental conditions (s. e.g. Ref. ¹³⁴). The CO_2 input rates under good conditions are of the order of 1–4 nmoles

i) in some plants light increases the rate of respiration. This process is referred to as "photorespiration".

$\text{CO}_2 \cdot \text{s}^{-1} \cdot \text{cm}^{-2}$. On the basis of average chlorophyll concentration this corresponds to 100 to 400 $\mu\text{moles CO}_2/\text{h} \cdot \text{mg chlorophyll}$.

4.1.2. The Chemical Reactions at the Biocatalysts Leading to CO_2 -Fixation

The "resistance" R_{CHL} in Fig. 4 includes the whole machinery which is responsible for CO_2 incorporation into carbohydrates according to Eq. (6). Hence, the question arises about the details of the realization of the overall reaction. Irrespective of the different mechanisms shortly to be discussed below the first step of CO_2 incorporation includes generally the binding of CO_2 into an organic acceptor molecule symbolized by AH. Thus, this primary event of chemical CO_2 -fixation can be formulated as the formation of a carboxylic group in the acceptor molecule:



CO_2 has polarized double bonds leaving the carbon atom slightly positively charged ($\delta - 2\delta + \delta -$ ($\text{O}=\text{C}=\text{O}$)). Since the reaction (10) occurs in an aqueous phase generally two possibilities for the mechanism have to be discussed. Either dissolved CO_2 reacts directly with AH via an electrophilic attack on AH or it reacts in the form of HCO_3^- (generated by nucleophilic attack of OH^- on CO_2).

The reaction described by Eq. (10) is catalyzed by an enzyme. The details of the mechanism of this initial step of CO_2 -fixation have not yet been clarified. This primary step of CO_2 -binding is followed by a sequence of enzyme catalyzed reactions. In this respect it is important to note, that none of these reactions requires light. Hence, the whole reaction mechanism of the CO_2 -fixation in the stroma region includes only secondary processes of photosynthesis.

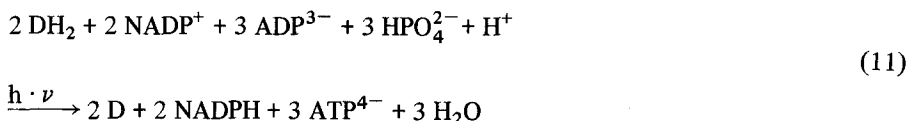
Generally 3 different types of mechanisms can be distinguished for CO_2 -fixation²²⁾:

- a) In most plants CO_2 is accepted by ribulose-1,5-diphosphate. As the primary stable product of chemical CO_2 -binding appears phosphoglyceric acid (PGA) containing 3 carbon atoms. Therefore, the organisms realizing CO_2 -fixation in this way are referred to as C_3 -plants. The details of the mechanisms have been elucidated mainly by M. Calvin and co-workers²³⁾ by the use of ^{14}C -tracer analysis. Hence, this reaction sequence is designated as Calvin cycle. The essential steps of this mechanism are schematically drawn in Fig. 2.
- b) In a number of tropical plants (e.g. sugarcane) the so-called C_4 -mechanism is realized²⁴⁾. As the first stable products of CO_2 -fixation dicarboxylic acids (malic and aspartic acid) are formed by CO_2 -incorporation into phosphoenolpyruvate. Therefore, such organisms are often referred to as C_4 -plants. The C_4 -acid then reacts with ribulose-1,5-diphosphate (RuDP) to form phosphoglyceric acid. Then the normal Calvin-circle will be passed. Instead of direct incorporation of CO_2 into the Calvin-cycle, CO_2 forms in C_4 -plants a C_4 -acid, which then serves to add carbon to RuDP. However, for the generation of C_4 -acids additional ATP is required.
- c) Some plants exist (e.g. crassulaceae) which fix CO_2 just as well in the dark as in the light. Whereas the CO_2 -fixation in the light occurs via the C_3 -pathway, in the dark CO_2 is incorporated into C_4 -acids which serve as an internal CO_2 -pool. This

CO₂-fixation mechanism is referred to as CAM-(crassulacean acid metabolism) typ²⁵⁾.

4.2. The Oxygen Evolution in the Thylakoid Region

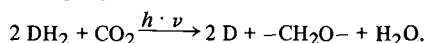
In the thylakoid region (symbolized in Fig. 1 by a big black box), a structurally highly organized membraneous system, the essential steps of light energy conversion into chemical energy take place. The overall reaction consists of the resynthesis of NADPH and ATP with the aid of light and by the use of a suitable hydrogen donor DH₂. For physiological conditions the overall reaction can be formulated in the following way:



Considering Eq. (11) firstly the question arises about the chemical nature of donor DH₂, because this substance is irreversibly consumed during photosynthesis^{j)}. Simple organisms like photosynthetic bacteria utilize comparatively strong (easily oxidizable) donor substances like H₂S or simple organic compounds as will be discussed in 4.3. However, the reservoir of these substances was limited, so that a significant increase of population of photosynthetic organisms required the evolution of systems being able to use substances with higher redox potentials as natural electron donors DH₂. This evolution process was accomplished 2–3 gigayears ago^{11, 12)} with the development of a system which can utilize the water as universally abundant donor substance giving rise to oxygen evolution. Since then the anaerobic atmosphere became enriched with oxygen until by the metabolic activity of newly developed oxygen consuming organisms the present dynamic quasi equilibrium state in the atmosphere has been attained. With the advent of oxygen in the atmosphere biological systems reached a new level of functional organization based on the significantly higher energetic efficiency of food utilization, but on the other hand, the problem of the protection of the living cells to oxidative destruction arose. This will be discussed later (see Chapter 6). Because all higher photosynthesizing organisms (above the evolutionary level of blue green algae) evolve oxygen, in a first order approximation, photosynthesis can be considered as the photolytic water cleavage by visible light into molecular free oxygen, and hydrogen bound in the form of NADPH, accompanied by ATP-synthesis. Hence watersplitting by visible light (including the red region) is the fundamental process of solar energy conversion by biological systems.

The water cleavage can be easily performed in the laboratory via electrolysis by the use of electrical energy instead of visible light. For the electrolytical water decomposition into its isolated elements two operational units are required: a) an electrical

j) Taking together Eqs. (6) and (11) the overall process of photosynthesis can be described by:



generator leading by electron flux to the production of positive (holes) and negative (electrons) charges, b) separate reaction spaces for holes and electrons. In the cathodic space electrons reduce protons to molecular hydrogen whereas in the anodic space the holes oxidize hydroxyl ions to molecular oxygen. The geometrical separation of the reaction spaces is essential in order to avoid dissipative back reactions. Principally, an analogous functional organization scheme of water cleavage is also realized by nature in the microscopic world of the thylakoid membrane system (see *e.g.* Ref.²⁶⁾). Thus, for the performance of the overall reaction of Eq. (11) four main functional elements are necessary:

- a) Generator systems leading by visible light to electronic displacement, thus giving rise to the production of electrons and holes.
- b) "Anodic space" building up the "reaction vessel" for the oxidation of water to molecular oxygen by holes of sufficient oxidizing power.
- c) "Cathodic space" building up the "reaction vessel" for the reduction of NADP^+ to NADPH by electrons of sufficient reducing power.
- d) ATP-synthesizing system realizing the ATP-production from ADP and inorganic phosphate by energetical coupling to electro-chemical energy supply.

With respect to the subject of inorganic gas exchange to be discussed in this paper the functional elements a) and b) are of special interest, whereas only a few remarks will be made about c) and d).

4.2.1. The Photoelectric Generators of Photosynthesis

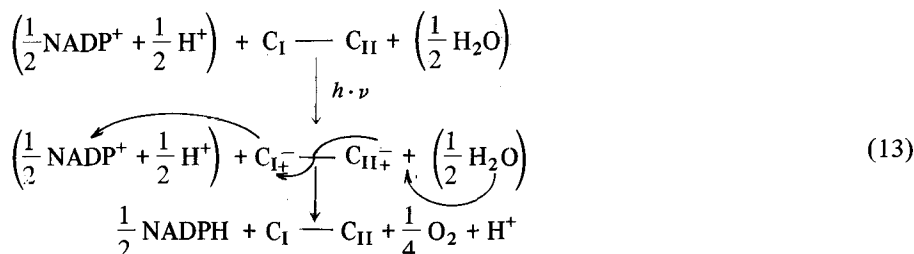
In the photoelectric generators the fundamental steps of solar energy conversion into chemical energy take place. The principal reaction sequence at the photoelectric generators, symbolized by C, can be described by Eq. (12):



where C^* represents the electronic excited state of a molecular component of C, which directly leads to the charge separation, characterized by the symbol C_{+}^{-} . The holes (+) and electrons (−) of C_{+}^{-} can react independently of each other and in this way the photoelectric generators can be envisaged as molecular solar batteries. It has been found (for rev. see Ref.²⁷⁾) that in all oxygen evolving organisms there exist two different types of photoelectric generators, called C_I and C_II . These are clamped together in series in such a way that via intermediate redox carriers the electrons of $\text{C}_{\text{II}+}^{-}$ discharge the holes of $\text{C}_{\text{I}+}^{-}$. The holes of $\text{C}_{\text{II}+}^{-}$ lead to oxygen evolution, whereas the electrons of $\text{C}_{\text{I}+}^{-}$ reduce NADP^+ . Thus the overall reaction of Eq. (11) can be described by the scheme of Eq. (13) on page 53 (for the sake of simplicity the coupling with the ATP-synthesis is omitted).

With respect to the mechanism and the realization of the light induced charge separation at C according to Eq. (12) four questions have to be answered:

- a) In which way does light generate the electronic excited state C^* ?
- b) In which way does the charge separation take place?
- c) Which chemical components form the photoelectric generators?
- d) In which way are the photoelectric generators C arranged in the thylakoid membrane?



In nature light intensity varies over many orders of magnitude (about $0,01\text{--}10\text{ mW} \cdot \text{cm}^{-2}$). Hence, photosynthetic organisms have evolved suitable adaptation systems. The generation of C^* by direct light absorption of C would not provide the above mentioned regulatory mechanism. Thus, nature has chosen another way. Already in 1932 it was shown by Emerson and Arnold²⁸⁾ that more than 99,5% of the total chlorophyll content is not included into the photochemical processes. Later, it was concluded that a bulk pigment system exists containing about 250 chlorophyll-a-molecules and accessory pigments (chlorophyll b, carotenoids and biliproteins) which is functionally connected with a photoelectric generator C^{29} . Principally the same type of functional connection between photoelectric generators C_I and C_II and the bulk pigment systems I and II, respectively, does exist. The subtleties of this point will not be discussed here, for rev. see Refs.^{30, 31)}. The functional entities consisting of photoelectric generator and bulk pigment system are referred to as *photosynthetic unit* of system I and II, respectively^{k)}.

The bulk pigment systems I and II provide the adaptation to the different light intensities (see Fig. 5). They solve essentially two problems.

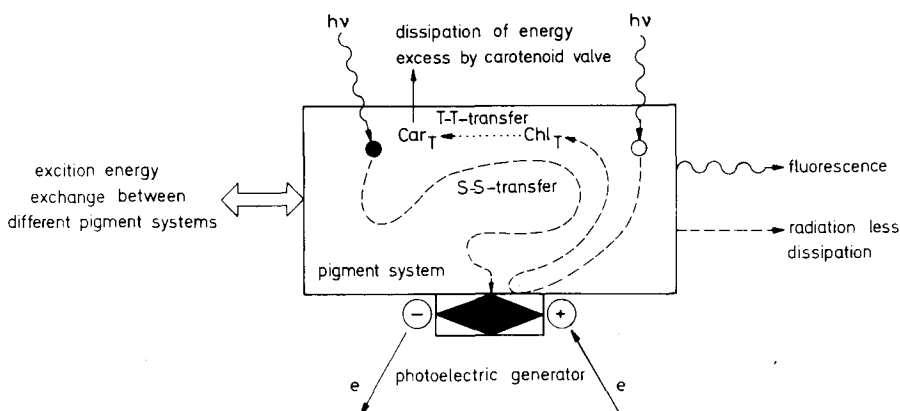


Fig. 5. Excitation energy fluxes in the pigment system of photosynthetic units (for details and explanation see text)

k) It must be emphasized that the photosynthetic units are not the functional units of all photosynthetic activities, e.g. for electrical and ion transport phenomena and ATP-synthesis the thylakoid as a whole represents the functional unit (see Ref.²⁷⁾).

At low intensities the few quanta of light absorbed, building up excitons within the bulk pigment systems, are funnelled to C_I and C_{II} via singlet-singlet resonance energy transfer (S-S-transfer, see Fig. 5)^{32–34}. Thus, the bulk pigment systems function at low light intensities as powerful antennae for the capture of radiation energy. As the photochemical quantum yield at the photoelectric generators was found to be nearly 100%^{35, 36} practically all light quanta are transformed into electrochemical energy up to moderate intensities. Thus, the photoelectric generators (as natural solar batteries of molecular dimensions) exceed significantly the efficiency of artificial macroscopic solar batteries³⁷. From fluorescence (yield and depolarization) measurements it has been inferred that on average 150–300 individual energy transfer steps occur until the exciton reaches the photoelectric generators³⁸. The individual hopping time is of the order of picoseconds^{30, 34}.

The reverse problem arises at high light intensities. The photochemical transformation rate of excitons at C_I and C_{II} is limited by the secondary electron transfer reactions in the dark leading to discharge of the functional inactive states C_I^- and C_{II}^- , C_I^+ and C_{II}^+ , C_{I+} and C_{II+} . Hence, at high light intensities an overloading of the bulk pigment systems with excitons could occur. This would lead by intersystem crossing to the generation of triplet states of bulk chlorophyll-a which are sensitive to destructive oxygenic attack (see Chapter 6.2.) The normal dissipative pathways of fluorescence and heat emission are not sufficient for protection, because carotenoidless mutants are known to be violable by visible light³⁹. The protective function of carotenoids has been clarified recently^{40, 41}. It was shown that a rapid triplet-triplet-energy transfer (T-T-transfer, see Fig. 5) occurs from chlorophyll-a to carotenoids. The carotenoid triplet rapidly decays in a few microseconds so that it acts as a protective valve supporting the dissipation of harmful excess energy.

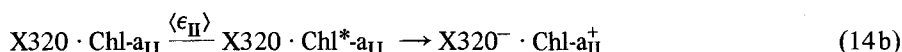
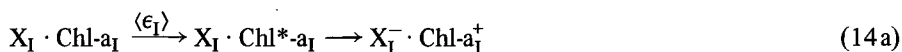
Lately it was found, that the same mechanism is realized also in bacteria^{41a, b}. Exciton fusion processes observed by excitation of photosynthesis with very intensive ps- or ns-flashes^{41c, d} practically do not occur under natural excitation conditions (s. Ref.^{41b}).

Thus, the bulk pigment systems provide a very effective adaptation of the photosynthetic organisms to the different environmental light intensities (s. p. 53).

The excitons reaching C_I and C_{II} are captured in times of 200 ps at C_{II} , at C_I (30–80 ps) as well as in bacteria (see later) this time seems to be even shorter^{42–45}. Laser-flash photometric measurements have shown that the charge separation at C_I and C_{II} is accomplished within ≤ 20 ns⁴⁶. The details of the mechanism of this process are completely unknown.

Very recent results present indirect evidence for the formation of a triplet state as an intermediate in the route of charge separation at C_I ⁴⁷ as well as on C_{II} ^{47a}.

It has been found that C_I contains a special chlorophyll-a^{48, 49} very probably in a dimer form^{50, 51}, called chlorophyll-a_I (Chl-a_I), which is primarily photooxidized with the concomitant reduction of an as yet not unequivocally identified primary electron acceptor (very recently evidence has been presented for the characterization as an Fe-S-protein, see Ref.⁵²). Similarly, the photoelectric generator C_{II} contains a special chlorophyll-a⁵³, called chlorophyll-a_{II} (Chl-a_{II}), which is also oxidized during the primary photoact^{54, 55}. The primary electron acceptor was found to be a special plastoquinone molecule which is reduced to the semiquinone form^{56, 57}. It is called X 320⁵⁶. Thus, the reactions at C_I and C_{II} can be explicitly formulated:



where $\langle \epsilon_I \rangle$ and $\langle \epsilon_{II} \rangle$ represent excitons which are able to excite C_I (excitable with light $\lambda \leq 730$ nm) and C_{II} (excitable with light $\lambda \leq 700$ nm), respectively (s. Ref.²⁷), and X_I is the primary electron acceptor of system I.

The photoelectric generators C_I and C_{II} are clearly distinguished by the asymmetric electrochemical behaviour of their electrons and holes, respectively. The charge separation at C_I leads to electrons of rather strong reducing power (the midpoint potential¹⁾ $E_{m,7}$ of X_I/X_I is $\leq -0,58$ V, see Ref.^{58,59}), whereas the holes are of moderate oxidizing power ($E_{m,7} \geq +0,43$ V, see Ref.^{60,61}). On the other hand, the charge separation at C_{II} produces electrons of only moderate reducing power ($E_{m,7} = -0,1$ to 0 V, see Ref.^{62,63}), whereas the holes are very strongly oxidizing species ($E_{m,7} \geq +0,9$ V^m). The photoelectric generators are embedded into the thylakoid membrane. Direct information (e.g. by X-ray-diffraction) is not available about the structural arrangement. However, it can be indirectly shown that C_I and C_{II} are anisotropically arranged. It was found that in the light within ≤ 20 ns an electrical field is established across the thylakoid membrane⁶⁴) and that systems I and II contribute to nearly the same degree to the total field if excitation occurs with short flashes^{65, 66}). This event kinetically coincides with the electron transfer at the photoelectric generators. Hence, it can be concluded that the electrical field is generated by the electronic displacement at C_I and C_{II} . This coupling between electron transfer at photoelectric generators and field formation is only possible if C_I and C_{II} are anisotropically arranged perpendicular to the plane of the thylakoid membrane. Furthermore, the direction of the electrical field indicates that the acceptor sides of C_I and C_{II} (X_I and X_{320} , resp.) are located near the outer phase, whereas the donor sides ($\text{Chl-}a_I$ and $\text{Chl-}a_{II}$ resp.) are located near the inner phase of the thylakoids^{55, 67-69}). This has been confirmed very recently by the application of structurally selective proteolytic enzymes⁷⁰). Hence, the thylakoid membrane builds up the barrier for the spatial separation between the reduction of NADP^+ at the outer side and the oxidation of water near the inner side of the thylakoid.

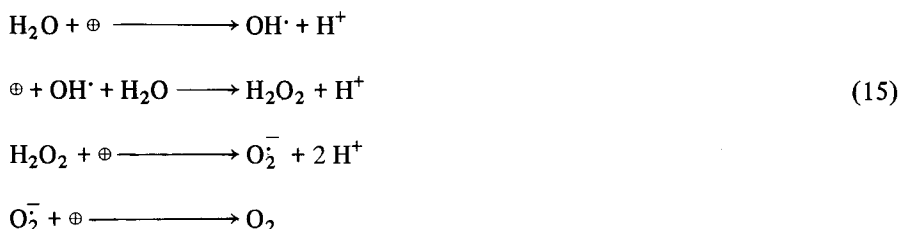
Very recently the synthesis of a covalently bound chlorophyll-a-dimer analogue has been reported^{70a}). It was shown that bis-(chlorophyllide-a)ethylene glycol diester with porphyrin rings held together via nucleophilic hydrogen bridging closely resembles in its spectral properties, photochemical activity and redox potential to $\text{Chl-}a_I$ and therefore can serve as an in vitro model for the native $\text{Chl-}a_I$ -dimer-protein complex.

1) As the redox potential of many biological relevant redox systems is pH-dependent, it is convenient to use the redox potential for $[\text{Ox}] = [\text{Red.}]$ at $\text{pH} = 7$, the so-called midpoint potential $E_{m,7}$, instead of the normal potential $E_{m,0}$ at the unphysiological $\text{pH} = 0$, where almost all biological activities are blocked.

m) The oxidation of water to molecular oxygen at $\text{pH} = 6,0$ requires a redox component of at least $E_{m,6} = +0,88$ V. Thus, if the electron transfer at the primary electron donor is not coupled with a protonation the midpoint potential is independent of pH. According to a theoretical model discussed in Chapter 4.2.2. the midpoint potential should be even higher ($E_{m,7} \geq +1,0$ V).

4.2.2. The Watersplitting Enzyme System

The strong oxidizing holes produced by C_{II} ultimately cause the water oxidation to molecular oxygen. The performance of this process is a serious challenge to biological systems. If one supposes a univalent pathway, then the overall process of water oxidation can be subdivided into four individual electron transfer steps in the following way (different protonation reactions have been omitted for the sake of simplicity):



\oplus represents a hole of sufficient oxidizing power.

As is seen in scheme Eq. (15) during the overall reaction very reactive intermediates are formed. Among these species the $OH\cdot$ -radical is the most potent oxidant known to chemistry which reacts with many organic substances at rates near the diffusion controlled theoretical limitⁿ⁾. The superoxide radical O_2^- is also a reactive species and even hydrogenperoxide as an intermediate species is a powerful oxidant. Thus, in order to prevent deleterious damage of the biological organisms, nature has developed a reaction mechanism which does not include the generation and accumulation of the above mentioned free radicals. This can be achieved by formation of a special "reaction vessel" for shielding the dangerous process from the sensitive organic material and by protective enzyme systems which rapidly destroy the reactive species if they occur outside of the "reaction vessel".

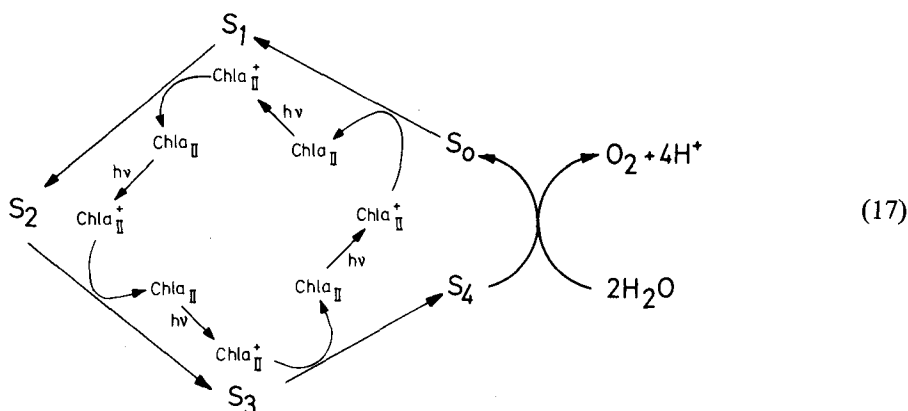
The oxidation of water to molecular oxygen requires in any case the cooperation of four holes. Generally, two different mechanisms are possible for the realization of this charge cooperation:

- a) A *statistical* cooperation of four holes generated at four different C_{II} -units. This could be achieved either, if the total inner aqueous phase of the thylakoid acts as "anodic space" with the total inner membrane side containing $Chl-a_{II}$ as source of holes or by a special watersplitting enzyme system (indicated here by the symbol Y) which is functionally connected with the $Chl-a_{II}$ -component of at least four different C_{II} -units. The first alternative seems to be very unfavorable because in this case the total inner side of the thylakoid membrane has to be made of inert material, which is very difficult to realize. For the second alternative one obtains the general scheme of Eq. (16):



n) The $OH\cdot$ -radical is isoelectronic with the fluorine atom, an extremely powerful oxidizing atom in the nature.

- b) Cooperation by *sequential charge accumulation*. In this case each watersplitting enzyme system Y is functionally connected with the Chl- a_{II} of only one C_{II} -unit, so that the state S_4 [see Eq. (17)] necessary for water oxidation can be attained only by four subsequent electron transfer steps and charge storage in system Y. Hence, the general reaction scheme is given by:



where S_i represents the storage state of the watersplitting enzyme system Y and index i ($i = 0, \dots, 4$) gives the number of holes stored in Y.

An experimental decision about the type of charge cooperation was achieved as the development of a very sensitive polarographic method for oxygen detection by Joliot *et al.*⁽⁷¹⁾ made it possible to measure the oxygen evolved due to excitation with only one short (duration \leq few microseconds) saturating flash. Under these conditions each saturating short flash of a flash train can induce one and only one turn-over at the photoelectric generators C_{II} ; that means just one hole is produced per C_{II} -unit and per flash. Hence, if the indispensable charge cooperation is realized statistically according to Eq. (16) each flash of a train should give rise to the same amount of oxygen. On the other hand, a completely different pattern is expected for the cooperation by sequential charge accumulation. According to Eq. (17) four consecutive steps are required to transform S_0 into S_4 . Thus, only the last flash of a group of four flashes can induce oxygen production. If one supposes a finite lifetime for the holes stored in the watersplitting enzyme system Y then the state S_0 should prevail in the dark adapted organisms. The theoretical patterns of oxygen yield per flash as a function of flash number in a train of short saturating flashes are given for both types of the above mentioned charge cooperativity in Fig. 6 in comparison with the experimental data^(72, 73). Though these values do not fit any of the theoretical patterns of Fig. 6 one can infer that a simple statistical charge cooperation is not realized (otherwise the first two flashes should lead to oxygen evolution). It has been shown that the experimental data are reconcilable with the model of the cooperation by sequential charge accumulation if additional assumptions (stability of state S_1 , non zero probabilities of misses and double hits for charging processes of system Y, see Ref.^(73, 74)), or by the introduction of the elaborated matrix model of Lavorel, Ref.⁽⁷⁵⁾) are introduced. Hence, each watersplitting enzyme system Y is functionally connect-

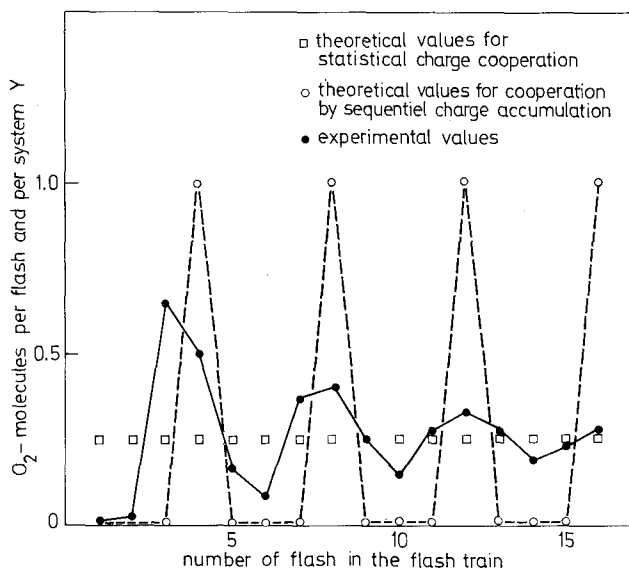


Fig. 6. Patterns of oxygen evolution in a sequence of short saturating flashes (for details and explanation see text)

ed with only one C_{II} -unit. A charge cooperation between different systems Y does not take place (in this respect it should be noted that experimental evidence points to a possible functional interaction between two C_{II} -units, see Ref.^{76, 77}). The realization of cooperation by sequential charge accumulation has a remarkable consequence. The lifetime of the holes stored in system Y is finite (order of a few seconds, Ref.^{78, 79}). Thus, oxygen evolution is only possible if the mean temporal distance between the holes transferred to system Y is smaller than or comparable to the lifetime of the stored holes. This effect is shown in Fig. 7. Under repetitive excitation conditions the normalized average oxygen yield per flash $\phi(t_d)$ as a function of the time t_d between the flashes firstly increases with t_d (Emerson rise-curve due to rate limitation by electron transport, see Ref.²⁸), but decreases at higher t_d . In this range the flux of holes into system Y becomes small in comparison to the lifetime of S_3 , the indispensable precursor state for water oxidation [see Eq. (17)]. Obviously, a decrease of the lifetime of S_3 would lead to a steeper decline of $\phi(t_d)$ with increasing t_d . This has been observed to occur by the application of some chemical species (ADRY^o-effect, see Ref.⁸⁰) in isolated spinach chloroplasts as is shown in Fig. 7 (in algae the reverse effect was found, Refs.^{81, 82}). Thus, the storage behaviour of the watersplitting enzyme system Y can be selectively modified by these ADRY-agents (for details see Ref.^{83, 84}).

The above mentioned considerations have shown that the photosynthetic oxygen evolution occurs within functionally isolated entities, the watersplitting enzyme systems Y. Thus, the systems Y can be suggested as being a highly specialized microscopic

^o) ADRY = Acceleration of the Deactivation Reactions of the water-splitting enzyme system Y.

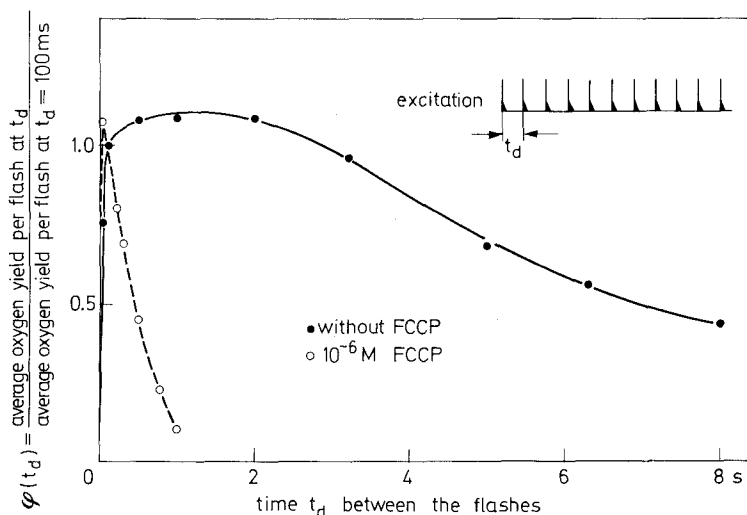


Fig. 7. Relative average oxygen yield per flash, $\varphi(t_d)$, as a function of the time t_d between the flashes in spinach chloroplasts²⁶⁾

“reaction vessels” of twofold functional importance: a) by performing the charge co-operation and b) by screening up the highly reactive intermediates of water oxidation from the sensitive organic material. In this respect now the question arises: By which molecular construction has this problem been solved by nature?

Until now hardly anything is known about the structural organization of system Y. The only facts clearly established are the central role of manganese^{85, 86)} and the high sensitivity of Y to irreversible destruction by temperature treatment⁸⁷⁾, Tris-washing⁸⁸⁾ (a regeneration of the oxygen evolving capacity is possible, see Ref.⁸⁹⁾), UV-irradiation⁹⁰⁾ and treatment with chaotropic agents⁹¹⁾. The inhibition is accompanied by a manganese release. The functional integrity of C_{II} is not destroyed by these treatments, as was shown by direct measurements of the reactions of $Chl-a_{II}$ ⁹²⁾ and X 320⁹³⁾ [see Eq. (14b)], respectively.

On the basis of the above mentioned data a hypothetical molecular model for system Y has been proposed⁹⁴⁾. In this model it is assumed that the watersplitting enzyme system Y is a mangano-protein with specially coordinated manganese as the storage sites for the holes transferred from $Chl-a_{II}^+$ via intermediate carrier D (or carriers D_i ?) into Y. Taking into account the important screening function of system Y, the above mentioned hypothesis is now extended by the assumption, that an ordered array, with manganese as the cornerstones, forms a cage which closes up a *small* membered cluster of *few* water molecules (G. Renger, in prep.). Because of the realization of the fundamental cooperation of four holes by sequential charge accumulation it is basically assumed that with respect to the wateroxidation a special 4-step univalent electron transfer mechanism resembling that of Eq. (15) takes place. The thermodynamics of electron abstraction clearly differs for the intermediate univalent electron transfer steps of Eq. (15), as is indicated by the corresponding midpoint potentials. Hence, in order to improve the energetic feasibility of the overall process a molecular reaction mechanism is supposed which avoids thermodynamically

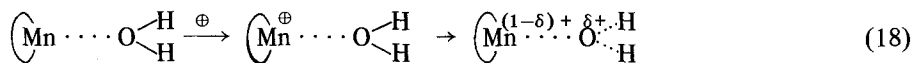
unfavoured reactions like the formation of free hydroxyl radicals. This specific hypothetical mechanism includes 4 essential postulates:

- 1) The charging of a storage place with a hole by $\text{Chl-a}_{\text{II}}^+$ leads to the formation of a bonding state designated as "cryptohydroxyl radical".
- 2) The transfer of a second hole by $\text{Chl-a}_{\text{II}}^+$ into a system Y already containing one "crypto-hydroxyl radical" gives rise to the generation of a second "crypto-hydroxyl radical" at another storage place.

If two "crypto-hydroxyl radicals" are located at neighbored storage places, a binuclear complexed "cryptoperoxide" is formed.

- 3) The complexed "cryptoperoxide" is further oxidized to the superoxide radical probably complexed at a manganese center in a transition valence state.
- 4) The superoxide radical in its complex state is easily oxidizable to molecular oxygen by an internal electron acceptor of rather poor oxidizing power.

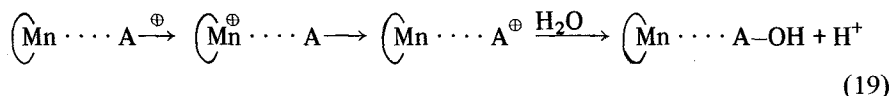
Now some remarks should be made about the chemical and mechanistical realization of this specialized reaction sequence. The formation of a "crypto-hydroxyl radical" has been discussed already implicitly in Ref.⁹⁵⁾. It can be accomplished in two ways: a) If the central manganese ion of a storage place is coordinated directly with a water molecule, then a univalent oxidative valence change of the manganese by electron transfer to $\text{Chl-a}_{\text{II}}^+$ can lead to an electronic redistribution between the central ion and the inner sphere water ligand in the form:



where $\left(\text{Mn}^{(1-\delta)+} \cdots \overset{\delta+}{\text{O}} \begin{array}{c} \text{H} \\ \diagup \quad \diagdown \\ \text{H} \end{array} \right)$ represents a "crypto-hydroxyl radical" and $\left(\text{Mn} \right)$ indicates the manganese central ion in its dark adapted oxidation state^{p)} surrounded by a special ligand shell, except for the water ligand.

The water oxidation via inner sphere aquo-complexes seems to be realized in vitro in $[\text{Co}(\text{H}_2\text{O})_6]^{3+}$ solutions⁹⁸⁾.

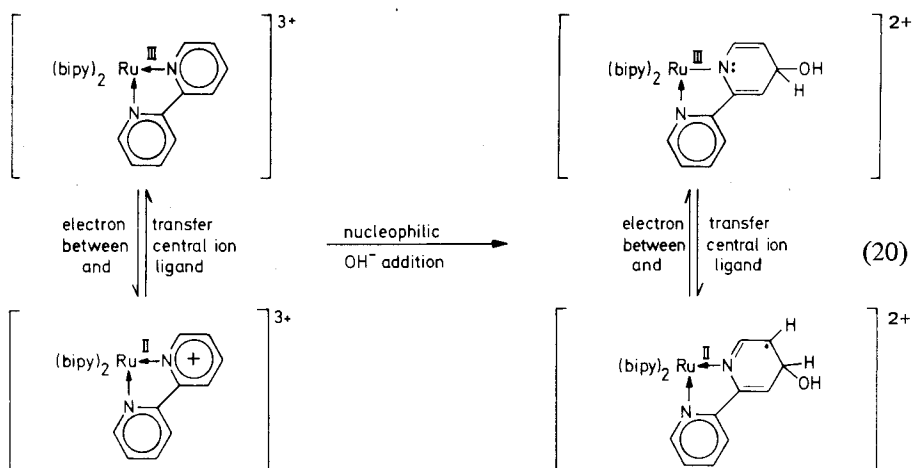
b) It could also be possible that the hole transferred to a storage place of system Y oxidizes one component of the ligand shell with the subsequent nucleophilic attack of an hydroxyl ion:



An example for the second type of "crypto-hydroxyl radical" formation has very recently been reported to exist in an in vitro model system for water oxidation consisting of tris(bipyridine)-ruthenium(III)-salts⁹⁹⁾. In the complex an internal charge

p) The valence state of manganese in dark adapted algae or chloroplasts is not known. On the basis of light activation experiments an oxidation state of +4 of the central manganese ion was inferred⁹⁶⁾ but very recent measurements of water proton spin lattice relaxation in chloroplast thylakoid membrane suspension suggest that manganese exist as a mixture of oxidation states, probably of +2 and +3⁹⁷⁾.

transfer occurs from one bipyridinium ligand to the central ruthenium ion followed by a nucleophilic addition of hydroxide to the 4-position of the ligand, as is described by Eq. (20), thus giving rise to a special form of a "crypto-hydroxyl radical". The most important aspect of this reaction is the oxidation of hydroxide by a relatively mild oxidant which is not able to oxidize water into a free hydroxyl radical^{q)}:



Thus, the formation of "cryptohydroxyl radicals" is energetically favoured in comparison to the water oxidation into free hydroxyl radical. At the present stage of knowledge it is premature to speculate which type of the above mentioned mechanism for "crypto-hydroxyl-radical" formation could be realized in the photosynthetic water splitting enzyme system Y.

However, irrespective of the real mechanism, the formation of a "crypto-hydroxyl radical" is postulated to be energetically feasible by redox components of a midpoint potential of +1,0–1,1 V. This is in close agreement with the above mentioned experimental data (see footnote^{q)}).

The second postulate of the present molecular model claims the generation of a "cryptoperoxide". Theoretically also the formation of a "crypto-oxygen atom" by the oxidation of a "crypto-hydroxyl radical" has to be taken into consideration as has been done in an earlier proposed reaction scheme⁹⁵⁾. However, in the watersplitting enzyme system Y containing more than one storage group the predominant generation of a "crypto-oxygen atom" would only occur if its formation is kinetically or energetically favoured in comparison with that of a second "crypto-hydroxyl radical". But, on the basis of the corresponding midpoint potentials ($\text{OH} \rightarrow \text{O} + e + \text{H}^+$, $E_{m,7} = +1,92 \text{ V}$, see Ref.¹⁰⁰⁾, versus $\text{OH} + \text{H}_2\text{O} \rightarrow \text{H}_2\text{O}_2 + e + \text{H}^+$, $E_{m,7} = +0,4 \text{ V}$, (see Ref.¹⁰⁰⁾) the formation of "crypto-oxygen atoms" seems to be energetically much more difficult than that of a second "crypto-hydroxyl radical", even if a mod-

^{q)} The normal redox potential of the system $[\text{Ru}(\text{bipy})_3]^{3+}/[\text{Ru}(\text{bipy})_3]^{2+}$ is +1,26 V⁹⁹⁾ which is far from the potential of the system $\text{H}_2\text{O}/\text{OH}$ ($E_{m,7} = 2,33 \text{ V}$, see Ref.¹⁰⁰⁾). Later, surface active derivatives of $[\text{Ru}(\text{bipy})_3]^{2+}$ aggregated to monolayers have been discussed as to be suitable catalysts for in vitro models of photolytic water cleavage^{100a)}.

ification of the thermodynamics by specific complexation will be taken into account. Hence, the degree of "crypto-oxygen atom" production can be neglected.

Furthermore, it has been assumed that two "crypto-hydroxyl radicals" located at neighboring storage places lead by interaction to the preformation of an O—O-bond of peroxide type, complexed via two manganese centers. Hence, this state represents a binuclear complexed "cryptoperoxide".

Thus, according to the present model free peroxide will not be evolved as an intermediate during the process of photosynthetic water oxidation to molecular oxygen. This is in accordance with experimental data obtained for the water oxidation at the binuclear $[(\text{H}_2\text{O})_4\text{CoOH}]_2^{4+}$ -complex excluding also the formation of a hydrolyzable complete peroxide bond⁹⁸). But, on the other hand, these results support clear evidence for the importance of a binuclear complex for the water oxidation. Recently Calvin reported about the light induced water oxidation to molecular oxygen by the binuclear manganese catalyst di- μ -oxotetrakis(2,2'-bipyridine)dimanganese(III,IV)perchlorate¹⁰¹).

It is interesting to note, that the formation of "bridged peroxide" has been discussed also for the reverse overall process, *i.e.* the O_2 -reduction to H_2O , occurring in cytochrome oxidase (see Chapter 6.4.2.). The "cryptoperoxide"-formation in the watersplitting enzyme system Y is assumed to occur practically without free energy change. Thus, in a rough approximation the redox energy required for the generation of "cryptoperoxide" by water oxidation results in about +1,0 V per abstracted electron at pH = 7 (in comparison for the synthesis of free H_2O_2 an energy supply of +1,4 V per electron is necessary, see Ref.¹⁰⁰). Accordingly, a rather high stabilization energy of "cryptoperoxide" compared to free H_2O_2 of 75–80 kJ/mole arises.

In the third postulate the formation of a complexed superoxide radical is supposed. This is in complete agreement with the experimental evidence for the occurrence of the superoxide radical as intermediate in a model system for water oxidation by aquo-complexes of Co(III)-salts⁹⁸) described above. However, in the present molecular model it is postulated that for energetical reasons a complexed superoxide is formed (see also 6.2.) which needs less redox energy than the formation of a free superoxide radical by oxidation of water. The stabilization energy of complexed superoxide is assumed to be nearly the same as for "cryptoperoxide", *i.e.* 70–80 kJ/mole. Taking into account this value, three univalent redox steps of about +1,0 V per electron, abstracted from water, are required for the formation of complexed superoxide (versus +1,3 V needed for the generation of free superoxide).

In the last step the oxidation of the complexed superoxide (postulate 4) takes place by an electron acceptor of comparatively poor oxidizing power. But because of the above mentioned stabilization energy — in contrast to the oxidation of free superoxide into O_2 ($E_{m,7} = -0,6$ V, see Ref.¹⁰²) — for the electron abstraction from the complexed superoxide stronger oxidizing equivalents are required. Considering the above introduced assumptions about the energetics of the formation of complexed superoxide a substance M with a midpoint potential of +0,2 to +0,3 V should be sufficient. It is assumed that the component M is stable in its oxidation state M^+ in the dark. Hence, in dark adapted algae or chloroplasts maximal oxygen yield is obtained in the third flash of a flash train (see Fig. 6). This explains the apparent stability of one hole stored in the watersplitting enzyme system Y on a molecular

basis. The midpoint potential of the component carrying this positive hole has been estimated to about $\pm 0,2 \text{ V}^{103}$. However, in contrast to the widespread assumption, according to the present model this stable trapped hole does not represent the stabilization of the first oxidation state of water in photosynthesis, but it rather serves to perform the last step of water oxidation.

The above mentioned redox component M leading to superoxide oxidation could be postulated as to be cytochrome b 559. It is known that cytochrome b 559 localized in system II has a sufficiently high midpoint potential¹⁾. It is oxidized by photoelectric generator C_{II} under certain conditions^{106, 107}. In this respect it is interesting to note that cytochromeoxidase responsible for the catalysis of the reverse process (oxygen reduction to water) also contains cytochromes as functional groups (see Chapter 6.4.). However, it must be mentioned that some experimental data point against a participation of cytochrome b 559 in the process of water oxidation to O_2 ^{105, 108}.

The water oxidation not only leads to oxygen evolution, but in addition it is coupled with a proton release. Generally, two possible mechanisms have to be considered. If the sequential charge accumulation in the watersplitting enzyme system Y via single electron transfer steps is not accompanied by deprotonation reactions [see Eq. (17)] then the proton liberation should coincide with the specific oscillatory pattern found for oxygen production (see Fig. 6). On the other hand, it could be anticipated that the intermediates of the water oxidation could be acids with pK-values low enough for proton release (see Ref.⁹⁵). Under these circumstances the kinetical patterns would not be identical for the liberation of protons and oxygen, respectively. Earlier experimental data favour the first mechanism¹¹⁰. However, later experiments obtained either with highly sensitive glass electrodes^{100a} or with special pH-indicators^{110b} cast some doubts onto this interpretation, because they strongly support the second mechanism^{110c}.

It is interesting to note that according to latest data the reduction kinetics of $Chl-a_{II}^+$ is influenced by the inner thylakoid H^+ -concentration^{110d}, which might reflect a regulatory role of protons near the watersplitting enzyme system Y. But, at the present stage of knowledge it is premature to speculate about this effect.

The molecular model of photosynthetic water oxidation discussed here is only a hypothesis, but it is compatible with a number of experimental data. One essential feature of this model is the assumption that chlorophyll itself is not directly included in the process of water cleavage. However, in contrast to this hypothesis, some authors propose a direct participation of chlorophyll itself in the photosynthetic water oxidation, either via $Chla \cdot H_2O$ -aggregates¹¹¹⁻¹¹³ or via oxidative formation of a "dioxolium ion" at chlorophyll-a including the carbonyl groups of the cyclopentanone ring and of the neighboring methylester group, respectively¹¹⁴. Though direct evidence for the acception or rejection of these models does not exist several reasons seem to unfavour these models. Firstly, chlorophyll is the unique molecule for the realization of very efficient photochemistry, which has been applied by nature as the cornerstone of the photoelectric generators in all photosynthesizing organisms (either as chlorophyll or in its dihydroform as bacteriochlorophyll) irre-

¹⁾ There exist at least two forms of cytochrome b 559: high potential form with $E_{m,7} = +0,35 \text{ V}$ and low potential form with $E_{m,7} = +0,08 \text{ V}$ (see Ref.¹⁰⁴). It is interesting to note that ADPR-agents lead to transformation of high into the low potential form¹⁰⁹.

spective of whether they are able to evolve oxygen or not, *i.e.* it was introduced into biological systems long before the evolution of water cleavage capacity of photosynthesis. Hence, chlorophyll by itself appears not to be the “fittest” molecule for the realization of water oxidation. Secondly, the watersplitting enzyme system Y can be completely destroyed without serious influence on the functional integrity of the photoelectric generators, indicating that intact photochemistry of Chl- a_{II} is not sufficient for water oxidation to molecular oxygen. Thirdly, the d -orbitals and the variability of the valence state of transition metal ions seem to be very useful for the stabilisation as well as for activation of the different intermediates of water oxidation to molecular oxygen (s. Chapter 6). Fourthly, until now the fundamental step of the hypothetical “dioxolium-ion” mechanism, *i.e.* the oxidative transformation of 1,3-dicarbonyls into oxygen and a cyclopropylum-cation, could not be experimentally confirmed at in vitro model systems¹¹⁴). Fifthly, from the lack of incorporation of ^{18}O into chlorophyll of *Chlorella* grown in highly enriched H_2^{18}O it has been concluded that the carbonyl group of the cyclopentanone-ring does not play a role in water oxidation¹¹⁵).

Thus, summarizing this point, chlorophyll – though generating via photochemical processes the holes required – is probably not directly included into the molecular reactions leading to water oxidation. It seems that nature has developed a special microscopic reaction vessel with a wall containing the functionally active catalytic sites. In this respect it is interesting to note that the principal functional organization scheme of photosynthetic water oxidation has been already entirely accomplished within the earliest phylogenetic ancestors of oxygen evolving organisms¹¹⁶).

Furthermore, it should be mentioned that in analogy to the phylogenetic evolution also in the ontogenesis the formation of the watersplitting enzyme system Y appears to be the last step of the development of algae and higher plants^{117, 118}).

The preceding discussion was based on the widely accepted assumption that oxygen evolution occurs by water oxidation. However, it should be mentioned that also CO_2 could function as the reactant for oxygen formation. Arguments have been presented favouring the CO_2 -hypothesis (for rev. see Ref.¹¹⁹). Though HCO_3^- addition to HCO_3^- depleted suspensions has been found to stimulate the rate of oxygen evolution^{120, 121}), very recent experimental data point against a stoichiometric participation of HCO_3^- in the oxygen evolving process^{122–123}).

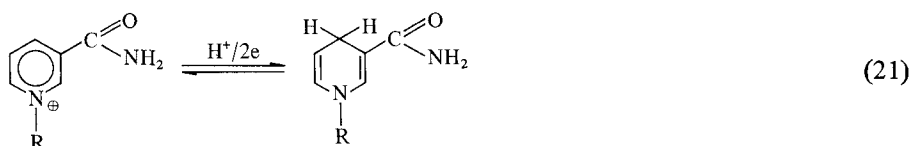
However, it could be possible that CO_2 acts catalytically as ligand A for “cryptohydroxyl radical” formation according to Eq. (19) (see Ref.⁹⁵).

As two light reactions are necessary for the electron transport from H_2O to NADP^+ and four positive charges generated by photoelectric generator C_{II} are required for water oxidation, a minimal quantum requirement of $8 h \cdot \nu / \text{O}_2$ should be observed. The experimental data of $8\text{--}10 h \cdot \nu$ per O_2 ¹²⁴) are in excellent agreement with the theoretical value.

4.2.3. The Reduction of NADP^+ and the Possibility of the Evolution of Molecular Hydrogen

The reducing power of the electrons produced by photoelectric generator of system I, C_I , which is characterized by the midpoint potential of the primary acceptor sub-

stance X_I ($E_{m,7} \leq -0,5$ V; see 4.2.1.) should be energetically sufficient for the evolution of molecular hydrogen, even under physiological pH-conditions ($E_{m,7} = -0,43$ V for the process $\frac{1}{2} H_2 \rightarrow H^+ + e$). However, the generation of molecular hydrogen would impose a high dissipative backlash in the economics of cellular metabolism. Because of the chemical inertia molecular hydrogen is a comparatively poor reactant in reductive processes in the absence of suitable catalysts, as is well known from the problems arising for the realization of technical hydrogenation processes. Furthermore, special carrier systems would be required for storage and transport of hydrogen within the cell. Otherwise, hydrogen would rapidly escape into the atmosphere and react by a dissipative reaction with oxygen. Thus, any significant hydrogen evolution has to be prevented. This can be achieved by the use of suitable carrier substances which are both, stable enough to transport reductive equivalents very effectively without loss to places in the organism, where they are needed, and reactive enough for sufficiently high turnover rates at the reactive sites. Many classes of organic substances undergoing redox reactions coupled with protonation/deprotonation equilibria are known to fulfil this condition (see also Chapter 6.3. and 6.4.). The terminal acceptor substance of the primary processes of photosynthesis was found¹²⁵ to be nicotinamide-adenine-dinucleotidephosphate ($NADP^+$). The functional electron carrier group is the aromatic nicotinamide part which can be reversibly reduced to the chinoidic dihydrogroup:



with a midpoint potential of $E_{m,7} = -0,32$ V. $NADP^+$ is not directly reduced by X_I^- , but the electron transfer occurs via the univalent redox carrier ferredoxin¹²⁶, a metalloprotein enzyme system containing iron coordinated with sulfur groups^{127, 128} and via the enzyme ferredoxin-NADP-reductase¹²⁹. NADPH then enters as the reductive agent into the CO_2 -fixation mechanism (see 4.1.).

Since 1942 it has been known, that under special conditions by keeping the oxygen tension very low in a number of algae the production of molecular hydrogen can be induced by light^{130, 131}, if they contain a hydrogenase activity, responsible for H_2 -evolution. Recently it has been shown¹³², that it is possible to alter the conditions in such a way, that solar energy can be used for H_2 -production from water. An improvement of artificial systems leading to hydrogen formation from water by visible light has been achieved by combining isolated chloroplasts with bacterial hydrogenase and chemical binding of the evolved oxygen¹³³. Artificial variations of the photosynthetic apparatus leading to photolytic water cleavage into its elements hydrogen and oxygen, respectively, in separate compartments could be of immense importance for the construction of technical solar energy converters (see also Refs.^{101, 132}).

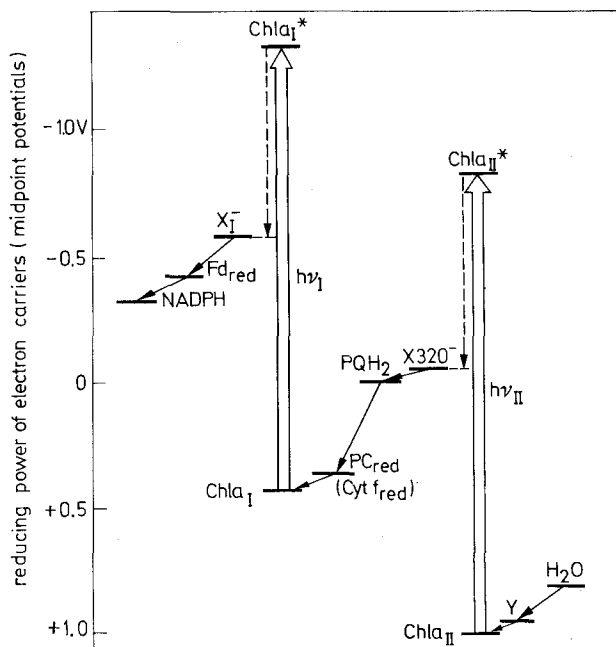


Fig. 8. Simplified free energy diagram of the photosynthetic electron transport chain (for details see Ref. 27, 69). For the sake of simplicity only the reduced forms of the corresponding redox carriers are given. The electronic excitations are symbolized by thick open arrows, thermal redox reactions in the dark are indicated by thin arrows. Abbreviations: Cyt f_{red} = reduced cytochrome f, NADPH = reduced nicotinamide adenine dinucleotidphosphate, PC_{red} = reduced plastocyanine, PQH_2 = plastoquinone, X_I^- and X_{320}^- are the reduced forms of the primary electron acceptor of C_I and C_{II} , respectively [see Eq. (14a, b)], Y = watersplitting enzyme system

4.2.4. Properties of the Electron Transport Chain of the Primary Processes of Photosynthesis

On the basis of the corresponding midpoint potentials there is given in Fig. 8 a free energy diagram of the main steps of the photosynthetic electron transport chain. According to the relation $\Delta G = -n \cdot \mathcal{F} \cdot \Delta E$ (n = number of electrons transferred, \mathcal{F} = Faraday constant and ΔE = electrochemical potential difference) upward directed electron transfer steps are endergonic and downward steps are exergonic. It is seen, that the overall electron transport from water to NADP^+ is driven by light induced electronic excitation at chlorophyll- a_I (Chl- a_I) and chlorophyll- a_{II} (Chl- a_{II}), respectively, [see Chapter 4.2.1. and Eqs. (14a, b) and p. 55]. The electronic excitation energy amounts 1,76 eV ($\lambda = 700$ nm) at Chl- a_I and 1,83 eV ($\lambda = 680$ nm) at Chl- a_{II} . About 70% of this energy should be maximally available for free energy conversion according to theoretical considerations^{135–137}, i.e. 1,23 eV and 1,28 eV, respectively. The redox potential span at the photoelectric generators C_I and C_{II} representing the primarily stored free energy is nearly 1,0 eV (see p. 55). Because additionally free energy is stored in the form of ionic gradients across the thylakoid membrane (see next Chapter 4.2.5.) the above mentioned theoretical values are practically reached. The other

steps of the electron transport chain are conventional exergonic redox reactions (for details of the kinetics and the properties of the corresponding redox components see Ref.⁶⁹⁾ not specific for photosynthesis (see respiratory chain, Chapter 6.4.).

4.2.5. The ATP-Synthesizing System

The mechanism of ATP-synthesis plays a central role in bioenergetics (see also 6.4.2.) because ATP can be envisaged as a universal free energy carrier in biological systems which provides the driving force for nearly all endergonic metabolic reactions. However, it must be strongly emphasized, that ATP is not stored in depots and therefore does not act as free energy reservoir. Since the reactions leading to the formation of ATP as well as to its consumption do not include the direct participation of gaseous compounds only a few remarks will be made within the present framework about the fundamental principles of this energy coupling (for rev. see Ref.^{69, 138, 139)}).

In the ATP-synthesizing system the very important interconversion of electrochemical energy generated by redox reactions into chemical energy (in the form of an "energy-rich" phosphate bond^{s)} takes place. At the present stage of knowledge according to Mitchells theory¹⁴⁰⁾ the light induced (in respiring systems the substrate mediated, see Chapter 6.4.) anisotropic electron transfer within the membrane system (thylakoid or mitochondrial cristae membrane, respectively), leads to the formation of an electrochemical potential gradient across the membrane acting as *coupling membrane* for energy transduction. In photoautotrophs this gradient consists of an electrical component $\Delta\psi$ of maximal 200 mV^{142, 143)} and a proton gradient Δ_{pH} of maximal 3–4 units¹⁴⁴⁾. In this way the coupling membrane becomes energized. The ATP-synthesis occurs within a special enzyme system denoted as ATP-ase¹⁴⁵⁾. This enzyme consists of 3 fundamental elements¹⁴⁶⁾: a) a basepiece bound into the membrane b) a coupling factor containing 5 different types of subunits^{t)} being the site of ATP-synthesis and c) a stalk piece connecting the coupling factor with the base-piece. Mitchells theory postulates that ATP-synthesis is driven by the decay of the electrochemical transmembrane gradient via proton flux through the ATP-ase. However, it is not yet clarified by which mechanism this proton transfer causes the formation of the "energy-rich" chemical bond. Similarly, the details of the chemical reaction sequence leading to ATP-synthesis from ADP and orthophosphate remain to be elucidated.

According to Eq. (6) the fixation of one CO₂-molecule requires 2 NADPH and 3 ATP-molecules, respectively. However, stoichiometrical measurements indicate that the linear noncyclic flow of two electrons from water to NADP⁺ leading to one NADPH-molecule is coupled with the generation of only one ATP-molecule (see e.g. Ref.¹⁴⁷⁾). Thus, an additional ATP-source is necessary. It is often assumed, that there exists a cyclic electron flow driven solely by the photoelectric

s) "Energy-rich" does not refer to the absolute bonding energy. It rather means that the hydrolytic cleavage of this bond leads to a free energy supply ($\Delta G^{\circ'} = -32,6$ kJ/mole at physiological conditions, see Ref.¹⁴¹⁾).

t) The coupling factor has the subunit structure $\alpha_3\beta_3\gamma\delta\epsilon$ where α – ϵ denote the type of subunit and the index the corresponding stoichiometrical number.

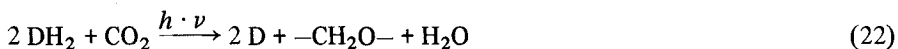
generator C_1 , thus leading only to ATP-synthesis but not to NADP^+ -reduction^{147, 148}). A direct experimental proof for this hypothesis is lacking. Very recently, an interesting mechanism of accommodation of the ATP/NADPH-ratio to the varying metabolic conditions¹⁴⁹) has been proposed¹⁵⁰). It has been found that the site of regulation is probably located at the ferredoxin (see 4.2.3.). Because ferredoxin is a univalent redox carrier of sufficient reducing power ($E_{m,7} = -0,42 \text{ V}$) this substance not only reduces NADP^+ , but in addition is autoxidizable (for the different reactivities of O_2 with univalent and bivalent electron donors see Chapter 6.). It is assumed that NADP^+ and O_2 compete for the electron at reduced ferredoxin¹⁵⁰). At low levels of NADPH, i.e. under metabolic conditions, where reducing equivalents are required, NADP^+ is preferentially reduced with practically no loss of electrons. At high NADPH-levels however, the electrons are transferred to oxygen, so that reducing equivalents are dissipatively destroyed, but ATP-synthesis remains unaffected. In this way the ATP/NADPH-ratio can vary in the wide range of 1 to ad infinitum. However, it should be emphasized that also other types of regulation of the ATP/NADPH-ratio via ferredoxin have been proposed¹⁴⁷). Thus, further experiments are required in order to decide which of these mechanisms is really the *in vivo* regulator.

The problems arising with the reduction of oxygen and the mechanism established to protect living matter to oxidative destruction will be discussed later (chapter 6.2.).

With the development of higher organisms cell differentiation increased leading to the incorporation of other organelles like peroxisomes and mitochondria (see Fig. 3). Thus, all higher plants contain simultaneously autotrophic and heterotrophic systems within the cell. In the light the activity of photosynthesis exceeds significantly that of respiration (see Chapter 4.1.), whereas in the dark plants act as heterotrophs in the same way as is described in Chapter 6.

4.3. Non-oxygen Evolving Autotrophic Organisms

In the philogenetic evolution of photoautotrophic organisms the development of the oxygen evolving machinery appears as the last step (see 4.2.). The primitive autotrophic precursors are the photo-synthetic bacteria which are still able to convert solar radiation energy into chemical energy, but beyond CO_2 and H_2O they need in addition comparatively good donor substances DH_2 (see footnote^{d)}). The photosynthetic bacteria also differ in their pigment content. In contrast to oxygen evolving organisms they contain various forms of bacteriochlorophyll^{u)} instead of chlorophyll. According to the pigmentation mainly caused by carotenoids two types of photosynthesizing bacteria can be distinguished: a) green coloured chloraceae containing bacteriochlorophyll c and d, and b) brownish-red coloured purple bacteria (thiorhodaceae and athiorhodaceae) containing bacteriochlorophyll a and b (for rev. see Ref.^{151, 152}). The overall reaction of bacterial photosynthesis can be described by:



^{u)} Bacteriochlorophyll is a dihydrochlorophyll.

Chloraceae which can live only under strict anaerobic conditions oxidize H_2S as electron donor to elementary sulfur. Sulfur-compounds are also the predominant substrates for thiorhodaceae oxidizing these agents up to the state of sulfate. Some of the species of thiorhodaceae can use certain organic compounds such as fatty acids. Under special conditions they can also be adapted to use molecular hydrogen as electron donor for CO_2 -fixation^{151, 152}. The class of athiorhodaceae preferentially utilizes simple organic compounds (*e.g.* isopropanol is oxidized to acetone), but some species can also be adapted to use molecular hydrogen.

The photosynthetic apparatus of these bacteria is driven by light excitation of photogenerators of principally the same organization scheme as has been reported in 4.2.1. for green plants. The photoelectric generators of the bacteria are pigment-protein complexes, the so-called reaction center complexes, containing bacteriochlorophyll (probably in tetrameric form)^{v)}, bacteriopheophytin and an as yet not unequivocally identified acceptor substance $\text{X}^{153, 154}$. The bacteriochlorophyll-dimer^{v)} acts as primary electron donor in a similar way as Chl-a_I and Chl-a_{II} , respectively, in the photoelectric generators in green plants. However, the redox properties of the electrons and holes produced by the reaction center complex of bacteria closely resembles those of system I in oxygen evolving plants. The midpoint potential of the bacteriochlorophyll-dimer ($E_{m,7} = 0,45 \text{ V}$, see Ref.^{154, 155}) is practically the same as for Chl-a_I (see 4.2.1., p.55). Lately evidence has been presented for bacteriopheophytin as to be acting as primary electron acceptor^{156, 156a}). Therefore, the electrons of the reaction center complex ($E_{m,7} = -0,55 \text{ V}$, Ref.¹⁵⁶) are also of nearly the same reducing power as those of system I in green plants.

As has been reported for green algae (see 4.2.3.) a photoproduction of H_2 can also occur in photosynthetic bacteria. But, in comparison to green algae the H_2 -generation appears to be ATP-dependent¹⁵⁷) and seems to be caused by the action of the nitrogenase system of these organisms¹⁵⁸). The main function of the nitrogenase system, however, is the fixation of nitrogen. This very important biological activity is not restricted to photosynthetic bacteria. Hence, the mechanism of nitrogen incorporation will be described in a separate chapter.

5. Nitrogen Fixation

Nitrogen is an essential nutrient for all living systems. It is indispensable for amino acid synthesis. Amino acids contain nitrogen in the reduced form (oxidation state -3). There are different nitrogen sources available, either in the elementary form as gaseous N_2 -molecules or chemically bound in a variety of organic or inorganic compounds. According to the guiding line of this article only the process of biological N_2 -fixation will be considered.

According to latest estimates¹⁵⁹) metabolic activities lead to the fixation of about 0,18 giga tons nitrogen per annum. Thus, the biological N_2 -fixation rate is rather small

v) It is assumed, that the electronic excitation is delocalized via strong exciton coupling over the whole ensemble of 4 bacteriochlorophylls, whereas the positive charge remaining after photochemical electron transfer is restricted to a bacteriochlorophyll-dimer.

in comparison to the turnover quantities of CO_2 and O_2 (see Chapter 2, p.44). With respect to the total amount of fixed nitrogen about 65% are contributed by biological N_2 -fixation, 20% are provided mainly by industry as chemical fertilizers and 15% by other chemical fixation processes, such as combustion (coal, motor car exhausts) or UV-irradiation. Hence, it is interesting to note that nearly one third of the total amount of nitrogen fixed is caused by the work of man.

The main important chemical property of N_2 is its very high inertia to chemical reactions. As is well known from the technical realization (Haber-Bosch-method, Birkeland-Eyde-method or cyanamid formation by the use of calciumcarbide, see Ref.⁶⁾) special reaction conditions are necessary for N_2 -fixation, which are not applicable in biological systems. Hence, special catalysts of high activity at room temperature are required.

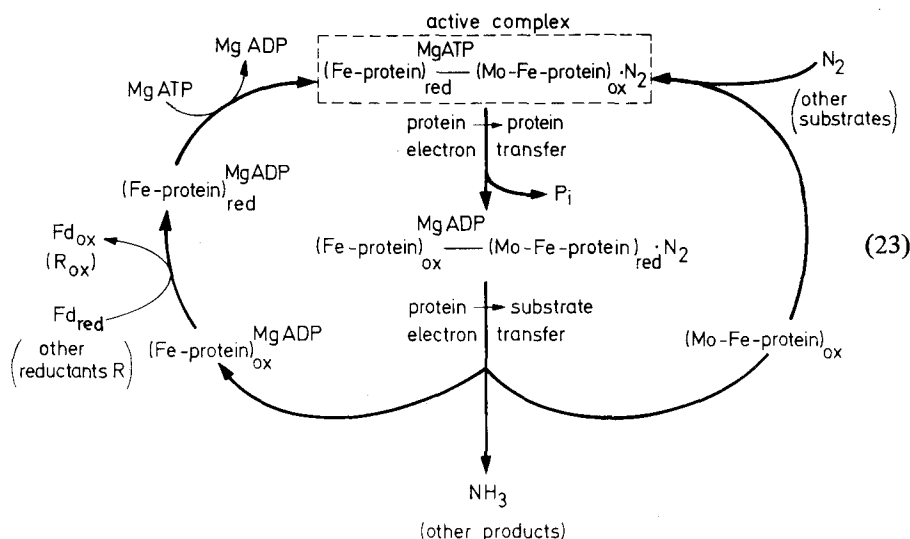
The metabolic N_2 -fixation occurs practically exclusively by microorganisms^{160, 161)} living under different conditions (aerobic, anaerobic, autonom or symbiotic) and it is not restricted to photoautotrophs. Though the diversity of the metabolic states, the N_2 -fixation seems to be performed according to a unique functional principle. N_2 -fixation occurs practically exclusively by reduction to the state of ammonium. All N_2 -fixing organisms contain an enzyme system called *nitrogenase*, which is responsible for N_2 -reduction. For the performance of N_2 -reduction the nitrogenase enzyme system has to solve two problems: a) Activation of the inert N_2 -molecule via distortion of the interatomic bond probably by a sufficient energy supply^{w)} and b) Reduction of activated N_2 by the use of an appropriate electron source of sufficient reducing power.

The nitrogenase is composed of two protein systems^{162, 163)}: a) a larger protein ($M \approx 220\,000$) of a four-subunit structure $\beta_2\gamma_2$ containing 20–30 iron atoms, 2 molybdenum atoms and 20–30 acid labile sulfur groups. This protein will be symbolized here by (Mo-Fe-protein). b) A smaller protein ($M \approx 60\,000$) of two-subunit structure α_2 containing 4 iron atoms and 4 acid labile sulfur groups, referred to as (Fe-protein). Neither of both proteins alone in the isolated form show nitrogenase activity.

Because of its strong reducing power the nitrogenase enzyme system is very sensitive to oxygen. Thus, in aerobic N_2 -fixing organisms a suitable protection to oxygen is required. This can be achieved either by a high respiration rate leading to low oxygen tension (e.g. in *Azotobacter*) or by conformational change induced compartmentation¹⁶⁴⁾ or by separate heterocyst-formation (thick-walled cells lacking oxygen evolving capacity) in blue-green algae¹⁶⁵⁾.

The molecular mechanism of nitrogenase catalyzed N_2 -fixation still remains to be elucidated. It is known that ferredoxin acts as natural electron donor¹⁶⁶⁾ and that ATP (together with mandatory presence of Mg^{2+}) is indispensable for N_2 -reduction at nitrogenase. Five ATP molecules have been found to be required for each electron pair transferred to N_2 ¹⁶⁷⁾. Thus, enzymatic N_2 -fixation needs a high amount of free energy. However, the functional role of ATP is not yet clarified. According to the present stage of knowledge¹⁶⁸⁾ the following general reaction scheme can be drawn. (see Eq. (23))

w) For the complete dissociation of N_2 into nitrogen atoms an energy of 941 kJ/mole is required.



The lower indices 'red' and 'ox' denote the functional important redox states of the protein components^{x)} and the upper indices 'MgADP' and 'MgATP' the binding of these agents to (Fe-protein), respectively.

The activation of N_2 is assumed generally to occur by interaction of the $\sigma_g 2p$ - and $\pi_g 2p$ -molecular orbitals of N_2 with the d -atomic orbitals of Fe and/or Mo, respectively. This should lead in N_2 to a population of the antibonding $\pi_g 2p$ -MO's and to a depopulation of the bonding $\sigma_g 2p$ -MO, respectively, thus giving rise to a weakening of the bonding between the nitrogen atoms (see *e.g.* Ref.¹⁶⁹). Generally two modes for metal- N_2 -interaction of N_2 -coordination can be distinguished, given by Eq. (24 a, b):



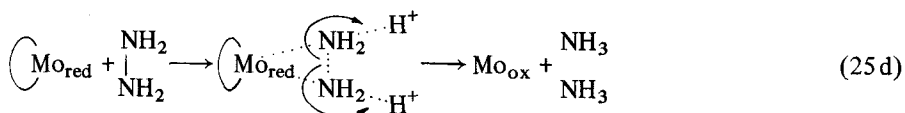
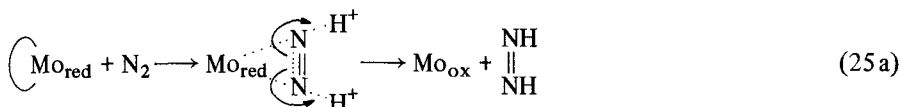
(a) "end-on"-complex

(b) "side-on"-complex

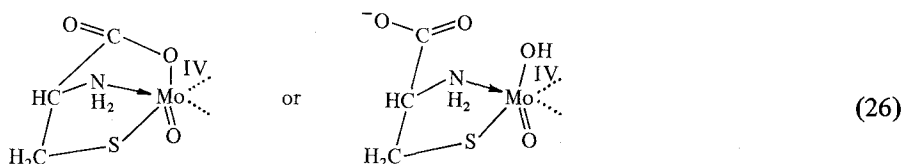
where M represents a transition metal ion.

The "side-on"-coordinated N_2 attains a nitride-like structure and is comparatively reactive. Thus, the formation of a "side-on" metal $\cdot N_2$ -complex in the nitrogenase is a reasonable way for N_2 -activation (for rev. see Ref.¹⁷⁰), but it should be mentioned that "end-on"-complexes have also been discussed as models¹⁷¹). Recent experiments showed¹⁷⁰ that "side-on"-metal $\cdot N_2$ -complexes built up on reduced oxomolybdenum in the valence state +4 and coordinated by cysteine lead to diimid-formation followed by a rapid disproportion or decomposition of diimid and subsequent reduction of the generated hydrazine to NH_3 . The reaction sequence is given by:

^{x)} The indices 'red' and 'ox' do not describe the absolute redox state. Only redox changes occurring in the in vivo cycle will be indicated by these symbols. Furthermore, the scheme does not include the stoichiometrical ATP/e-ratio.



where $\left(\text{Mo} \right)$ symbolizes molybdenum coordinated by cystein in the form:



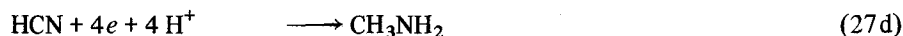
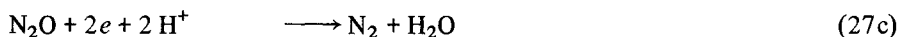
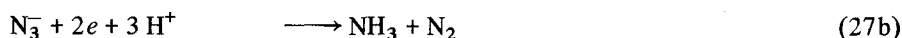
The oxidized molybdenum resulting by reactions (25 a)–(25 d) can be rereduced to its active state *inter alia* by ferredoxin-model compounds of the form $\text{Fe}_4\text{S}_4(\text{SR})_4^{n-}$ (R = alkyl, $n = 2$ in oxidized state and $n = 4$ in reduced state). On the basis of these model systems it has been inferred¹⁷⁰⁾ that the active site for substrate binding and reduction in the nitrogenase is composed of an oxomolybdenum coordinated by a cysteine (or cysteine-like) sulfur group of the apoenzyme. This site, which is active only in the reduced state is assumed to be surrounded by $\text{Fe}_4\text{S}_4(-\text{S-protein})_4^{n-}$ -clusters ensuring the maintenance of the reduced state of the oxomolybdenum.

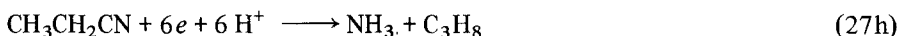
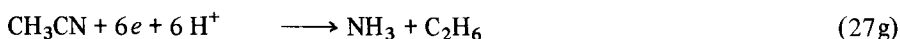
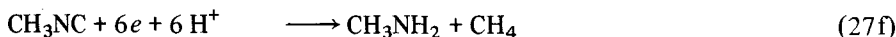
The reduction of N_2 could occur either via a similar way as described above by Eqs. (25 a)–(25 d) or by special stabilization of the diimid and its subsequent direct reduction to NH_3 via N_2H_4 , thus avoiding diimid-disproportionation.

Though these ideas appear to be attractive, for their acceptance direct experimental evidence for this nitrogenase model is required.

It should be emphasized that the above discussed model reactions are not only relevant for a better understanding of the nitrogenase mechanism, but even more important, they could open a door for new technologies of “mild”- N_2 -fixation (see *e.g.* Ref.¹⁶⁹⁾).

Lastly, it should be mentioned, that the enzyme system of nitrogenase is not substrate specific for N_2 . A number of other substances can be also reduced by cell-free nitrogenase. A compilation of the reactions known to occur on nitrogenase is given in the following scheme:

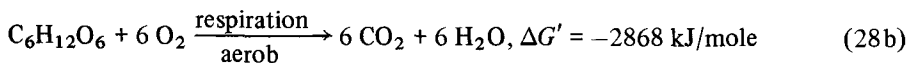
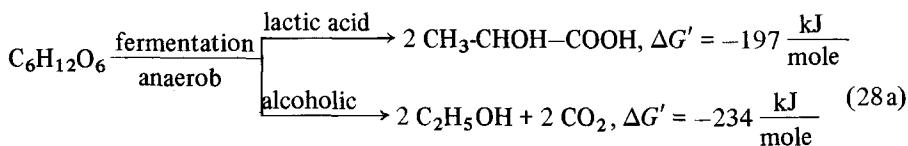




The last reaction leads to the formation of molecular hydrogen. From the dependence of hydrogen evolution of many bacteria it has been inferred¹³¹⁾ that – in contrast to algae (see 4.2.3.) – this process occurs via the nitrogenase catalyzed reaction (27j).

6. Metabolic Processes in Heterotrophic Organisms Involving Gaseous Compounds

Heterotrophic organisms are not able to utilize solar radiation as a source of free energy for their development and sustenance. Hence, they have to uptake from the environment exogeneous compounds of high enough free energy content, so that the chemical reactions of these substances within the biological organisms provide the required free energy. As in the earliest times of evolution the atmosphere was practically anaerobic (see Chapter 3.) only moderate oxidants were available. Thus, the free energy which could be made available from a certain amount of organic material for the energetic demand of the biological organisms was limited by the oxidizing power of the oxidants. However, with the development of oxygen evolving photoautotrophs (see 4.2.) and the advent of significant amounts of oxygen in the atmosphere, the energetical situation of the heterotrophic organisms dramatically changed. Now the same amount of foods became potential providers of much more free energy. This will be illustrated by the comparison of the energetics of the overall reactions of glucose via anaerobic fermentation^{y)} and aerobic respiration^{y)}, respectively.



^{y)} It must be emphasized that the terms “fermentation” and “respiration” are not precisely defined in the literature. Here the term “respiration” includes only catabolic degradation of foods with O₂ via the “respiratory chain”, but not the so-called “substrate respiration”.

Furthermore, other substances being not able to be used under anaerobic conditions became available as free energy sources through the oxidation by oxygen. However, the great advantage of the possibility of having much better energetics in food utilization includes also concomitantly a much higher thermodynamic instability of the biological systems. Thus, the evolution of the oxygenic atmosphere was both, on the one side an opportunity for the development of much higher organized animals with a very much increased free energy requirement and on the other hand a serious challenge for the survival of the existing systems adopted to anaerobic conditions. Most of the anaerobic biological ancestors deceased, some of the simple bacteria being obligate anaerobic, sustained in muds and niches of water which still remained anaerobic. A few hundred megayears later some of them found a new home within the oxygen free spaces (e.g. intestine) of the very highly organized mammals. But, except for these small relicts, a new type of biological systems was developed which acquired the ability to use oxygen as the unique metabolic oxidant for the very efficient exploitation of foods and in addition for the synthesis of new oxygen containing organic compounds. Furthermore, they have had to "construct" special protective systems to the toxic attack by oxygen.

In order to gain an optimal efficiency nature has developed a special machinery for food oxidation by oxygen. These energy converters transform the chemical energy of the foods directly into other forms of chemical energy by synthesis of new compounds or indirectly into osmotic energy by active transport or into mechanical work within muscle cells. It should be clearly emphasized that the biological way of utilization of organic compounds drastically contrasts with man's exploitation of these materials as free energy source. Whereas all biological oxidations are nearly isothermal and thus can be referred to as "cold combustions" resembling in principle to energy conversion in fuel cells, nearly all conventional technical machines are of the heat engine type, i.e. energy transformation occurs via heat as intermediate energy form ("hot combustion"). This way appears to be much less effective. Thus, the question arises: How are the processes of "cold combustion" handled by nature?

Because of the key role which oxygen plays it seems to be worthwhile to discuss first of all some of its properties making this substance the "fittest" oxidant in the biological world, before going into details of the realization of metabolic "cold combustion".

6.1. Thermodynamic and Kinetic Properties of Molecular Oxygen

In the preceding section the bioenergetical advantage of the use of a strong oxidant has been briefly mentioned, however, this is not sufficient for an understanding of the role of molecular oxygen in biology. The oxidizing power of oxygen at physiological pH is slightly lower in comparison to those of chlorine and bromine, respectively, but much less so than that of fluorine²⁾. Thus, these substances, especially flu-

²⁾ The midpoint potential, $E_{m,7}$, of the reactions $\frac{1}{2} X_2 + e \rightarrow X^-$ and $\frac{1}{4} O_2 + e + H^+ \rightarrow \frac{1}{2} H_2O$ are + 2,87; 1,36 and 1,07 V for X = F, Cl and Br, respectively, and 0,82 V for the reduction of O_2 to H_2O .

orine, would allow an even significantly higher energetical expenditure of foods. However, for thermodynamical reasons they are also able to oxidize water. An application of the above mentioned agents in biological systems would be possible only if their reactivity is sufficiently low, but this is known not to be the case. Fluorine avidly reacts with water and practically all organic matter, chlorine is also known to be very aggressive and even bromine leads to rapid destruction of biological systems. Accordingly, the crucial point for the possible use of molecular oxygen as a powerful metabolic oxidant is its reactive property. In order to prevent a spontaneous damage of the biological organisms a rather sluggish reactivity is required. On the other hand, for high biological turnover rates a sufficiently large reactivity is necessary. Thus, a powerful oxidant for biological "cold combustion" should be kinetically nearly inert in the absence, but very reactive in the presence of suitable biocatalysts.

The rather low reactivity of molecular oxygen is caused firstly by its molecular orbital structure, given by $(1\sigma_g)^2(1\sigma_u)^2(2\sigma_g)^2(2\sigma_u)^2(3\sigma_g)^2(1\pi_u)^4(1\pi_g)^2$. Because of the degeneracy of the $1\pi_u$ - and $1\pi_g$ -MO's, respectively, the ground state of oxygen is a triplet (see Fig. 9). On the other hand, practically all stable organic compounds are singlets in their electronic ground states with an electron pair of antiparallel spin in

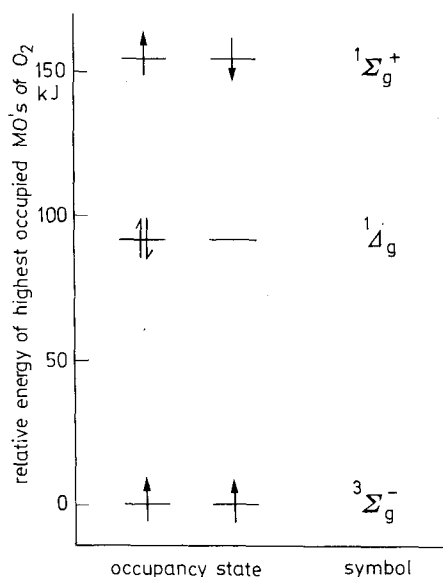
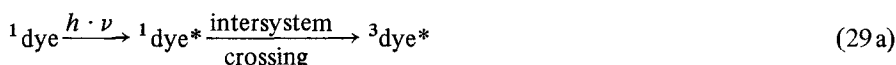


Fig. 9. Energy levels of different electronic occupancy states of the highest degenerated molecular orbitals (MO's) of O_2 (for details see text)

the highest occupied MO. Thus, a simple bimolecular reaction including a two electron transfer from a singlet state donor DH_2 to molecular oxygen in the ground triplet state is spin-forbidden. Ground state O_2 is preferentially reduced by univalent electron donors or via radical chain reactions. But these types of electron transfer reactions do not occur with many organic agents, so that the special electronic situation of O_2 really leads to a rather sluggish reactivity with organic matter as is required for a suitable bio-oxidant. A second factor diminishing the reactivity of O_2 in aqueous solutions is its hydrophobicity. This leads via orientation effects of the water molecules surrounding the O_2 -molecule to a "thermodynamic milieu effect"

which hampers the electron transfer to O_2 ¹⁷²⁾. Thirdly, the bonding energy of O_2 is high enough^{α)} to exclude oxygen atom formation under biological conditions. These facts, together with its gaseous state ensuring a rapid distribution throughout the atmosphere make the molecular oxygen really the "fittest" oxidant for biological systems (for a detailed discussion of the "fitness of oxygen" see Ref.¹⁰⁰⁾). The situation, however, drastically changes for singlet oxygen (see Fig. 9). As the state $^1\Sigma_g$ is very short lived, it is not as dangerous as the $^1\Delta_g$ -state, which is stable enough¹⁷³⁾ to cause serious malign destructions of the organisms. Energetically the singlet state of oxygen could be formed by excitation with visible light (see Fig. 9, Ref.¹⁷⁴⁾). Fortunately, oxygen does not absorb in this wavelength range (otherwise biological organisms could hardly survive under illumination in an oxygenic atmosphere), but indirect light induced singlet oxygen formation can occur via excited sensitizer dyes according to:



or by dark chemical reactions (see Ref.^{175, 176)}).

Thus, the suppression of singlet oxygen formation is an indispensable prerequisite for the survival of living matter under aerobic conditions. Furthermore, as has been mentioned in 4.2.2. very reactive intermediates exist in the reductive pathway of molecular oxygen to water. An accumulation of these intermediates could also destroy the biological systems. Therefore, aerobic organisms have evolved suitable protective mechanisms.

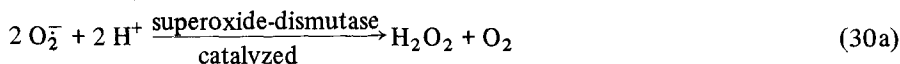
6.2. The Protection of Biosystems to Toxic Attack by Oxygen

Bioluminescence emitting systems have been postulated to be developed by certain bacteria as the earliest defence mechanism to toxic attack by O_2 ¹⁷⁷⁾. It is assumed that the bacteria synthesize special substrates reacting with O_2 under the formation of excited electronic states. Thus, these substrates act as scavenger preventing oxygen from reactions with other materials being necessary for sustenance of the biological apparatus. However, the appearance of bioluminescence in higher animals (fireflies, hatched fish) indicates that bioluminescence probably includes biological functions beyond the simple defence mechanism to oxygen¹⁷⁸⁾. Bioluminescence is not commonly used by biological systems for protection to O_2 , but other mechanisms have been developed. According to Eqs., (29a, b) singlet oxygen formation appears to be a serious problem especially in pigmented and illuminated systems, such as in photoautotrophs. A protective action is possible in a twofold manner: a)

^{α)} The standard free enthalpy of oxygen atom formation is + 233 kJ/mole (gas) and + 254 kJ/mole (aqueous solution), see Ref.¹⁰⁰⁾.

prevention of triplet population of dyes. This protective mechanism has been found to be realized in photo-synthesizing organisms by the carotenoid valve, discussed in 4.2.1., b) rapid quenching of $^1\Delta_g\text{-O}_2$. Carotenoids have been discovered to act also as very effective oxygen singlet quenchers^{179, 180}. Thus, carotenoids play a central role as protective agents as well by triplet dissipation of sensitizer dyes, thus preventing the formation of singlet oxygen, as by singlet oxygen quenching. The carotenoid function is clearly manifested by the fact that carotenoid deficient mutants of photoautotrophs are not viable under aerobic conditions^{39, 181, 182}.

A second problem arises for the protection to the reactive intermediates of the oxygen reduction pathway. A perfect protection should be achieved if oxidations with O_2 in biological systems would be activated by biocatalysts which completely avoid any formation of free intermediate species. Though many enzymes catalyzing O_2 -reduction, like cytochromeoxidase (see 6.4.), seem to act in this manner, a complete suppression of free superoxide radical, O_2^- , and peroxide formation could not be attained. Thus, nature has evolved special enzyme systems acting as scavengers which catalyze rapid disproportion. There exist two types of enzymes: superoxide-dismutases^{183, 184} and catalases^{185, 186}. Their catalytic function is described by:



Furthermore, H_2O_2 decay is also catalyzed by peroxidases^{187, 188} if a suitable electron donor substance, RH_2 , is available:



The above mentioned enzyme systems all contain at the catalytic site transition metal ions specifically coordinated by groups of the apoprotein either directly or indirectly via a porphyrin ring. For the activity the interaction between the d -orbitals of the transition metal ion and the π -molecular orbitals of the substrates seems to play a central role.

Recently, the protective function of the above mentioned enzyme systems has been illustrated on oxygen sensitive superoxide-dismutase deficient bacteria¹⁸⁹. In this respect it is interesting to note that oxygen toxicity and the impossibility of a perfect protection could be also one factor responsible for senescence and ultimate death of the bioorganisms (see also Ref.¹⁸⁹).

6.3. Oxygen Transport Systems

The actual chemical reactions of O_2 occur inside the cells. As the reaction sites are not in direct contact with air and because the solubility of O_2 is comparatively low

an appropriate oxygen transport system is required. Its capacity should be well adaptable to the different metabolic conditions. The oxygen transport occurs via special carrier-protein molecules, myoglobin and hemoglobin. The carrier-proteins bind oxygen reversibly. Whereas in myoglobin oxygen uptake and release follow a hyperbolic curve, hemoglobin shows a characteristic sigmoidal saturation behaviour (see Ref.¹⁹⁰) as is shown in Fig. 10. Hemoglobin has a tetrameric $\alpha_2\beta_2$ -subunit structure. Each

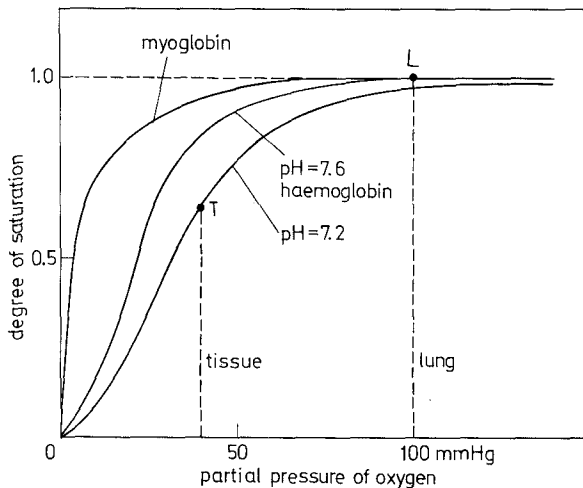


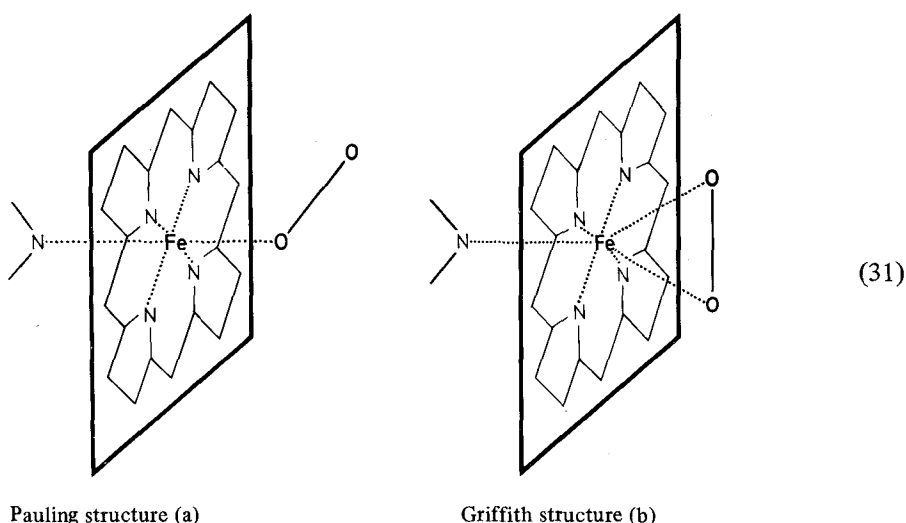
Fig. 10. Degree of saturation with O_2 of myoglobin and hemoglobin as function of partial pressure of O_2 (for details see text)

subunit can attain 2 different conformational states characterized by specific binding capacities. The functional interaction (cooperation) of these subunits is responsible for the sigmoidal saturation curve^{191, 192}. On the other hand, myoglobin has no subunit structure organization. As the protein structure determining the oxygen binding is additionally dependent on other environmental parameters, e.g. pH (Bohr-effect, see Ref.^{193, 194}), the oxygen transport via hemoglobin is adaptable to a wide range of metabolic states. In Fig. 10 the influence of pH on the O_2 -saturation behaviour of hemoglobin is shown. The pH-value of the environment is dependent on CO_2 concentration. In the lung the CO_2 partial pressure is comparatively low (pH higher) and the O_2 partial pressure rather high. Thus, hemoglobin is nearly completely saturated with O_2 (working point L). On the contrary, in the tissue, the CO_2 partial pressure is higher due to the metabolic activity (pH lower) and the O_2 partial pressure is significantly decreased (see Chapter 6.4.). This leads to O_2 release from oxygenated hemoglobin (working point T). In this way hemoglobin realizes the O_2 -transport in animals by switching between the different working states. Typical values for the working states *in vivo* are given in Fig. 10 (see Ref.¹⁹⁵).

The essential functional group, *i.e.* the binding site for O_2 is in myoglobin and in the α - and β -chains of hemoglobin, the sixth position of a five-coordinated ferrous ion (the nitrogen atoms of the four pyrrole groups of the porphyrin ring form a planar quadridentate ligand, the fifth position is coordinated to an imidazole of a histidine-rest of the apoprotein). It is assumed that the reversible O_2 -binding is caused by or-

bital interaction between d -orbitals of the ferrous ion and molecular orbitals of O_2 . It has been suggested¹⁹⁶ that the electrical field of a central metal ion can break the degeneracy of the $1\pi_g(p_x)$ and $1\pi_g(p_y)$ -molecular orbitals of O_2 , respectively. In this way oxygen reaches a "ground state ethylene-like" electronic configuration with four "lone pair" orbitals oriented in the same manner as the hydrogen atoms in ethylene. The lowest unoccupied orbital of O_2 is the $1\pi_g(p_x)$ -MO. The energetic levels of the d -orbitals of the metal ion depend on the coordination shell. Because of the geometric characteristics of the d -orbitals specific interactions are possible depending on the nature of the transition metal ion and the structure of the complex (see Ref.^{197, 197a}). There occurs a two fold interaction between O_2 and the metal ion. Firstly, the "lone pair" orbitals of O_2 interact with single occupied highest d -orbitals (or unoccupied lowest d -orbital) and secondly a "back donation" from occupied metal d -orbitals into the empty antibonding $1\pi_g(p_x)$ -MO of O_2 takes place (back-bonding).

The coordination of O_2 to the metal ion can be directed either towards the "lone pair" orbital of one oxygen atom of O_2 [Pauling-structure, Eq. (31 a), see Ref.¹⁹⁸] or to both oxygen atoms of O_2 [Griffith-structure, Eq. (31 b), see Ref.¹⁹⁶]:



Both types of O_2 -metal complexes are known to exist *in vitro* model systems (for ref. see Ref.^{197, 197a}). An unequivocal decision about the real structure of O_2 -hemoglobin and O_2 -myoglobin has not been reached because some studies favor the Pauling-structure^{199, 200}, other data the Griffith-structure^{197, 201}.

The unique biological O_2 -carrier system, however, has a serious sensitivity to blockage. It does not only bind O_2 but other strong field ligands such as CO. Therefore, these agents act as very dangerous poisons which are able to cause a rapid death of the animals. It is interesting to note, that CN^- is not appreciably bound to reduced hemoglobin. The fatal effect of CN^- -poisoning is mainly caused^{197a} by preventing the catalytic function of cytochrome a in the respiratory chain (s. Section 6.4.2).

6.4. The Metabolic Chemical Reactions of O₂

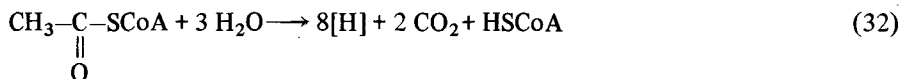
Molecular oxygen serves in biology as substrate for two metabolic important categories of reactions:

- a) Exergonic reduction of O₂ to H₂O by hydrogen donors coupled with the endergonic synthesis of "energy rich" components (see 4.2.5. and footnote⁸).
- b) Introduction of either only one atom or both oxygen atoms of O₂ into substrates catalyzed by mono- and dioxygenases, respectively.

Though the second category of reactions plays an important role for the synthesis of many compounds (*e.g.* hydroxy-derivatives) it will not be discussed here (for *rev. see e.g. Refs.*^{202–204}). The first category represents in the light of the overall process of substrates and products, respectively, the reversal of photosynthesis [see Eq. (1)]. However, with respect to energy transformation it is certainly not the complete back reaction of photosynthesis because no light quanta are produced but rather an inter-conversion of the free chemical energy of substrates either directly into another form of free chemical energy (ATP-synthesis) or indirectly into mechanical work (muscle action) or simply into heat (temperature regulation). It must be clearly emphasized that generally the same structural and functional principles of energy transduction are applied as has been described in chapters 4.1. and 4.2. Thus, only a comparatively short contribution to this subject seems to be justified. The forward reaction of Eq. (1), *i.e.* photosynthesis is localized in special organellae, the chloroplasts. Similarly, the reversal of Eq. (1) also occurs in highly specialized systems, the mitochondria (*e.g. Ref.*^{205, 206}). As was shown in Chapter 4. the overall reaction of photosynthesis is functionally and structurally subdivided into two parts: the cleavage of water by light energy into free molecular oxygen and hydrogen bound to a metabolic carrier (NADPH) accompanied by ATP-synthesis. These reactions take place in a structurally highly organized membraneous system. In the second part the enzyme catalyzed reduction of CO₂ to carbohydrates takes place in an aqueous phase. In analogy, the oxidation of substrates in mitochondria is also functionally and structurally subdivided into two parts. Firstly, the substrates are decarboxylated via an enzyme catalyzed reaction sequence, the Krebs-cycle (see *Ref.*²⁰⁷), under the formation of bound hydrogen (NADH, FADH, succinate) and secondly the hydrogen donors reduce O₂ to water in a special electron transport sequence, the respiratory chain, localized in a structurally highly organized membraneous system within the mitochondria. These reactions are coupled with ATP-synthesis (see *Ref.*^{208, 209}).

6.4.1. The Decarboxylations Leading to the Formation of Metabolically Bound Hydrogen

The overall process leading to the formation of hydrogen bound to metabolic carriers can be separated into two main reaction sequences. Firstly, carbohydrates, amino acids and fatty acids, obtained by enzyme catalyzed cleavage of polysaccharides, proteins and lipids, respectively, are transformed into "active" acetic acid, CH₃–CO–SCoA (where -SCoA represents coenzyme A). Secondly, the "active" acetic acid is degraded into CO₂ and metabolically bound hydrogen (symbolized by [H]) according to Eq. (32):



The reaction Eq. (32) proceeds via a sequence of steps catalyzed by a multi-enzyme system. Because of the chemical nature of the primary acceptor of "active" acetic acid the sequence is referred to as "citric acid cycle", firstly postulated 1937 by Krebs²⁰⁷. The reaction scheme is depicted in Fig. 1.

Most of the reactions are localized in the soluble matrix space (a gel like phase containing 40–50% protein) of the mitochondria. The reaction sequence leading to degradation of "active" acetic acid according to Eq. (32) is slightly exergonic ($\Delta G^{o'} = -105 \text{ kJ/mol}$). The free energy available by oxidation of the products (8[H]) to H_2O is lower by only about 10% ($\Delta G^{o'} = -800 \text{ kJ/mol}$) in comparison to that of the "cold combustion" of "active" acetic acid ($\Delta G^{o'} = -905 \text{ kJ/mol}$) (s. textbooks of biochemistry, e.g. Ref.¹⁹⁵). Thus, the main steps of free energy conversion are coupled with the electron transport leading to oxidation of [H] by O_2 to H_2O . The hydrogen [H] is bound to a few metabolic carriers. The most important of these carriers is NADH, which has the same functional group and practically identical redox properties as NADPH, the main hydrogen acceptor of photoautotrophic organisms (see 4.2.3.). Other carriers for [H] are flavin adenine dinucleotide (FADH) and succinate.

6.4.2. The Oxidation of Metabolically Bound Hydrogen to Water

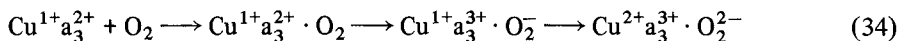
The oxidation by O_2 of [H] (either as NADH or FADH, succinate or directly as "active" acetic acid) occurs via a sequence of electron transfer steps between redox components being incorporated (more or less deeply) into the inner mitochondrial membrane. As is shown in Fig. 11 in the above mentioned electron transport chain, referred to as respiratory chain, the electronic energy is successively decreased step by step. Oxygen is introduced only into the last step of the chemical events in the respiratory chain. Nature has developed a special enzyme system, the cytochrome oxidase, for the realization of oxygen reduction to water. It is assumed that this enzyme system provides the indispensable cooperation of four electrons and protons, respectively, which is required for oxygen reduction:



Thus, cytochrome oxidase can be envisaged as to be the functional counterpart of the watersplitting enzyme system Y, extensively discussed in 4.2.2.

Cytochrome oxidase appears to be a large 6-subunit oligomeric molecule, containing two functional cytochromes (cytochrome a and cytochrome a_3) and two functional copper protein groups, which anisotropically spans the whole inner mitochondrial membrane²¹⁰. It has been found that during the reduction processes of O_2 a change in the valency state of the central copper ions takes place^{211, 212}. On the basis of very recent low temperature experiments²¹³ it has been inferred that in

the reduction pathway leading from O_2 to water, probably peroxide “bridged” between a pair of metal atoms is formed as intermediate^{β)}, according to Eq. (34):



where the indices denote the oxidation states of the central iron of the cytochrome a_3 moiety and of the copper group, respectively. The protonation state of the peroxide is not yet clearly resolved. The exact mechanism of the cooperation of four electrons and protons in the cytochrome oxidase remains to be elucidated.

In the respiratory chain the electrons from NADH traverse exactly the same total redox span as the electrons in the primary processes of photosynthesis as is shown by the dotted scheme in Fig. 11 (compare Fig. 8). However, whereas in the latter process the electronic energy increases due to the expenditure of the light energy, in the respiratory chain the free energy of the electrons falls down to the level of water. This loss of electronic energy is coupled with a gain of free chemical energy by other processes like formation of “energy-rich” bonds (ATP-synthesis) or creation

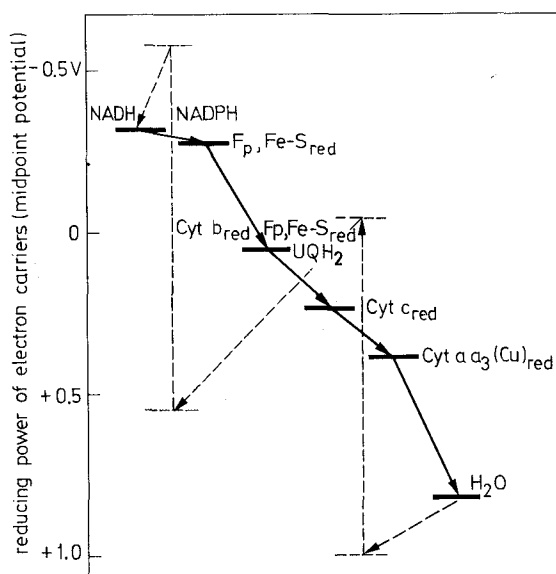


Fig. 11. Simplified free energy diagram of the respiratory electron transport chain (for details see Ref. 208, 209) and text). For the sake of simplicity only the reduced forms of the corresponding redox carriers are given. Electron transfer steps are indicated by thick arrows. For comparison the free energy diagram of photosynthetic electron transport chain is given by dotted lines (excited singlet states of chlorophyll- a_I and chlorophyll- a_{II} are omitted, see Fig. 9). Abbreviations: Cyt aa_3 (Cu) = cytochromoxidase, Cyt b = cytochrome b, Fp = different flavoproteins, Fe-S = different non haem iron-sulfur proteins, UQH_2 = ubiquinone, NADH = reduced nicotinamide adenine dinucleotide

^{β)} The assumption of a bound peroxide is compatible with the fact that H_2O_2 has not been detected in the cytochrome oxidase reaction.

of chemical gradients by active transport. Generally, the inner mitochondrial membrane plays the same important role as functional unit for energy transducing processes as the thylakoid membrane in the chloroplasts. Thus, for the ATP-synthesis principally the same coupling mechanism between electrochemical energy and "energy rich" bond formation is assumed to be realized as has been already discussed in 4.2.4.

The oxidation by oxygen of 2 hydrogen atoms bound to NADH leads to the formation of 3 ATP-molecules, whereas other forms of a metabolically bound [H]-pair (FADH, succinat) can produce only 2 ATP molecules.

Though all higher biological organisms mainly⁷⁾ utilize O₂ as oxidant for the energetical expenditure of organic material some simple bacteria exist using other electron acceptors, such as CO₂, NO₃⁻ or SO₄²⁻. However, these organisms will not be discussed here (see *e.g.* Refs.^{214, 215}).

7. Conclusions

In the present paper it has been shown that quantitatively two gaseous compounds play a central role in the biological world: CO₂ and O₂. Despite their importance (especially N₂ appears to be indispensable as the nitrogen source) other gaseous molecules play a minor role in comparison to the paramount importance of CO₂ and O₂. Both gaseous compounds provide the basis for fundamental processes.

CO₂ is the cornerstone — either as primary substrate in photosynthesis for the anabolism of organic materials or as terminal product of their catabolic degradation — of the immense variety of bio-organic chemistry in living matter. These processes occur mainly in aqueous liquid or gel-like phases and are catalyzed by numerous enzymes.

On the other hand, the H₂O/O₂ system provides the molecular basis for the fundamental processes of bioenergetics. The water cleavage by visible light into O₂ and [H] (accompanied by ATP-synthesis) appears as the primary stable product of transformation of solar radiation into chemical energy, whereas the water formation from O₂ and [H] provides the energetic basis for nearly all heterotrophic organisms. In contrast to the biochemistry including CO₂ the energy transducing reactions connected with cleavage as well as with formation of water require a structurally highly organized membraneous system. The electrochemical potential gradients across biological membranes are of vital importance, because they were shown to represent the basic convertible energy source for nearly all biological activities (for *rev. s.* Ref.²¹⁶).

In the preceding sections it has also been shown that fundamental dynamic quasi equilibrium states exist between the activities of autotrophic and heterotrophic organisms, respectively. The unique role of ozone as indispensable protective agent has been discussed.

⁷⁾ Under special metabolic conditions (O₂-deficiency) other processes (*e.g.* lactate formation, "Pasteur-effect", see Ref.¹⁹⁵) can occur.

Last but not least, it should be strongly emphasized that the immense complex biosphere developed during a very long evolutionary process is very sensitive to rapid deviations above or below critical limits. Thus, "hidden" dangers exist to distort the above mentioned mechanisms by "mankind's work" to a point of no return leading to nearly complete destruction of the basis of life of all higher organized animals.

Acknowledgements. The author would like to thank Dr. P. Gräber, Prof. Dr. W. Junge and Dr. U. Siggel for a critical reading of the manuscript, Miss D. Difiore for correcting the English version and Mrs. B. Sander for drawing the figures. I am also very indebted to my wife for the help in preparing the manuscript.

The financial support by Deutsche Forschungsgemeinschaft und by ERP-Sondervermögen is gratefully acknowledged.

8. References

- 1) Morowitz, H. J.: Energy flow in biology. New York: Academic Press 1968.
- 2) Boltzmann, L.: Der zweite Hauptsatz der Wärmetheorie, in: Populäre Schriften. Leipzig: J. A. Barth 1905.
- 3) Broda, E.: *Naturwiss. Rundschau* 28, 365 (1975).
- 4) Bolin, B.: *Sci. Amer.* 223, 124 (1970).
- 5) Fairbridge, R. W. (ed.): *The Encyclopedia of Geochemistry and Environmental Science*. New York 1972.
- 6) See textbooks of Inorganic or Physical Chemistry.
- 7) Menzel, D. L.: *Ann. Rev. Pharmacol.* 10, 379 (1970).
- 8) Seliger, H. H., McElroy, W. D.: *Light: Physical and biological action*. New York: Academic Press 1965.
- 8a) Löber, G., Kittler, L.: *Photochem. Photobiol.* 25, 215 (1977)
- 9) van Valen, L.: *Science* 171, 439 (1971).
- 10) Berkner, L. V., Marshall, L. C., in: *The origin and evolution of atmosphere and oceans* (Brancazio, P. J., Gameron, A. G. W., eds.), p. 102. New York: Wiley 1964.
- 11) Cloud, P. E.: *Science* 148, 27 (1965).
- 12) Barghorn, E. A.: *Sci. Amer.* 224, 30 (1971).
- 13) Chapman, S.: *Memoirs Roy. Meteorol. Soc.* 3, 103 (1930).
- 14) Johnston, H. S.: *Ann. Rev. Phys. Chem.* 26, 315 (1975).
- 15) Hearing, W. S., Borden Jr., T. R.: *AFCRL-Report*, p. 65 (1965).
- 16) Cicerone, R., Stolarsky, R., Walters, S.: *Science* 185, 1165 (1974).
- 17) Blackman, F. F., Smith, A. M.: *Proc. Roy. Soc. B* 83, 389 (1911).
- 18) Van Niel, C. B.: *Advanc. Enzymol.* 1, 263 (1941).
- 19) Hill, R.: *Proc. Roy. Soc. B* 127, 192 (1939).
- 20) Held, H. W., Werdan, K., Milovancev, M., Geller, G.: *Biochim. Biophys. Acta* 314, 224 (1973).
- 21) Moss, D. N.: *Nature (London)* 193, 587 (1962).
- 22) Black, C. C.: *Ann. Rev. Plant Physiol.* 24, 280 (1973).
- 23) Calvin, M.: *Angew. Chem.* 74, 165 (1962).
- 24) Hatch, M. D., Slack, C. R.: *Ann. Rev. Plant Physiol.* 21, 141 (1970).
- 25) Osmond, C. B., Ziegler, H.: *Naturwiss. Rundschau* 28, 323 (1975).
- 26) Renger, G.: *Physiol. Veg.* 10, 329 (1972).
- 27) Witt, H. T.: *Quart. Rev. Biophys.* 4, 365 (1971).
- 28) Emerson, R., Arnold, W.: *J. gen. Physiol.* 16, 191 (1932).
- 29) Gaffron, H., Wohl, K.: *Naturwiss.* 24, 81 (1936).
- 30) Borisov, A. Yu., Godik, V. I.: *Biochim. Biophys. Acta* 301, 227 (1973).
- 31) Seely, G. R.: *J. Theor. Biol.* 40, 173 (1973).
- 32) Duysens, L. M. N.: *Prog. Biophys.* 14, 1 (1964).
- 33) Robinson, G. W.: *Brookhaven Symp., Biol.* 19, 16 (1967).
- 34) Knox, R. S. in: *Bioenergetics of photosynthesis* (Govindjee, ed.), p. 183. New York: Academic Press 1975.
- 35) Sun, A. S. K., Sauer, K.: *Biochim. Biophys. Acta* 234, 399 (1971).
- 36) Wraight, C. A., Clayton, R. K.: *Biochim. Biophys. Acta* 333, 246 (1974).
- 37) Mytton, R. J.: *Solar Energy* 16, 33 (1974).
- 38) Teale, F. W.: *Biochim. Biophys. Acta* 42, 69 (1960).
- 39) Griffith, M., Sistro, W. R., Cohen-Bazire, G., Stanier, R. Y.: *Nature* 176, 1211 (1955).
- 40) Wolff, Ch., Witt, H. T.: *Z. Naturforsch.* 24b, 1031 (1969).
- 41) Mathis, P., Galmiche, J. M.: *C. R. Acad. Sci., Paris*, 264, 1903 (1967).
- 41a) Monger, T. G., Cogdell, R. J., Parson, W. W.: *Biochim. Biophys. Acta* 449, 136 (1976).
- 41b) Renger, G., Wolff, Ch.: *Biochim. Biophys. Acta* 460, 47 (1977).
- 41c) Manzerall: *Biophys. J.* 16, 87 (1976).
- 41d) Swenberg, C. E., Geacintov, N. E., Pope, M.: *Biophys. J.* 16, 1447 (1976).
- 42) Müller, A., Lumry, R., Walker, M. S.: *Photochem. Photobiol.* 9, 113 (1969).
- 43) Wu, W., Ho, P. P., Alfano, R. R., Seibert, M.: *Biochim. Biophys. Acta* 387, 159 (1975).

- 44) Paschenko, V. Z., Protasov, S. P., Rubin, A. B., Timofeev, K. N., Zamazova, L. M., Rubin, L. B.: *Biochim. Biophys. Acta* 408, 143 (1975).
- 45) Kaufmann, K. J., Dutton, P. L., Netzel, T. L., Leigh, J. S., Rentzepies, P. M.: *Science* 188, 1301 (1975).
- 46) Witt, K., Wolff, Ch.: *Z. Naturforsch.* 25b, 387 (1970).
- 47) Blankenship, R., McGuire, A., Sauer, K.: *Proc. Nat. Acad. Sci. US* 72, 4943 (1975).
- 47a) McIntosh, A. R., Bolton, J. R.: *Nature* 263, 443 (1976).
- 48) Beinert, H., Kok, B.: *Natl. Acad. Sci. - Natl. Res. Council Publ.* 1145, 131 (1963).
- 49) Witt, H. T., Müller, A., Rumberg, B.: *Nature* 192, 967 (1961).
- 50) Norris, J. R., Uphaus, R. A., Crespi, H. L., Katz, J.: *Proc. Nat. Acad. Sci. US* 68, 625 (1971).
- 51) Philipson, K. D., Sato, V. L., Sauer, K.: *Biochemistry* 11, 4591 (1972).
- 52) Evans, M. C., Sihara, C. K., Bolton, J. R., Cammack, R.: *Nature* 256, 668 (1975).
- 53) Döring, G., Renger, G., Vater, J., Witt, H. T.: *Z. Naturforsch.* 24b, 1139 (1969).
- 54) Wolff, Ch., Gläser, M., Witt, H. T., in: *Proc. IIIrd Int. Congr. on Photosynthesis, Rehovot (Avron, M., ed.), p. 295. Amsterdam: Elsevier 1975.*
- 55) Gläser, M., Wolff, Ch., Renger, G.: *Z. Naturforsch.* 31c, 712 (1976).
- 56) Stiehl, H. H., Witt, H. T.: *N. Naturforsch.* 23b, 220 (1968).
- 57) Bensasson, R., Land, E. J.: *Biochim. Biophys. Acta* 325, 175 (1973).
- 58) Ke, B.: *Biochim. Biophys. Acta* 301, 1 (1973).
- 59) Evans, M. C. W., Reeves, S. G., Cammack, R.: *FEBS Letters* 49, 111 (1974).
- 60) Beinert, H., Kok, B., Hoch, G.: *Biophys. Biochem. Res. Commun.* 7, 209 (1962).
- 61) Rumberg, B., Witt, H. T.: *Z. Naturforsch.* 19b, 693 (1964).
- 62) Erixon, K., Butler, W. L.: *Biochim. Biophys. Acta* 234, 381 (1971).
- 63) Knaff, D. B.: *FEBS Letters* 60, 331 (1975).
- 64) Wolff, Ch., Buchwald, H. E., Rüppel, H., Witt, H. T.: *Z. Naturforsch.* 24b, 1038 (1969).
- 65) Junge, W., Witt, H. T.: *Z. Naturforsch.* 23b, 244 (1968).
- 66) Schliephake, W., Junge, W., Witt, H. T.: *Z. Naturforsch.* 23b, 1571 (1968).
- 67) Kraan, G. P. B., Amesz, J., Velthuys, B. R., Steemers, R. G.: *Biochim. Biophys. Acta* 223, 129 (1970).
- 68) Junge, W., in: *Proc. IIIrd Int. Congr. on Photosynthesis, Rehovot (Avron, M., ed.) p. 273. Amsterdam: Elsevier 1975.*
- 69) Witt, H. T., in: *Bioenergetics of photosynthesis (Govindjee, ed.), p. 493. New York: Academic Press 1975.*
- 70) Renger, G.: *Biochim. Biophys. Acta* 440, 287 (1976).
- 70a) Wasielewski, M. R., Studier, M. H., Katz, J. J.: *Proc. Natl. Acad. Sci. US* 73, 4282 (1976).
- 71) Joliot, P., Barbieri, G., Chabaud, R.: *Photochem. Photobiol.* 10, 309 (1969).
- 72) Joliot, P., Joliot, A., Bouges, B., Barbieri, G.: *Photochem. Photobiol.* 14, 287 (1971).
- 73) Kok, B., Forbush, B., McGloin, M. P.: *Photochem. Photobiol.* 11, 457 (1970).
- 74) Forbush, B., Kok, B., McGloin, M. P.: *Photochem. Photobiol.* 14, 307 (1971).
- 75) Lavorel, J.: *J. Theor. Biol.* 57, 171 (1976).
- 76) Siggel, U., Renger, G., Rumberg, B., in: *Proc. IIInd Int. Congr. Photosynthesis Res., Stresa (Forti, G., Avron, M., Melandri, A., eds.) Vol. 1, p. 753. The Hague: Dr. W. Junk Publ. 1972.*
- 77) Diner, B.: *Biochim. Biophys. Acta* 368, 371 (1974).
- 78) Lemasson, C., C. R. Acad. Sci., Paris, 270, 250 (1970).
- 79) Lemasson, C., Barbieri, G.: *Biochim. Biophys. Acta* 245, 386 (1971).
- 80) Renger, G.: *Biochim. Biophys. Acta* 256, 428 (1972).
- 81) Renger, G., Bouges, B., Delosme, R.: *Biochim. Biophys. Acta* 292, 796 (1973).
- 82) Lemasson, C., Etienne, A. L.: *Biochim. Biophys. Acta* 408, 135 (1975).
- 83) Renger, G., Bouges, B., Büchel, K. H.: *J. Bioenergetics* 4, 491 (1973).
- 84) Renger, G.: *Biochim. Biophys. Acta* 314, 390 (1973).
- 85) Cheniae, G. M., Martin, I. F.: *Biochim. Biophys. Acta* 197, 219 (1970).
- 86) Cheniae, G. M., Martin, I. F.: *Biochim. Biophys. Acta* 253, 167 (1971).
- 87) Katoh, S., San Pietro, A.: *Arch. Biochem. Biophys.* 122, 144 (1967).
- 88) Yamashita, T., Butler, W. L.: *Plant Physiol.* 43, 1978 (1968).
- 89) Yamashita, T., Tomita, G.: *Plant and Cell Physiol.* 15, 69 (1974).

- 90) Yamashita, T., Butler, W. L.: *Plant Physiol.* **43**, 2037 (1968).
- 91) Lozier, R., Baginsky, M., Butler, W. L.: *Photochem. Photobiol.* **14**, 323 (1971).
- 92) Döring, G.: *Biochim. Biophys. Acta* **376**, 274 (1975).
- 93) Renger, G., Wolff, Ch.: *Biochim. Biophys. Acta* **423**, 610 (1976).
- 94) Renger, G.: *Z. Naturforsch.* **25b**, 966 (1970).
- 95) Renger, G.: *Eur. J. Biochem.* **27**, 259 (1972).
- 96) Radmer, G., Cheniae, G. M.: *Biochim. Biophys. Acta* **253**, 182 (1971).
- 97) Wydrzynski, T., Zumbulyadis, N., Schmidt, P. G., Govindjee: *Biochim. Biophys. Acta* **408**, 349 (1975).
- 98) Anbar, M., Pecht, I.: *J. Am. Chem. Soc.* **89**, 2553 (1967).
- 99) Creutz, C., Sutin, N.: *Proc. Nat. Acad. Sci. US* **72**, 2858 (1975).
- 100) George, P., in: *Oxidases and related redox systems*, (King, T. E. H., Mason, H. S., Morrison, M., eds.) Vol. 1, p. 3. New York: Wiley 1965.
- 100a) Sprintschnik, G., Sprintschnik, H. W., Kirsch, P. P., Whitten, D. G.: *J. Am. Chem. Soc.* **98**, 2337 (1976).
- 101) Calvin, M.: *Science* **184**, 375 (1974).
- 102) Bray, R. C.: *Proc. Biochem. Soc.* **1969** 13 P.
- 103) Bouges-Bocquet, B.: *Biochim. Biophys. Acta* **292**, 772 (1973).
- 104) Cramer, W. A., Fan, H. N., Böhme, H.: *J. Bioenerg.* **2**, 289 (1972).
- 105) Cox, R. P., Bendall, D. S.: *Biochim. Biophys. Acta* **283**, 124 (1972).
- 106) Bendall, D. S., Sofrova, D.: *Biochim. Biophys. Acta* **234**, 371 (1971).
- 107) Vermeglio, A., Mathis, P.: *Biochim. Biophys. Acta* **292**, 763 (1973).
- 108) Phung Nhu Hung, S.: *Z. Pflanzenphysiol.* **72**, 389 (1974).
- 109) Ben Hayyim, G.: *Eur. J. Biochem.* **41**, 191 (1974).
- 110) Fowler, Ch. F., Kok, B.: *Biochim. Biophys. Acta* **357**, 299 (1974).
- 110a) Fowler, Ch. F.: *Biochim. Biophys. Acta* **459**, 351 (1977).
- 110b) Junge, W., Renger, G., Ausländer, W.: *FEBS-Letters* (in press).
- 110c) Renger, G.: *FEBS-Letters* (in press).
- 110d) Renger, G., Gläser, M., Buchwald, H. E.: *Biochim. Biophys. Acta* (in press).
- 111) Kuttyurin, V. M., in: *Proc. IIInd. Int. Congr. Photosynthesis Res.*, Stresa (Forti, G., Avron, M., Melandri, A., eds.) Vol. 1, p. 93. The Hague: Dr. W. Junk Publ. 1972.
- 112) Harbour, J. R., Tollin, G.: *Proc. Nat. Acad. Sci. US* **69** 2066 (1972).
- 113) Tollin, G.: *J. Bioenergetics* **6**, 69 (1974).
- 114) Mauzerall, D., Chivvis, A.: *J. Theor. Biol.* **42**, 387 (1973).
- 115) Byrn, M. P., Ph. D. thesis, University of California 1966.
- 116) Ley, A. C., Babcock, G. T., Sauer, K.: *Biochim. Biophys. Acta* **387**, 379 (1975).
- 117) Strasser, R. J., Sironval, C.: *FEBS Letters* **28**, 56 (1972).
- 118) Ninnemann, H., Strasser, R. J., in: *Proc. IIIrd Int. Congr. on Photosynthesis*, Rehovot (Avron, M., ed.), Vol. III, p. 1639. Amsterdam: Elsevier 1975.
- 119) Metzner, H.: *J. Theor. Biol.* **51**, 210 (1975).
- 120) Warburg, O., Krippahl, G.: *Z. Naturforsch.* **15b**, 367 (1960).
- 121) Metzner, H.: *Naturwiss.* **53**, 141 (1966).
- 122) Stemler, A., Babcock, G. T., Govindjee: *Proc. Nat. Acad. Sci. US* **71**, 4679 (1974).
- 123) Stemler, A., Radmer, R.: *Science* **190**, 457 (1975).
- 124) Emerson, R., Chalmers, R.: *Plant Physiol.*, Lancaster, **30**, 504 (1955).
- 125) Vishniac, W., Ochoa, S.: *Nature*, London, **167**, 768 (1951).
- 126) Shin, M., Arnon, D. I.: *J. Biol. Chem.* **240**, 1405 (1965).
- 127) Mayerle, J. J., Frankel, R. B., Holm, R. H., Ibers, J. A., Phillips, W. D., Weiher, J. F.: *Proc. Nat. Acad. Sci. US* **70**, 2429 (1973).
- 128) Mason, R., Zubieta, J. A.: *Angew. Chem.* **85**, 390 (1973).
- 129) Shin, M., Tagawa, K., Arnon, D.: *Biochem. Z.* **338**, 84 (1963).
- 130) Gaffron, H., Rubin, J.: *J. Gen. Physiol.* **26**, 219 (1943).
- 131) Stuart, T. S., Gaffron, H.: *Planta* (Berlin) **106**, 91 (1972).
- 132) Benemann, J. R., Berenson, J. A., Kaplan, N. O., Kamen, M. E.: *Proc. Nat. Acad. Sci. US* **70**, 2317 (1973).

- 133) Rao, K. K., Rosa, L., Hall, D. O.: *Biochem. Biophys. Res. Commun.* 68, 21 (1976).
- 134) Nobel, P. S.: *Introduction to plant physiology*. San Francisco: Freeman 1974.
- 135) Duysens, L. M. N.: *Brookhaven Sympos. Biol.* 11, 18 (1959).
- 136) Ross, R. T., Calvin, M.: *Biophys. J.* 7, 595 (1967).
- 137) Knox, R. S.: *Biophys. J.* 9, 1351 (1969).
- 138) Greville, G. D., in: *Current topics of bioenergetics* (Sanadi, D. R., ed.), Vol. 3, p. 1. New York: Academic Press 1969.
- 139) Jagendorf, A. T., in: *Bioenergetics of photosynthesis* (Govindjee, ed.), p. 413. New York: Academic Press 1975.
- 140) Mitchell, P.: *Biol. Rev.* 41, 445 (1966).
- 141) Rosing, J., Slater, E.: *Biochim. Biophys. Acta* 267, 275 (1972).
- 142) Jackson, J. B., Crofts: *FEBS Letters* 4, 185 (1969).
- 143) Gräber, P., Witt, H. T.: *Biochim. Biophys. Acta* 333, 389 (1974).
- 144) Rumberg, B., Siggel, U.: *Naturwiss.* 56, 130 (1969).
- 145) Vambutas, V. K., Racker, E.: *J. Biol. Chem.* 240, 2660 (1965).
- 146) Senior, A. E.: *Biochim. Biophys. Acta* 301, 249 (1973).
- 146a) Nelson, N.: *Biochim. Biophys. Acta* 456, 314 (1976).
- 147) Arnon, D. I., Chain, R. K.: *Proc. Nat. Acad. Sci. US* 72, 4961 (1975).
- 148) Simonis, W., Urbach, W.: *Ann. Rev. Plant Physiol.* 24, 89 (1973).
- 149) Heber, U., Kirk, M. R.: *Biochim. Biophys. Acta* 376, 136 (1975).
- 150) Allen, J. F.: *Nature*, London, 256, 599 (1975).
- 151) Gest, H., Kamen, M. D., in: *Handbuch der Pflanzenphysiologie* (Ruhland, W., ed.), Vol. V/2, p. 568. Berlin – Göttingen – Heidelberg: Springer 1960.
- 152) Frenkel, A. W.: *Biol. Rev.* 45, 569 (1970).
- 153) Clayton, R. K.: *Ann. Rev. Biophys. Bioenerg.* 2, 131 (1973).
- 154) Parson, W. W., Cogdell, R. J.: *Biochim. Biophys. Acta* 416, 105 (1975).
- 155) Kuntz, I. D., Loach, P. A., Calvin, M.: *Biophys. J.* 4, 227 (1964).
- 156) Fajer, J., Brune, D. C., Davis, M. S., Forman, A., Spaulding, L. D.: *Proc. Nat. Acad. Sci. US* 72, 4956 (1975).
- 156a) Grondelle, R. V., Romijn, J. C., Holmes, N. G.: *FEBS-Letters* 72, 187 (1976).
- 157) Gray, C. T., Gest, H., *Science* 148, 186 (1965).
- 158) Hardy, R. W. F., Burns, R. C.: *Ann. Rev. Biochem.* 37, 331 (1968).
- 159) Burns, R. C., Hardy, R. W. F., in: *Nitrogen fixation in bacteria and higher plants*, p. 47. Berlin – Heidelberg – New York: Springer 1975.
- 160) Hardy, R. F. W., Burns, R. C., Parshall, G. W., in: *Inorganic biochemistry*, (Eichhorn, G. K., ed.) Vol. 2, p. 745. Amsterdam: Elsevier 1973.
- 161) Dalton, H., Mortenson, L. E.: *Bacteriol. Rev.* 36, 231 (1971).
- 162) Huang, T. C., Zumpft, W. G., Mortensen, L. E.: *J. Bacteriol.* 113, 884 (1973).
- 163) Burns, R. C., Holstein, R. D., Hardy, R. W. F.: *Biochem. Biophys. Res. Commun.* 39, 90 (1970).
- 164) Yates, M. G., Jones, C. W.: *Advanc. Microbiol. Physiol.* 11, 97 (1974).
- 165) Tel-Or, E., Stuart, W. P. D.: *Nature* 258, 715 (1975).
- 166) Bothe, H., in: *Proc. II Int. Congr. Photosynthesis Res.*, Stresa (Forti, G., Avron, M., Melandri, A., eds.) Vol. 3, p. 2169. The Hague: Dr. W. Junk Publ. 1972.
- 167) Hadfield, K. L., Bulen, W. A.: *Biochemistry* 8, 5103 (1969).
- 168) Zumpft, W. G., Mortensen, L. E.: *Biochim. Biophys. Acta* 416, 1 (1975).
- 169) Fischler, I., Koerner von Gustorf, E.: *Naturwiss.* 62, 63 (1975).
- 170) Schrauzer, G. N., Kiefer, G. W., Tano, K., Doemeny, P. A., *J. Amer. Chem. Soc.* 96, 641 (1974).
- 171) Postgate, J. R. (ed.): *The chemistry and biochemistry of nitrogen fixation*. London: Plenum Press 1971.
- 172) Stauff, J., in: *Biochemie des Sauerstoffs* (Hess, B., Staudinger, H., eds.), p. 26. Berlin – Heidelberg – New York: Springer 1968.
- 173) Arnold, S. J., Kutso, M., Ogryzlo, E. A.: *Advanc. Chem. Ser.* 77, 133 (1968).
- 174) Foote, C. S.: *Science* 162, 963 (1968).

- 175) Kearns, D. R., *Chem. Rev.* **71**, 395 (1971).
- 176) Bonneau, R., Pottier, R., Bagno, O., Jousset-Dubien, J.: *Photochem. Photobiol.* **21**, 159 (1975).
- 177) McElroy, W. D., Seliger, H. H.: *Advanc. Enzymol.* **25**, 119 (1963).
- 178) White, E. H., Miano, J. D., Watkins, C. J., Breaux, E. J.: *Angew. Chem.* **86**, 292 (1974).
- 179) Foote, C. S., Denny, R. W.: *J. Amer. Chem. Soc.* **90**, 6233 (1968).
- 180) Foote, C. S., Chang, Y. C., Denny, R. W.: *J. Amer. Chem. Soc.* **92**, 5216 (1970).
- 181) Stanier, R. Y.: *Brookhaven Sympos. Biol.* **11**, 143 (1959).
- 182) Claes, H.: *Z. Naturforsch.* **9b**, 461 (1954).
- 183) Fridovich, I.: *Acc. of Chem. Res.* **5**, 321 (1972).
- 184) Lumdsen, J., Hall, D. O.: *Biochem. Biophys. Res. Commun.* **58**, 35 (1974).
- 185) Nicholls, P., Schonbaum, G. R., in: *The enzymes* (Boyer, P., Lardy, H., Myrbäck, K., eds.) 2nd ed., Vol. 8, p. 147. New York: Academic Press 1964.
- 186) Brill, S., in: *Comprehensive biochemistry* (Florkin, M., Stotz, E. H., eds.), Vol. 14, p. 447. Amsterdam – London – New York: Elsevier 1966.
- 187) Paul, K. G., in: *The enzymes* (Boyer, P., Lardy, H., Myrbäck, K., eds.) 2nd ed., Vol. 81, p. 227. New York: Academic Press 1964.
- 188) Yamazaki, I., Yokata, K., Nakajima, R., in: *Oxidases and related redox systems* (King, T. E. H., Mason, H. S., Morrison, M., eds.) Vol. 1, p. 485. New York: Wiley 1965.
- 189) Fridovich, I., in: *Horizons biochemistry and biophysics* (Quagliariello, E., Palmieri, E., Singer, E. T., eds.), Vol. p. 1. London: Addison – Wesley Publ. 1974.
- 190) Mahler, H. R., Cordes, E. H.: *Biological chemistry*. New York – Evanston – London: Harper and Row 1967.
- 191) Monod, J., Wyman, J., Changeux, J. P.: *J. Mol. Biol.* **12**, 88 (1965).
- 192) Schuster, T. M., Ilgenfritz, G., in: *Nobel Sympos.* **11** (Engstrom, A. and Strandberg, B., eds.). Stockholm: Almquist and Wiksell 1969.
- 193) Bohr, C., Hasselbalch, K. A., Krogh, A.: *Scand. Arch. Physiol.* **16**, 402 (1904).
- 194) Rollema, H. S., de Bruin, S. H., van Os, G. A. J.: *FEBS-Letters* **61**, 148 (1976).
- 195) Lehninger, A. L.: *Biochemistry*, 2nd ed., New York: Worth Publ. 1975.
- 196) Griffith, J. S.: *Proc. Roy. Soc. A* **235**, 23 (1956).
- 197) Henrici-Olivé, G., Olivé, S.: *Angew. Chem.* **86**, 1 (1974).
- 197a) Hanzlick, R. P.: *Inorganic aspects of Biological and Organic Chemistry*. New York-San Francisco-London: Academic Press 1976.
- 198) Pauling, L., in: *Hemoglobin* (Roughton, F. J. W., Kendrew, J. C., eds.), p. 60. New York: Interscience 1949.
- 199) Watson, H. C., Nobbs, C. L., in: *Biochemie des Sauerstoffs* (Hess, B., Staudinger, H., eds.), p. 37. Berlin – Heidelberg – New York: Springer 1968.
- 200) Maggiora, G. M., Viale, R. O., Igraham, L. L., in: *Oxidases and related redox systems* (King, T. E. H., Mason, H. S., Morrison, M., eds.) Vol. 1, p. 88. New York: Wiley 1965.
- 201) Lang, G.: *J. Appl. Phys.* **38**, 915 (1967).
- 202) Hayaishi, O., Ishimura, Y., Nakazawa, T. and Nozaki, M., in: *Biochemie des Sauerstoffs* (Hess, B., Staudinger, H., eds.) p. 196. Berlin – Heidelberg – New York: Springer 1968.
- 203) Mason, H. S.: *Science* **125**, 1185 (1957).
- 204) Mason, H. S., North, J. C., Vanneste, M.: *Fed. Proc.* **24**, 1172 (1965).
- 205) Green, D. E., Baum, H.: *Energy and mitochondrion*. New York: Academic Press 1970.
- 206) Wainio, W. W.: *The mammalian mitochondrial respiratory chain*, New York: Academic Press 1970.
- 207) Krebs, H. A., Lowenstein, J. M., in: *Metabolic pathways* (Greenberg, D. M., ed.), Vol. 1, p. 129. New York: Academic Press 1960.
- 208) Chance, B., Williams, G. R.: *Advanc. Enzymol.* **17**, 65 (1956).
- 209) Slater, E. C.: *Quart. Rev. Biophys.* **4**, 35 (1971).
- 210) Eytan, G. D., Carroll, R. C., Schatz, G., Racker, E.: *J. Biol. Chem.* **250**, 8598 (1975).
- 211) van Gelder, B. F., Beinert, H.: *Biochim. Biophys. Acta* **189**, 1 (1969).
- 212) Malmström, B. G.: *Quart. Rev. Biophys.* **6**, 389 (1974).
- 213) Chance, B., Saronio, C., Leigh, J. S.: *J. Biol. Chem.* **250**, 9226 (1975).

G. Renger

214) Payne, W. J.: *Bac. Rev.* 37, 409 (1973).

215) Le Gall, J., Postgate, J. R.: *Advanc. Microbiol. Physiol.* 10, 82 (1973).

216) Skulachev, V. P.: *FEBS Letters* 74, 1(1977).

Received March 12, 1976, March 8, 1977

Complex Formation of Monovalent Cations with Biofunctional Ligands

Dr. Wolfgang Burgermeister

Laboratory of Chemistry, NIAMDD, National Institutes of Health, Bethesda, Maryland
20014, U.S.A.

Dr. Ruthild Winkler-Oswatitsch

Max-Planck-Institut für Biophysikalische Chemie, 3400 Göttingen-Nikolausberg, West-Germany

Table of Contents

1. Introduction	93
2. Selectivity and Stability of Complex Formation	94
2.1. Theoretical Aspects on Metal Complex Equilibria	94
2.2. Methods for the Determination of Complex Stability Constants	101
2.3. Stability Constants (Tables 3–14)	108
3. Kinetics and Mechanism of Complex Formation	128
3.1. Theoretical Aspects on Complexation Kinetics	128
3.2. Methods for the Determination of Rate Constants	135
3.3. Rate Constants (Tables 15–19)	138
4. Carrier Mediated Ion Transport through Artificial and Biological Membranes	144
4.1. Carrier Mechanism	146
4.2. Channel Mechanism	149
5. Structure and Conformation of Ionophoric Ligands and their Complexes	151
5.1. Depsipeptides	151
Valinomycin	151
Enniatins and Beauvericin	155
5.2. Depsides	158
Nonactin and its Homologs	158
5.3. Peptides	161
Antamanide	161
Synthetic Cyclopeptides	166






Alamethicin and Suzukacillin	168
Gramicidins A, B and C	169
5.4. Nigericin and Related Openchain Compounds	172
5.5. Synthetic Macrocyclic Polyethers	176
5.6. Synthetic Macrobicyclic and -tricyclic Ligands (Cryptands)	180
5.7. Synthetic Non-Cyclic Ligands	184
6. Application of Carriers	184
6.1. Use of Crown Polyethers as Lipophilizers	184
6.2. Carriers as Elements of Ion Selective Electrodes	185
6.3. Biomedical Applications	185
7. Appendix	
Compilation of Recent Publications on Biomedical Applications of Valinomycin	187
8. References	189

1. Introduction

Over many years alkali ions in solution almost escaped the attention of the chemists. The alkali metals belong to a group of elements which in their common state of ionization possess a closed electronic shell and hence should show a noble-gas-like chemistry. Being charged particles and differing in size the various members of this series of course show individual characteristic interactions with other charged, di- or multi-polar ligands, well understood in terms of classical theory.

Most of the recent interests in this group of metal ions — as far as their properties in solution are concerned — arose in biology, more specifically in neurobiology. Sodium and potassium ions are the major ionic constituents of all inter- and extracellular liquids, and play an outstanding role in electric communication across membranes. The excitation of the nervous membrane, for instance, is closely linked with a rapid exchange of sodium and potassium ions, which in the resting state are separated by means of an active transport mechanism.

Table 1.

Alkali metal	Crystal radius r [Å]	Charge density [Coulomb/Å ³]	Stokes radii ^{a)} of hydrated ions r_s [Å]	Relative size of alkali metal ions	Free energy of hydration $-\Delta G_H$ [kcal/mole]	Rate constant of inner sphere substitution k [sec ⁻¹]
Li	0.6	0.22	3.7		122	$\sim 5 \times 10^8$
Na	0.95	0.088	3.3		98	$\sim 8 \times 10^8$
K	1.33	0.045	2.4		81	$\sim 1 \times 10^9$
Rb	1.48	0.036	2.2		76	$\sim 2 \times 10^9$
Cs	1.69	0.029	2.2		68	$\sim 5 \times 10^9$

^{a)} Corrected according to R. A. Robinson and R. H. Stokes in *Electrolyte Solutions*, Butterworths Scientific Publications, London (1959) p. 125.

In looking at the various physical properties of these cations (cf. Table 1) one realizes especially the differences in size, which manifest themselves clearly in energy parameters. However, the effective sizes of the solvated ions — *i.e.* the Stokes radii — apart from showing a reversed order do not differ greatly. Any simple model based on Brownian motion of totally solvated metal ions under the influence of an electric field gradient could not explain pronounced specificities of electric transport across membranes. In realizing this fact physiologists proposed the idea of a carrier, which via its peculiar molecular architecture could specifically interact with an ion of a

given size. This concept had its true renaissance when C. Moore and B. Pressman in 1964 discovered that the antibiotic valinomycin induces selectively the uptake of potassium ions in mitochondria. In the following years many other antibiotics and also many newly synthesized compounds were found to facilitate the transport of alkali ions across natural and artificial lipid membranes.

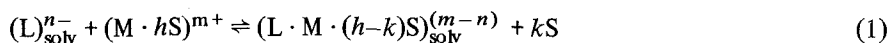
The chemist got confronted with exciting new tasks as to synthesize organic molecules with structures specifically adapted for the binding of metal ions. Natural selection once more proved to be the guiding principle for the elucidation of a scientific problem. The unique biological behaviour now appears to be explainable in terms of physical properties such as complex stability and rates of ligand substitution.

2. Selectivity and Stability of Complex Formation

2.1. Theoretical Aspects on Metal Complex Equilibria

Selectivity of metal carrier action can, in many cases, be reduced to binding equilibrium properties of the metal ions and ligands involved. Where such a model can be applied the information required relates solely to the free energies of the initial and final states of the complexing process, irrespective of the particular type of reaction mechanism. However, selectivity of ion transport could depend on kinetic behaviour, if the rate of equilibration for the complex is slow compared with the rates of decisive steps of transport.

The equilibrium between a metal ion, a multidentate ligand and the resulting complex, can be formally represented by the substitution reaction-scheme:



where L is the (multidentate) ligand, M the metal ion, and S the solvent molecule. The stoichiometry is defined by k , n , m , and h which refer to coordinated solvent molecules replaced by L, (negative) charges of L, (positive) charges of M, and the solvent molecules coordinated by M, respectively. The subscript «solv» refers to additional solvation not further specified.

Thus the relationship:

$$\Delta G^0 = RT \ln K$$

is given by the difference of two sum terms (K is the complex equilibrium constant and RT the thermal energy). Each of these sum terms relates to one of the sides of the equilibrium and encompasses all contributions of the standard free energy G^0 of the corresponding state.

The differences of the two binding energies due to the competition between ligand and solvent molecule constitute the significant contributions to ΔG^0 . The decisive factor is whether the incoming ligand group be more, or less, tightly bound than the replaced solvent molecule. It is important to emphasize that the total binding strength of a multidentate ligand is by no means the simple sum of identical in-

crements of all its single-dentate binding sites. Contributions from charge- and steric-interactions between individual groups and from the possible conformational changes of the ligand as a complete entity, will be present in the sum-total. Effects due to the replacement of solvent molecules from the inner coordination shell of the metal ion have to be taken into consideration as well. This substitution process requires, with decreasing metal ion radius, an increase in energy to compensate for the higher solvation energy. It is known from kinetic data⁶⁶⁾ that one of the solvent molecules in the aqueous coordination shell of an alkali ion can be replaced so easily, that the overall process is diffusion-controlled. Only a fraction of average energy of a solvating water molecule is expended in replacing one of the solvent molecules in the shell. To achieve a comprehensive understanding of the differences in the behaviour of various ligands, a detailed analysis of the reaction mechanism has to account for all these electrostatic influences, which in addition must include relative changes in the solvation of the ligand, and changes in polarization of the medium due to charge neutralization. A consequence of these numerous contributions, the superposition of which may lead to quite varying results, is the discriminating specificity of complexation. This is observed for classes of metal-ions such as alkali and alkaline-earth, which, owing to their noble-gas-like electronic configurations, do not offer particular "chemical" characteristics with respect to the different ligands.

The permutations of intimately interacting energetic influences presents to preparative chemistry the possibility of "tailoring" ligands with any desired cation specificity or selectivity.

This discussion does not attempt a detailed theoretical description. In order to understand the principles of selectivity, based on equilibrium properties, it is sufficient to analyze the major terms of the electrostatic, steric, and solvation energies and to obtain an indication of their orders of magnitude. The free energy of solvation, ΔG_{solv}^0 , is particularly important in this connection. In Table 2 data for ΔG_{solv}^0 are given for the alkali and alkaline-earth ions in water and in methanol. Generally, candidates for effective binding are chelating ligands, which, through their binding energies compete favourably with the solvent molecules.

Table 2. Heat of solvation and free energy of solvation of alkali ions and alkaline earth ions

	$-\Delta H (\text{H}_2\text{O})$		$-\Delta G (\text{H}_2\text{O})$		$-\Delta G_t (\text{H}_2\text{O} \rightarrow \text{CH}_3\text{OH})$ Strehlow
	Noyes	Latimer	Noyes	Latimer	
Li^+	130	121	122		
Na^+	104	95	98	91	-0.41
K^+	83	76	81	75	-0.03
Rb^+	78	70	76	70	+0.06
Cs^+	70	62	68	65	+0.15
Mg^{2+}	473		454		
Ca^{2+}	395		380		
Sr^{2+}	359		340		
Ba^{2+}	325		314		

[Values from Ref.^{275, 276, 325)].}

One can consider a case in which the binding strength of such a multidentate ligand is of the same order of magnitude as that of the solvent molecules in the coordination shell of the cation. Further it can be assumed that the various binding sites of the ligand can be arranged as freely around the metal ion as are the mutually unconnected (or weakly connected) solvent molecules, and that their mutual repulsion, resulting from charge-charge or dipole-dipole interactions, does not exceed the corresponding effects between the solvent molecules in the inner coordination sphere of the metal ion. Whenever these conditions apply simultaneously, one of the extreme monotonic binding-strength dependences, would be expected.

1. The incoming ligand is more tightly bound than the solvent molecule to be substituted. The stability of the complex decreases with increasing radius of the metal ion. Thus, the smaller the metal ion, the larger is the gain in binding energy for each binding site.

2. The incoming ligand is less tightly bound than the solvent molecule. In this case the relationship between complex stability and cation size is reversed, since the relative preference for the solvent molecule increases with decreasing metal ion radius.

This behaviour is depicted in Fig. 1. As mentioned previously, it applies only, if the multidentate ligand is so flexible, that its conformation presents no steric hindrance for any metal ion in the alkali cation series. This means that the ligand binding groups can position themselves as freely around the metal ion as can the solvent molecules.

The alternative extreme is a multidentate ligand, in which the chelating cavity has all the binding groups at fixed positions. A metal ion of appropriate size would

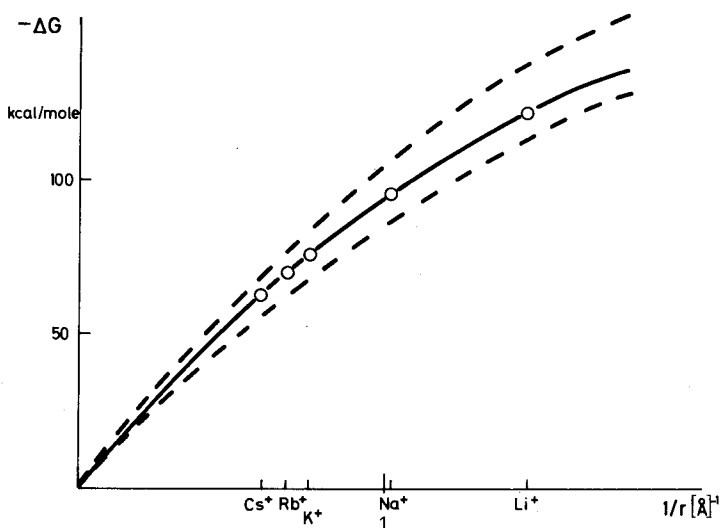


Fig. 1. Free energy ($-\Delta G$) of ligand binding (dashed lines) and of hydration (solid line) of alkali ions as a function of their reciprocal radius

fit optimally into the cavity, and would be distinguished by a maximal (relative) binding strength. A cation of smaller radius than that of the cavity will "rattle". The absolute binding energies of all ions in this category are virtually independent of their size. In an idealized electrostatic picture, these cations could be treated as point charges, whenever they are sufficiently small to fit easily into the cavity. The higher solvation energy of a smaller cation (solvation energy increases with decreasing ion size) destabilizes the complex formation relative to a larger ion which also fits into the cavity.

However, ions requiring more space than the cavity provides, can be accommodated only through introduction of conformational strains in the ligand molecule with respect to the groups constituting the cavity. Therefore the decrease in strength of ligand binding is greater than the decrease in strength of solvation.

The optimum size of the chelating cavity, however, is not determined purely by space requirements. Optimal stability of the metal-ion-binding to the multidentate ligand can only result from an extremum in free energy where all terms involved are superimposed, *i.e.* for the free energy associated with the total substitution process. This situation may or may not coincide with mere spacial fitting.

The lower limit of cavity size is determined by steric interference, as well as by electrostatic repulsion between the coordinating groups. The upper limit, on the other hand, depends strongly on the conformational flexibility of the binding sites within the ligand molecule. J. M. Lehn¹⁶⁷⁾ has demonstrated this effect most clearly by alkali ion complex formation with cryptands. The left curve in Fig. 2 shows the binding of the alkali ion with a sterically fixed cryptand (cf. Fig 67), whereas the right part of Fig. 2 demonstrates the effect of cryptands possessing flexible binding sites which results in a plateau of binding strength for the larger cations.

If one examines the absolute values of the binding curves in comparison with the free energies of solvation, (as illustrated in Fig. 1) it is apparent that there are various alternatives of monotonic dependences and of their superposition, as depicted in Fig. 3 for example. Curve a describes the ion size dependence of the free energy of solvation. The upper curves b and c represent two different series of free energy of ligand binding with respect to the reciprocal metal ion radius. Each individual curve

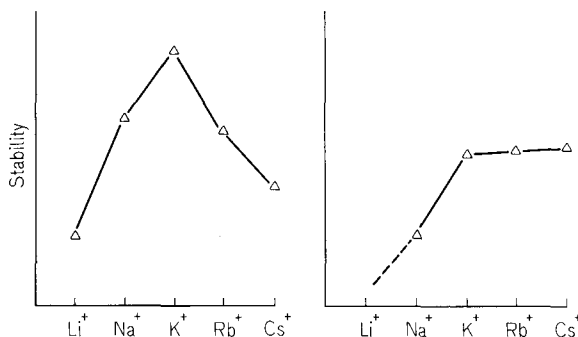


Fig. 2. Selectivity behaviour of a typical rigid ligand ([2.2.2.] $m = n = 1$) expressed as peak selectivity (left) and of a typical flexible ligand ([3.3.3.] $m = n = 2$) exhibiting a plateau selectivity (right). (cf. Fig. 67).

[Reproduced from Lehn, J. M.: Structure and Bonding, 16, 54 (1973).]

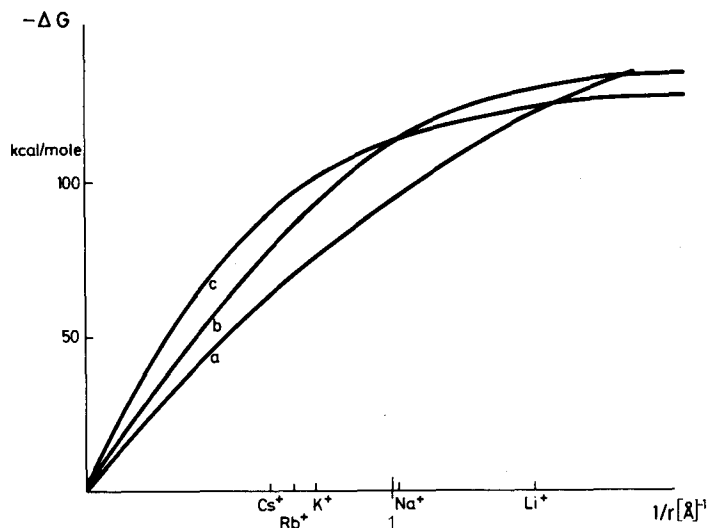


Fig. 3. Free energy ($-\Delta G$) of hydration of alkali ions (curve a) as compared with free energy ($-\Delta G$) of ligand binding for two hypothetical cases of ligand interaction in a chelating cavity (curves b and c), as a function of the reciprocal ionic radius

appears to be monotonic. That is to say: the smaller the ion, the larger its energy of interaction. However, the curvature of these energy relations might differ considerably. The reason for this lies in the very special architecture of the complexing ligand. Selectivity in metal cation complex formation then is the consequence of the superposition of two such energy profiles differing in their curvatures. Such a superposition might in particular lead to a more or less sharp maximum in the binding strength for a given metal ion radius as was shown for the example in the left part of Fig. 2.

How large such an effect could be, may be easily estimated from the magnitude of free energies involved. The discrepancy in free energy of solvation between sodium and potassium ions is of the order of 20 kcal/mole (cf. Table 2). Only a fraction of this amount is effective in the difference between solvation and ligand-binding-energy. Therefore *chelating* ligands play an important role in selective complex formation since they solely are able to substitute a major part or even all of the solvent molecules bound in the inner coordination shell of the metal ion. At this stage it has to be pointed out that 1.4 kcal/mole difference in free energy at room temperature corresponds to a ten-fold change in the stability constant due to $K = \exp(-\Delta G^0/RT)$. Hence one might imagine selectivities, discriminating sodium from potassium, expressed by stability constants which differ by several orders of magnitude. Even larger effects may be expected for alkaline earth ions where the discrepancy in solvation free energies, e.g. between Mg^{2+} and Ca^{2+} , reach values of 60 to 70 kcal/mole.

We may briefly summarize the main consequences of these qualitative considerations. A non-monotonic relationship between free energy and reciprocal ion radius, i.e. selective binding strength, is *not* the result of a particular chemical property of the metal ion as is often the case for the transition metal ions, but is rather the out-

come of a superposition of two partially compensating forces: chelation and desolvation.

From consideration of the whole series of alkali ions, one might conclude, that the rank order of selectivity can be shifted around arbitrarily by using varying architectures for the multidentate ligand. However, this is not the case, since there is always a regularity maintained for the alkali ions within their relative order. As noted in a paper by P. B. Chock and E. O. Titus⁴⁹⁾ theoretically, $5! = 120$ different selectivity patterns should exist, of which only 14 have been observed⁸⁹⁾ thus far. In a summary of his systematic study on selectivity of monovalent cations by means of specific glass electrodes, G. Eisenman reported the following series:

I.	Cs ⁺	>	Rb ⁺	>	K ⁺	>	Na ⁺	>	Li ⁺	
II.	Rb ⁺	>	Cs ⁺	>	K ⁺	>	Na ⁺	>	Li ⁺	or
IIa.	Cs ⁺	>	K ⁺	>	Rb ⁺	>	Na ⁺	>	Li ⁺	
III.	Rb ⁺	>	K ⁺	>	Cs ⁺	>	Na ⁺	>	Li ⁺	or
IIIa.	K ⁺	>	Cs ⁺	>	Rb ⁺	>	Na ⁺	>	Li ⁺	
IV.	K ⁺	>	Rb ⁺	>	Cs ⁺	>	Na ⁺	>	Li ⁺	
V.	K ⁺	>	Rb ⁺	>	Na ⁺	>	Cs ⁺	>	Li ⁺	
VI.	K ⁺	>	Na ⁺	>	Rb ⁺	>	Cs ⁺	>	Li ⁺	
VII.	Na ⁺	>	K ⁺	>	Rb ⁺	>	Cs ⁺	>	Li ⁺	or
VIIa.	K ⁺	>	Na ⁺	>	Rb ⁺	>	Li ⁺	>	Cs ⁺	
VIII.	Na ⁺	>	K ⁺	>	Rb ⁺	>	Li ⁺	>	Cs ⁺	
IX.	Na ⁺	>	K ⁺	>	Li ⁺	>	Rb ⁺	>	Cs ⁺	
X.	Na ⁺	>	Li ⁺	>	K ⁺	>	Rb ⁺	>	Cs ⁺	
XI.	Li ⁺	>	Na ⁺	>	K ⁺	>	Rb ⁺	>	Cs ⁺	

Several of these patterns have also been found with cryptands or other synthetic macrocyclic compounds (such as polyethers and polyamines), antibiotics as well as proteins (cf. below).

Another conclusion suggested by these qualitative reflections is that of solvent dependent complex stability constants. There is a general electrostatic force owing to the metal ion – and possibly the ligand as well – since it is an electrically charged particle. Charging-up always results in an expenditure of work (or increase of free energy). Transferring a charge of valency z from vacuum to a dielectric with the dielectric constant ϵ then corresponds to an equivalent gain in free energy, which can be calculated from the well known Born equation³¹⁾:

$$\Delta G_B = \frac{z^2 e_0^2}{2r} \left(1 - \frac{1}{\epsilon} \right) \quad (2)$$

Similarly, transferring the charge from a medium 1 to a medium 2, characterized by the dielectric constants ϵ_1 and ϵ_2 respectively, means an expenditure or gain of free energy according to:

$$\Delta_{1-2} G_B = \frac{z^2 e_0^2}{2r} \left(\frac{1}{\epsilon_2} - \frac{1}{\epsilon_1} \right) \quad (3)$$

The concept of treating the solvent as a continuous medium of dielectric constant ϵ does not represent a very good approximation in the close vicinity of the cation, which shows the specific structure of the solvation shell. It was therefore suggested^{164, 275, 288}) that at least part of the solvation shell in the apparent ionic radius r should be included and Eq. (2) applied only in order to characterize the long range effects which it indeed describes more satisfactorily. Thus it is important for the discussion of solvent influences on the stability constant to take into account explicitly differences arising from solvation energies — in addition to the term introduced in Eq. (3). Those influences usually are quite large and may shift the stability constant for a given metal-ion-ligand-complex, if transferred from one medium to another, by orders of magnitude. Moreover, they may as well alter the selectivity pattern.

Clear evidence for this phenomenon has been established by D. Haynes and B. C. Pressman^{121b}). The selectivity of valinomycin with respect to Rb^+ , for instance, changes (cf. Table 3) from 0,60 to 2,75 (as expressed by ratios of stability constants relative to K^+ , for which the selectivity number is unity) when transferred from a solvent mixture of 70% toluene and 30% n-butanol to a medium containing 56% toluene and 44% n-butanol. Another example is the reversal of selectivity of dibenzo-18-crown-6 for the fluoryl salts of sodium and potassium. The sodium over potassium selectivity in tetrahydrofuran switches in oxetane to potassium over sodium as reported by K. W. Wong *et al.*³¹²).

However, metal ion solvation and long range dielectric forces are not the only quantities to be considered in analyzing the various alternations of complex stabilities associated with a change of solvent. As an example, the stability constants of alkali ion complexes with macrocyclic ligands are compared in the two solvents water and methanol. They generally show values differing by about four orders of magnitude, with the complex strength in methanol being correspondingly higher than in water. H. Strehlow²⁷⁵) has calculated that the free energies of solvation of the alkali ions should not change by more than 0,5 kcal/mole when transferred from water to methanol (cf. Table 2). The four orders of magnitude discrepancy in stability constants, seen as an energy quantity, is adequate to about 5 to 6 kcal/mole. This discrepancy may in part be due to the fact that solvation energy is a sum (or integral) of several energy terms, which contribute with differing weights to the substitution process. The major portion, however, may be attributed to the solvation changes which the ligand undergoes during complex formation, which are expected to be quite substantial, even if the ligand consists only of polar groups carrying no excess negative charge. The differences in solvent properties with respect to their solvation energies respond particularly to positive and negative charges and to polarities respectively.

Attempts have been made to calculate the mentioned forces more quantitatively. W. Simon and coworkers¹⁹⁵) have been successful in representing their, and other, data by semi-empirical model, so that a reasonable quantitative account of the various reported phenomena can be presented in terms of molecular structure data. To date, little work has been done to apply more rigorous, non-empirical methods of quantum chemistry to problems other than solvation^{67, 157, 261, 269}).

After a short review on equilibration methods we shall present a summary of data on complex stability constants of alkali ions with various chelating ligands.

Details about the chemical nature and the structure of the ligands involved can be found in Section 5. The data in the tables of Section 2.3. reflect the main issue of our discussion, such as selectivity, which sometimes – as e.g. for valinomycin or for certain specially designed cryptands – shows peak values for Li^+ , Na^+ or K^+ , orders of magnitude above the other members of the alkali series. At the same time they demonstrate that the rank order of selectivity within this series might vary considerably.

2.2. Methods for the Determination of Complex Stability Constants

The methods applied for the determination of stability constants of metal complex formation are, as far as the principles are concerned, generally the classical ones. However, important novel sophistications have come into use recently. The methods range from the typical thermodynamic techniques such as vapour pressure osmometry^{150,235,315}, calorimetry^{12,51,101,135,173}, potentiometric recording with ion specific electrodes^{9,90,169,191,245}, to solvent extraction^{91,100,121b,240,241}, and in particular to the various titration concepts utilizing specific chemical couplings (indicators)^{262,263} or unique optical, electrical or magnetic properties of one of the reactants or products. To explain them all in detail is the purpose of a textbook; we therefore restrict ourselves to the description of some recent innovations. (The reader is requested to forgive any bias in the present account towards our own approach to the problem of stability and kinetics of complex formation. Authors from other laboratories also have demonstrated preferences for their own special solutions to this very problem in a variety of review articles published in the past three years^{49, 92, 115, 218, 277}).

Among the techniques mentioned above the more recent advancements were made with alkali ion specific electrodes^{9, 90, 169, 191, 245}. The conventional method here is to use the cation concentration by direct potentiometric recording after calibration with solutions of known content. The electrode potential is given by:

$$E = E_0 + k \log [\text{Me}^+] \quad (4)$$

with coefficient k ranging from 0.045 to 0.065 depending on cation concentration. The sensitivity of the electrode permits detection of the following magnitudes of stability constants¹⁶⁹:

Water:	$\text{Li}^+, \text{Rb}^+, \text{Cs}^+$:	$10 < K_s < 10^4$	$[\text{M}^{-1}]$
	Na^+, K^+	:	$10 < K_s < 10^{5.5}$	$[\text{M}^{-1}]$
Methanol:	Li^+	:	$10 < K_s < 10^5$	$[\text{M}^{-1}]$
	Rb^+, Cs^+	:	$10 < K_s < 10^6$	$[\text{M}^{-1}]$
	Na^+, K^+	:	$10 < K_s < 10^7 \text{ to } 10^8$	$[\text{M}^{-1}]$

W. Simon and coworkers^{9, 245} have refined the concept of ion selective lipid membrane electrodes. Out of the large number of specific ionophores soluble in membranes only few are useful candidates. A series of non-cyclic ligands has been prepared

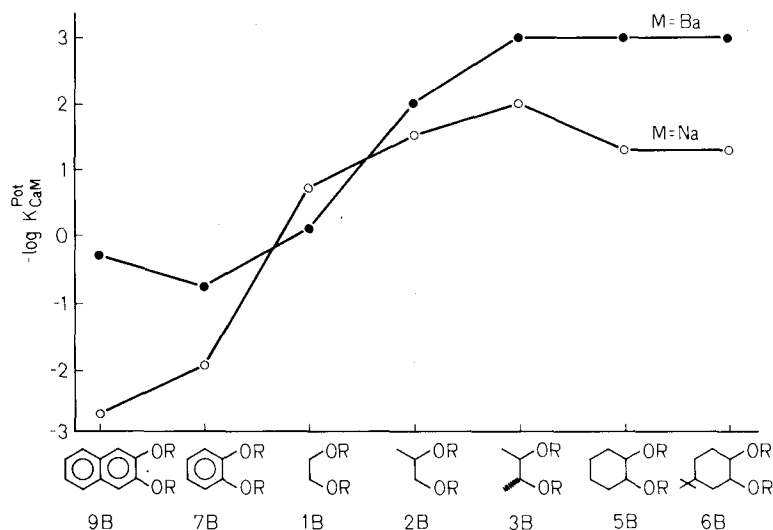


Fig. 4. Influence of structure of ion carrier on the selectivity of the corresponding liquid membrane electrodes. [Reproduced from Amman, D., *et al.*: *Helv. Chim. Acta*. 58, 1539 (1975).]

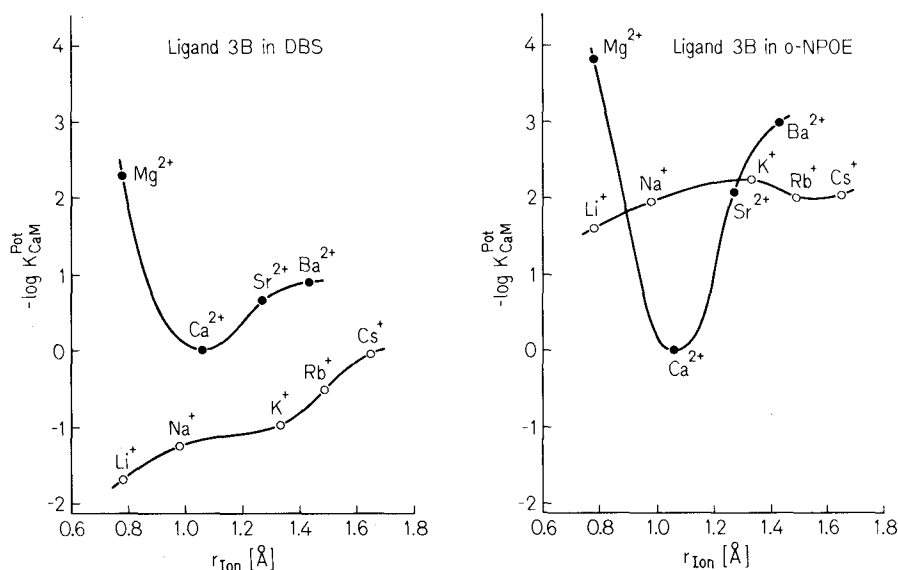
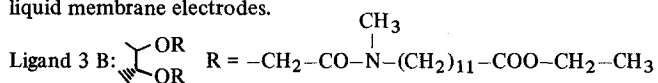


Fig. 5. Influence of the membrane solvent on the selectivity of the corresponding neutral carrier liquid membrane electrodes.



DBS = dibutyl sebacate; O-NPOE = o-nitro-phenyl n-octyl ether.

[Reproduced from Amman, D., *et al.*: *Helv. Chim. Acta*, 58, 1539 (1975).]

which exhibits very high ion selectivity as well as membrane carrier properties. Figs. 4 and 5 show the selectivity of the liquid membrane electrodes studied⁹⁾. The potentiometric selectivity factor K_{NM}^{Pot} is a measure of the preference of cation M relative to cation N exerted by the membrane. Direct use of the membrane soluble ionophore to extract cations from an aqueous phase into an organic phase is also a straight-forward approach. It has been applied preferentially by the research group of G. Eisenman⁹¹⁾, by H. K. Frensdorff¹⁰⁰⁾ as well as by B. C. Pressman and D. Haynes^{121, 240, 241)}. The latter authors have used this technique to study the interaction of Na^+ , K^+ , Rb^+ and Cs^+ with carrier ligands such as valinomycin, macrolide actins, enniatin B and dibenzo-18-crown-6.

A given volume of the organic phase, such as cyclohexane or a mixture of toluene and n-butanol, chloroform of various proportions is shaken with the aqueous phase containing the metal salt, centrifuged and sampled. The radioactive isotopes tested for were: $^{22}Na^+$, $^{42}K^+$, $^{86}Rb^+$ and $^{137}Cs^+$, and the anion to accompany the metal ion into the organic phase in most cases was CNS^- . In the presence of an ionophore the extraction processes become much more efficient. The selectivity ratios obtained through this method are included in Table 3.

With respect to the various titration procedures ingenuity of the researcher is mainly focused on finding a good signal for monitoring the process of complex formation. One obvious choice is conductometry¹⁰⁾ the other spectrophotometry. For the latter the existence of suitable metal ion indicators is of special help. Murexide — once proposed by G. Schwarzenbach^{262, 263)} for Ca^{2+} -titration in aqueous media — works well with most of the alkali ions in non-aqueous phases^{66, 85, 305)}. Otherwise the visible range of the spectrum is not useable for alkali-ion complexes with most of the macrocyclic ligands. Characteristic structures in the spectra of these compounds, of course, are to be expected in the infra-red as well as in the ultra-violet. The UV-spectra of valinomycin, enniatin and certain cryptands have been shown to be sensitive to the presence of alkali ions, with slight differences exhibited for the various cations. Hence stability constants of complexes with biofunctional ligands could be determined by spectrophotometric titration^{48, 115a, b, 103)}. Furthermore, optical rotatory dispersion and circular dichroism provide recordable signals for the detection of alkali metal complexes with carrier compounds. They have especially been applied to enniatin and valinomycin^{112, 115a, b, 132)}. The fluorescence of Tl^+ — as a substituent for alkali ions — turned out to be very useful for measuring stabilities of ionophores with alkali ions as well⁵⁶⁾.

Last but not least nuclear magnetic resonance spectroscopy has to be mentioned in this connection. New advances which have made available more nuclei for a quantitative resonance study increased the applicability of this technique for a study of complex bio-organic structures. NMR-studies^{114, 244, 265)} based on the resonances of H, ^{23}Na and ^{13}C in order to detect metal ion-ionophore interactions (nonactin, dibenzo-18-crown-6 and valinomycin) have been described recently.

Titration methods yield the most direct access to a determination of stability constants, since they provide a means of detecting concentrations of individual reaction partners. The basic purpose of titration was quantitative analysis. Its usefulness for measuring stability constants of the reaction products arrived with the observation of smooth transitions, where originally a sharp end point was expected. Out of

this, the question arises, is it justified to assume that the variation of the composition of a binary reaction in response to an added standard of calibrated concentration really is the best way of obtaining information about the equilibrium parameters? The composition of a system as represented by one of the "true" concentrations, for instance that of the complex due to the law of mass action can be defined as a function of

- i) the total (or weighed-in) concentrations of the sample,
- ii) the total (or weighed-in) concentration of the standard, and
- iii) the stability constant (or the apparent stability constant, referring to a given condition of ionic strength).

In classical titration procedures one looks at the variation of the chemical composition with respect to the change of the standard concentration — utilizing a suitable signal sensitive to any shift in concentration. This variation is dependent on the equilibrium constant and hence provides quantitative information about its value.

There exists another more direct way for determining the equilibrium constant, where the change of chemical composition is brought about by a perturbation of the equilibrium. Variation of temperature, pressure or electric field strength will alter the equilibrium constant. The resulting shift in the proportion of concentrations within the reaction system is a direct measure of the equilibrium constant and the reaction quantity complementary to the external parameter changed (e.g. for T : ΔH and for p : ΔV). This technique proves to be still sensitive under conditions, where the classical titration procedures begin to fail delivering precise data about the binding strength, especially at high complex stabilities. The monitored signals are obtained as amplitudes in relaxation experiments⁸⁷⁾, which refer directly to the shift of the concentration c_{complex} e.g. in case of a temperature jump:

$$\delta c_{\text{complex}} = \frac{\partial c_{\text{complex}}}{\partial \ln K_s} \cdot \frac{\partial \ln K_s}{\partial T} \cdot \delta T = \Gamma \frac{\Delta H}{RT} \cdot \frac{\delta T}{T} \quad (5)$$

Γ represents the desired function, providing the information about the stability constant K_s . ΔH is the enthalpy of reaction, R the gas constant and T the (absolute) temperature. The chemical shift expressed by $\delta c_{\text{complex}}$ has to be recorded instantaneously as a relaxation signal, since only then does it reflect exclusively the chemical response (proceeding with its characteristic time constant), and can clearly be separated from other — physical — changes, brought about by the rapid temperature alternation. In Figs. 6 and 7 the quantity Γ , to be determined by such experiments is plotted as a function of the total standard concentration (at fixed sample concentration). These relaxational titration plots are to be seen in comparison with the well-known classical titration curves and with the derivatives (Figs. 8 and 9), which contain more detailed information about complex stabilities.

For ordinary titration functions, three basic situations have to be distinguished

- i) The stability constant is small compared with the reciprocal weighed-in concentration of the sample, e.g. the ligand: $K_s c_L^0 \ll 1$. An excess of metal ion concentration c_M^0 has to be added in order to arrive at the half-point of the titration curve

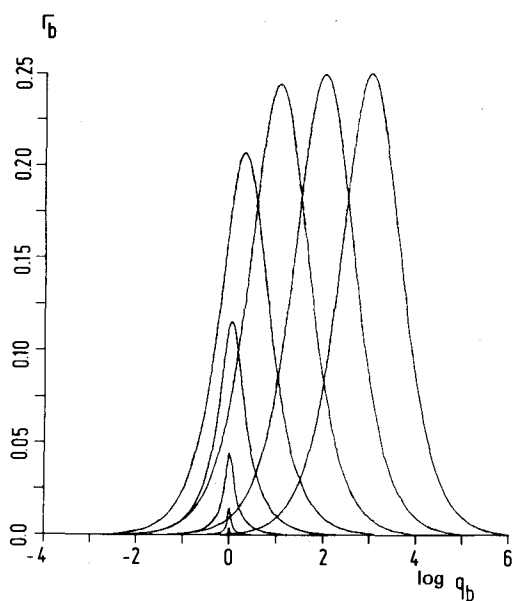


Fig. 6. Relaxation amplitude (Γ_b) as a function of the logarithm of concentration ratio $q_b = c_{\text{stand}}/c_{\text{sample}}$ for various parameters $p_b = K_{\text{stab}}^{-1}/c_{\text{sample}}$

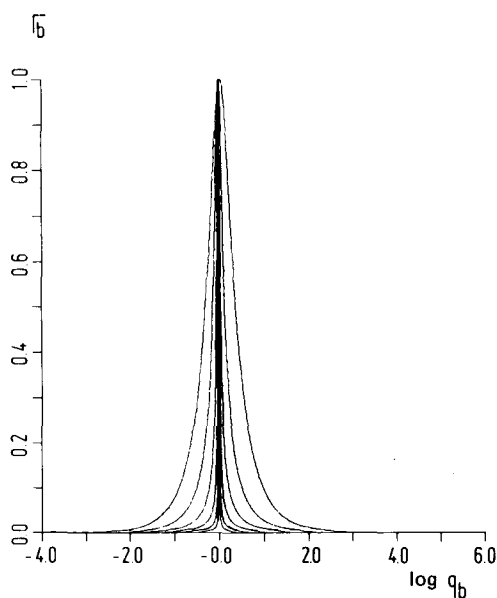


Fig. 7. The variation of the relaxational amplitude (Γ_b) with the parameter p_b normalized to the same maximum value (cf. Fig. 6)

(i.e. where half of the ligand molecules are complexed). The excess of metal over ligand concentration required to reach the half-point is then characteristic of the stability constant. Since at this point c_L^0 is relatively small c_M^0 is a direct measure of K_s^{-1} . Here the titration curve plotted as a function of $\log c_M^0$ possesses an universal shape.

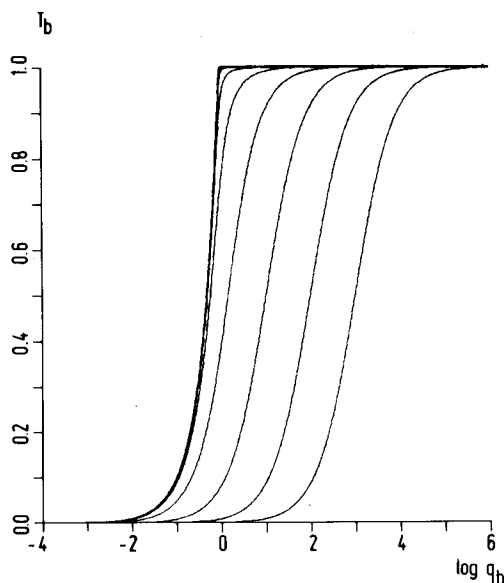


Fig. 8. Classical titration curves, showing the degree of binding (T_b) as plotted versus the logarithm of concentration ratio $q_b = c_{\text{stand}}/c_{\text{sample}}$ for different parameters p_b

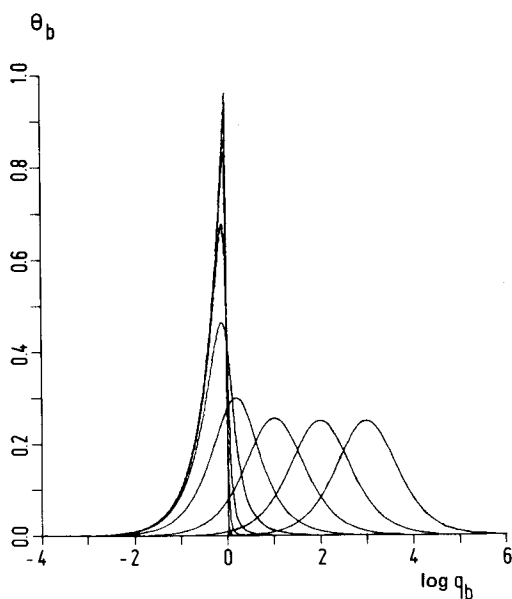


Fig. 9. Slopes of titration curves (cf. Fig. 8): $\theta_b = \frac{dT_b}{d \ln q_b}$. As is seen, for $p_b > 1$ the position of the maximum slope, indicating the inflection point of the titration curve, is a direct measure of p_b . For $p_b \rightarrow 0$, however, a limiting curve is approached

ii) The stability constant is of the same order of magnitude as the reciprocal ligand concentration: $K_s c_L^0 \approx 1$. The amount of excess at the half way point of the titration curve is not a measure of K_s . c_M^0 is rather equivalent to $K_s^{-1} + c_L^0/2$. This means that the shape of the titration curve is characteristic of the complexing constant, since it deviates markedly from the invariant standard form. There exist many useful linear plots – such as the one suggested some time ago by Hildebrand and Benesi²²⁾ – which yield directly data for K_s .

iii) In the limit where $K_s c_L^0 \gg 1$ the titration function again assumes a constant shape marked by an abrupt change of the observable at the equivalence point: $c_M^0 = c_L^0$. Information about K_s is exclusively comprised in the curvature of this changing region. Here the classical titration procedure turns out to be inappropriate for a determination of K_s .

Relaxational titration — as suggested by Figs. 6 or 7 yields results equivalent to the conventional ones (Figs. 8 or 9) under conditions (i) and (ii), whereas it offers considerable advantages in the third case (iii). It is true that also the maximal relaxation effect for $c_M^0 = c_L^0$ decreases with $K_s c_L^0$ becoming larger than unity, however, there exists quite a large range of $K_s c_L^0 \gg 1$ where relaxational signals still can be recorded with sufficient precision. Since the absolute magnitude of the signal depends on K_s , amplification yields a true enhancement. For an optimal evaluation of the titration curve signal enhancement does not help very much, because the information of K_s originates exclusively from relative changes — namely from the second derivative of the titration function —. Another advantage of relaxation amplitude studies is the concomitant determination of reaction enthalpies, based on rather small temperature variations (*i.e.* T -jumps of one to a few degrees in any suitable range). This is a very important prerequisite for the investigation of carrier complexes, which undergo conformation changes with increasing temperature.

The relaxation titration technique has been elaborated to include multiple step processes, for which it offers much more detailed information about equilibrium and rate parameters of individual reaction steps^{305, 88)}. In such situations, conventional titration only delivers data on overall chemical shifts.

Another important application refers to substitution titration. Suppose the ligand (as well as the metal ion) does not exhibit any easily recordable electromagnetic property so that alterations in chemical composition are not directly detectable. For this experimental problem, the use of a suitable indicator is suggested, which complexes favourably with the metal ion or couples to the ligand via some protonation equilibrium and thereby shows specific spectral behaviour. Relaxation titration procedures proved to be specially successful for studies of the complexation of alkali ions with various macrocyclic ligands^{35, 36, 50, 88)} yielding the stability constants originally asked for as well as reaction enthalpies and finally also rate parameters. All the data are listed in the tables, presented in the following section.

2.3. Stability Constants (Tables 3—14)

Table 3. Ion specific ratios for ionophoric ligands determined in several solvents

Ligand	Solvent	Na ⁺	K ⁺	Rb ⁺	Cs ⁺	Ref.
Valinomycin	70% toluene/30% n-butanol	0.00011	1.0	0.60	0.48	121b)
	56% toluene/44% n-butanol	0.0025	1.0	2.75	0.50	121b)
	toluene	0.001	1.0	1.0	0.015	121b)
	50% toluene/50% CHCl ₃	0.024	1.0	1.0	—	121b)
	CH ₂ Cl ₂	0.000017	1.0	1.95	0.62	91)
Nonactin	70% toluene/30% n-butanol	~0.021	1.0	0.54	0.43	121b)
	CH ₂ Cl ₂	0.015 ^{a)}	1.0	0.43 ^{a)}	0.052 ^{a)}	91)
Monactin	70% toluene/30% n-butanol	~0.05	1.0	0.67	0.40	121b)
	hexane	0.0035 ^{b)}	1.0	0.53 ^{b)}	0.19 ^{b)}	91)
	64% hexane/36% CH ₂ Cl ₂	0.0046	1.0	0.22	0.011	91)
	CH ₂ Cl ₂	0.0094	1.0	0.34	0.029	91)
Dinactin	70% toluene/30% n-butanol	~0.021	1.0	1.0	0.21	121b)
	CH ₂ Cl ₂	0.013	1.0	0.40	0.023	91)
Trinactin	70% toluene/30% n-butanol	~0.012	1.0	0.64	0.088	121b)
	CH ₂ Cl ₂	0.011	1.0	0.29	0.019	91)
Enniatin B	70% toluene/30% n-butanol	0.011	1.0	0.15	0.13	121b)
Perhydro-18-crown-6 ^{c)}	70% toluene/30% n-butanol	0.0035	1.0	0.38	0.047	121b)

a) Average values of Table 15 of Ref.⁹¹⁾.b) Based on K_3 -values of Ref.⁹¹⁾ which may have been influenced by ion pairing in the organic phase.c) Mixtures of A and B isomers (cf. Ref.¹⁰⁰⁾).[Table according to Ref.^{121b)}].

Table 4. Stability constants of alkali metal ion complexes

Ligand	Solvent	Temp.	Cation	$K_{stab} [M^{-1}]$	Ref.
OH ⁻	H ₂ O; $\mu \rightarrow 0$	25 °C	Li	8.3×10^{-1}	316)
			Na	2.0×10^{-1}	316)
NO ₃ ⁻	H ₂ O; $\mu \rightarrow 0$	25 °C	Na	$5 \rightarrow 3.2 \times 10^{-1}$	316)
			K	6.3×10^{-1}	
			Cs	1.1 \rightarrow 1.5	
HPO ₄ ²⁻	H ₂ O; $\mu \rightarrow 0$	25 °C	Li	5.2	316)
			Na	4.0	
			K	3.1	
P ₂ O ₇ ⁴⁻	H ₂ O; $\mu \rightarrow 0$	25 °C	Li	1.3×10^3	316)
			Na	2.2×10^2	
			K	2.0×10^2	
			Cs	2.0×10^2	
P ₃ O ₁₀ ⁵⁻	H ₂ O; $\mu \rightarrow 0$	25 °C	Li	7.9×10^3	316)
			Na	6.3×10^2	
			K	6.3×10^2	
			Cs	6.3×10^2	
SO ₄ ²⁻	H ₂ O; $\mu \rightarrow 0$	25 °C	Li	4.0	316)
			Na	5.2	
			K	9.1	
EDTA ⁴⁻	H ₂ O; $\mu = 0.32$ M	25 °C	Li	7.1×10^2	316)
			Na	6.2×10^1	
			K	9.1	
			Rb	3.9	
			Cs	1.4	
			Tl(I)	3.5×10^6	
Dibenzoyl-methane	0.1 M 75% Dioxan	20 °C 30 °C	Li	8.9×10^5	316)
			Na	1.5×10^4	
			K	4.7×10^3	
			Rb	3.3×10^3	
			Cs	2.6×10^3	
Cryptand [1.1.1.] (cf. Fig. 67)	H ₂ O	20 °C	Na	4.0×10^3	68)
			K	1.3×10^5	
			Rb	5.0×10^3	
ATP ⁴⁻	H ₂ O; $\mu = 0.1$	30 °C	Na	1.5×10^1	316)
			K	1.4×10^1	

EDTA⁴⁻: Ethylene-diamino-tetraacetate.ATP⁴⁻: Adenosine triphosphate.

Table 5. Stability constants of complex formation between murexide and several open chain ionophoric ligands with alkali cations

Ligand	Solvent	Temp.	Cation	$K_{stab} [M^{-1}]$	Method	Ref.
Murexide ^{a)}	MeOH	25 °C	Li	7.1×10^2	OD	305)
			Na	2.5×10^3		
			K	1.1×10^3		
Nigericin (cf. Fig. 53)	MeOH	25 °C	Na	9.2×10^3	EFP	50)
			Na	1.0×10^4	CAL	173)
			K	5.0×10^5		
Monensin (cf. Fig. 53)	MeOH	25 °C	Na	1.3×10^6	CAL	173)
			K	9.5×10^4	EMF	172)
			Tl(I)	2.6×10^4	FL	56)
X-537 A (cf. Fig. 53)	EtOH	25 °C	Na	1.5×10^6	FL	56)
			K	1.4×10^6		
			Rb	1.2×10^6		
			Cs	9.5×10^5		
			Tl(I)	2.5×10^6		
	MeOH	25 °C	Tl(I)	2.4×10^4	FL	56)

OD: Optical density.

FL: Fluorescence.

EFP: Electric field pulse.

EMF: Electromotive force.

a)

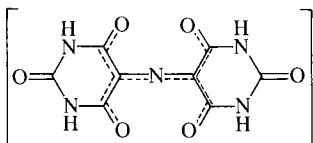


Table 6. Stability constants of the complex formation of depsides with alkali cations

Ligand	Solvent	Temp.	Cation	$K_{stab} [M^{-1}]$	Method	Ref.
Nonactin	MeOH	25 °C	Li	< 2	UV, Ind.	50)
			Na	2.3×10^2		
			K	1.4×10^4		
			Rb	1.4×10^4		
			Cs	1.5×10^3		
			NH ₄	2.4×10^4		
		30 °C	Tl	1.4×10^4	FL VPO	56) 315)
			Na	2.7×10^2		
			K	4.9×10^3		
			Rb	4.2×10^3		
			Cs	9.2×10^2		
			Na	2.3×10^3		
Monactin	MeOH	25 °C	Li	< 2	UV, Ind.	50)
			Na	4.0×10^2		
			K	2.4×10^4		
			Rb	2.4×10^4		
			Cs	2.0×10^3		
			NH ₄	4.8×10^4		
		30 °C	Tl	3.7×10^4	FL VPO	56) 315)
			Na	4.2×10^2		
			K	1.4×10^4		
			Rb	4.2×10^3		
			Cs	1.4×10^3		
			Na	3.8×10^3		
Dinactin	MeOH	25 °C	Li	< 2	UV, Ind.	50)
			Na	1.1×10^3		
			K	4.3×10^4		
			Rb	4.2×10^4		
			Cs	4.2×10^3		
			NH ₄	9.1×10^4		
		30 °C	Tl (I)	7.1×10^4	FL VPO	56) 315)
			Na	9.6×10^2		
			K	6.7×10^3		
			Rb	5.3×10^3		
			Cs	2.2×10^3		
			Na	5.5×10^3		
Dinactin	EtOH	30 °C	Na	3.8×10^3	VPO	315)
			K	3.7×10^3		
			Na	3.8×10^3		
			K	3.7×10^3		
			Na	3.8×10^3		
			K	3.7×10^3		
		30 °	Na	3.8×10^3	VPO	315)
			K	3.7×10^3		
			Na	3.8×10^3		
			K	3.7×10^3		
			Na	3.8×10^3		
			K	3.7×10^3		

Complexformation of Monovalent Cations with Biofunctional Ligands

Ligand	Solvent	Temp.	Cation	$K_{stab}[M^{-1}]$	Method	Ref.
Trinactin	MeOH	25 °C	Li	< 2	UV, Ind.	50)
			Na	1.7×10^3		
			K	9.1×10^4		
			Rb	7.7×10^4		
			Cs	1.0×10^4		
			NH ₄	2.1×10^5		
	EtOH	30 °C	Rb	9.0×10^3	VPO	315)
			Cs	2.8×10^3		
			Na	4.5×10^3		

UV: Ultraviolet absorption.

Ind.: Use of indicator

VPO: Vapour pressure osmometry.

FL: Fluorescence.

Table 7. Stability constants of complex formation of depsipeptides with alkali cations

Ligand	Solvent	Temp.	Cation	K_{stab} [M ⁻¹]	Method	Ref.		
Valinomycin	H ₂ O	25 °C	K	1.5×10^{-1}	Extrapolated from values below	115b) 94)		
			K	2.3				
			Rb	5.9				
			Cs	1.2×10^{-1}				
	90% MeOH/10% H ₂ O	25 °C	K	4.7×10^3	UV, CD	115a)		
	80% MeOH/20% H ₂ O		K	8.7×10^2				
	70% MeOH/30% H ₂ O		K	9.3×10^1				
	50% MeOH/50% H ₂ O	25 °C	K	1.1×10^1	TJ	115b)		
	90% MeOH/10% H ₂ O		K	4.5×10^3				
	$\mu = 0.1$ M LiCl		K	6.0×10^2				
	80% MeOH/20% H ₂ O							
	$\mu = 0.1$ M LiCl							
	70% MeOH/30% H ₂ O	25 °C	Cs	1.5×10^2	UV, CD	112)		
			K	6.5×10^1				
			Li	< 5				
			Na	4.7				
			Na	1.2×10^1				
	MeOH	25 °C	K	8.0×10^4	EMF	307)		
			K	$> 8.0 \times 10^3$	UV, CD	112)		
			Rb	1.8×10^5	EMF	307)		
			Cs	2.6×10^4	UV, CD	112)		
			NH ₄	4.7×10^1	FL	56)		
			Guani-	2.5				
			dinium					
			Tl(I)	5.4×10^3				
			Tl(I)	2.3×10^4				
			MeOH	25 °C	K	3.0×10^4	US, TJ	103)
	$\mu = 0.1$ M TBAP							
	EtOH	25 °C	Rb	6.5×10^4	COND ¹³ C-NMR COND	10) 115b) 268)		
			Cs	8.0×10^3				
K			2.0×10^6					
K			1.5×10^6					
K			2.0×10^6					
Rb			2.6×10^6	FL	56)			
Cs			6.5×10^5					
Tl(I)			4.2×10^4					
Na			$< 1 \times 10^{-2}$			UV, CD	113)	
K			1.2					
Rb	1.4							
Membranebound	25 °C	Cs	3.0×10^{-1}					
		K	1.2×10^3	EMF	307)			
		Enniatin A	MeOH	25 °C	K	1.2×10^3	EMF	307)

Table 7. (continued)

Ligand	Solvent	Temp.	Cation	$K_{stab} [M^{-1}]$	Method	Ref.		
Enniatin B	MeOH	25 °C	Li	1.9×10^1	UV, CD	112)		
			Na	2.6×10^2	EMF	307)		
			Na	2.4×10^2				
			K	8.4×10^2				
			K	8.3×10^2	UV, CD	112)		
			Rb	5.5×10^2				
			Cs	2.2×10^2				
			NH ₄	8.3×10^1				
			Tl(I)	5.2×10^2	UV, CD	115a)		
	90% MeOH/10% H ₂ O	25 °C	K	2.8×10^2				
			80% MeOH/20% H ₂ O	K			1.2×10^2	
			70% MeOH/30% H ₂ O	K			4.4×10^1	
			50% MeOH/50% H ₂ O	K			1.5×10^1	
			EtOH	25 °C			Na	1.3×10^3
	Na	2.6×10^3					ORD	132)
	K	3.7×10^3			COND	267)		
	K	6.5×10^3			ORD	132)		
	Rb	4.0×10^3			COND	268)		
	Cs	2.2×10^3						
	Membrane-bound	25 °C			Na	$< 2 \times 10^{-2}$	UV, CD	113)
					K	8		
			Rb	2.5				
			Cs	1×10^{-1}				
Enniatin C	EtOH	25 °C	Na	2.5×10^3	COND	267)		
			K	5.5×10^3				
			Rb	7.5×10^3				
			Cs	4.1×10^3				
Beauvericin	EtOH		Li	1.0×10^2	COND	212)		
			Na	3.0×10^2				
			K	3.1×10^3				
			Rb	3.5×10^3				
			Cs	3.5×10^3				

UV: Ultraviolet absorption, CD: Circular dichroism, ORD: Optical rotatory dispersion.

TJ: Temperature-jump relaxation method.

EMF: Electromotive force.

FL: Fluorescence.

US: Ultrasonic absorption.

NMR: Nuclear magnetic resonance.

COND: Conductometry.

TBAP: Tetrabutylammonium perchlorate.

Table 8. Stability constants of the K^+ complex and antibiotic activity of valinomycin and some of its analogs²¹⁷⁾

Analog number	Compound	$K_{stab} [M^{-1}]$ (EtOH, 25 °C)	Antimicrobial activity against <i>Staphylococcus aureus</i> UV-3 (minimal growth inhibiting concentration $\mu g/ml$)
1	Cyclo[(-D-Val-L-Lac-L-Val-D-HyIv-) ₃] = Cyclo(-A ₃ -) Valinomycin	2×10^6	0.2 – 0.4
2	Cyclo(-A ₂ -) "Octa-valinomycin"	$< 5 \times 10^1$	> 100
3	Cyclo(-A ₄ -) "Hexadeca-valinomycin"	1×10^2 a)	> 50
4	Cyclo(-D-Leu-L-Lac-L-Leu-D-HyIv-A ₂ -)	1.3×10^5	2
5	Cyclo(-D-Val-L-Ala-L-Val-D-HyIv-A ₂ -)	3×10^5	0.1
6	Cyclo(-D-Val-L-Lac-L-HyIv-D-HyIv-A ₂ -)	2.5×10^3	> 50
7	Cyclo(-D-Val-L-Lac-L-MeVal-D-HyIv-A ₂ -)	$< 5 \times 10^1$	> 50

a) Cs^+ complex: $K_{stab} = 5 \times 10^2 [M^{-1}]$.

Table 9. Stability constants of complex formation of cyclic peptides with alkali cations

Ligand	Solvent	Temp.	Cation	$K_{stab} [M^{-1}]$	Method	Ref.
Antamanide	MeOH	25 °C	Li	< 10	UV	301)
		45 °C	Na	5.0×10^2	VPO	
		25 °C	K	10	UV	
	EtOH	45 °C	Na	2.5×10^4	VPO	35a)
			K	2.8×10^2		
		25 °C	Na	2.8×10^3	COND	11)
	96% EtOH/4% H ₂ O		K	2.7×10^3		
		45 °C	Na	2.0×10^3	VPO	300, 301)
		25 °C	K	1.8×10^2	CSE	300, 301)
	CH ₃ CN	45 °C	Na	3.0×10^4	VPO	301)
Cyclo(Pro-Gly) ₃ (cf. Fig. 45)	96% CH ₃ CN/4% H ₂ O		K	2.9×10^2		
		45 °C	Li	1.3×10^2	VPO	301)
			Na	2.6×10^3		
	92% CH ₃ CN/8% H ₂ O		K	2.0×10^1		
		45 °C	Na	1.2×10^3	VPO	301)
					CD	175)
	H ₂ O	25 °C	Na	2.2		
	80% MeOH/20% H ₂ O	25 °C	Li	1.8×10^2	CD	175)
			Na	1.1×10^2		
			K	2.9×10^1	CD	

COND: Conductometry.

VPO: Vapour pressure osmometry.

CSE: Cation selective electrode.

UV: Ultraviolet absorption, CD: Circular dichroism.

Table 10. Stability constants of complex formation of antamanide analogs with sodium and potassium in several solvents

Ligand	Solvent	$K_{stab} [M^{-1}]$ Na^+	$K_{stab} [M^{-1}]$ K^+	Method	Ref.
Leu ¹ -Antamanide	96% EtOH/4% H ₂ O	1.0×10^3	—	CSE	301)
Ile ¹ -AA	96% EtOH/4% H ₂ O	2.3×10^3	—	CSE	301)
Abu ¹ -AA	96% EtOH/4% H ₂ O	1.5×10^3	—	VPO	301)
Ala ¹ -AA	96% EtOH/4% H ₂ O	1.5×10^2	—	CSE	301)
Gly ¹ -AA	96% EtOH/4% H ₂ O	1.8×10^2	—	CSE	301)
Tyr ⁶ -AA	96% EtOH/4% H ₂ O	2.0×10^3	—	CSE	301)
[O-glucosido]-Tyr ⁶ -AA	96% EtOH/4% H ₂ O	1.7×10^3	—	CSE	301)
[O-dodecyl]Tyr ⁶ -AA	96% EtOH/4% H ₂ O	< 10	—	CSE	301)
(Br ₂)-Tyr ⁶ -AA	96% EtOH/4% H ₂ O	3.5×10^3	—	VPO	301)
Gly ⁷ -AA	96% EtOH/4% H ₂ O	6.0×10^1	—	CSE	301)
Des-Pro ⁸ -AA	96% EtOH/4% H ₂ O	< 10	—	CSE	301)
Gly ¹ , Gly ⁴ -AA	CH ₃ CN	1.9×10^3	—	VPO	301)
	MeOH	4.0×10^1	—	VPO	301)
	96% CH ₃ CN/4% H ₂ O	2.5×10^2	$\begin{cases} 2.0 \times 10^2 (Li^+) \\ 7.0 \times 10^1 (K^+) \end{cases}$	VPO	301)
Ala ¹ , Gly ⁴ -AA	96% EtOH/4% H ₂ O	1.0×10^2	—	CSE	301)
Ala ¹ , Val ⁴ -AA ^{a)}	96% EtOH/4% H ₂ O	1.2×10^2	—	CSE	301)
Phe ¹ , Ala ⁹ -AA	EtOH	4.0×10^2	1.0×10^2	—	217)
Pro ⁶ , Phe ⁷ -AA	EtOH	6.0×10^3	5.0×10^2	—	217)
Val ⁶ , Ala ⁹ -AA	96% EtOH/4% H ₂ O	5.0×10^1	—	CSE	301)
Cha ⁵ , Cha ⁶ , -AA ^{b)}	EtOH	2.5×10^4	1.0×10^3	—	217)
Cha ⁸ , Cha ⁹ , -AA ^{b)}	96% CH ₃ CN/4% H ₂ O	3.6×10^3	$\begin{cases} 3.8 \times 10^2 (Li^+) \\ 2.3 \times 10^2 (K^+) \end{cases}$	VPO	301)
	CH ₃ CN	1.5×10^4	—	VPO	301)
	MeOH	5.0×10^2	—	VPO	301)
	EtOH	2.0×10^3	5.0×10^1	—	217)

Cha ⁵ , Val ⁶ , Ala ⁹ , Cha ¹⁰ -AA	EtOH	1.7 × 10 ³	1.0 × 10 ²	—	217)
D-Phe ⁵ , Val ⁶ , Ala ⁹					
D-Phe ¹⁰ -AA	EtOH	2.6 × 10 ⁴	2.6 × 10 ⁴	—	217)
all-D-AA ^{c)}	EtOH	2.5 × 10 ³	2.0 × 10 ²	—	217)

AA = Antamanide.

a) = Retro-antamanide.

b) = Perhydro-antamanide.

c) = Enantio-antamanide.

Abu = α-Aminobutyric acid; Cha = Cyclohexylalanine.

CSE = Cation selective electrode.

VPO = Vapour pressure osmometry (measurements carried out at 45 °C).

Table 11. Stability constants of the Na^+ complex and antitoxic activity of antamanide and some of its analogs^{301, 303, 217)}

Analog-number	Compound	$K_{\text{stab}} [\text{M}^{-1}]$ (EtOH, 25 °C)	Antitoxic activity*)
1	$\text{Pro}^8\text{--Phe}^9\text{--Phe}^{10}\text{--Val}^1\text{--Pro}^2$ $\quad \quad \quad \quad \quad \quad \quad \quad $ $\text{Pro}^7\text{--Phe}^6\text{--Phe}^5\text{--Ala}^4\text{--Pro}^3$ Antamanide (AA)	2.4×10^3	0.5
2	[Ile ¹]-AA	2.3×10^3	0.5
3	[Abu ¹]-AA (Abu = α -Aminobutyric acid)	1.5×10^3	2.5
4	[Ala ¹]-AA	1.5×10^2	15
5	[Gly ¹]-AA	1.8×10^2	10
6	[Ala ¹ , Val ⁴]-AA "Retro-antamanide"	4×10^2	~10
7	[Gly ⁷]-AA	6×10^1	>20
8	[Pro ⁶ , Phe ⁷]-AA	5×10^1	>20
9	Des-[Pro ⁸]-AA	$<1 \times 10^1$	>20
10	[Val ⁶ , Ala ⁹]-AA	2.5×10^4	>10
11	[Cha ⁵ , Cha ⁶ , Cha ⁹ , Cha ¹⁰]-AA (Cha = Cyclohexylalanine) "Perhydro-antamanide"	2×10^3	>10
12	all-D-AA "Enantio-antamanide"	2.5×10^3	10

*) Dose in mg/kg which protects white mouse against 5 mg/kg phalloidin.

Table 12. Stability constants of complex formation of macrocyclic polyethers with alkali cations

Ligand	Solvent	Temp.	Cation	$K_{stab} [M^{-1}]$	Method	Ref.
Tetramethyl-12-crown-4 (cf. Fig. 58, 0)	MeOH	25 °C	Na	2.57×10^1	POT-CSE	99)
Perhydrobenzo-14-crown-4 (cf. Fig. 58, 1)	MeOH	25 °C	Na K	1.52×10^2 2.0×10^1	POT-CSE	99)
Benzo-15-crown-5 (cf. Fig. 58, 2a)	50% THF / 50% H ₂ O	25 °C	K	9.33	CSE	317)
Perhydrobenzo-15-crown-5 (cf. Fig. 58, 2b)	H ₂ O	25 °C	Rb Li Na K	2.88 < 10 < 2 4.0	POT-CSE	99)
	MeOH		Na K*)	5.13×10^3 { $K_1 : 3.80 \times 10^3$ $K_2 : 7.60 \times 10^1$ $K_1 : 6.03 \times 10^2$ $K_2 : 8.13 \times 10^1$ }		
18-Crown-6 (cf. Fig. 58, 3a)	H ₂ O	25 °C	Na K Cs	< 2 1.15×10^2 6.3	POT-CSE	99)
	MeOH	25 °C	Na K Cs*)	2.09×10^4 1.26×10^6 { $K_1 : 4.17 \times 10^4$ $K_2 : 2.0 \times 10^1$ 3.7×10^4 7.1×10^4 }		
	EtOH		Tl(I) Tl(I)		FL	56) 56)
Benzo-18-crown-6 (cf. 58, 3b)	MeOH	25 °C	Na K	3.4×10^4 1.12×10^5	POT	318)
4-Nitrobenzo-18-crown-6 (cf. Fig. 58, 3b)	MeOH	25 °C	Na K	8.9×10^3 5.13×10^4	POT	318)

Table 12. (continued)

Ligand	Solvent	Temp.	Cation	$K_{\text{stab}} [\text{M}^{-1}]$	Method	Ref.					
Pehydrobenzo-18-crown-6 (cf. Fig. 58, 3c)	H ₂ O	25 °C	Li	< 5	POT-CSE	99)					
			Na	6.3							
			K	7.9×10^1							
			Cs	6.3							
	MeOH		NH ₄	1.3×10^1							
			Na	1.23×10^4							
			K	7.76×10^5							
			Cs*)	$\{K_1 : 2.0 \times 10^4$ $\{K_2 : 3.3 \times 10^1$							
			Dibenzo-18-crown-6 (cf. Fig. 58, 3d)	MeOH			25 °C	Na	2.30×10^4	POT-CSE	99)
								K	1.0×10^5		
Cs*)	$\{K_1 : 3.55 \times 10^3$ $\{K_2 : 8.32 \times 10^2$										
50% THF / 50% H ₂ O	25 °C	K			7.94×10^1	CSE		317) 317)			
		Rb		2.5×10^1							
Perhydrodibenzo-18-crown-6 A-Isomer (cf. Fig. 58, 3f)	H ₂ O	25 °C		Li	4.0	POT-CSE	99)				
		Na		5.0×10^1							
		10 °C		K	1.41×10^2	CAL	135)				
		25 °C			1.05×10^2						
				40 °C		1.51×10^2	POT-CSE CAL	99) 135)			
			10 °C	Rb	8.13×10^1						
25 °C			4.07×10^1								
40 °C			3.31×10^1								
		40 °C		2.5×10^1	CAL	135)					
		10 °C	Cs	1.0×10^1							
		25 °C		9.12							
		1.78 × 10 ¹	POT-CSE CAL	99) 135)							
		40 °C						9.12			
		25 °C	NH ₄	2.14×10^1			POT-CSE	99)			
			2.5×10^1								

Perhydrodibenzo-18-crown-6 B-Isomer (cf. Fig. 58, 3f)	MeOH	25 °C	Na K Cs*)	1.21×10^4 1.02×10^6 $ K_1 : 4.07 \times 10^4 $ $ K_2 : 3.9$	POT-CSE	99)
	H ₂ O	25 °C	Na	2.5×10^1	POT-CSE	99)
		10 °C	K	6.17×10^1	CAL	135)
		25 °C		4.27×10^1		
		40 °C		6.03×10^1	POT-CSE	99)
		10 °C	Rb	3.16×10^1	CAL	135)
		25 °C		8.9		
		40 °C		7.41		
		25 °C		7.24		
	MeOH	25 °C	Cs	7.94	POT-CSE	99)
Perhydrodibenzo-21-crown-7 (cf. Fig. 58, 4a)		25 °C	NH ₄	6.3	POT/CAL	99, 135)
		25 °C	Na	4.77×10^3	POT-CSE	99)
		25 °C	K	2.40×10^5		
			Cs*)	$ K_1 : 3.09 \times 10^3 $ $ K_2 : \sim 1$		
	H ₂ O	25 °C	Cs	7.9×10^1	POT-CSE	99)
	MeOH	25 °C	K	2.57×10^4	POT-CSE	99)
			Cs*)	$ K_1 : 1.05 \times 10^5 $ $ K_2 : \sim 1$		
	MeOH	25 °C	K	3.01×10^3	POT-CSE	99)
			Cs	6.03×10^3		
	MeOH	25 °C	K	3.02×10^3	POT-CSE	99)
			Cs	1.41×10^4		
Dibenzo-24crown-8 (cf. Fig. 58, 4d)						
24-crown-8 (cf. Fig. 58, 4e)						

Table 12. (continued)

Ligand	Solvent	Temp.	Cation	$K_{gab}[M^{-1}]$	Method	Ref.
Dibenzo-30-crown-10 (cf. Fig. 58, 4g)	MeOH	25 °C	Li Na	< 1 1.3 × 10 ² 1.0 × 10 ² 6.3 × 10 ² 3.7 × 10 ⁴ 4.0 × 10 ⁴ 1.7 × 10 ⁴ 4.4 × 10 ⁴ 1.7 × 10 ² 2.7 × 10 ² 3.2 × 10 ⁴ 2.5 × 10 ¹ 4.0 × 10 ¹ 3.3 × 10 ² 4.68 × 10 ⁴ 7.9 × 10 ³	OD POT-CSE POT OD POT-CSE POT OD	48) 99) 318) 48) 99) 318) 48)
			Rb Cs NH ₄ Tl(I) K Rb			
Dimethyldibenzo-30-crown-10 (cf. Fig. 58, 4g)	50% THF / 50% H ₂ O				CSE	317)
	MeOH	25 °C	Na K		POT	318)
Dibenzo-60-crown-20 (4h) (cf. Fig. 58, 4h)	MeOH	25 °C	K		POT-CSE	99)
Di(<i>tert</i> -butylperhydrobenzo) 18-crown-6	H ₂ O	25 °C	Li Na K Cs	< 8.0 2.63 × 10 ¹ 1.20 × 10 ² 8.0	BMM	319)
Pentaglyme = CH ₃ (OCH ₂ -CH ₂) ₅ OCH ₃	MeOH	25 °C	Na K	3.31 × 10 ¹ 1.58 × 10 ²	POT	99)

*) Crown : cation = 2 : 1

POT: Potentiometry.

POT-CSE: Potentiometry with cation-selective electrodes.

CAL: Calorimetric titration.

BMM: Bilayer membrane measurement (permeability ratio vs. conductance ratio).

FL: Fluorescence.
OD: Optical density.

Table 13. Stability constants of complex formation of cryptands with alkali cations

Ligand (cf. Fig. 67)	Solvent	Temp.	Cation	$K_{\text{stab}} [\text{M}^{-1}]$	Method	Ref.
[2. 1. 1]	H_2O $\mu = 0.05$	25 °C	Li	3.2×10^5	pH-metric titration	169)
			Na	1.6×10^3		
			K	$< 10^2$		
			Rb	$< 10^2$		
			Cs	$< 10^2$		
	95% MeOH / 5% H_2O $\mu = 0.01$		Li	3.8×10^7		
			Na	1.2×10^6		
			K	1.8×10^2		
			Rb	$< 10^2$		
			Cs	$< 10^2$		
	MeOH $\mu = 0.01$		Li	$> 10^6$		
			Na	1.3×10^6		
			K	2.0×10^2		
			Rb	7.9×10^1		
			Cs	$< 10^2$		
[2. 2. 1]	H_2O $\mu = 0.05$	25 °C	Li	3.2×10^2	pH-metric titration	169)
			Na	2.5×10^5		
			K	8.92×10^3		
			Rb	3.55×10^2		
			Cs	$< 10^2$		
	95% MeOH / 5% H_2O $\mu = 0.01$		Li	1.52×10^4		
			Na	6.92×10^8		
			K	2.82×10^7		
			Rb	6.3×10^5		
			Cs*)	7.9×10^3		
	MeOH $\mu = 0.01$		Li	$(> 10^5)$		
			Na	$> 10^8$		
			K	$> 10^7$		
			Rb	$> 10^6$		
			Cs*)	$\sim 1.0 \times 10^5$		
[2. 2. 2]	H_2O $\mu = 0.05$	25 °C	Li	$< 10^2$	pH-metric titration	169)
			Na	7.9×10^3		
			K	2.5×10^5		
			Rb	2.24×10^4		
			Cs	$< 10^2$		
	95% MeOH / 5% H_2O $\mu = 0.01$		Tl(I)	2.0×10^6		
			Li	6.3×10^1		
			Na	1.62×10^7		
			K	5.62×10^9		
			Rb	2.5×10^8		
	MeOH $\mu = 0.01$		Cs	3.47×10^3		
			Li	4.0×10^2		
			Na	$> 10^8$		
			K	$> 10^7$		
			Rb	$> 10^6$		
			Cs	2.5×10^4		

Table 13. (continued)

Ligand (cf. Fig. 47)	Solvent	Temp.	Cation	$K_{stab} [M^{-1}]$	Method	Ref.				
[3. 2. 2]	H_2O $\mu = 0.05$	25 °C	Li	$< 10^2$	pH-metric titration	169)				
			Na	4.47×10^1						
			K	1.58×10^2						
			Rb	1.12×10^2						
			Cs	1.0×10^2						
	95% MeOH/ 5% H_2O $\mu = 0.01$		Li	$< 10^2$						
			Na	3.72×10^4						
			K	1.0×10^7						
			Rb	2.0×10^7						
			Cs	1.0×10^7						
	MeOH $\mu = 0.01$		Li	2.0×10^2						
			Na	6.3×10^4						
			K	$> 10^7$						
			Rb	$> 10^6$						
			Cs	$> 10^6$						
[3. 3. 2]	H_2O $\mu = 0.05$	25 °C	Li	$< 10^2$	pH-metric titration	169)				
			Na	$< 10^2$						
			K	$< 10^2$						
			Rb	$< 10^5$						
			Cs	$< 10^2$						
	MeOH $\mu = 0.01$		Na	1.6×10^3						
			K	1.0×10^6						
			Rb	1.4×10^6						
			Cs	$> 10^6$						
			[3. 3. 3]	H_2O $\mu = 0.05$			25 °C	Li	$< 10^2$	pH-metric titration
	Na							$< 10^2$		
	K							$< 10^2$		
	Rb							< 3.2		
	Cs							$< 10^2$		
	MeOH $\mu = 0.01$			Na				5.0×10^2		
K		2.5×10^5								
Rb		5.0×10^5								
Cs		7.9×10^5								
[2.2. C_8] $m = 1$, third bridge = – $(CH_2)_8$ –		95% MeOH / 5% H_2O $\mu = 0.01$		25 °C	Na	1.0×10^3		pH-metric titration	70)	
	K				2.24×10^4					
	MeOH $\mu = 0.01$	Li			$\leq 10^2$					
		Na			3.2×10^3					
		K			1.6×10^5					
		Rb			2.5×10^3					
		Cs	5.0×10^2							

*) External complexes of 2 : 1 ligand cation stoichiometry may be present.

Table 14. Thermodynamic parameters for the complex formation of macrotetrolide compounds with sodium and potassium determined by microcalorimetry and relaxation methods at 298 °K (Table from Ref. 315)

Ligand	Cation	ΔH° [kJ/mole]	ΔG° [kJ/mole]	ΔS° [J/mole · K]	$\log K$	K [kg/mole]	Solvent	Ref.
Nonactin	Na	-11.1 ± 0.2 ^{a)}	-15.5	14.8	2.71 ± 0.03	5.2 × 10 ²	MeOH	315)
		~ -20	-12	-27	2.11	1.3 × 10 ²	MeOH	50) b)
Nonactin	K	-43.6 ± 0.9 ^{a)}	-25.6 ^{a)}	-60.3 ^{a)}	4.49 ± 0.08 ^{a)}	3.1 × 10 ^{4a)}	MeOH	315)
	Na	-27.4 ± 0.5	-18.7	-29.4	3.27 ± 0.03	1.9 × 10 ³	EtOH	315)
	K	-52.2 ± 0.1	-30.0	-74.4	5.26 ± 0.23	1.8 × 10 ⁵	EtOH	315)
	Na	-22.4					MeOH	101)
Monactin	Na	-25.1	-14.8	-34	2.6	4 × 10 ²	MeOH	305) b)
Dinactin	Na	-27.6	-16.5	-37	2.9	8 × 10 ²	MeOH	50) b)
Trinactin	Na	-30.5	-17.7	-43	3.11	1.3 × 10 ³	MeOH	50) b)

a) Values of Ref. 101 corrected for difference of salt dilution heats in sample and reference cell as discussed elsewhere¹⁷³⁾.

b) Values converted to [kg/mole] respectively [kJ/mole].

3. Kinetics and Mechanism of Complex Formation

3.1. Theoretical Aspects on Complexation Kinetics

Metal complex formation in solution is generally a very rapid reaction process. A few decades ago textbooks commonly described the recombination of two ions of opposite charge as occurring "instantaneously". In other words, such a process was assumed to be completed at every encounter of the two entities¹⁹⁰). The introduction of new techniques for the study of fast reactions in solution such as relaxation spectrometry and nuclear magnetic resonance has thoroughly revolutionized this point-of-view. Certainly metal complex formation belongs to the area of rapid reactions, but the process itself can, by no means, be considered a simple one-step reaction between the charged or dipolar ligand and the cation. The reaction, often described by the basic scheme,



usually includes a number of intermediate steps of substitution of one or several solvent molecules from the inner coordination shell of the metal ion or of internal rearrangements of the ligand. This is especially so if L represents a multidentate chelating agent. We have referred to this situation already in Chapter 2.1, where we characterized the metal ion ligand interaction by a more realistic reaction model [cf. Eq. (1)].

A primitive picture of metal ion ligand interaction might create the impression that the recombination becomes faster, the greater the force of interaction between the two reaction partners. In fact, the opposite is true. The smaller the metal ion, the stronger is the electrostatic force exerted at its surface (cf. Table 1), where solvent molecules form a tightly fixed coordination sphere. The ligand, in order to bind to the metal ion, has to penetrate through this solvation sheath by substitution of one or several solvent molecules. The rate of substitution is lower the smaller the metal ion, where the solvent molecules of the inner coordination shell are more tightly bound.

The inner solvation shell itself appears to possess a highly ordered structure. This follows from even the most simple picture one could draw of such a regular arrangement: the metal ion attracts the polar solvent molecules and tries to attach them as closely as possible to its surface. On the other hand, the closer the approach of the polar groups, the stronger their mutual repulsion. Since the potential energy of the charge-dipole interaction varies with the square of the reciprocal radius,

$+ \frac{1}{r^2}$, while that for dipole-dipole interaction exhibits a $-\frac{1}{r^3}$ dependence (cf. Fig. 10),

one should expect a minimum for superposition of both counteracting terms. In a more realistic treatment¹⁹⁾, one has to account for van der Waals forces, and for polarization of both the metal ion and the solvent molecules. For transition-metals, additionally, some specific influences must be considered resulting from a splitting of electronic energy terms, brought about by the ligand-field interactions. These

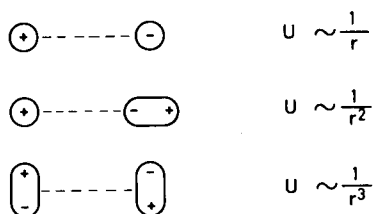


Fig. 10. The distance relations of potential energies (U) of electrostatic interactions

effects all together require a modification of the concept of the solvation shell as an even more highly ordered structure.

Given this picture we may formally distinguish two limiting mechanisms of substitution^{81b)}: (cf. Fig. 11)

i) S_N1 : The solvent molecule to be substituted by a ligand leaves the coordination shell prior to the entry of the ligand. The intermediate state is thus characterized by a lower coordination number than the initial and final state.

ii) S_N2 : The ligand enters the solvation shell by "squeezing-in" and forming an intermediate with a larger coordination number than the initial state. The reaction is completed by expulsion of either the incoming ligand, or more likely, one of the solvent molecules, depending on which is more tightly bound.

The distinction of these limiting cases certainly is a formal one and the real mechanism might be intermediate, e.g. resembling some type of "push-pull" process. However, the two mechanisms lead to quite different consequences in their rate

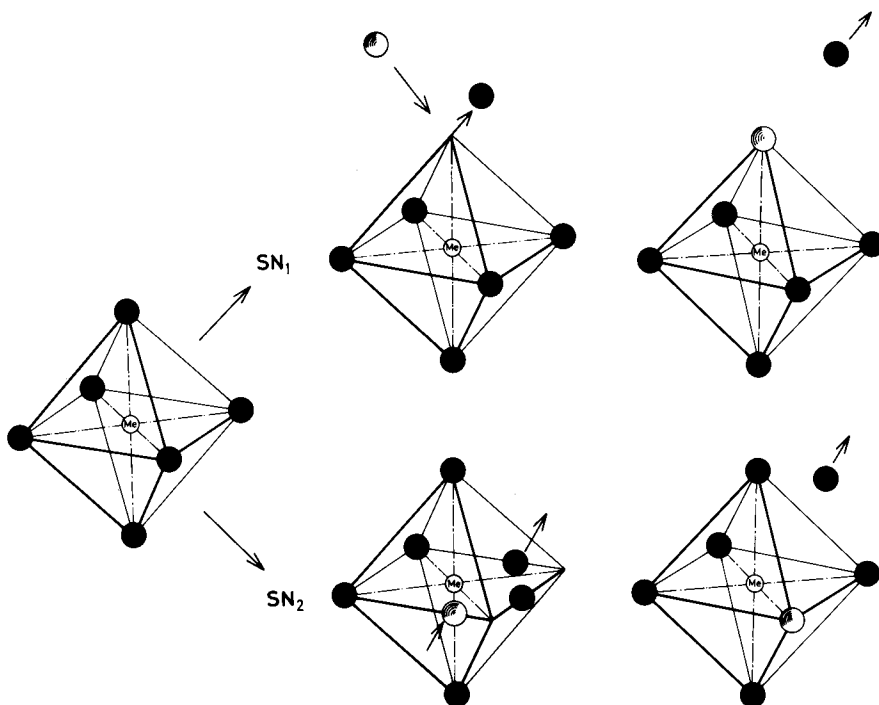


Fig. 11. The two limiting mechanisms of ligand substitution in an octahedral metal complex [Reproduced from Eigen, M: Ber. Bunsenges. Phys. Chem. 67, 753 (1963)]

behaviour which can easily be tested in relaxation experiments. The S_N1 mechanism should, for a given solvent, show a substitution rate which is independent of the ligand and a characteristic of the metal ion only.

On the other hand, the competition between ligand and solvent molecule occurring in the S_N2 mechanism should render the rate of substitution clearly ligand dependent.

With water as solvent, the majority of the substitution processes studied so far yielded results in agreement with the mechanism postulated for the first limiting case^{81b, 84}). The S_N1 type of substitution applies particularly to most of the main group metal ions, and many of the octahedrally coordinated transition metal ions. There are many impressive examples in which rates of substitution of water by a variety of ligands remain within a few percent constant, while the complex stabilities of those ligands differ by many orders of magnitude. The fact that the metal ion is decisive for the rate behaviour has led to the establishment of a "table of characteristic rate constants" correlating substitution rates with the electronic configuration of the metal ions due to position in the periodic table of elements^{66, 81b, 82}). This assumes that steric influences caused by the ligands, and the effects of ligand charge, have been taken into account.

Examples conforming with the S_N2 mechanism can also be provided^{81b, 83}). They were found, as one would expect them, for metal ions possessing a distorted coordination shell (e.g. mercury complexes with their preferred coordination number two, square planar configurations with weakly coordinated axial ligands, etc.).

An analysis of the rates, and their observed orders of magnitude yields the surprising result, that simple substitution processes, i.e. those in which a solvent molecule leaves the inner coordination sphere and is immediately replaced by a ligand, are exceedingly fast. In the following discussion we shall concentrate on main group metal ions; particularly the alkali ions. Given the relatively large solvation energies, and recalling that at room temperature 1.4 kcal/mole is equivalent to a tenfold change of the Boltzmann factor, it is indeed surprising that substitution at these ions occurs so rapidly (cf. Table 1). A solvent molecule from an otherwise complete coordination shell is replaced within a time, which is not much larger than that required to move the particles across a pathlength equivalent to the diameter of the complex. This accounts for the fact that the second order recombination process of metal ion and ligand must occur at a rate near the diffusion controlled limit⁶⁶). This also holds for most of the alkaline earth ions, which are characterized by appreciably larger solvation energies. The exceptions are Mg^{2+} and, of course, Be^{2+} , which show rates much smaller than predicted for uninhibited "diffusional" substitution⁸²). Analyzing the rate data in more detail, one realizes that Ca^{2+} and Li^+ are close to, but clearly below that limit. This means that it costs very little in terms of energy to remove one solvent molecule (or ligand) from the inner coordination sphere if a competing substituent is available. It furthermore indicates that the mechanism is close to the extreme of an S_N1 -type. In this connection one should remember that Stoke's ionic radii for alkali ions (cf. Table 1), as resulting from their electric mobilities in solution, are clearly larger than crystal radii, and definitely smaller than radii of tightly closed solvation shells²⁵¹). Apparently the flexibility in the coordination shell is sufficient for single solvent molecules to leave the shell while

the metal ion is pushed around by thermal motion. On the other hand, energy expenditure should increase considerably, when simultaneous removal of several solvent molecules from the coordination sphere occurs. This actually may be required for the formation of a complex between a metal ion and a multi-dentate chelating ligand.

One of the principal requirements for selectivity, as discussed in Section 2.1, is based on multiple substitution of solvent molecules. The more solvent molecules are replaced, the larger is the fraction of free energy of solvation relative to free energy of ligand binding which can be utilized for stability of the complex. A ligand with a chelating cavity, having sufficient binding sites, suitably placed to enclose the metal ion completely, proves to be the most favourable structure for selective binding. Moreover, if non-polar groups make up the surface providing a lipophilic coat for the carrier, the whole complex will be membrane soluble.

Here, an apparent contradiction arising from the two opposite requirements, namely to be highly selective and, at the same time, to be dynamically efficient, has to be resolved. In order to function optimally, the carrier must load and unload the metal ion as rapidly as possible. This would not be the case for a rigid chelating ligand, whose cavity is a fixed structure of a size which neatly accommodates the metal ion. Loading the carrier in such a case requires the metal ion to strip off its entire solvation shell prior to its entry into the cavity. By the same argument, unloading of the metal ion out of the chelate would have to be a one-step process. This would be very costly in activation energy and thus occur exceedingly slowly.

Rate measurements, which were carried out with various antibiotics, revealed the astonishing fact that even for highly selective ligands the reactions of complex formation are very fast, even approaching the diffusion controlled limit.

At this stage we may briefly re-examine the conditions for a diffusion controlled process. (For a more detailed discussion cf.⁸⁶⁾). Any reaction between two separate particles M and L is preceded by an encounter, in which the partners owing to their diffusional motion meet within a critical distance R_{ML} before they undergo reaction, e.g. the substitution of solvent molecules by binding groups of the ligand L. The overall process can be represented formally as



where the rate constants are ascribed to the following steps.

- k_{12} diffusional encounter
- k_{21} diffusional separation
- k_{23} reactive association
- k_{32} reactive separation

Note that the reaction steps defined by the rate constants k_{23} and k_{32} themselves may be related to sequences of individual steps. This certainly is the case for any substitution involving a multidentate ligand. In the formal treatment above, the diffusional encounter and separation are each represented by only one reaction step, whereas in reality they constitute a distribution of processes, owing to the distribution of distance correlations between M and L. Such an approach is justified if the

proportion of states, characterized by the distance R_{ML} is small in comparison with all other distance correlations summed up under $M + L$, as well as to the number of final products denoted by ML . The overall rate constants for association and dissociation can then be expressed as

$$\vec{k} = \frac{k_{12} \cdot k_{23}}{k_{21} + k_{23}} \quad \overset{\leftarrow}{k} = \frac{k_{32} \cdot k_{21}}{k_{21} + k_{23}} \quad (8)$$

Whether a chemical reaction is diffusion controlled is solely decided by the relative magnitude of the two (first order) rate constants k_{21} and k_{23} . If diffusional separation, expressed by the rate constant k_{21} , occurs faster than the reaction (e.g. substitution, the partners undergo several encounters before reaction occurs.

The overall rate constant is thus determined by the product of k_{23} and the ratio k_{12}/k_{21} , the equilibrium constant of two reaction partners M and L within the critical distance R_{ML} . Only if the step represented by k_{23} is fast with respect to diffusional separation, will each encounter be successful, and the process as a whole can be described as diffusion controlled. From this it follows that k_{12} will become

the overall rate constant while the rate of the reverse reaction is given by $k_{21} \frac{k_{32}}{k_{23}}$.

Both k_{12} and k_{21} can be estimated to be within the order of magnitude of 10^9 to 10^{10} with units $[M^{-1} s^{-1}]$, and $[s^{-1}]$ for k_{12} and k_{21} respectively depending on charges and distances of the reacting compounds as well as on the dielectric constant of the solvent^{64, 81a}.

Returning now to the discussion of alkali ion-ionophore interactions we realize that any measured rate constant of recombination with a value of around 10^9 to $10^{10} [M^{-1} s^{-1}]$ indicates a diffusion controlled process, such that every single substitution step is completed within a period shorter than 10^{-9} s.

Open chain antibiotics such as nigericin⁵⁰ in methanol (cf. Table 15) indeed show rate constants around $10^{10} [M^{-1} s^{-1}]$ for the recombination with alkali ions just as expected for a diffusion controlled reaction between two univalent ions of opposite charge in a solvent having that particular dielectric constant. Very similar results had been obtained for the anion of the indicator murexide^{85, 305}, forming complexes with the alkali ions in the same medium. Since the nigericin molecule wraps around the metal ion, we have to assume that substitution can be extremely rapid on the basis of a stepwise mechanism, i.e. if the solvent molecules are replaced one after the other, so that in each single substitution step the solvation energy is compensated by the ligand binding energy.

Such a treatment could not easily apply to macrocyclic structures, unless conformational changes assist loading or unloading of the metal ion. The free molecule should exhibit a wide opening of its ring shape bringing all the polar binding sites in close contact with the solvent.

The metal ion within the vicinity of the critical distance R_{ML} should be able to replace its coordinated solvent molecules step-by-step by the ligand binding groups. Concomitantly, the conformation of the macrocycle shrinks so that the chelating cavity in its interior adapts to the size of the unsolvated metal ion. Such a mechanism is formally depicted in Fig. 12.

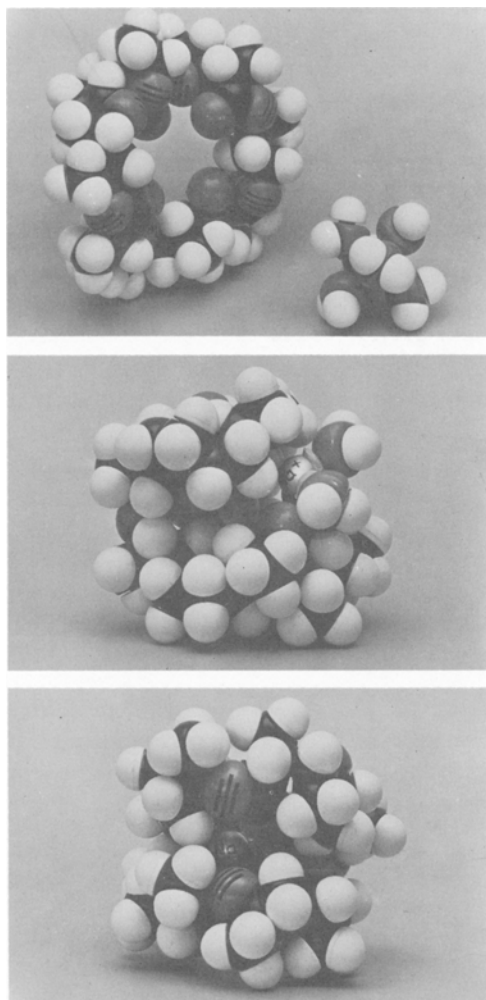


Fig. 12. Model representation of the loading of a macrocyclic ionophore (monactin) with Na^+ . The solvated metal ion approaches the carrier, the conformation of which permits its polar groups to be in close contact with the solvent. The uptake of the metal ion then occurs under stepwise substitution of the solvent molecules by the polar groups of the ionophoric ligand. In its final conformational state the carrier completely encloses the metal ion with its non-polar groups being accumulated at the surface

This concept was first put forward 1969^{85, 305)} in order to interpret the unpredicted high rates of recombination found for alkali metal ions with macrolide actins in methanol. For these compounds, conformational changes result from their flexible molecular structure, which converts from an open ring to a “tennis-ball-seam” configuration. Later, more detailed kinetic studies⁵⁰⁾ yielded direct information about these conformational transformations. They show up as discrete reaction steps. In depsipeptide- (valinomycin)^{111, 115a)} and peptide-structures (antamanide)³⁶⁾, where intermediate conformations are characterized by a varying number of hydrogen bonds, they appear even more distinctly. These intermediates can be stabilized in suitable solvents, which permits a direct determination of the rates of conformational changes by sound absorption measurements¹¹¹⁾. The complete processes of loading and unloading, passing through all the intermediates, are still rapid (cf. Tables 15 and 19) though markedly slower than for the macrolide actins and especially

for open chain antibiotics. For cryptands with highly fixed structures¹⁶⁵⁾, rates of exchange should be even smaller, which has been verified experimentally (cf. Table 16). Also in the case of these very rigid compounds, we may assume a somewhat modified stepwise mechanism for the complexing of the metal ion to ligand, whereby it is not required for all solvent molecules to leave the coordination shell simultaneously. The rate conditions referring to homogeneous solution are quantitatively different, if they occur at the solvent interface of a membrane, although their qualitative behaviour and characteristic features are maintained. P. Luger and coworkers^{160, 271)} have studied the rate of metal ion uptake and release with ionophores sitting in the interface of a lipid bilayer membrane using an electrical relaxation technique. Their data are reported in Table 17. The loading of the carrier through the interface is slower than in homogeneous medium, while the unloading appears to be faster than that in methanol. The selectivity pattern is qualitatively equivalent to that found in homogeneous solution. The mechanism of facilitated metal ion transport through a membrane by a mobile carrier might be visualized as that shown in Fig. 13. Ion transport may also be brought about by a pore which will be as selective as a mobile carrier, if it requires the alkali ion to dispose of its solvation sphere, before entering the pore. Here, the steps for loading and unloading should be similar to the mobile carrier. Such a pore, in order to com-

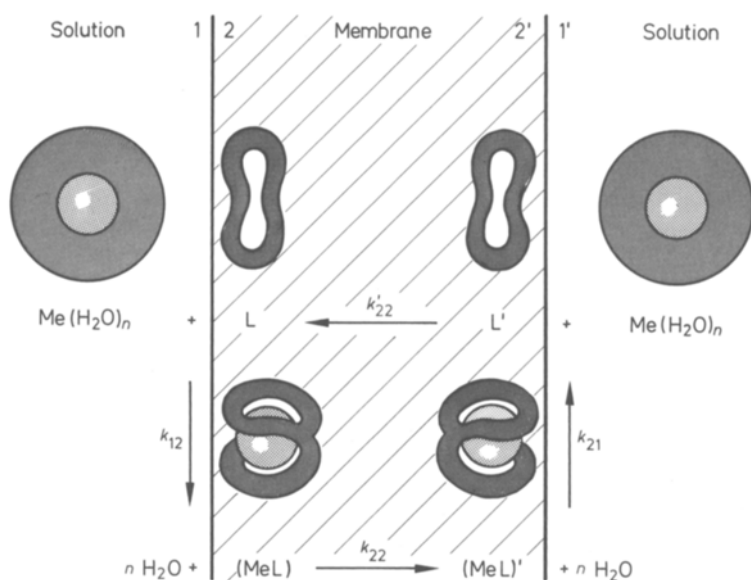


Fig. 13. Scheme for ionophoric action. The processes (12) and (21) on both sides of the membrane represent loading and unloading of the carrier. They occur at the interface membrane-solution and involve the substitution of solvent molecules by the ligand groups as well as conformational changes of the ligand. Transport across the membrane of the loaded and unloaded carrier is represented by the processes (22) and (22)'.

The maximum rates V_m are for:

$$k_{21} \gg k_{22} : V_m = k_{22} \cdot K_{MeL} \cdot C_{Me(H_2O)_n}^{solv} \cdot C_L^{memb.}$$

$$k_{21} \gg k_{22} : V_m = \frac{1}{2} k_{12} \cdot C_{Me(H_2O)_n}^{solv} \cdot C_L^{memb.}$$

compensate for desolvation, must offer binding sites for the metal ions, otherwise it may be less selective though kinetically more efficient. A more detailed discussion of the mechanism of facilitated transport across membranes is found in Section 4.

The two (apparently contradictory) requirements, high selectivity, and high speed of metal ion uptake can be satisfied by the special architecture of an ionophore allowing for fast conformation changes and thereby transforming solvated metal ions by stepwise compensation of binding energy into specific adapted complexes showing selective stabilities.

3.2. Methods for the Determination of Rate Constants

Techniques for the study of alkali metal complex formation involve devices to measure fast reactions. There are only few exceptions, namely very stable cryptand complexes where the binding of metal ions might be elucidated using classical methods. Any of the recording instruments mentioned in Section 2.2 should be suitable to follow the kinetics of the reactions, possibly in combination with a flow apparatus. Processes with half times as low as 1 ms could easily be investigated in this way. (For technical detail cf.⁴⁶⁾).

Most of the data reported in the next section have been obtained by means of relaxation studies⁸⁷⁾. The principle is based on a rapid perturbation of the equilibrium through the alteration of an external physical parameter (such as temperature, pressure or electric field strength) with a subsequent — or simultaneous — monitoring of the resulting chemical shift of equilibrium. The perturbation of the system may be effected as a pulse or periodically, and the observation can either be direct, *i.e.* by following the temporal shift of a recordable parameter, or indirect, *e. g.* by measuring the phase difference between the external perturbation and the internal chemical change.

The first mentioned methods are most appropriate for time ranges smaller than 0.1 s. The relaxational signal to be recorded has to exploit any electromagnetic quantity, characteristic of alkali metal complex formation, as outlined in Section 2.2. Since the alkali metal ions themselves do not exhibit any suitable optical properties, the availability of sufficiently sensitive indicators is desirable. Murexide (the anion of purpuric acid) has proved to be suitable for most of the alkali ions in methanolic solutions^{85, 305, 306)} and should be relevant also for certain other nonaqueous media. In water, the stability constants for the various alkali ion complexes with murexide are much too low in order to allow useful applications. Therefore murexide has been used in aqueous media preferentially for the indication of Ca^{2+} ²⁶²⁾ and other di- and tri-valent ions¹⁰⁵⁾. One of the fundamental prerequisites of an indicator is excellently fulfilled by murexide: its reactions with all the cations of the alkali series (and with Ca^{2+} as well) are exceedingly fast^{85, 305, 306)}, so that changes in concentration of the complexing system under study can be recorded without delay. In methanol, its stability constant (cf. Table 5) is of such a magnitude, that murexide can be employed as a truly competitive ligand for the investigation of many macrocyclic ionophores both of natural and artificial origin.

As for equilibrium studies, UV-absorption spectra as well as optical rotatory dispersion and circular dichroism of various ligands and their complexes have also proved useful for kinetic investigations^{103, 113}). Detailed analyses of relaxation effects have actually led to a deeper insight into the mechanism of complex formation and hence has provided a better understanding of the reasons underlying selectivity.

The relaxation response to a sudden increase of an external parameter — in the form of a temperature jump — usually appears as a sum of exponentials⁸⁷⁾

$$\Delta x(t) = \sum A_i e^{-t/\tau_i} \quad (9)$$

where t is time, x the concentration or a concentration dependent parameter to be recorded, A_i an amplitude reflecting the amount of equilibrial shift of the investigated reaction and τ_i the corresponding relaxation time. The index i refers to a number of steps characterizing the particular mechanism. For a reaction scheme of the type



where ML_1 , ML_2 and ML_3 denote three distinct forms of the complex (*e.g.* different substitution states or different ligand conformations), three relaxation terms may be recorded. These, however, are not immediately related to the three reaction steps but rather to some normal modes of reaction which result from the coupling of the three steps. Methods have been worked out which allow a complete analysis of the relaxation spectrum^{87, 88, 137, 280}), *i.e.* of the time constants and their attributed amplitudes. (An example of a single step relaxation curve is presented in Fig.14.). The evaluation of amplitudes has already been indicated in Section 2.2. The relaxa-

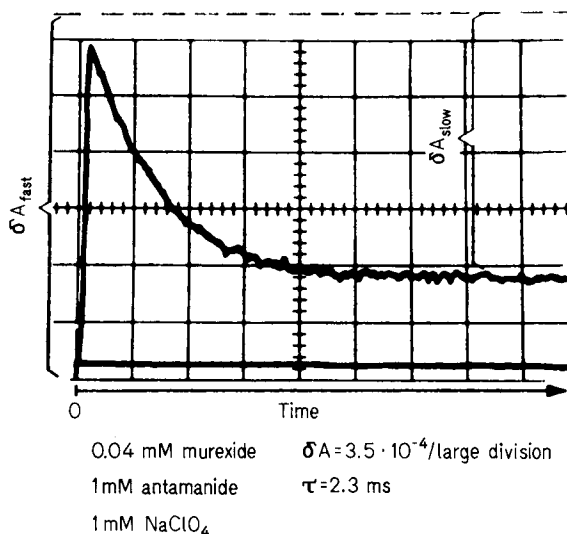


Fig. 14. Oscillogram of a temperature jump relaxation effect of the system containing antamanide, murexide, and Na^+ in methanol

tion times, and the amplitudes, are obtained by variation of c_L° or c_M° or of both keeping their sum constant. The plots for τ yield in the case of such a multiple step process similar sharp maxima as do the amplitudes at the various equivalence points (cf. Fig. 6), which enables a separate determination of individual rate constants. If it is possible to measure several relaxation effects and to resolve them clearly, the resulting information is sufficient to determine parameters such as the equilibrium and rate constants of the individual steps during complex formation. A more complete description of those special relaxation methods is given elsewhere⁸⁸⁾.

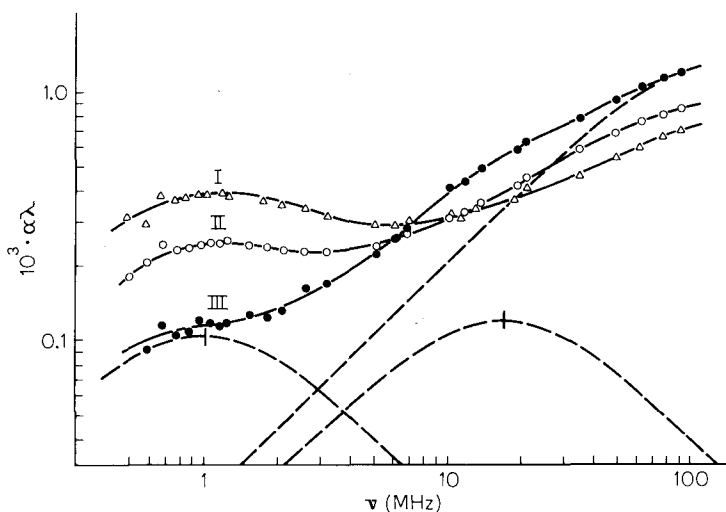


Fig. 15. Ultrasonic absorption of antamanide in methanol (I) and of antamanide with varying sodium concentrations: (II) low Na^+ concentration, (III) high Na^+ concentration. [The analysis given in this picture refers to curve (III).]

Sound absorption spectra yield similar data. Here the relaxation effects are observed in the form of maxima in the coefficient of "absorption per wave length" ($\alpha\lambda$). They are expressed in terms of the following relation:

$$\Delta\alpha\lambda = \sum A_i \frac{\omega\tau_i}{1 + \omega^2\tau_i^2} \quad (11)$$

where $\omega = 2\pi\nu$ is the angular frequency of the soundwave, A_i and τ_i the corresponding amplitudes and time constants of the single reaction steps.

This technique has been used by F. Eggers, Th. Funck and E. Grell^{80, 102, 115a)} as well as by the present authors^{36, 50)} to determine fast conformation changes of macrocyclic ligands such as valinomycin, enniatin and antamanide. In each example, several relaxation effects could be detected and correlated with conformational changes brought about by opening or closing the H-bonds which stabilize the spatial structures of these ionophoric compounds.

Data from relaxation and other studies are listed in Section 3.3.

3.3. Rate Constants (Tables 15–19)

Table 15. Overall rate constants for complex recombination (k_R) and dissociation (k_D) of alkali ions with a variety of ligand compounds

Ligand	Solvent	Temp.	Cation	$k_R [M^{-1} sec^{-1}]$	$k_D [sec^{-1}]$	Method	Ref.
[NTA] ³⁻ (Nitrilo-triacetate)	H ₂ O; pH > 12 $\mu = 2$ M	25 °C	Na	1.9 × 10 ⁸	3.1 × 10 ⁷	US	66)
			K		1.0 × 10 ⁸		
			Rb		1.5 × 10 ⁸		
			Cs		2.1 × 10 ⁸		
[EDTA] ⁴⁻ (Ethylene-diamino-tetraacetate)	H ₂ O; pH > 12 $\mu = 2$ M	25 °C	Li	1.0 × 10 ⁸	1.4 × 10 ⁷	US	66)
			Na	1.7 × 10 ⁸	2.3 × 10 ⁷		
			K	8.5 × 10 ⁷	3.9 × 10 ⁷		
			Rb		1.3 × 10 ⁸		
			Cs		2.0 × 10 ⁸		
			Li	1.7 × 10 ⁸	2.8 × 10 ⁷		
[DCITA] ⁴⁻ (2,2-Ethylene-dioxy-bis (ethylimino-diacetate))	H ₂ O; pH > 12 $\mu = 2$ M	25 °C	Na	2.0 × 10 ⁸	6.1 × 10 ⁷	US	66)
			K	2.0 × 10 ⁸	9.0 × 10 ⁷		
			Rb		2.3 × 10 ⁸		
			Cs		3.1 × 10 ⁸		
			Li	5.5 × 10 ⁹	7.7 × 10 ⁶		
			Na	1.5 × 10 ¹⁰	5.9 × 10 ⁶		
Murexide	MeOH	25 °C	K	~2 × 10 ¹⁰	~1 × 10 ⁷	EFP	305)
Nonactin	80% MeOH / 20% CDCl ₃	21 °C	K	>1.6 × 10 ⁵	32	NMR	121a)
Monactin	MeOH	25 °C	Na	3 × 10 ⁸	6 × 10 ⁵	US	305, 50)
Dinactin	80% MeOH / 20% CDCl ₃	21 °C	K	>1.1 × 10 ⁵	23	NMR	121a)
	MeOH	25 °C	Na	6.5 × 10 ⁷	5.8 × 10 ⁴	TJ	50)
	80% MeOH / 20% CDCl ₃	25 °C	Na	5 × 10 ⁷	4.6 × 10 ⁴	US	50)
			Cs	3.4 × 10 ⁸	8.2 × 10 ⁴	US	50)
Trinactin	80% MeOH / 20% CDCl ₃	21 °C	K	>1.1 × 10 ⁵	21	NMR	121a)
Nigericin	MeOH	25 °C	Na	7.2 × 10 ⁷	4.2 × 10 ⁴	TJ	50)
	80% MeOH / 20% CDCl ₃	21 °C	K	>0.9 × 10 ⁵	18	NMR	121a)
	MeOH	25 °C	Na	≥1 × 10 ¹⁰	≥1.1 × 10 ⁵	EFP	50)
Dibenzo-18-crown-6	DMFA	25 °C	Na	6 × 10 ⁷	1 × 10 ⁵	NMR	265)

Table 15. (continued)

Ligand	Solvent	Temp.	Cation	$k_R [M^{-1} \text{sec}^{-1}]$	$k_D [\text{sec}^{-1}]$	Method	Ref.
Dibenzo-30-crown-10	MeOH $\mu = 0.15 \text{ M LiCl}$	25 °C	Na	$> 1.6 \times 10^7$	$> 1.3 \times 10^5$	TJ	48)
			K	6×10^8	1.6×10^4		
			Rb	8×10^8	1.8×10^4		
			Cs	8×10^8	4.7×10^4		
			NH ₄ Tl(I)	$> 3 \times 10^7$ 8×10^8	$> 1.1 \times 10^5$ 2.5×10^4		
Valinomycin	MeOH $\mu = 0.1 \text{ M TBAP}$	25 °C	Na	1.3×10^7	1.8×10^6	US, TJ	103)
			K	3.5×10^7	1.3×10^3		
			Rb	5.5×10^7	7.5×10^2		
			Cs	2×10^7	2.2×10^3		
			NH ₄ K	1.3×10^7 1.3×10^7	2.5×10^5 2.9×10^3		
Antamanide	90% MeOH/10% H ₂ O $\mu = 0.1 \text{ M LiCl}$ 80% MeOH/20% H ₂ O $\mu = 0.1 \text{ M LiCl}$ 70% MeOH/30% H ₂ O $\mu = 0.15 \text{ M LiCl}$ 80% MeOH/20% CDCl ₃	25 °C	K	5.5×10^6	1.3×10^4	TJ	115b)
			Rb	7.5×10^6	6×10^3		
			Cs	3×10^6	2×10^4		
			K	1.3×10^6	2.8×10^4		
			K	$> 1.1 \times 10^5$	21	NMR	121a)
Perhydro-Antamanide	MeOH CH ₃ CN MeOH	20 °C	Na	1.1×10^5	2.1×10^2	TJ	35b)
		20 °C	Na	7.7×10^5	2.6×10^1	TJ	35b)
		20 °C	Na	4.1×10^5	4.1×10^2	TJ	35b)
Cryptand [2.1.1]	H ₂ O	25 °C	Na	1.2×10^4	1.5×10^2	¹³ C-NMR	115b)

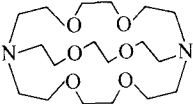
US: Ultrasonic absorption.

EFP: Electric field pulse.

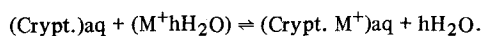
TJ: Temperature jump.

NMR: Nuclear magnetic resonance.

Table 16. Exchange rates and free energies of activation for cation exchange in cryptand [1.1.1] (according to Ref.¹⁶⁵)

Ligand	Alkali ion	Counter ion	$T\text{ }^{\circ}\text{C} (\pm 4^{\circ})$	$k[\text{sec}^{-1}]$	$\log K (20\text{ }^{\circ}\text{C})$
	Na^+	Cl^-	3	27	3.6
	K^+	F^-	36	38	5.1
		Cl^-	36	38	5.1
		Br^-	35	42	5.1
	Rb^+	Cl^-	9	38	3.7

T is the temperature, at which the NMR-signals coalesce due to line broadening. The exchange rate (k) was determined from the associated frequency distances of the cryptand and cryptate resonances. The rate k refers to the coalescence temperature. The data favour an exchange mechanism of the type.

Table 17. Rate constants k_R , k_D , k_{MS} , k_S of valinomycin and trinactin mediated cation transport through glycerol monooleate/n-decane bilayer membranes at $25\text{ }^{\circ}\text{C}$ (cf. Fig. 18)

Carrier	Ion	k_R [$\text{M}^{-1} \text{sec}^{-1}$]	k_D [sec^{-1}]	k_{MS} [sec^{-1}]	k_S [sec^{-1}]	Ref.
Valinomycin	K^+	2.9×10^5	2.7×10^5	2.1×10^5	3.8×10^4	24)
	Rb^+	3.7×10^5	2.4×10^5	2.7×10^5	3.5×10^4	
	Cs^+	2.2×10^5	5.6×10^5	2.5×10^5	4.1×10^4	
Trinactin	NH_4^+	1.9×10^5	2×10^4	8×10^3	5.4×10^4	23)
	K^+	6.5×10^4	6.4×10^4	1.6×10^4	5.4×10^4	
	Rb^+	1.1×10^5	1.6×10^5	1.6×10^4	5.4×10^4	

Table 18. Rate constants of single steps associated with the complex formation of valinomycin, dinactin and trinactin with several monovalent cations in methanol at 25 °C according to*): $L + M^+ \xrightleftharpoons[k_{21}]{k_{12}} L \cdots M^+ \xrightleftharpoons[k_{32}]{k_{23}} LM^+$

Ligand	Cation	K' [M ⁻¹]	k_{12} [M ⁻¹ sec ⁻¹]	k_{21} [sec ⁻¹]	$K_{12} = \frac{k_{12}}{k_{21}}$ [M ⁻¹]	k_{23} [sec ⁻¹]	k_{32} [sec ⁻¹]	$K_{23} = \frac{k_{23}}{k_{32}}$	Method	Ref.
Valinomycin	NH ₄	47	1×10^9	1.5×10^8	6.5	2×10^6	2.5×10^5	8	US	115a)
	Na	4.7	7×10^7	2×10^7	3.5	4×10^6	2×10^6	2	US	115a)
	K ^{a)}	3×10^4	4×10^8	1×10^8	4.0	1×10^7	1.3×10^3	7.7×10^3	US, TJ	115a)
a) Apparent stability constant was determined in the presence of 0.1 M TBAP.										
K': The apparent stability constants were determined by spectrophotometric titration.										
US: Ultrasonic absorption.										
TJ: Temperature jump relaxation.										
according to*): $L' + M^+ \xrightleftharpoons[k_{10}]{k_{01}} L + M^+ \xrightleftharpoons[k_{21}]{k_{12}} LM^+$										
Ligand	Cation	$K_{10} = \frac{k_{10}}{k_{01}}$	k_{01} [sec ⁻¹]	k_{10} [sec ⁻¹]	k_{12} [M ⁻¹ sec ⁻¹]	k_{21} [sec ⁻¹]	Method	Ref.		
Dinactin	Na	1.7	6.5×10^7	1.1×10^8	1.3×10^8	4.3×10^4	US	50)		
	Cs	1.7	6.5×10^7	1.1×10^8	1.6×10^8	5.4×10^4	TJ	50)		
Trinactin	Na	1.2			7.8×10^8	5.1×10^4	US	50)		
					1.6×10^8	4.2×10^4	TJ	50)		

*) The first order transformations: $L' \rightleftharpoons L$ or $L \cdots M^+ \rightleftharpoons LM^+$ are interpreted as conformation changes of the ligand or its metal complex respectively.

Table 19. Conformational transitions of depsipeptide ligands in different solvents (Table taken from Ref. 115a)

Ligand	Solvent	Minimal number of equilibrium states and relaxation times as obtained by ultrasonic absorption measurements
Valinomycin	n-Hexane	$\dots V_1 \xrightleftharpoons[2 \times 10^{-9} \text{ s}]{\tau_1} V_2 \xrightleftharpoons[2 \times 10^{-8} \text{ s}]{\tau_2} V_3$
	n-Hexane/ Ethanol 5:1 (v/v)	$\dots V_1 \xrightleftharpoons[2 \times 10^{-9} \text{ s}]{\tau_1} V_2 \xrightleftharpoons[2 \times 10^{-8} \text{ s}]{\tau_2} V_3 \xrightleftharpoons[10^{-7} \text{ s}]{\tau_3} V_4$
	Methanol	$\dots V_{n-1} \xrightleftharpoons[\tau_n]{\tau_n} V_n$ <p>spectrum of relaxation times</p>
Enniatin B	n-Hexane	$\dots E_1 \xrightleftharpoons[2 \times 10^{-9} \text{ s}]{\tau_1} E_2$
	n-Hexane/ Ethanol 5:1 (v/v)	$\dots E_1 \xrightleftharpoons[10^{-9} \text{ s}]{\tau_1} E_2 \xrightleftharpoons[9 \times 10^{-8} \text{ s}]{\tau_2} E_3$
	Ethanol	$\dots E_1 \xrightleftharpoons[5 \times 10^{-9} \text{ s}]{\tau_1} E_2 \xrightleftharpoons[10^{-7} \text{ s}]{\tau_2} E_3$

4. Carrier Mediated Ion Transport through Artificial and Biological Membranes

Since the discovery in 1964 that valinomycin induces K^+ uptake of mitochondria¹⁹²), the investigation of mechanisms by which certain substances facilitate ion transport in lipid membranes has developed into a major field in biophysics. Depending on the inducing substance, two principal modes of ion transport have been deduced from experimental findings: the "carrier" and the "channel" mechanism.

In this text both concepts and individual properties of the inducers will be briefly described. For a detailed treatment of the subject, the reader is referred to current reviews^{53, 124, 162, 279, 291}).

Wipf and Simon have shown that the various effects of valinomycin- and nigericin-type antibiotics can be rationalized on the basis of their complex formation and carrier properties³¹⁰). Because of the complexity of biological membranes, artificial lipid membranes have proved more suitable for studying the details of the transport mechanisms. Lipid bilayer membranes, formed in a hole between two aqueous compartments, have been most widely used^{159, 196}). Such a membrane consists of a bimolecular layer of oriented lipid molecules, *e.g.*, lecithin. As shown in Figure 16, the polar head groups of the lipid molecules point toward the aqueous medium, whereas the hydrocarbon chains form the lipophilic interior of the membrane. The membrane has a thickness of 35 to 60 Å (depending on the lipid) and an electrical conductance of 10^{-9} to 10^{-7} [$\Omega^{-1} \text{ cm}^{-2}$].

The function of carriers (cf. Fig. 13) and channels in lipid bilayer membranes is illustrated in Figure 17²⁹¹). The carrier molecule is assumed to reside at the aqueous-lipid interface, where it chelates a cation from the aqueous solution. The carrier-cation complex then migrates across the lipid interior of the membrane to the opposite interface, where it dissociates, releasing the ion into the aqueous phase. In Section 3.1 certain rules have been formulated for the design of an efficient metal-ion carrier⁸⁵):

1. The carrier molecule should possess electrophilic groups that can compete with the solvent molecules for metal-ion binding. These groups should be inside an otherwise lipophilic structure which easily dissolves in membranes.
2. As many solvent molecules of the inner coordination sphere as possible should be replaced by coordinating sites of the carrier molecule.
3. The ligand should form a cavity adapted to the size of the metal ion to be selected.
4. The carrier molecule should be sufficiently flexible providing a fast stepwise substitution of the solvate shell of the cation. Rule (1) fulfills the requirement of gating an ion through a lipid membrane. Rules (2) and (3) explain high ion selectivity, whereas rule (4) permits rapid loading and unloading of the carrier.

Ion conducting channels across the membrane are formed either by parallel or serial alignment of suitable organic molecules. The outside of a channel should be lipophilic, in order to allow for an energetically favourable interaction with the lipid chains of the membrane. Inside the channel, electrophilic groups should produce a polar cylindrical cavity through which partially or completely desolvated cations can permeate.

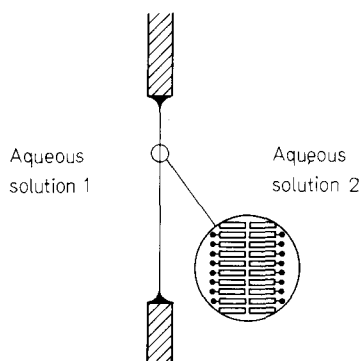


Fig. 16. Schematic representation of a lipid bilayer
[From Luger, P.: Science 178, 24 (1972).]

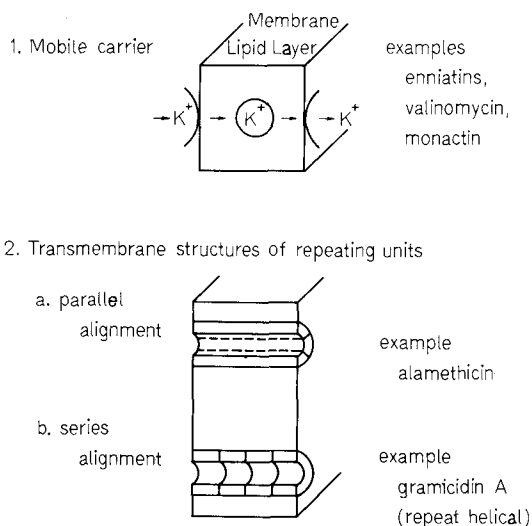


Fig. 17. Molecular mechanisms of cation permeation of membranes
[Reproduced from Urry, D. W., *et.al.*: Ann. N. Y. Acad. Sci. 264, 203 (1975).]

Through experimental methods, it has been possible to distinguish between the two mechanisms of ion transport. The conductance of lipid bilayers varies linearly with the concentration of a carrier, indicating that 1 : 1 carrier-ion complexes are the conducting units. (For carriers which also form other than 1 : 1 complexes, this is at least observed at low concentrations.) In case of a channel former, the membrane conductance shows a second or higher power dependence on the concentration, implying that two or more molecules are required to make one conducting pathway^{43, 159}).

“Freezing” and “melting” of lipid bilayers greatly alters the conductance mediated by a carrier, because it influences its mobility in the membrane. In contrast, the conductance induced by a channel former is not influenced¹⁵⁸). Similarly, an increase of the membrane viscosity, by addition of cholesterol, reduces carrier-, but not channel- mediated conductance^{278, 217}).

4.1. Carrier Mechanism

Valinomycin and the *macrotetrolides* are the compounds of this group which have been most widely investigated. Using radioactive valinomycin and macrotetrolides, Simon and coworkers demonstrated that ligand and cation are transported in equimolar amounts across a bulk lipid membrane. Since an exchange of ligand occurred during the transport, a carrier-relay mechanism was suggested by the authors^{308, 309}.

Detailed lipid bilayer studies with valinomycin and macrotetrolides established that both antibiotics have the following effects on (i) membrane potential and (ii) conductance^{92, 126, 159, 279}: (i) If the aqueous solutions on both sides of the membrane contain different K^+ concentrations, a potential is observed which shows approximately Nernstian dependence on the K^+ -concentration gradient. By using K^+ in one aqueous solution and a different alkali ion in the other aqueous solution, potentials are also measured. From these, cation permeability ratios can be calculated which give the same cation selectivity sequence as observed with complexation. (ii) The membrane conductance (measured with the same alkali ion solution in both aqueous compartments) increases linearly with the aqueous concentration of the antibiotic. At fixed concentration of the antibiotic, the membrane conductance increases linearly with the alkali ion concentration. The conductance values measured with different alkali cations correlate with the ion selectivity sequence of complexation.

From the similarity of the above findings for both antibiotics it was concluded that valinomycin and macrotetrolides are carriers of the same type, transporting cations in the form of 1:1-complexes²⁷⁹.

The kinetics of carrier-mediated cation transport through bilayer membranes have also been investigated. Figure 18 shows a scheme of four different processes,

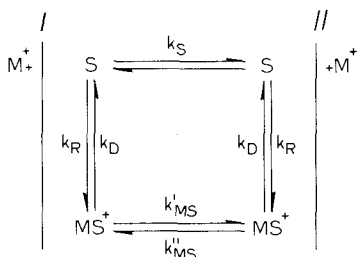


Fig. 18. Mechanism of carrier-mediated ion transport through a lipid bilayer membrane [Reproduced from Stark, G., *et.al.*: *Biophys. J.* 11, 981 (1971) and Benz, R., Stark, G.: *Biochem. Biophys. Acta* 382 (1), 27 (1975).]

describing the complex formation in the membrane/aqueous interface (vertical arrows) and the translocations across the membrane (horizontal arrows)²⁷¹. From analysis of the current/voltage characteristics and voltage jump measurements, the four rate constants have been evaluated by different groups^{23, 125, 154, 162, 271}. Recently a charge pulse method has also been applied to the determination of the rate constants^{24, 95}. Table 17 shows rate constants of different cation complexes of valinomycin and trinactin. The rate constants are all within the relatively narrow limits of 8×10^3 and 5.6×10^5 . For a given complex, the complexation rate constant,

k_R , and the decomplexation rate constant, k_D , differ by less than one order of magnitude. In methanolic solution, on the other hand, k_R exceeds k_D by three to four orders of magnitude (cf. Table 15).

From k_R and k_D , stability constants of the complexes in the membrane/aqueous interphase can be calculated. For the valinomycin complexes, stability constants in the order of 1 M^{-1} are obtained. Likewise, stability constants of about 1 M^{-1} were found by cation titrations of valinomycin bound to lipid bilayer vesicles in aqueous dispersion^{115a}. On the other hand, 10^5 times larger stability constants were obtained in homogeneous methanolic solution (cf. Table 7). As was pointed out by Grell and coworkers, the complex stability constants of membrane-bound valinomycin correspond to those determined in homogeneous 70% water/30% methanol solution^{115a}. The molecular factors determining the rate constants in the membrane/aqueous interphase are not completely understood. As a result of their influence, all processes involved in the ion transport (binding, translocation, release) run at comparable rates. From the expression

$$f = (1/k_S + 1/k_{MS} + 2/k_D)^{-1}$$

given by Luger¹⁵⁹, one can calculate the turnover number, f (maximal number of ions which may be transported per second by a single carrier molecule). For valinomycin and K^+ ions, the large value of $f = 2.5 \times 10^4 \text{ s}^{-1}$ is obtained. A turnover number of the same order was found for the valinomycin- and nonactin-mediated cation transport at the tylakoid membrane²⁵⁸. Haynes and coworkers reported a turnover number of $2 \times 10^3 \text{ s}^{-1}$ for valinomycin and K^+ ions at the mitochondrial membrane¹²².

The peptide analog of valinomycin, cyclo-(D-Val-L-Pro-L-Val-D-Pro)₃ (= PV) forms more stable complexes with alkali metal cations than valinomycin (cf. Section 5.3). From NMR data, dissociation rate constants of 5 s^{-1} for the Li^+ complex and $\leq 1 \text{ s}^{-1}$ for the Na^+ and K^+ complexes in solution have been estimated⁶¹. At lipid bilayers, a 10^4 times higher concentration of PV than of valinomycin is required to produce a comparable increase in K^+ conductance²⁸². It has been proposed that the dissociation of the complex could be the rate limiting factor of the ion transport by PV in bilayer membranes⁶¹.

Effects of the *enniatins* at lipid bilayers have been studied by several groups^{133, 197, 268, 285}. Considerably higher concentrations of these antibiotics are required to obtain membrane conductance and potential values comparable with those induced by valinomycin and the macrotetrolides. Ivanov *et al.* observed first, second, and third power dependence of membrane conductance on enniatin B concentration, but only, first power dependence on the concentration of bis-enniatiin B (cf. Section 5.1). They concluded that complexes with 1 : 1, 2 : 1, and 3 : 2 carrier-cation stiochiometry are involved in the ion transport mediated by enniatin B and beauvericin. In the limiting case, stacking of many enniatin complex molecules can be postulated, which could lead to a channel mechanism of cation transfer by enniatiin¹³³.

Despite its complex formation ability, *antamanide* does not mediate ion transport through artificial or biological membranes. This is probably due to its poor

solubility in lipid membrane constituents. The synthetic derivative, perhydro-antamanide, which has a high lipid solubility, was found to enhance the cation permeability of lecithin liposomes²¹⁴).

The carrier action of *macrocyclic polyethers* has been demonstrated in bilayer experiments²⁷⁹). The membrane conductance induced by bis(*t*-butyl) dicyclohexyl-18-crown-6 has a second-power dependence on polyether concentration in the region of 10^{-6} M and a third power dependence at 10^{-5} M to 10^{-4} M polyether. This indicates that besides the 1 : 1 complex, 2 : 1 and 3 : 1 (or 3 : 2) carrier-cation complexes are formed in the membrane. The incomplete chelation of the cation by the flat polyether ring obviously favours the formation of sandwich complexes (cf. Section 5.5).

Ion transport by *macrobicyclic ligands (cryptands)* has been investigated using a bulk liquid membrane¹⁴⁹). It was found that the relative transport rates are not proportional to complex stability. *E.g.* cryptand (Fig. 67; $m = n = 1$) which forms a very stable K^+ complex, is an inefficient K^+ carrier, because of the slow exchange rate of the complex¹⁶⁷). On the other hand, cryptand (Fig. 68; 3) which forms a more lipophilic and less stable complex, is quite an efficient K^+ carrier. It appears that the cryptands display efficient carrier properties for those cations which form complexes with stability constants of about 10^5 in methanol.

The *synthetic non-cyclic ligands* described in Section 5.7 induce selective cation transport through bulk membranes. The current-voltage characteristics and the mobility of the ligands in the membrane are consistent with a carrier mechanism³¹⁴). Some of these compounds have been used as the cation carrier component in liquid membrane electrodes (cf. Section 6.2). Their ion selectivity sequence in membrane electrodes does not always correlate with the selectivity sequence obtained from their complex stability constants in alcoholic solution. According to Kirsch and Simon, this is due to the presence of complexes with varying stoichiometry in the liquid membrane electrode. As a consequence, not only one species determines the potentiometric ion selectivity¹⁵¹).

The *nigericin antibiotics* differ from the carriers mentioned so far by the fact that they form electrically neutral 1 : 1 antibiotic-cation complexes. It was therefore assumed that they induce nonelectrogenic exchange of equal amounts of different ions, which has no influence on the electrical characteristics of membranes²⁴⁰). Mueller and Rudin found, however, that nigericin induces conductivity in lipid bilayers, although this effect is relatively weak as compared with other carriers. They also detected that transmembrane potential differences are generated by nigericin in presence of an ion gradient¹⁹⁸). In a recent investigation, nigericin was found to increase the bilayer membrane conductivity by a factor of 20 and to produce a transmembrane potential of variable polarity¹⁷⁹). In order to explain the observed effects, the authors assumed that besides undissociated nigericin molecules, HA (A is the anionic form of the antibiotic), and the neutral potassium-complex, KA, charged dimers of the form $(HA_2)^-$ and $(KA_2)^-$ permeate in the membrane. In another study⁴⁵), antibiotic X-537 A was reported to increase the bilayer conductance to monovalent and bivalent ions by a factor of 10^4 . From biionic potential measurements, the following two ionic selectivity sequences were derived: $H^+ \gg Cs^+ > Rb^+$, $K^+ > Na^+ > Li^+$; and $Ba^{++} > Ca^{++} > Mn^{++} > Sr^{++} \gg Mg^{++}$. The membrane conduc-

tance for H^+ and Ca^{++} is proportional to the H^+ and Ca^{++} concentration; it has, however, approximately second power dependence on the antibiotic concentration. From this, it was concluded that the permeant species for the H^+ conductance is the dimer $(HA_2)^-$, and for the Ca^{++} conductance the dimer $(CaHA_2)^+$.

4.2. Channel Mechanism

In the presence of very small amounts of *linear gramicidins* (A, B, C), a constant applied electrical potential yields a membrane current which fluctuates in the manner shown in Figure 19. The current levels are equally spaced and consistent with

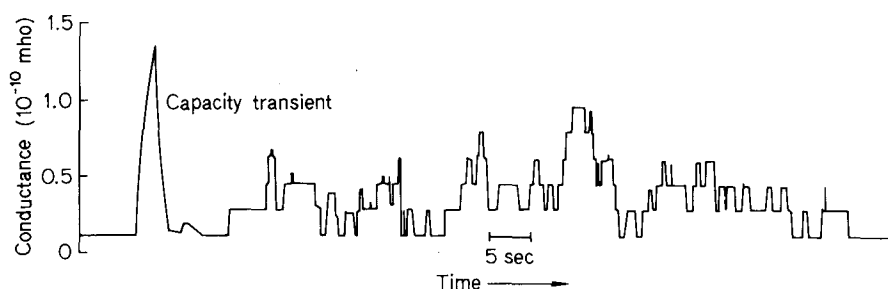


Fig. 19. Conductance transitions in a lipid bilayer membrane containing gramicidin A. The aqueous solution was 0.5 M NaCl and the applied potential was 100 mV [Reproduced from Hladky, S. B., *et al.*: *Ann. Rev. Phys. Chem.* 1974, 11.]

the notion that individual channels are opening and closing¹²⁴). Membrane potential measurements in the presence of relatively large amounts of gramicidin showed that only certain univalent ions can pass the channels. Among the alkali ions, a permeability sequence of $Rb^+ = Cs^+ > NH_4^+ > K^+ > Na^+ > Li^+$ was observed¹²³). In comparison to carriers like valinomycin and nonactin, gramicidin channels exhibit poor ion selectivity. The individual ion permeabilities through the channels are in the order of magnitude of their mobilities in aqueous solution. The channels are therefore extremely efficient in their transfer rate. At a potential difference of 100 mV, as many as 3×10^7 K^+ ions per second can be transported by one channel¹⁵) (cf. the corresponding number of 2.5×10^4 s^{-1} for valinomycin).

The membrane conductance increases with the second power of the gramicidin concentration, indicating that the conductance channel is a dimer of gramicidin^{108, 294}). A study of the channel formation kinetics also showed that the reaction is second order^{15, 155}). According to Urry, gramicidin dimers are formed by head-to-head dimerization via hydrogen bonds of two molecules in helical conformation^{287, 289}) (cf. Section 5.3.). From the temperature dependence of the rate constants, Bamberg and Lauser determined the activation energies of channel formation ($E_R = 20$ kcal/mole) and disappearance ($E_D = 17$ kcal/mole). On the basis of Urry's model, they interpreted the rather high value of E_D as representing the energy required for breakage of the hydrogen bonds during dimer dissociation¹⁶). A covalently head-to-head connected gramicidin A dimer, N, N'-(dideformyl gramicidin A)-malonamide was

synthesized by Urry and coworkers²⁸⁸). In support of the model, this compound induces membrane conductance comparable to gramicidin, but increasing with a first power dependence on concentration.

Veatch and coworkers proposed a different class of gramicidin dimers, constituting double stranded helices (cf. Section 5.3.)^{292, 293}). This model has been included in recent discussions of the mechanism of gramicidin channel formation^{17, 291}).

At lipid bilayer membranes, *alamethicin* generates voltage-dependent ion conductance changes, with characteristics identical to those found in excitable cells. Thus, the steady-state conductance is a steep exponential function of the membrane potential, it saturates at high potential, and there is rectification^{109, 116, 199, 255}). Corresponding effects have been observed with the related peptide, *suzukacillin*²⁹), and with *monazomycin*^{18, 193}). The induced membrane conductance shows sixth- to ninth-power dependence on alamethicin concentration, indicating that six to nine alamethicin molecules are necessary for one conducting unit¹²⁴). As with gramicidin, the ion fluxes are so large that they cannot reasonably be accounted for by diffusion of a carrier-ion complex, but rather by an ion conducting channel. Alamethicin conductance shows almost no ion selectivity; the channels are permeable to both mono- and divalent cations and anions of less than some critical size. At very low levels of conductance, membranes containing alamethicin show current fluctuations similar to those for gramicidin^{28, 124}). In the case of alamethicin, however, the conductance levels are not equally spaced.

In order to account for the experimental findings, especially for the cooperative character of the gating action, a model was proposed by Baumann and Mueller which is presented in Fig. 20²⁰). According to this concept, an applied voltage induces inser-

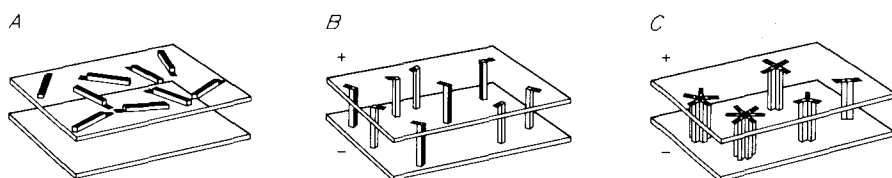


Fig. 20. A model of the gating process of alamethicin-like channel formers in a membrane. Explanation in the text
[Reproduced from Mueller, P.: Ann. N. Y. Acad. Sci. 264, 247 (1975).]

tion of the alamethicin molecules into the membrane. By lateral diffusion, they aggregate forming the walls of a transmembrane channel, like the staves of a barrel. Trimers and higher oligomers form a central opening suitable for the flow of ions. According to Mueller, the conductance steps observed at low alamethicin concentration can be interpreted as being caused by the changes of the channel diameter due to the insertion or removal of a single alamethicin molecule¹⁹⁹).

5. Structure and Conformation of Ionophoric Ligands and their Complexes

In this section we shall provide some more detailed information about the chemical composition and structure of the ligands listed in the various tables in Sections 2.3 and 3.3.

5.1. Depsipeptides

Valinomycin

In 1955, Brockmann and Schmidt-Kastner isolated valinomycin from extracts of *streptomyces fulvissimus*³³). The antibiotic was found to be active against a number of bacteria, yeasts, and fungi²⁰⁵). Valinomycin has a macrocyclic molecular structure consisting of three identical tetradepsipeptide fragments with alternating amino and hydroxy acid residues (Fig. 21). Its synthesis was first achieved by Shemyakin and

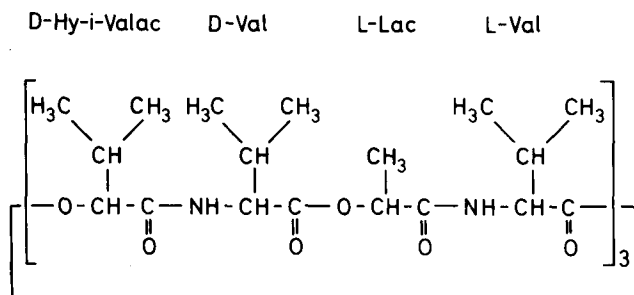


Fig. 21. Structure of valinomycin

coworkers²⁶⁶). In 1959 valinomycin was reported to uncouple oxidative phosphorylation of mitochondria¹⁸⁴). Further studies of its effects on mitochondria¹⁹²), and on the ion conductance of artificial bilayer membranes¹⁹⁷), led to the conclusion that valinomycin acts by "carrying" K^+ ions across lipophilic membranes. By various methods, it was then demonstrated that in alcoholic solution the depsipeptide forms very stable complexes with K^+ , Rb^+ , and Cs^+ ions, and very weak complexes with Li^+ , Na^+ , and NH_4^+ ions^{130, 267, 268, 307}). Complexes of valinomycin with KNCS, $KAuCl_4$, and KI_3/KI_5 have been isolated in the crystalline state^{201, 233, 236}). The latter two complexes were used for X-ray analyses.

The conformation of the valinomycin- K^+ complex in solution has been determined by the combined use of physico-chemical methods such as ORD, IR, and

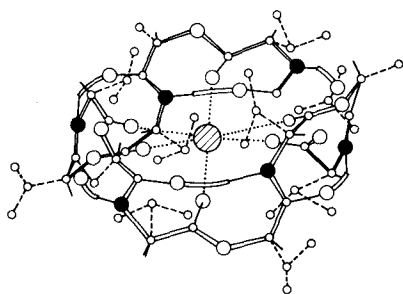


Fig. 22. Conformation of the valinomycin- K^+ complex in solution

[Reproduced from Ovchinnikov, Y. A., *et al.*: Membrane-active complexones. BBA Library, Vol. 12. Amsterdam: Elsevier 1974, p. 127]

NMR spectroscopy, and conformational energy calculations^{130, 182, 208, 221, 268}). The proposed structure (Fig. 22) is a bracelet-like conformation of the macro cycle, with the six ester carbonyl oxygen atoms coordinating the K^+ ion octahedrally. Six intramolecular hydrogen bonds of the $4 \rightarrow 1$ type are formed between the amide CO and NH groups. They provide considerable rigidity to this conformation, which is maintained throughout a range of solvents with widely differing polarities. X-ray analyses revealed the same conformation for the crystalline K^+ complex^{201, 233}). The exceptionally high ion selectivity of valinomycin can be explained on the basis of conformational features of its K^+ complex. The diameter of the chelating cavity (2.7–2.9 Å) corresponds to the size of K^+ or Rb^+ . With Cs^+ , steric strain arises, leading to a decrease in complex stability. Due to the rigid bracelet structure, the cavity cannot contract to fit the size of Na^+ . Thus, the ligand will not bind Na^+ sufficiently strongly to compensate for the much higher solvation energy of Na^+ over K^+ . Spectroscopic findings indicate that the conformation of the Na^+ complex is solvent dependent, and that the cation interacts effectively only with part of the ester carbonyl groups^{115 a}).

Non-complexed valinomycin shows considerable conformational variety. Spectroscopic studies led to the postulation of solvent dependent equilibria between three principal forms, A, B, and C (Fig. 23)^{130, 207, 209, 220, 268}). Form A which predom-

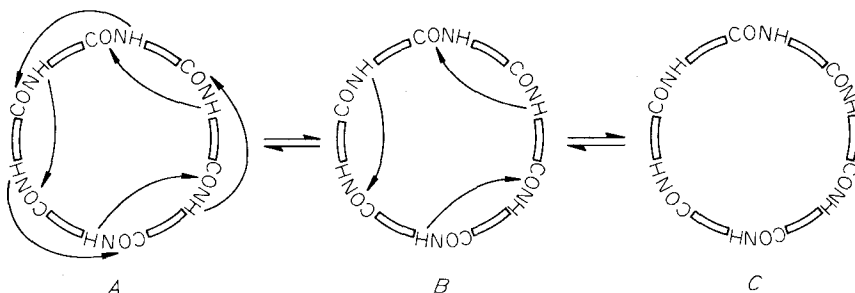


Fig. 23. Schematic representation of equilibria between valinomycin conformations A, B, and C [Reproduced from Ovchinnikov, Y. A., *et al.*: Membrane-active complexones. BBA Library, Vol. 12. Amsterdam: Elsevier 1974, p. 120]

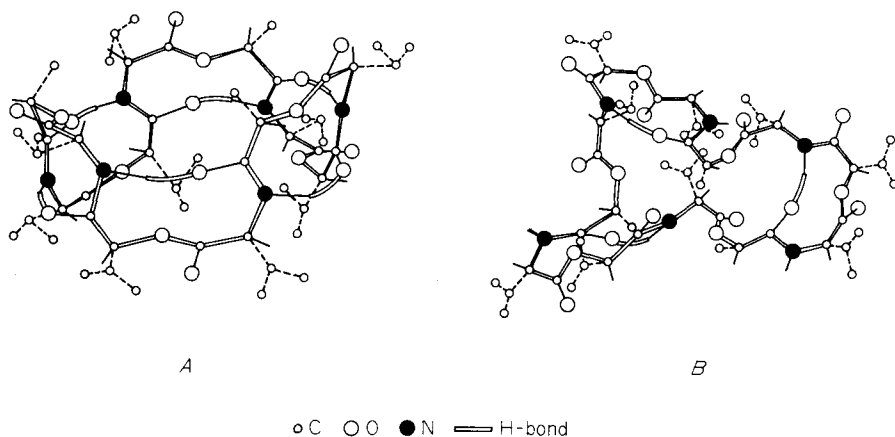


Fig. 24. Conformations of valinomycin in non-polar solvents (A) and in solvents of medium polarity (B)

[Reproduced from Ovchinnikov, Y. A., *et al.*: Membrane-active complexones. BBA Library, Vol. 12. Amsterdam: Elsevier 1974, p. 123]

inates in non-polar solvents (e.g., carbon tetrachloride) is a bracelet conformation similar to that of the K^+ complex^{a)} (Fig. 24).

In solvents of medium polarity (e.g. ethanol), form B of valinomycin predominates. It results from form A by opening the three hydrogen bonds in one plane of the bracelet. Form B resembles a propeller and is more flexible than form A (Fig. 24). Form C of valinomycin which occurs in solvents of high polarity (e.g., dimethyl sulfoxide), has no intramolecular hydrogen bonds. Instead, all NH groups are hydrogen-bonded to the solvent. Form C represents an equilibrium mixture of many flexible, energetically similar conformers. Besides the forms A, B, and C, intermediate conformations possessing five, four, two, or one intramolecular hydrogen bonds, can be assumed to exist. Evidence for the related conformational equilibria has been furnished by relaxation studies^{115 a)}.

X-ray analyses of uncomplexed valinomycin revealed a conformation of the crystalline depsipeptide which differs from all the proposed solution conformations (Fig. 25)^{77, 144, 270)}. The molecule has six intramolecular hydrogen bonds. Four of these are formed between amide CO and NH groups and belong to the $4 \rightarrow 1$ type. The other two hydrogen bonds, however, are of the $5 \rightarrow 1$ type and are formed by ester carbonyl groups. The resulting bracelet can be transformed into the complexed structure by a simple conformational change involving the change of the $5 \rightarrow 1$ type hydrogen bonds into those of the $4 \rightarrow 1$ type, as indicated by arrows in Fig. 25.

A Raman spectroscopic study of valinomycin has indicated that two conformations of the depsipeptide may exist in the solid state^{252, 254)}. When valinomycin was crystallized from n-octane or from acetone, Raman spectroscopic data of the crystal

a) For both the free and the complexed molecule, two bracelet forms (A_1 and A_2) can be formulated, differing in chirality of the ring system and orientation of the side chains. Figs. 22 and 24 show the actually occurring forms: A_1 for uncomplexed, A_2 for complexed valinomycin. For details see Ref. 217).

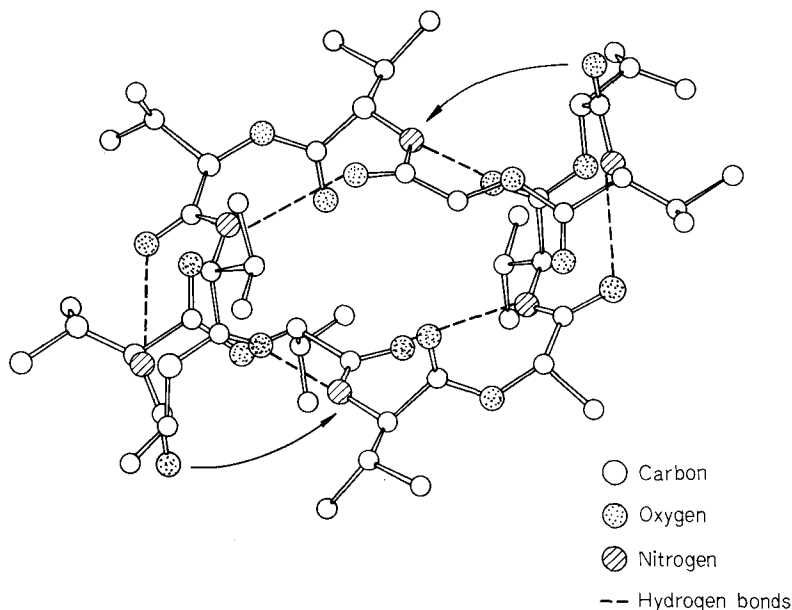


Fig. 25. Conformation of valinomycin in the crystalline state
[Reproduced from Duax, W. L., *et al.*: *Science* 176, 911 (1972).]

powder indicated a participation of ester carbonyl groups in intramolecular hydrogen bonding, in accordance with the structure revealed by X-ray analysis. If, however, the crystals were obtained from a solution in *o*-dichlorobenzene, the Raman spectroscopic findings were in agreement with the postulated valinomycin conformation in solvents of medium polarity (form B). For the valinomycin- K^+ complex the presence of a single conformation in solution as well as in the crystalline state was confirmed by the Raman spectra¹³⁾.

Other current work on valinomycin conformations includes a conformational calculation using a new spherical trigonometry method¹⁸¹⁾, and a 220 MHz proton-NMR reinvestigation leading to affirmation of *trans* orientation in the valyl residue side chains²⁹⁰⁾. Ion pairing of the valinomycin- K^+ complex has been studied by proton NMR using paramagnetic anions³⁰⁾. Proton-NMR signals of NH_4^+ ions were used to determine the rotational correlation time and the Stoke's radius of the valinomycin- NH_4^+ complex⁶⁰⁾. Recently, spectroscopic evidence for sandwich complex formation of valinomycin was reported¹³⁴⁾. The hypothetical structure of a (valinomycin)₂- K^+ sandwich complex is shown schematically in Fig. 26.

The study of more than 80 synthetic analogs of valinomycin has led to an understanding of the conformational requirements for complex formation and biological activity. Since a detailed discussion of the analogs has been given in Ref.²¹⁷⁾, only some characteristic examples are presented here (Table 8). Narrowing or widening of the cyclodepsipeptide ring affects the ion selectivity and complex stability. Analog 2 is capable of forming Na^+ and K^+ complexes, although formation of a bracelet conformation results in steric strain²¹⁶⁾. As is expected from the smaller

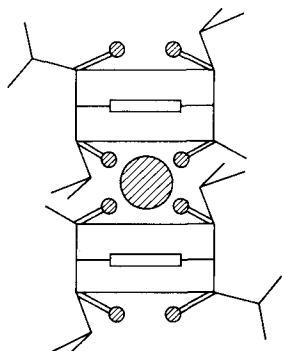


Fig. 26. Hypothetical structure of a 2:1 valinomycin-cation complex

[Reproduced from Ivanov, V. T.: Ann. N. Y. Acad. Sci. 264, 221 (1975).]

cavity, analog 2 exhibits $\text{Na}^+ > \text{K}^+$ ion selectivity. The internal cavity of analog 3 is too large to provide for effective interaction of all ester carbonyl groups with the metal ion. Therefore this analog complexes K^+ only weakly, Cs^+ somewhat better. Analogs 4 and 5 show that individual amino and hydroxy acids can be replaced by related compounds without substantially affecting the complex stability. If, however, an amino acid is replaced with a hydroxy acid (analog 6) or an N-methyl-amino acid (analog 7), intramolecular hydrogen bonds are lost and the stability constants decrease markedly.

According to Ovchinnikov and coworkers, the antibiotic activity of valinomycin is due to impairment of alkali ion transport in bacterial membranes²¹⁷. The main arguments for this theory are: (i) None of the synthetic non-complexing analogs has antibiotic activity; (ii) enantio-valinomycin has the same antibiotic activity as valinomycin, thus excluding interaction with a stereospecific receptor; (iii) valinomycin increases the cation permeability of bacterial membranes; (iv) the antimicrobial action of valinomycin depends on the cation composition of the medium.

Corresponding observations have been made with enniatins, macrotetrolides, and linear gramicidins. These antibiotics are therefore believed to have a mechanism of action, analogous to that of valinomycin.

Enniatins and Beauvericin

Enniatins A and B were isolated in 1947 by Plattner and coworkers from the culture fluid of several *Fusarium* species²³⁸. Beauvericin is a metabolite of the fungus *Beauveria bassiana*¹¹⁷. Syntheses of the enniatins were first reported in 1963^{239, 246}. Beauvericin was synthesized in 1971²¹². The structures of the three closely related antibiotics are shown in Fig. 27.

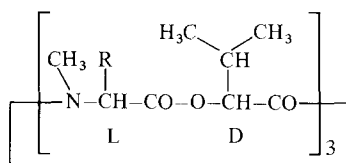


Fig. 27. Structures of enniatins A and B, and of beauvericin

R = sec-butyl Enniatin A
R = iso-propyl Enniatin B
R = benzyl Beauvericin

The compounds form 1 : 1 complexes with all alkali ions and with a large number of other metal ions in organic solvents^{267, 268, 307}. Among the alkali ions, K^+ is bound most strongly, but K^+ -complex stability as well as $K^+ > Na^+$ selectivity are much less pronounced than with valinomycin. In concentrated enniatin solutions, non-equimolar complexes are formed. NMR- und CD-spectroscopic titrations have demonstrated that 2 : 1 enniatin-cation complexes are formed with a stability order of $K^+ > Cs^+ > Na^+$. Evidence for formation of a 3 : 2 complex with Cs^+ was also obtained^{133, 216}.

Spectroscopic studies of enniatin B in solvents of different polarity have shown that two conformations are in equilibrium: A non-polar form N and a polar form P (Fig. 28)^{211, 216}. It is believed that the conformational change of enniatin is due to

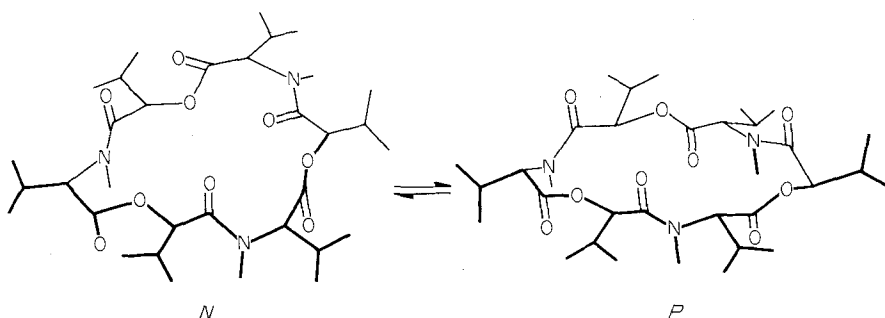


Fig. 28. Conformations of enniatin B in non-polar solvents (N) and in polar solvents (P) [Reproduced from Ovchinnikov, Y. A.: FEBS Letters 44, 1 (1974).]

solvation processes which change the orientation of the carbonyl and isopropyl groups, and hence the ring structure. A relaxation study of enniatin B in various solvents revealed the existence of several conformational equilibria¹¹¹. It can therefore be assumed that more conformations exist besides the basic N and P forms.

The conformation of the crystalline enniatin B- K^+ complex was determined by X-ray analysis⁷². NMR-spectroscopic analyses have shown that the same conformation is adopted by the complex in solution (Fig. 29)²¹¹. The conformation of the complex closely resembles the conformation of enniatin in polar solvents (form P, cf. Fig. 28). This was also confirmed by a molecular orbital calculation¹⁷⁷.

In the complex, the six carbonyl groups form an approximately octahedral coordination sphere for the cation. Due to the large angle which is formed between the carbonyl groups and the $K^+ \cdots O$ interaction, binding of the cation is weaker than in the case of valinomycin. The low cation selectivity of the enniatins is due to their high structural flexibility. Enniatins cannot form intramolecular hydrogen bonds, which in the case of valinomycin stabilize a rigid complex conformation. By appropriate rotations in the backbone structure, the chelating cavity of enniatin is fitted to different sizes of cations.

The enniatin complex molecule resembles a charged disc with lipophilic boundaries. In the crystal, many of these discs are stacked in columns. With respect to this property, sandwich structures have been proposed for the non-equimolar enniatin

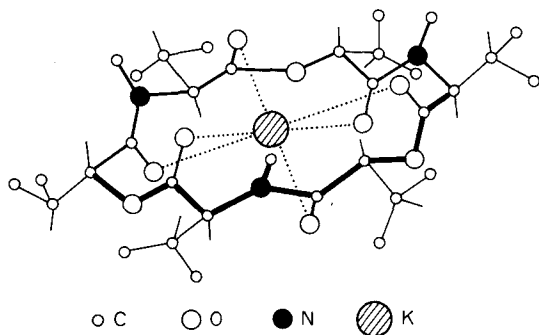


Fig. 29. Conformation of the enniatin B - K^+ complex in solution

[Reproduced from Ovchinnikov, Y. A., *et al.*: Biochem. Biophys. Res. Comm. 37, 668 (1969).]

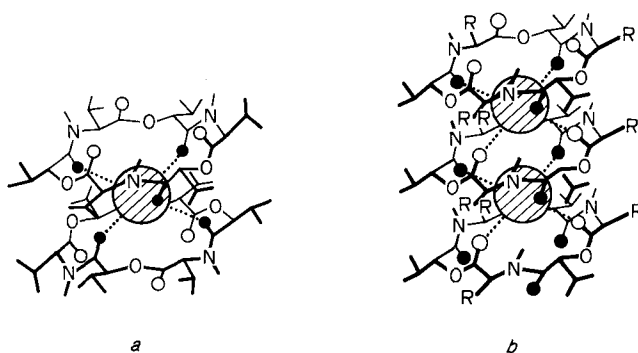


Fig. 30. Proposed conformations of (a) 2:1 and (b) 3:2 enniatin B - cation complexes [Reproduced from Ivanov, V. T., *et al.*: FEBS Letters 36, 65 (1973).]

complexes (Fig. 30). The conformation of enniatin in these complexes is probably similar to that of the 1:1 complex. This has been concluded from the similarity of the corresponding CD spectra¹³³.

Bis-enniatiin B (Fig. 31) which has the structural prerequisites for formation of an equimolar sandwich complex, has been synthesized in order to clarify the stoichiometry of enniatin complexes in lipid bilayers¹³³.

X-ray analysis of the crystalline 2:2 complex of beauvericin with Ba^{++} has revealed the interesting structure shown in Fig. 32¹¹⁸. The two Ba^{++} ions in the center of the complex are held together by three picrate anions which contribute to the coordination. Each of the two beauvericin molecules contributes three chelating amide oxygens. The resulting structure has much in common with the sandwich conformations shown in Fig. 30.

About 60 structural analogs of enniatin have been synthesized. A detailed discussion of their properties is given in Ref.²¹⁷. Compared to the valinomycin analogs, the various enniatins exhibit only weak correlation between their individual depsipeptide structure and complex stability/ion selectivity. The flexibility of the enniatin compounds and their inability to form intramolecular hydrogen bonds are believed to account for these characteristics.

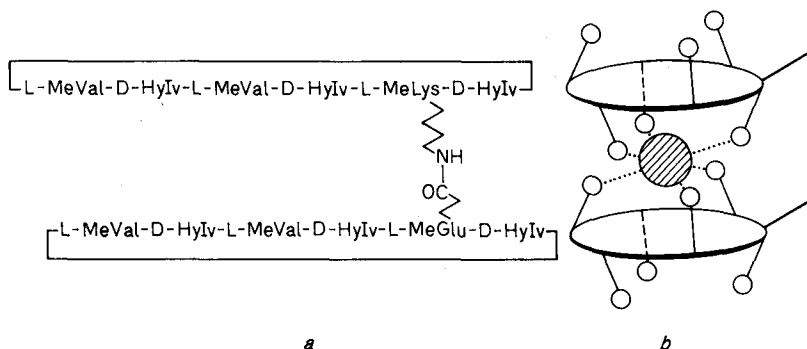


Fig. 31. Bis-enniatin B. a, Sequence of the depsipeptide; b, assumed structure of its equimolar sandwich complex

[Reproduced from Ivanov, V. T., *et al.*: FEBS Letters 36, 65 (1973).]

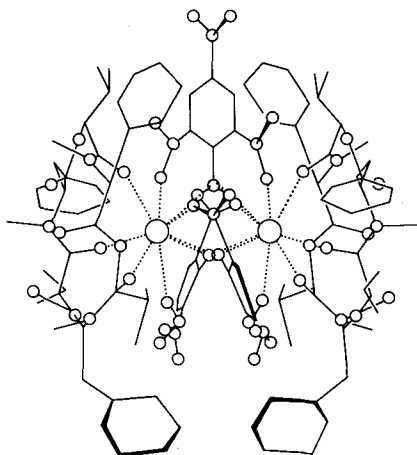


Fig. 32. Conformation of the crystalline 2:2 complex of beauvericin with barium picrate [Reproduced from Hamilton, J. A., *et al.*: Biochem. Biophys. Res. Comm. 64, 151 (1975).]

5.2. Depsides. Nonactin and its Homologs

Various species of Actinomyces produce a mixture of homologous macrotetrolides of the general formula shown in Fig. 33¹⁰⁶). The macrotetrolides were found to possess broad antimicrobial activity spectra¹¹⁾ as well as insecticidal qualities²¹⁷⁾. Recently, Gerlach and coworkers carried out the first synthesis of nonactin by a stepwise condensation of four nonactic acid molecules and subsequent cyclization¹⁰⁷⁾. Complex formation of the macrotetrolides with alkali metal ions has been thoroughly studied by NMR and IR spectroscopy and vapour pressure osmometry^{209, 235, 243, 244, 307)}. The macrotetrolides exhibit $K^+ > Na^+$ ion selectivity which increases with increasing number of ethyl side chains.

The conformation of crystalline nonactin and tetranactin have been resolved by X-ray analyses^{73, 129)} (Figs. 34 and 35). The two flat ring structures show consider-

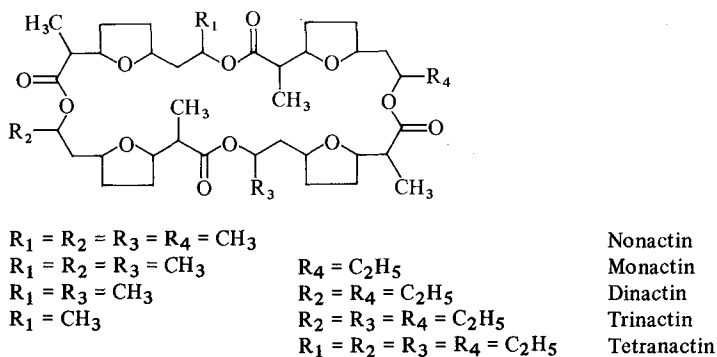


Fig. 33. Structures of nonactin and homologs

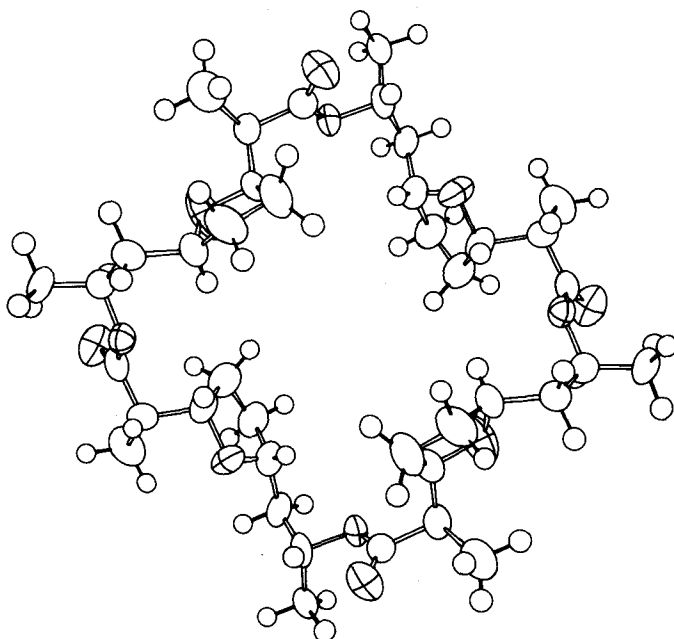


Fig. 34. Conformation of nonactin in the crystalline state. Cross-marked ellipsoids represent oxygen atoms

[Reproduced from Dobler, M.: *Helv. Chim. Acta* 55, 1371 (1972).]

able conformational differences, indicating a high degree of flexibility of the basic macrocycle.

A large number of macrocyclic-cation complexes has been analyzed by X-ray crystallography: Nonactin complexes with Na^+ , K^+ , and NH_4^+ were studied by Swiss workers^{71, 147, 202}, whereas tetranactin complexes with Na^+ , K^+ , Rb^+ , and

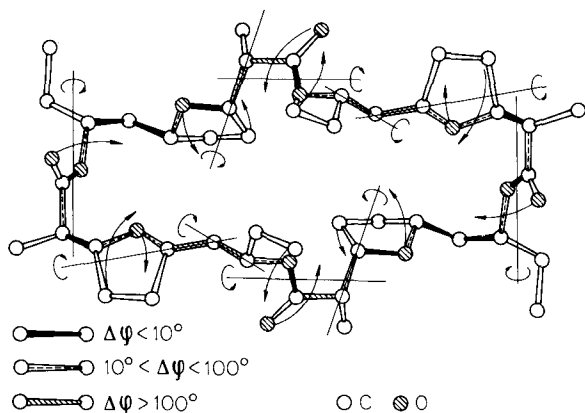


Fig. 35. Conformation of crystalline tetranactin. Atomic shifts and bond rotations accompanying complexation are shown by arrows. Bond representations along the backbone correspond as shown in the lower left-hand corner to the complexing-induced changes in the torsional angles [From Ovchinnikov, Y. A., *et al.*: Membrane-active complexones. BBA Library, Vol. 12. Amsterdam: Elsevier 1974, p. 184 and Iitaka, Y., *et al.*: Chem. Letters (Japan) 1972, 1225.]

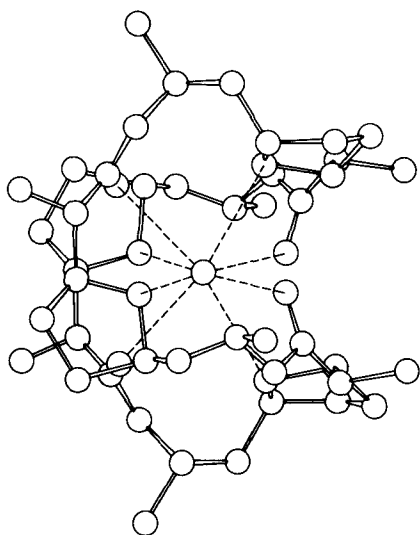


Fig. 36. Conformation of the crystalline nonactin- K^+ complex [Reproduced from Kilbourn, B. T., *et al.*: J. Mol. Biol. 30, 559 (1967).]

NH_4^+ were investigated by a Japanese group^{129, 200}). All these complexes proved to possess very similar conformations. In the nonactin- K^+ complex (Fig. 36) the desolvated K^+ ion is chelated by four tetrahydrofuran oxygens and four carbonyl oxygens. These eight oxygen atoms are nearly equidistant from the central ion (2.75 to 2.83 Å), providing an approximately cubic coordination sphere. The depside chain is shaped like the seam of a tennis ball, the side chains and tetrahydrofuran rings forming a hydrophobic exterior. The conformation of the nonactin- Na^+ complex is adapted to the smaller cation by a denser folding of the backbone, thereby providing

a distorted cubic coordination sphere. The four carbonyl oxygen atoms are closer to the Na^+ ion (2.42 Å) than the ether oxygen atoms (2.77 Å) which are sterically hindered from a closer approach. The preference of nonactin for K^+ with respect to Na^+ can be related to the change in coordination geometry from eight equidistant oxygens in the K^+ complex to only four first neighbour oxygen atoms in the Na^+ complex. In the nonactin- NH_4^+ complex (Fig. 37), the cubic coordination is distorted

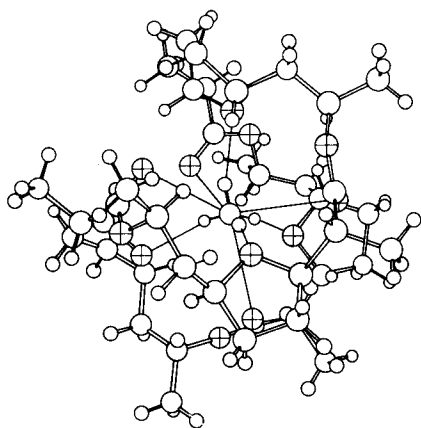


Fig. 37. Conformation of the nonactin- NH_4^+ complex in the crystalline state
[Reproduced from Neupert-Laves, K., Dobler, M.: *Helv. Chim. Acta* 59, 614 (1976).]

in such a way that the four ether oxygen atoms are appreciably closer to the nitrogen atom (2.83 to 2.89 Å) than the four carbonyl oxygen atoms (3.01 to 3.16 Å). The four hydrogen atoms of the NH_4^+ ion form almost linear hydrogen bonds with the ether oxygen atoms. NH_4^+ ions are more strongly bound by nonactin than by valinomycin. This may be attributed to the more favourable interaction of NH_4^+ with four tetrahedrally arranged oxygen atoms in nonactin than with six octahedrally arranged ones in valinomycin²⁰².

NMR studies of nonactin and its Na^+ , K^+ , and Cs^+ complexes in solution have shown independently that the complexes have quite similar conformations enclosing the desolvated cation^{243, 244}. The NMR data also indicated that the nonactin ring undergoes sizeable conformational changes on incorporation of these cations. As can be seen from the X-ray resolved structures, the conformational change affects eight torsional angles of the 32-membered ring. Thereby a reorientation from outward- to inward-pointing carbonyl and tetrahydrofuran oxygen atoms and formation of the cavity is accomplished.

5.3. Peptides

Antamanide

In 1968, Wieland and coworkers isolated antamanide from the poisonous mushroom, *Amanita phalloides*²⁹⁸. The substance was found to possess the unique property of

counteracting the toxic effects produced by phalloidin, a peptide from the same mushroom. If applied simultaneously with phalloidin, antamanide prevents the typical intoxication symptoms: accumulation of phalloidin in the liver, release of K^+ and enzymes from the liver cells³⁰², and dramatic changes of the cytoplasmic membrane of hepatocytes⁹³. Pretreatment of the perfused rat liver with a high phalloidin concentration did not reduce binding of antamanide to the organ, as could be expected if the two substances compete for the same receptor site. Therefore, it was suggested that antamanide acts by tightening the cytoplasmic membrane against penetration of phalloidin³⁰².

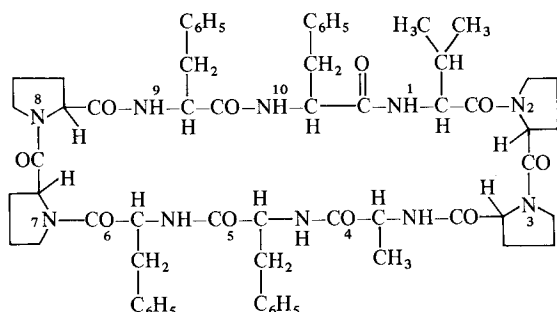


Fig. 38. Structure of antamanide

Antamanide is a cyclic decapeptide containing only L-amino acids (Fig. 38). It has been synthesized using either classical or solid phase methods^{298, 299}. The appearance of an ion corresponding to antamanide- Na^+ in the mass spectrum was the first indication to ion complexes of antamanide. IR spectroscopy (increase of carbonyl absorption in the presence of Na^+) and ORD spectral changes showed that the peptide interacts with cations by means of its amide carbonyl groups³⁰⁰. The stability of antamanide complexes with various cations was determined by vapour pressure osmometry, potentiometry, conductometry, spectrophotometric titrations³⁰⁰ as well as by two-phase partition experiments³⁰¹. In the alkali metal ion series, antamanide exhibits a selectivity order of



Among the alkaline earth metal ions, Ca^{++} is bound strongly, whereas only weak binding occurs with Sr^{++} and Ba^{++} , and no interaction with Mg^{++} . CD spectral changes also indicated complex formation with Tl^+ . Antamanide exhibits clearly a preference for ions of about 1 Å radius.

Considerable effort has been devoted to conformational studies of antamanide. The first CD and NMR spectroscopic investigation of the peptide in solution resulted in the conclusion that antamanide assumes a single conformation in solvents of widely varying polarity. The proposed structure has all-*trans* peptide bonds and no intramolecular hydrogen bonds²⁸³. Further studies, including IR spectroscopy, have provided evidence for the existence of several antamanide conformations differing in the number of intramolecular hydrogen bonds. A conformation of anta-

manide in non-polar solvents was proposed which exhibits some analogies to the conformation of valinomycin in non-polar solvents. It is a bracelet-like structure with the maximum number of six intramolecular hydrogen bonds^{131, 215}). A more recent NMR study by Patel revealed the existence of two *cis* X-Pro peptide bonds in the molecule. Since two different locations of these bonds were compatible with the NMR data and conformational calculations, two proposals were given for each of two solvent-dependent antamanide conformations^{222, 284}). The solution approach to antamanide conformations has thus led to a considerable variety of proposed structures.

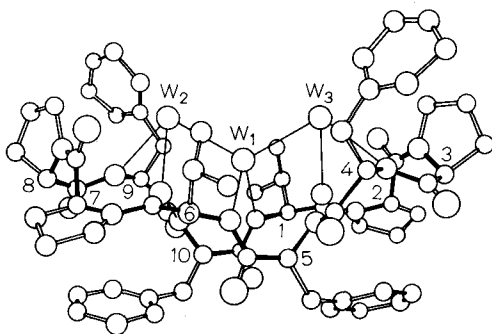


Fig. 39. Conformation of [Phe⁴, Val⁶] antamanide, crystallized from non-polar solvents. The water molecules associated with the peptide are labeled W_i, and hydrogen bonds are indicated by light lines

[Reproduced from Karle, I. L., *et al.*: Proc. Nat. Acad. Sci. USA 73, 1782 (1976).]

A recent X-ray analysis of the analog, [Phe⁴, Val⁶] antamanide, crystallized from non-polar solvents, revealed the conformation shown in Fig. 39¹⁴⁵). The molecule forms an elongated, relatively planar ring, containing two *cis* Pro-Pro peptide bonds. Since *cis-trans* interconversions of antamanide peptide bonds can be ruled out on grounds of the NMR data²²²), the earlier proposed conformations with all-*trans* peptide bond configuration appear very unlikely. The X-ray resolved structure has some unpredicted and unusual features: Only two intramolecular hydrogen bonds are formed, and these are of the rare 5 → 1 type. Nevertheless, the four remaining NH groups are also hydrogen bonded to an array of three water molecules. Antamanide is known to retain one to two water molecules even after drying in vacuo over P₂O₅ at 60° for one week. The resolved structure can in fact be considered as an H₂O complex of antamanide. An interesting feature is the interruption of the hydrophobic side and bottom exterior of the molecule by two rows of three carbonyl oxygens which do not participate in any hydrogen bonding. Karle and Duesler have now reported the X-ray analysis of [Phe⁴, Val⁶] antamanide, crystallized from a solution containing calcium nitrate, acetone and acetonitrile³²⁶). The peptide is uncomplexed and has the same conformation as shown in Fig. 39. The crystal contains 12 water molecules per peptide molecule. Three of these occupy the positions W₁, W₂, and W₃. Of the remaining water molecules, some are hydrogen-bonded to exterior peptide carbonyl groups, others are hydrogen-bonded only to other water molecules. Thereby continuous channels of water molecules are formed in the crystal.

Preliminary X-ray analytical data of [Phe⁴, Val⁶] antamanide, crystallized from organic solvent-water mixtures, indicate that in polar solvents the peptide assumes a conformation different from either the one in non-polar solvents or in the com-

plex (see below). From NMR spectroscopic data and ultrasonic absorption measurements in various solvents, the existence of three antamanide conformations has been suggested^{36, 222}). Further X-ray studies may reveal the related spatial structures.

Elucidation of the complex conformation of antamanide has also been a gradual process. From the first analysis on the basis of IR, ORD, and NMR spectra, a bracelet conformation similar to the valinomycin- K^+ complex was proposed, possessing all-



Fig. 40. Conformation of the antamanide- Li^+ complex, crystallized from acetonitrile. The phenyl groups of Phe⁵ and Phe¹⁰ have been omitted for clarity.

[Reproduced from Karle, I. L., *et al.*: Proc. Nat. Acad. Sci. USA 70, 1836 (1973).]

trans peptide bonds and four intramolecular hydrogen bonds¹³¹). As with the uncomplexed molecule, a reinvestigation brought evidence for two *cis* X-Pro peptide bonds and led to the proposal of two conformations with different locations of these bonds²²³).

X-ray analysis finally revealed the conformation of the antamanide- Li^+ complex as shown in Fig. 40^{141, 142}). As was pointed out by Patel and Tonelli, one of the proposed solution-conformations agrees with the crystal-conformation in the following features: Similar overall molecular shape, two *cis* Pro-Pro peptide bonds, two 4 → 1 type intramolecular hydrogen bonds in identical positions, similar arrangement of eight carbonyl groups²²⁴). The unpredicted and most unusual feature in the X-ray resolved structure is the penta-coordination of the Li^+ ion. The cation resides in a shallow cup and is coordinated by four carbonyl oxygen atoms, two of which also participate in intramolecular hydrogen bonds. The fifth ligand is provided by a molecule of acetonitrile which was the solvent of crystallization. Curiously,

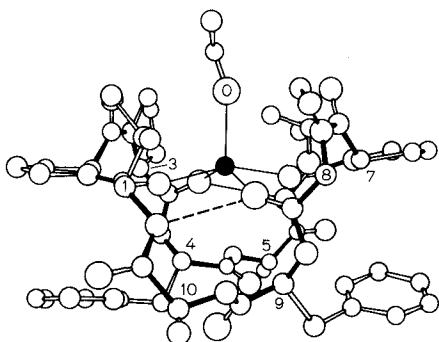


Fig. 41. Conformation of the [Phe⁴, Val⁶]antamanide- Na^+ complex, crystallized from ethanol. The phenyl groups of Phe⁵ and Phe¹⁰ have been omitted for clarity.

[Reproduced from Karle, I. L.: Biochemistry 13, 2155 (1974).]

there is another cavity in the molecule located below the Li^+ and lined with six carbonyl oxygen atoms, which remains empty.

The $[\text{Phe}^4, \text{Val}^6]$ antamanide- Na^+ complex has also been investigated by X-ray crystallography and was found to be isostructural with the antamanide- Li^+ complex (Fig. 41)^{141, 143}. Since the Na^+ complex was crystallized from ethanol, a molecule of this solvent figures as the fifth ligand of the Na^+ ion. As a consequence of introducing a larger metal ion, the upper cavity of the Na^+ complex is expanded in such a way that the two intramolecular hydrogen bonds are considerably widened. If antamanide retains the same conformation in forming a K^+ complex, it seems unlikely that the upper cavity can expand further in order to accommodate the size of this cation. This would explain the $\text{Na}^+ > \text{K}^+$ ion selectivity of antamanide. One may speculate that the K^+ ion could be placed somewhat further above the plane formed by the four chelating oxygen atoms, or it may alternatively occupy the interior of the lower cavity¹⁴³.

The close similarity of the two resolved complex conformations, despite the different solvents of crystallization, strongly suggests that they represent also the conformations in solution.

Recent CD and NMR studies have demonstrated the ability of antamanide to form also 2:1 peptide-cation complexes with Na^+ and Ca^{++} ions¹³⁴. A possible sandwich structure of these complexes was proposed by Ivanov and Ovchinnikov, taking into account the described coordination pattern of antamanide (Fig. 42)²¹⁸.

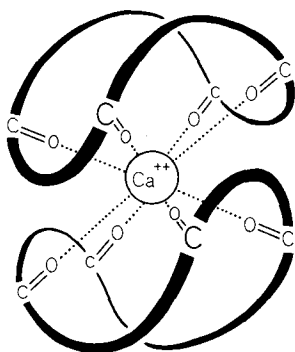


Fig. 42. Possible structure of an $(\text{antamanide})_2\text{-Ca}^{++}$ sandwich complex
[Reproduced from Ivanov, V. T.: *Ann. N. Y. Acad. Sci.* 264, 221 (1975).]

The same authors have proposed the following interesting hypothesis for the mode of action of antamanide which is illustrated in Fig. 43. Antamanide might coordinate to Ca^{++} or Na^+ ions which are bound to phospholipids on the cell membrane surface, thereby modifying the membrane properties sufficiently to inhibit penetration of phalloidin. Since the antitoxic action of antamanide is stereospecific (enantio-antamanide has only 1/20 of the biological activity of antamanide), protein components of the membrane are assumed to participate in the binding. Stacking of aromatic groups of the proteins with the phenyl groups of antamanide could contribute to the binding. This would explain why perhydro-antamanide (with cyclohexyl rings instead of the phenyl rings) is biologically inactive, although it forms as stable complexes as antamanide.

Besides the antamanide analogs already mentioned, more than 50 others have been synthesized in order to study relationships between structure, biological

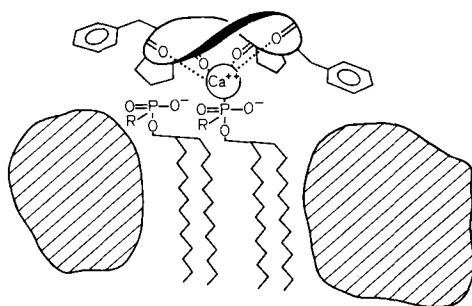


Fig. 43. Proposed principle of antamanide interaction with a cell membrane. Hatched areas symbolize protein globules
[Reproduced from Ivanov, V.T.: Ann. N. Y. Acad. Sci. 264, 221 (1975).]

activity, and complex formation. The analogs differ from the original compound in one or several amino acid residues, in ring size, in inversed configuration of all amino acid residues (enantio-antamanide), or in reversed direction of acylation (retro-antamanide). Since a detailed description has been given in Ref.²¹⁷⁾, only some examples are presented here (Tables 10 and 11).

As can be seen from Fig. 40, the isopropyl side chain of valine in position 1 contributes substantially to hydrophobic shielding of the complexed cation. It might also contribute to hydrophobic attachment of antamanide to the cell membrane (cf. Fig. 43). In analogs 2–5 the aliphatic side chain of residue 1 is modified. Extension of the side chain by one C atom (analog 2) leaves biological activity and complex formation unaffected. Shortening by one, two, or three C atoms (analog 3, 4, and 5) leads to a stepwise decrease in biological activity and Na^+ complex stability. The reduced biological activity of retro-antamanide (analog 6) can also be ascribed to the shortened side chain of residue 1. The higher complex stability of this analog in comparison to analog 4 is surprising.

Analog 7–9 illustrate the importance of a correct sequence in positions 7 and 8. In the antamanide- Na^+ complex, Pro^7 and Pro^8 form a *cis* peptide bond, resulting in a sharp turn of the macrocycle (Fig. 40). Like Val^1 , they are located along the “upper” opening of the cavity, contributing to effective enclosure of the cation and probably to hydrophobic interaction with membranes (Fig. 43). Exchange of Pro^7 (analog 7 and 8) or removal of Pro^7 (Pro^8) (analog 9) results in complete loss of biological activity and in the lowest complex stabilities of all analogs tested.

Analog 10, a symmetrical antamanide, exhibits exceptionally high complex stability. Its biological activity is, however, markedly reduced. As with analog 11, perhydro-antamanide, this may be due to the disappearance of phenyl rings which are required for the binding of antamanide to membrane proteins.

Apparently, complex formation is only one condition for the biological activity of antamanide analogs. Other molecular features, like certain lipophilic side chains and the chirality (cf. analog 12), also play an important role, thereby suggesting an interaction of the peptide with a stereospecific receptor.

Synthetic Cyclopeptides

The idea of obtaining sandwich complex forming compounds by connecting two cyclic peptides with a covalent bridge was first realized by Schwyzner and cowork-

ers²⁶⁴). They synthesized the pentapeptide *cyclo*(Gly-L-Cys-Gly-Gly-L-Pro) which showed no signs of complex formation with cations in methanol. By formation of a disulfide bridge between the cystein residues, the bicyclic peptide *S-S'-bis-[cyclo(Gly-L-Cys-Gly-Gly-L-Pro)]* was obtained. This compound forms cation complexes, exhibiting the following order of ion selectivity: $K^+ > Na^+ > Li^+ > Ca^{++}$. The structure of the sandwich complexes is schematically shown in Fig. 44.

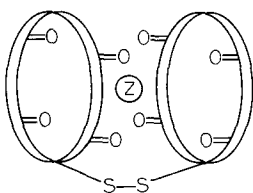


Fig. 44. Principle of sandwich complex formation of a cystin-bridged bicyclic peptide with a cation, Z.
[Reproduced from Schwyzer, *et al.*: *Helv. Chim. Acta* 53, 15 (1970) and Ovchinnikov, Y. A., *et al.*: *Membrane-active complexones*. BBA Library, Vol. 12. Amsterdam: Elsevier (1974).]

The hexapeptide, *cyclo*(L-Pro-Gly)₃, has been shown to form complexes with a number of metal ions¹⁷⁵). The compound exhibits ion selectivity for Li^+ and Na^+ over K^+ and larger alkali metal ions. It also forms a Ca^{++} complex which has a stability constant in acetonitrile of $K_{stab} = 1.1 \times 10^5 M^{-1}$. With Mg^{++} three different complexes with cyclopeptide-cation stoichiometries of 2:1, 1:1, and 1:2 are formed. Hypothetical structures of these complexes (Fig. 45) have been proposed which are reminiscent of the enniatin sandwich complexes.

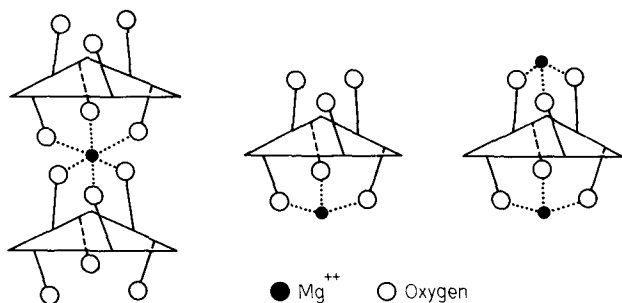


Fig. 45. *Cyclo*(L-Pro-Gly)₃ complexes with Mg^{++} . Schematic representation of possible structures
[Reproduced from Madison, V., *et al.*: *J. Am. Chem. Soc.* 96 (21), 6725 (1974).]

NMR and CD spectroscopy revealed the existence of several conformations of the cyclopeptide and its complexes^{27, 62}). In non-polar solvents, a C_3 symmetric conformation with *trans* peptide bonds and three 3→1 type hydrogen bonds exists. From this conformation, the complex is formed by rotation of the peptide bond units between Pro and Gly residues (Fig. 46). The complex conformation retains C_3 symmetry and all-*trans* peptide bonds, but it is devoid of intramolecular hydrogen bonds. In polar solvents, *cyclo*-(L-Pro-Gly)₃ forms an unsymmetric conformation with one *cis* Gly-Pro peptide bond.

Ion binding cyclopeptides have also been described which are structurally related to the depsipeptides, enniatin and valinomycin. Complex formation of the

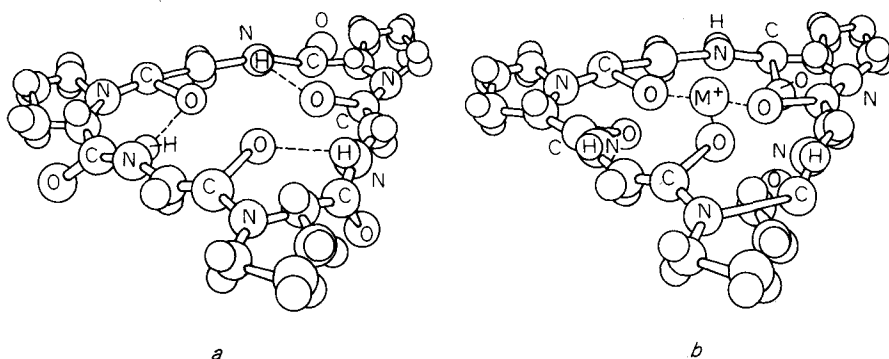


Fig. 46. Spatial structures of $\text{cyclo}(\text{L-Pro-Gly})_3$ in solution. a, Free peptide; b, cation complex [Reproduced from Deber, C. M., Pfeiffer, D. R.: *Biochemistry* 15 (1), 132 (1976).]

peptide analog of enniatin, $\text{cyclo}(\text{L-Val-Sar})_3$, was recently investigated in detail by Ivanov¹³⁴). It was found that this compound forms less stable alkali ion complexes than enniatin, preferring Na^+ to K^+ ions. In concentrated solutions, $\text{cyclo}(\text{L-Val-Sar})_3$ also forms 2 : 1 peptide-cation complexes with sandwich structure.

The peptide analog of valinomycin, $\text{cyclo}(\text{D-Val-L-Pro-L-Val-D-Pro})_3$, was studied by Davis and coworkers⁶¹). From NMR spectroscopic investigations, it was concluded that the cation complexes of the peptide are essentially isostructural with the K^+ complex of valinomycin. In contrast to valinomycin, the Li^+ and Na^+ complexes of the peptide analog are stable in methanol and have very slow dissociation rates. It was proposed that the peptide may have a higher affinity for cations than valinomycin because of its higher potential energy in the uncomplexed state.

Alamethicin and Suzukacillin

Alamethicin is a peptide antibiotic produced by the microorganism *Trichoderma viride*¹⁸⁷). A first determination of its primary structure was carried out in 1970 by Payne and coworkers²²⁵) and confirmed by mass spectroscopy²¹³). From this work, a cyclic structure was proposed for alamethicin which is shown in Fig. 47. Seventeen of the eighteen L-amino acids form the macrocycle. The eighteenth residue, glutamine, is attached as a side chain and has a free carboxyl group. On the basis of this primary structure, a conformation of alamethicin has been calculated³⁷) (Fig. 47), and conformational equilibria have been investigated by NMR and CD spectroscopy^{139, 138}). A recent reinvestigation of alamethicin by NMR spectroscopy arrived at a substantially different structure¹⁸⁰) (Fig. 48). The peptide was found to be linear, consisting of nineteen amino acids, an N-terminal blocking acetyl group, and a phenylalaninol side chain at the eighteenth residue.

Alamethicin has a relatively low antimicrobial activity. At mitochondrial and artificial membranes, alamethicin increases ion conductance, presumably by forming channels in the membrane (cf. Section 4.2.). Two-phase ion partition experiments have shown that the peptide also facilitates the transfer of alkali metal ions into an organic phase²⁴⁰). From these findings the formation of alamethicin-cation

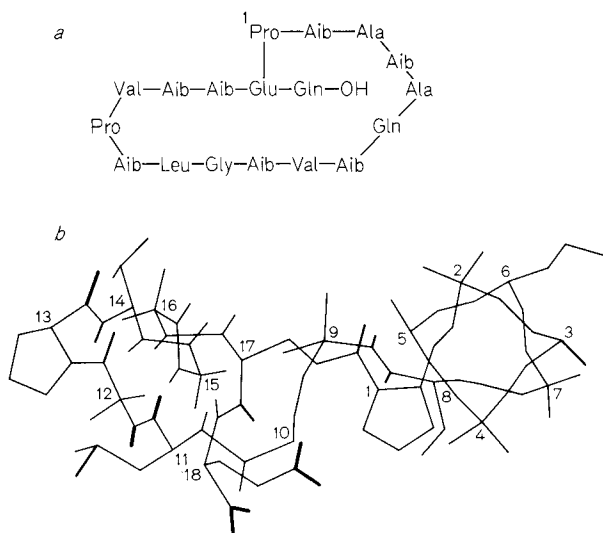


Fig. 47. Alamethicin. a, Primary structure after Payne *et al.* (1970); b, possible conformation after calculations of Burgess and Leach (1973) (Aib = α -Aminoisobutyric acid) [Reproduced from Jung, G., *et al.*: Hoppe Seyler's Z. Physiol. Chem. 355 (10), 1213 (1974).]

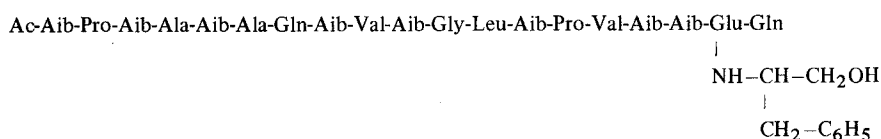


Fig. 48. Alamethicin sequence after Martin and Williams (1976)

complexes has been suggested. Since neither the CD spectra¹⁸³⁾ nor the NMR spectra¹²⁰⁾ of alamethicin are affected by the presence of univalent ions in solution, direct evidence of complex formation by this peptide is lacking.

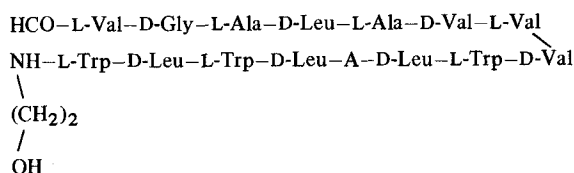
Suzukacillin is an antibiotic produced by the same microorganism as alamethicin²¹⁰⁾. Recent investigations have shown that suzukacillin is a linear peptide with an alamethicin-like sequence of twenty-three amino acids and one phenylalaninol residue¹⁴⁰⁾. Suzukacillin exhibits membrane modifying properties similar to alamethicin²⁹⁾.

Gramicidins A, B, and C

The antibiotic mixture produced by *Bacillus brevis* contains a group of related peptides, the gramicidins A, B, and C. Similar to alamethicin, the gramicidins were first assumed to have a cyclic structure¹²⁸⁾. Sarges and Witkop have, however, shown that they are linear pentadecapeptides, with an N-terminal blocking formyl group and ethanolamine as the C-terminal residue²⁵⁷⁾. The sequences of valine-gramicidins

A, B, and C are shown in Fig. 49. Isoleucine-gramicidins A, B, and C differ from these structures only by an isoleucine instead of a valine residue in position 1.

The gramicidins possess antibiotic activity against many Gram-positive microorganisms. Recent investigations have indicated that gramicidin and tyrocidin play an antagonistic regulatory role on the sporulation of *Bacillus brevis* which produces both of them^{248, 249, 250}.



A = L-Trp	Valine-gramicidin A
A = L-Phe	Valine-gramicidin B
A = L-Tyr	Valine-gramicidin C

Fig. 49. Structures of valine-gramicidins A, B, and C

At biological and artificial membranes, gramicidins produce large and stepwise changes of ion conductance. They are believed to act by forming ion conducting channels in the membrane (cf. Section 4.2.). The formation of a pseudo-cyclic, enniatin-like ion complexing conformation of gramicidin A has been suggested by Lardy and coworkers¹⁶³). A direct investigation of the ion binding properties of gramicidin A has, however, shown that the peptide binds cations very weakly, and that it transports cations through a chloroform layer much more poorly than a diffusional carrier⁴²).

Interesting hypotheses have been developed on the conformational states of gramicidin involved in transmembrane channel formation. Figure 50 shows a model suggested by Urry^{287, 289}). The ion conducting channel is formed by two gramicidin molecules in helical conformation which are connected "head-to-head" by hydrogen bonds. The dimer is long enough to span across a lipid bilayer membrane. In order to explain the experimental conductance effects, Urry has proposed a field-dependent equilibrium between conducting and non-conducting gramicidin conformations which is schematically shown in Fig. 51²⁸⁹). Structure b represents the conducting, helical conformation which is shown as a dimer in Fig. 50. In this conformation, the molecule has an internal cavity which can accommodate metal ions, and has a net dipole moment along the helix axis. Structure a shows the non-conducting, spiral conformation. The internal cavity of this form is closed by two intramolecular hydrogen bonds per turn, and there is no net dipole moment along the spiral axis.

Recent spectroscopic studies did not contradict Urry's hypotheses but revealed an additional type of gramicidin dimers^{98, 253, 292, 293}). According to this model which is schematically shown in Fig. 52, two gramicidin molecules form an anti-

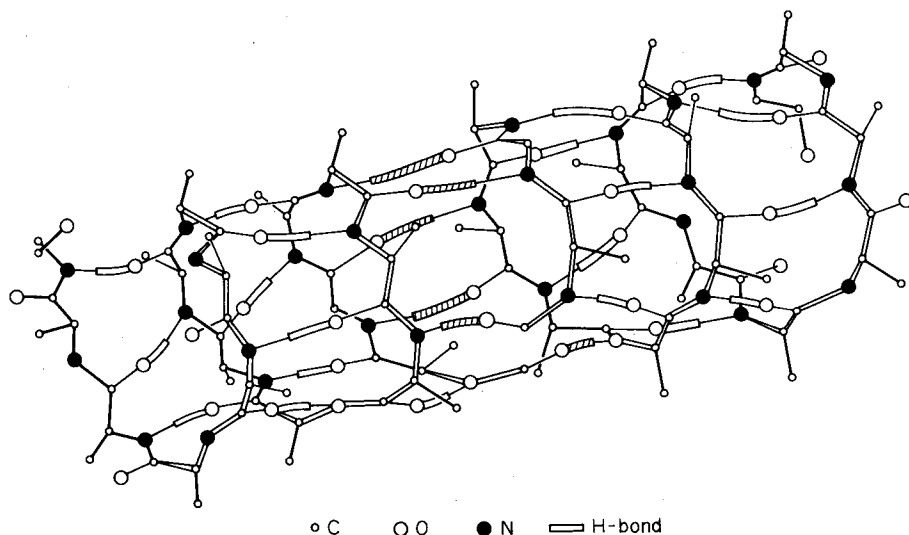


Fig. 50. A "head-to-head" dimer of gramicidin A in helical conformation. Side chains are not completely shown for sake of clarity

[Reproduced from Urry, D. W.: Proc. Nat. Acad. Sci. USA 68, 672 (1971).]

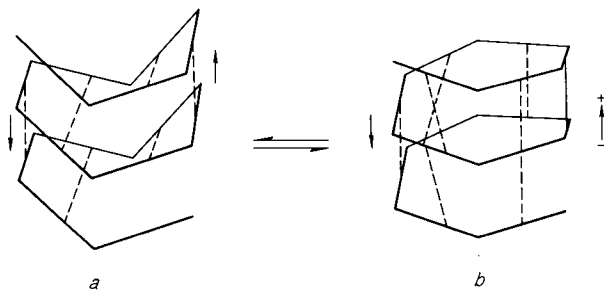


Fig. 51. Schematic representation of an equilibrium between a non-conducting (a) and a conducting (b) helical conformation of gramicidin A. Intramolecular hydrogen bonds are shown as dashed lines

[Reproduced from Urry, D. W.: Proc. Nat. Acad. Sci. USA 69, 1610 (1972).]

parallel- β -double-helical dimer with seven residues per turn and "even ends". The properties of this dimer (length, central hole) are also compatible with the requirements for an ion conducting transmembrane channel. Urry and coworkers have recently discussed the conditions under which each of the different types of gramicidin dimers is likely to exist²⁹¹.

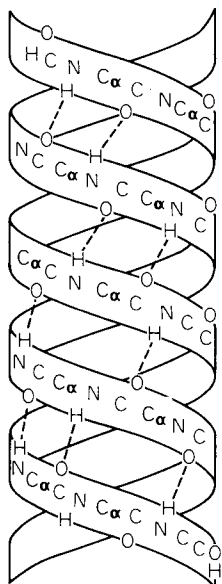


Fig. 52. Schematic diagram of an antiparallel- β -double-helical gramicidin dimer with seven residues per turn and "even ends". The dotted lines denote hydrogen bonds
[Reproduced from Veatch, W. R., *et al.*: *Biochemistry* 13, 5249 (1974).]

5.4. Nigericin and Related Openchain Compounds

Nigericin was the first known compound¹¹⁹⁾ of a group of structurally related antibiotics which are represented in Fig. 53. These compounds contain tetrahydrofuran and/or tetrahydropyran rings and a carboxyl function which is dissociated at physiological pH value. The nigericin antibiotics form electrically neutral complex salts with various cations. Different ion selectivities have been observed. Nigericin follows the selectivity order of $K^+ > Rb^+ > Na^+ > Cs^+ > Li^+$ ⁹⁴⁾. Monensin and dianemycin display $Na^+ > K^+$ selectivity¹⁴⁾. Antibiotic A 23187 prefers divalent ions over monovalent ions; its selectivity sequences are $Li^+ > Na^+ > K^+$ and $Ca^{++} > Mg^{++} > Sr^{++} > Ba^{++}$ ²³²⁾.

In recent years additional antibiotics of this class have been isolated, e.g. salinomycin^{148, 189)}, laidlomycin¹⁵²⁾, lysocellin⁷⁹⁾, septamycin¹⁴⁶⁾, alborixin⁴⁾, and emericid²⁰⁴⁾.

Cation complexes of the nigericin antibiotics are poorly soluble in water and highly soluble in organic solvents, indicating that the cation is surrounded by hydrophobic groups of the antibiotic. X-ray analyses of the silver salts have revealed that in the complexes a macrocyclic system is formed by stable intramolecular "head-to-tail" hydrogen bonds as schematically shown in Fig. 54. The silver salt of monensin was the first complex of this group to be investigated^{1, 234)} (Fig. 55). The Ag^+ ion is coordinated by six oxygen atoms, namely four ether oxygens and two hydroxyl

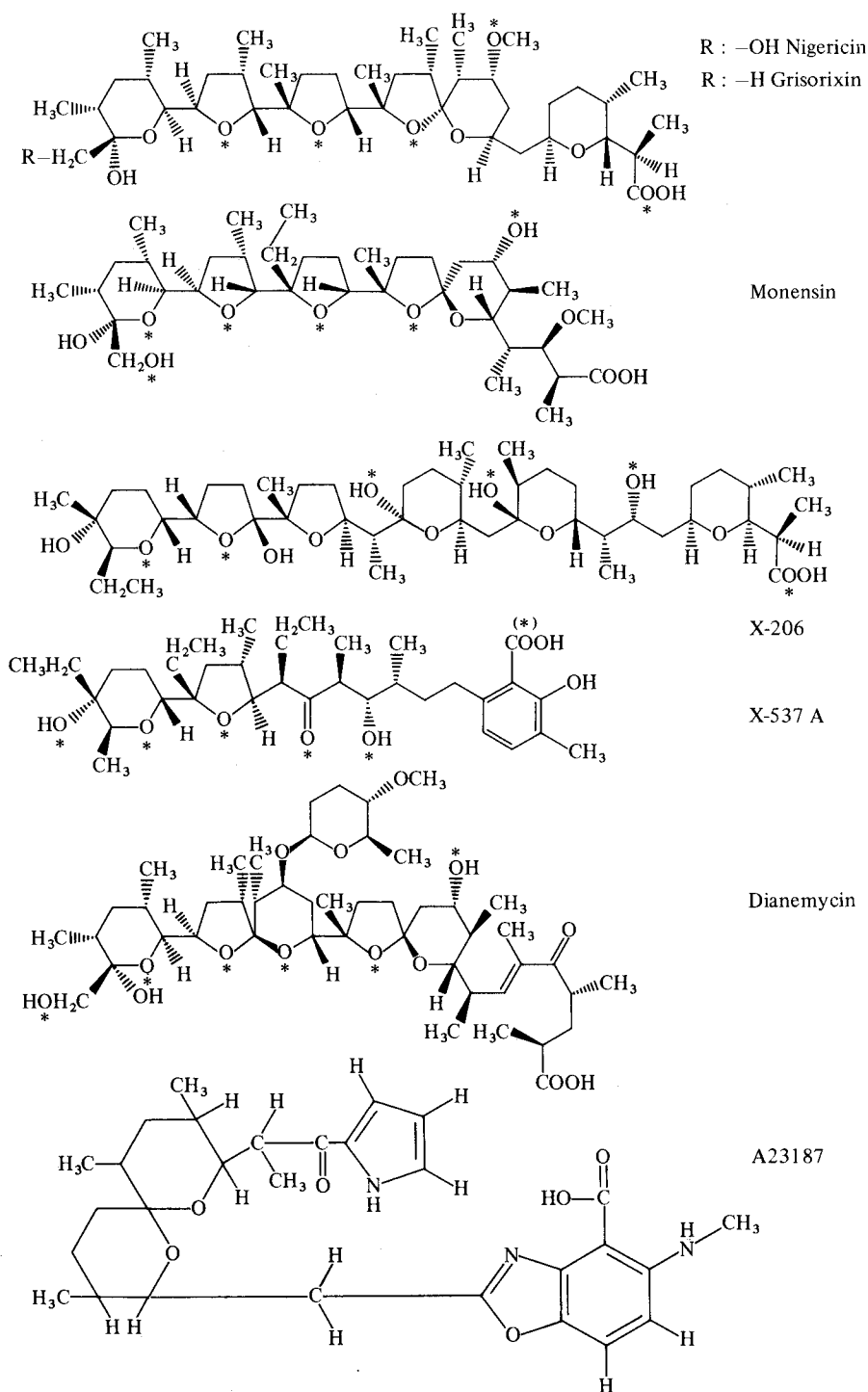
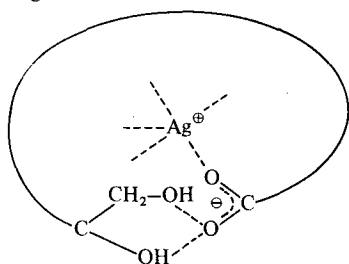
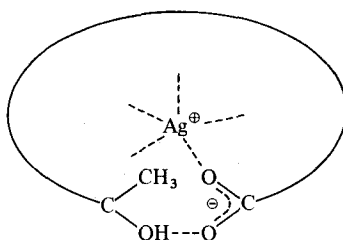


Fig. 53. Structures of nigericin and related antibiotics

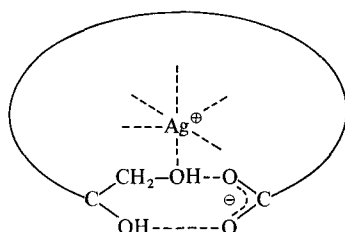
Nigericin



Grisorixin



Monensin



Dianemycin

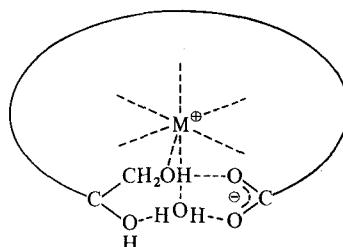


Fig. 54. Schematic representation of the complexes of antibiotics of the nigericin group [Reproduced from Simon, W., *et al.*: Structure and Bonding 16,113 (1973).]

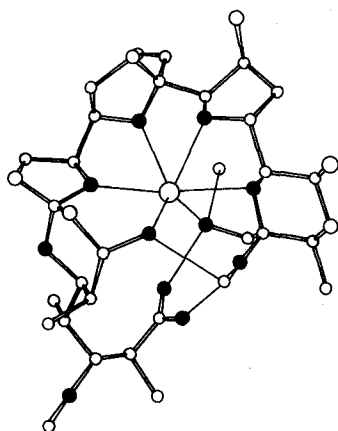


Fig. 55. Conformation of the crystalline Ag^+ salt of monensin [Reproduced from Pinkerton, M., Steinrauf, L. K.: J. Mol. Biol. 49, 533 (1970).]

oxygen. One hydrate water molecule participates in the intramolecular hydrogen bond system. X-ray analysis of free monensin revealed a cyclic conformation similar to the Ag^+ complex¹⁷⁴. The hydrogen bonding system of the free antibiotic is, however, quite different, as schematically shown in Fig. 56. An important part is played by the hydrate water molecule which occupies a central position like the cation in the complex. An analogous situation was described for grisorixin and its complex¹⁰⁴. IR spectroscopic studies have indicated that monensin and nigericin maintain a cyclic hydrogen bonded conformation also in solution¹⁷².

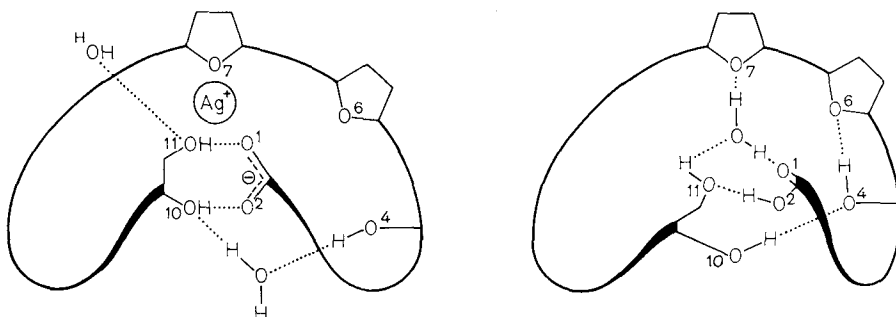


Fig. 56. Schematic representation of the hydrogen-bonding patterns in monensin-Ag salt and free monensin acid

[Reproduced from Lutz, W. K., *et al.*: *Helv. Chim. Acta* 54, 1103 (1971).]

Many other complexes of nigericin-type antibiotics have been analyzed by X-ray crystallography, *e.g.* the nigericin-Ag complex²⁷³⁾, grisorixin complexes with Ag^+ and $\text{Tl}^{+2, 3)}$, dianemycin complexes with Na^+ , K^+ , and $\text{Tl}^{+59, 274)}$, and the complex of X-206 with $\text{Ag}^{+26)}$. In spite of the structural differences, these complexes have remarkably similar conformations.

Antibiotic X-537 A, the smallest member of the group, forms dimeric complexes with $\text{Ag}^{+176)}$, $\text{Na}^{+259)}$ and $\text{Ba}^{++136)}$, as shown by X-ray analyses. The dimeric $(\text{X-537 A-Na})_2$ complex occurs in two different conformations, a "head-to-tail" structure as well as a "head-to-head" one, which are both shown in Fig. 57²⁵⁹⁾. Uncomplexed X-537 A crystallizes as a "head-to-head" dimer, too²⁵⁾. In the different complexes and the uncomplexed form, the conformations of the individual X-537 A molecules are very closely similar²⁵⁹⁾. With spectroscopic methods, the

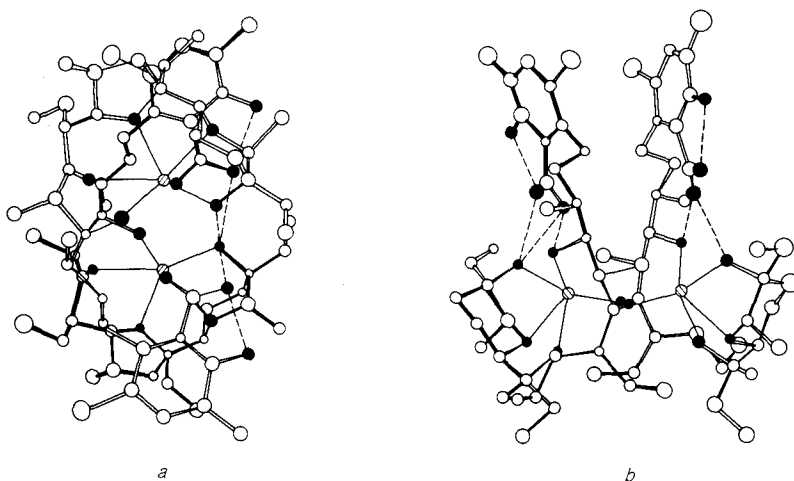


Fig. 57. Conformations of the dimeric Na^+ salt of antibiotic X-537 A. a, "Head-to-tail" modification I; b, "head-to-head" modification II. Oxygen atoms are shown as dark spheres, the sodium ions by line shading.

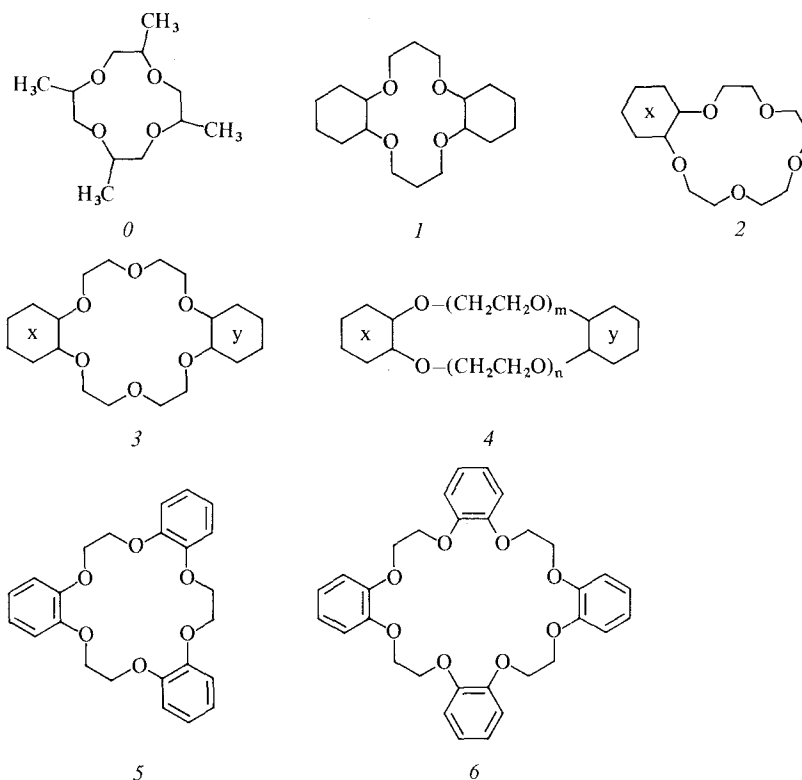
[Reproduced from Schmidt, P. G., *et al.*: *J. Amer. Chem. Soc.* 96, 6189 (1974).]

following complex types of X-537 A with mono- and divalent cations in solution have been identified: AM, AM^+ , AHM^+ , A_2M , A_2HM (A = antibiotic anion, AH = antibiotic acid, M = mono- or divalent cation, resp.)⁶⁵⁾.

In recent studies, antibiotic A23187 was found to form complexes of the type AM^I and A_2HM^I with monovalent cations, and of the type A_2M^{II} with divalent cations in solution^{63, 232)}. The solution conformation of the $(A23187)_2$ -Ca complex and of the free antibiotic were deduced from NMR spectroscopic data⁶³⁾.

5.5. Synthetic Macrocyclic Polyethers

The synthesis and complex formation of macrocyclic polyethers was first described by Pedersen^{227, 228, 229, 231)}. Some representative structures of these compounds are given in Fig. 58. Their names are listed according to the "crown" nomenclature introduced by Pedersen. Crown polyethers form complexes with a large number of mono-, di-, and trivalent metal ions^{52, 230)}. Their ion selectivity can be correlated to the polyether ring size, as was demonstrated for the alkali cation series by Frensdorff⁹⁹⁾. The selectivity order in methanol was found to change from $Na^+ > K^+$ for perhydrodibenzo-14-crown-4, to $Na^+ \sim K^+ > Cs$ for perhydrobenzo-15-crown-5, to $K^+ > Cs^+ > Na^+$ for perhydrobenzo-18-crown-6, to $K^+ \sim Cs^+ \gg Na^+$ for dibenzo-21-crown-7, and to $Cs^+ > K^+$ for dibenzo-24-crown-8. Polyethers with large and



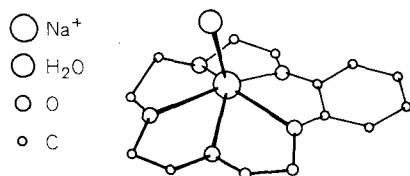
Compound		Nomenclature
0		Tetramethyl-12-crown-4
1		Perhydrodibenzo-14-crown-4
2a	$x = \text{C}_6\text{H}_4$	Benzo-15-crown-5
2b	$x = \text{C}_6\text{H}_{10}$	Perhydrobenzo-15-crown-5
3a	$x = y = \text{C}_2\text{H}_4$	18-crown-6
3b	$x = \text{C}_6\text{H}_4, y = \text{C}_2\text{H}_4$	Benzo-18-crown-6
3c	$x = \text{C}_6\text{H}_{10}, y = \text{C}_2\text{H}_4$	Perhydrobenzo-18-crown-6
3d	$x = y = \text{C}_6\text{H}_4$	Dibenzo-18-crown-6
3e	$x = \text{C}_6\text{H}_{10}, y = \text{C}_6\text{H}_4$	Benzo-perhydrobenzo-18-crown-6
3f	$x = y = \text{C}_6\text{H}_{10}$	Perhydrodibenzo-18-crown-6
4a	$m = 2, n = 3$	Perhydrodibenzo-21-crown-7
4b	$m = 2, n = 3, x = y = \text{C}_2\text{H}_4$	21-crown-7
4c	$m = n = 3$	Perhydrodibenzo-24-crown-8
4d	$m = n = 3, x = y = \text{C}_6\text{H}_4$	Dibenzo-24-crown-8
4e	$m = n = 3, x = y = \text{C}_2\text{H}_4$	24-crown-8
4f	$m = n = 4$	Perhydrodibenzo-30-crown-10
4g	$m = n = 4, x = y = \text{C}_6\text{H}_4$	Dibenzo-30-crown-10
4h	$m = n = 9, x = y = \text{C}_6\text{H}_4$	Dibenzo-60-crown-20
5		Tribenzo-18-crown-6
6		Tetrabenzo-24-crown-8

Fig. 58. Representative structures of crown polyethers

[Reproduced from Pedersen, C. J., Frensdorff, H. K.: *Angew. Chem. Internat. Ed.* 11, 16 (1972).]

flexible rings, however, do not follow this rule, since they may adopt folded ring conformations. For example, dibenzo-30-crown-10 has a selectivity order of $\text{K}^+ \sim \text{Rb}^+ > \text{Cs}^+ \gg \text{Na}^+ \gg \text{Li}^+$ ⁴⁸⁾. Ion selectivity has also been found to be solvent-dependent³¹¹⁾.

The spatial structure of many crown polyether complexes has been resolved by X-ray crystallography^{52, 286)}. In complexes with polyether rings containing four to six oxygen atoms, the cation is held by an annular arrangement of the oxygen atoms. In the case of benzo-15-crown-5-NaI, the hexa-coordination of the Na^+ ion is completed by a water molecule^{38, 40)} (Fig. 59). In $(\text{benzo-15-crown-5})_2\text{KI}$, sandwich complex formation leads to deca-coordination of the K^+ ion¹⁷⁸⁾ (Fig. 60). A recent X-ray analysis of the dibenzo-15-crown-5 complex with $\text{Ca}(\text{NCS})_2$

Fig. 59. Conformation of the crystalline benzo-15-crown-5 complex with Na^+ [Reproduced from Bush, M. A., Truter, M. R.: *J. C. S. Chem. Comm.* 1970, 1439.]

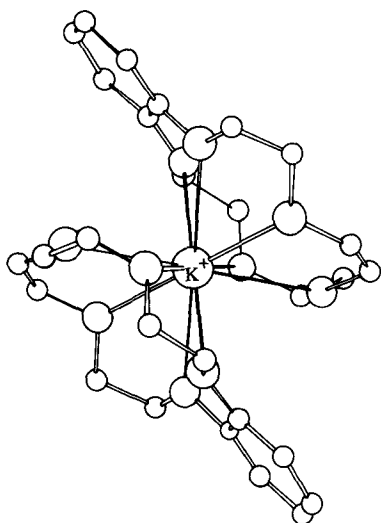
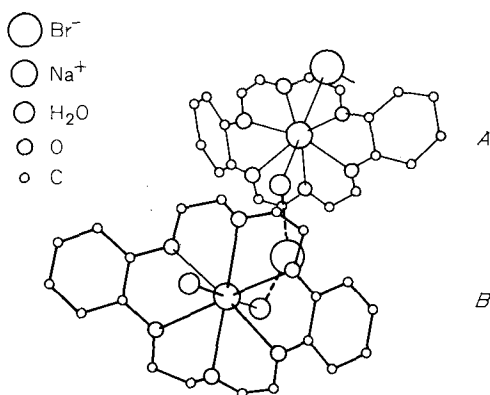


Fig. 60. Spatial structure of the $(\text{benzo-15-crown-5})_2\text{K}^+$ complex in the crystalline state
[Reproduced from Mallinson, P. R., Truter, M. R.: J. Chem. Soc. 1972, 1818.]



B Fig. 61. Asymmetric unit of crystalline $(\text{dibenzo-18-crown-6}) \text{NaBr} \cdot 2\text{H}_2\text{O}$
[Reproduced from Bush, M. A., Truter, M. R.: J.C.S. Chem. Comm. 1970, 1439.]

revealed that in this complex the arrangement of the oxygen atoms differs stronger from planarity than in the complexes mentioned before²¹⁹.

Two forms of the $\text{dibenzo-18-crown-6-Na}^+$ complex are present in the elementary cell (Fig. 61): In form B two water molecules, in form A one water molecule and one Br^- anion participate in the octahedral coordination of the Na^+ ion^{38, 39}.

The larger ring of $\text{dibenzo-24-crown-8}$ allows for a formation of a 1 : 2 polyether-cation complex with K^+ ions⁹⁶ (Fig. 62). As is schematically shown in Fig. 63, two aromatic rings and two NCS^- anions participate in the eightfold coordination of the K^+ ions.

The very large ring of $\text{dibenzo-30-crown-10}$ permits a complete enclosure of the complexed K^+ ion by one polyether molecule^{38, 41} (Fig. 64). The shape of the complex resembles the tennis ball seam conformation of the nonactin complexes. The free polyether has a flat and open conformation, reminiscent to free nonactin⁴¹ (Fig. 65).

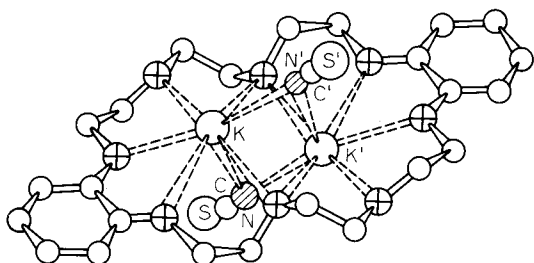


Fig. 62. Crystalline conformation of the complex, (dibenzo-24-crown-8) (KNCS)₂
[Reproduced from Fenton, D. E., *et al.*: J. C. S. Chem. Comm. 1972, 66.]

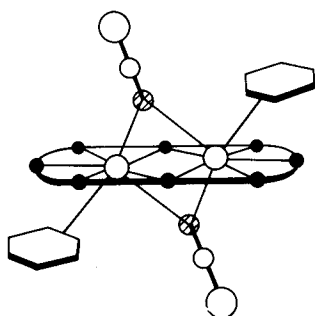


Fig. 63. Diagrammatic representation of the coordination in (dibenzo-24-crown-8) (KNCS)₂
[Reproduced from Fenton, D. E., *et al.*: J. C. S. Chem. Comm. 1972, 66.]

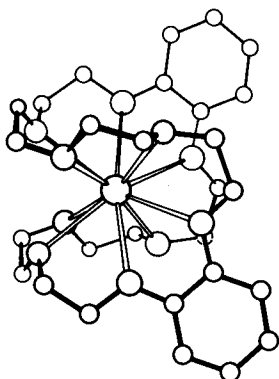


Fig. 64. Conformation of the crystalline complex, (dibenzo-30-crown-10)-K⁺
[Reproduced from Bush, M. A., Truter, M. R.: J. C. S. Chem. Comm. 1970, 1439.]

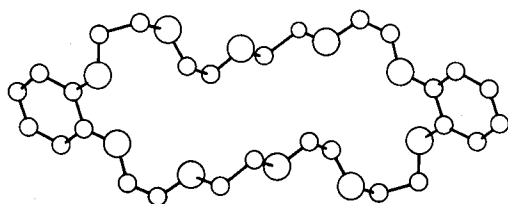


Fig. 65. Conformation of dibenzo-30-crown-10 in the crystal
[Reproduced from Bush, M. A., Truter, M. R.: J. C. S. Perkin II, 1972, 345.]

Starting from the "classical" crown polyethers, a variety of analogous compounds has been synthesized in recent years. Substitution of ring oxygen atoms in crown polyethers by NH, NR, or S groups was found to reduce the stability of alkali cation complexes, in accordance with the order of decreasing electronegativity^{99, 206, 297}, $O > NR > NH > S$. New macrocyclic polyethers have been synthesized containing 1.3-bridged benzene rings²⁴⁷, amino groups¹²⁷, furane rings^{247, 281}, or pyridine rings²⁰³. The influence of intraannular groups (pyridine-N-oxid, OCH_3 , NO_2 , $SOCH_3$, F) on complex formation of crown polyethers with five oxygen atoms has been studied²⁹⁶. Mixed polyether-esters have been introduced which possess two kinds of cation binding sites, namely ether oxygen atoms and 1.3-dicarbonyl groups³².

The ability of crown polyethers to form complexes with ammonium and alkylammonium salts⁹⁹ gave rise to the development of Cram's concept of "host-guest" chemistry⁵⁷. Asymmetric macrocyclic polyethers (host molecules) were designed and synthesized that distinguish between the enantiomers of chiral amine salts (guest molecules). For example, the (R,R)-form of polyether (Fig. 66) which was obtained in pure state, forms complexes of different

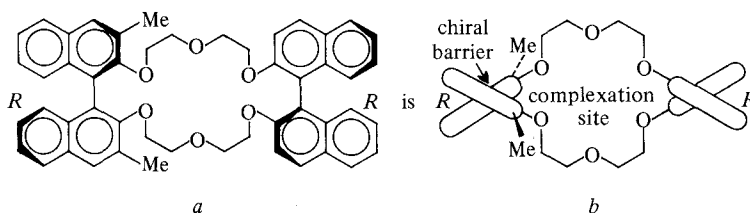


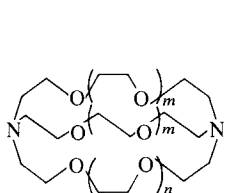
Fig. 66. a, Structure of a chiral macrocyclic polyether; b, cross section of a, viewed along axis of naphthalene-naphthalene bond from under side

[Reproduced from Peacock, S. C., Cram, D. C.: J. C. S. Chem. Comm. 1976, 282.]

stability with the L- and D-forms of amino acids²²⁶. With the same compound covalently attached to a resin, total chromatographic optical resolution of α -amino acids has been achieved⁷⁵. Instead of binaphthyl groups, L-amino acid residues²¹ or D-mannitol⁵⁸ have also been attached to the polyether macrocycle in order to obtain chiral host molecules.

5.6. Synthetic Macrobicyclic and -tricyclic Ligands (Cryptands)

A series of macrobicyclic compounds ([2]cryptands) of the general structure given in Fig. 67 has been synthesized by Lehn and coworkers^{68, 167}. These compounds form complexes ([2]cryptates) in organic solvents and in water with alkali as well as many other cations¹⁶⁹. The observed stability constants are very high, exceeding values of comparable crown polyethers by two or more orders of magnitude²³¹. This is obviously due to more effective chelation of the cation in the bicyclic, cage-like molecules. The cryptands exhibit ion selectivity. With increasing size of their



- [1.1.1] $m = n = 0$
 [2.1.1] $m = 0; n = 1$
 [2.2.1] $m = 1; n = 0$
 [2.2.2] $m = n = 1$
 [3.2.2] $m = 1; n = 2$
 [3.3.2] $m = 2; n = 1$
 [3.3.3] $m = n = 2$

Fig. 67. General structure of [2]cryptands
 [Reproduced from Lehn, J.-M.: Structure and Bonding 16, 1 (1973).]

intramolecular cavity, maximum alkali cation complex stability passes from the Li^+ to the Cs^+ complex¹⁶⁷). As in the case of the crown polyethers, replacement of ether oxygen atoms by sulfur⁶⁹) or amino groups^{166, 170}) leads to a decrease of alkali cation complex stability in the order of $\text{O} > \text{NR} > \text{S}$. By means of the ligands shown in Fig. 68, Lehn and coworkers have demonstrated how alkaline earth/alkali cation selectivity may be controlled by structural changes⁷⁰).

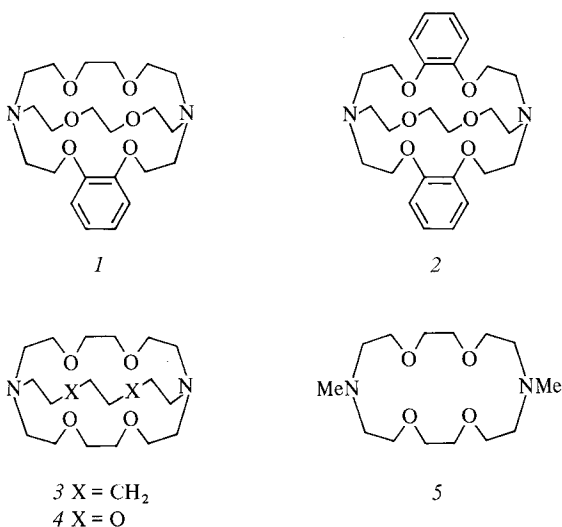


Fig. 68. Structures of macrobicyclic ligands and their $\text{Ba}^{++}/\text{K}^+$ selectivities: 1, $\text{Ba}^{++} > \text{K}^+$; 2, $\text{Ba}^{++} \sim \text{K}^+$; 3, $\text{Ba}^{++} \ll \text{K}^+$; 4, $\text{Ba}^{++} > \text{K}^+$; 5, $\text{Ba}^{++} \gg \text{K}^+$
 [Reproduced from Dietrich, B., *et al.*: J.C.S. Chem. Comm. 1973, 15.]

The conformations of a number of cryptands and their complexes have been analyzed by X-ray crystallography¹⁶⁷). Figure 69 shows the conformations of the cryptand (Fig. 67; $m = n = 1$) and of its Rb^+ complex^{185, 167}). Four ether oxygen atoms and the two nitrogen atoms participate in octahedral coordination of the cation. In both the complex and the free ligand, the two nitrogen atoms are in endo configuration.

Macrocyclic ligands have also been prepared, *e.g.* the structures shown in Fig. 70^{47, 186}). Both compounds form complexes ([3]cryptates) with alkali and other cations. The lower alkali ion selectivity and complex stability of [3] cryptand 1 in comparison to [2]cryptands is probably due to the larger size of its cavity which has a length of approximately 6 Å⁴⁷). The cavity of ligand 1 can even accommodate two cations which has been demonstrated by X-ray analysis of a LAg_2^{++} complex (L = ligand 1, Fig. 70)³⁰⁴).

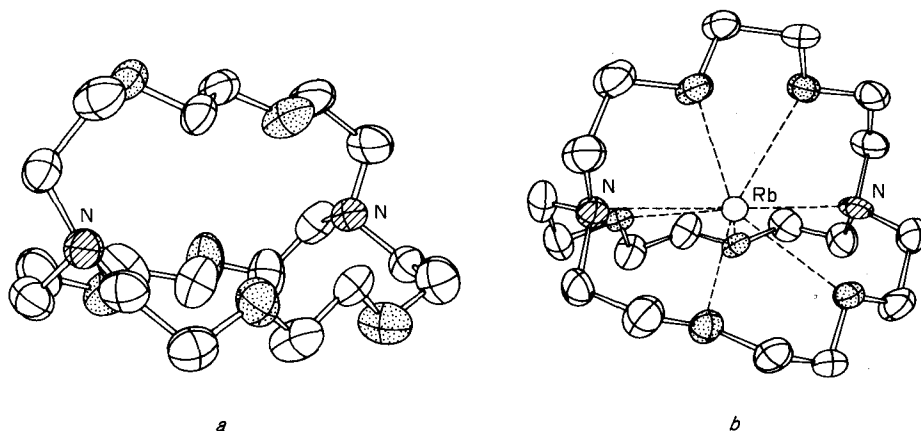


Fig. 69. Conformation of the macrobicyclic ligand [2.2.2.] a, and its Rb^+ complex, b [Reproduced from Metz, B., *et al.*: J. C. S. Chem. Comm. 1970, 217 and Lehn, J.-M.: Structure and Bonding 16, 1 (1973).]

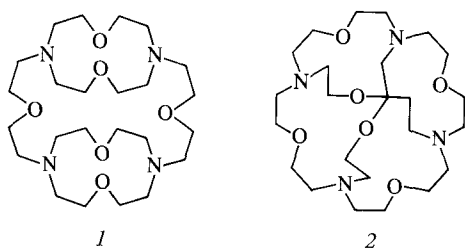


Fig. 70. Two macrotricyclic ligands [Reproduced from Cheney, J., *et al.*: J. C. S. Chem. Comm. 1972, 1100 and Metz, B., *et al.*: J. C. S. Chem. Comm. 1976, 533.]

Ligand 2 (Fig. 70) has a spherical intramolecular cavity lined with ten binding sites. The four nitrogen atoms are located at the corners of a tetrahedron, and the six oxygen atoms are at the corners of an octahedron. The compound exhibits an ion selectivity in water of $\text{K}^+ < \text{Rb}^+ > \text{Cs}^+$, forming the probably most stable Cs^+ complex known to date¹¹⁰). Recently, X-ray analyses of the NH_4^+ cation complex and the Cl^- anion complex of this ligand have been published¹⁸⁶) (Fig. 71). In the latter complex the tetraprotonated ligand LH_4^{4+} (L = ligand 2, Fig. 70) forms an anion inclusion complex with Cl^- , $[\text{ClLH}_4]^{3+}$. In both complexes, the central ions are probably held in place by four hydrogen bonds formed with the nitrogen or the protonated nitrogen atoms respectively of the macrotricyclic which are pointing into the cavity¹⁸⁶).

As a curiosity it may be mentioned that the structure of an inorganic [2]cryptate with Na^+ was recently revealed by X-ray analysis of an antimoniotungstate with antiviral activity⁹⁷).

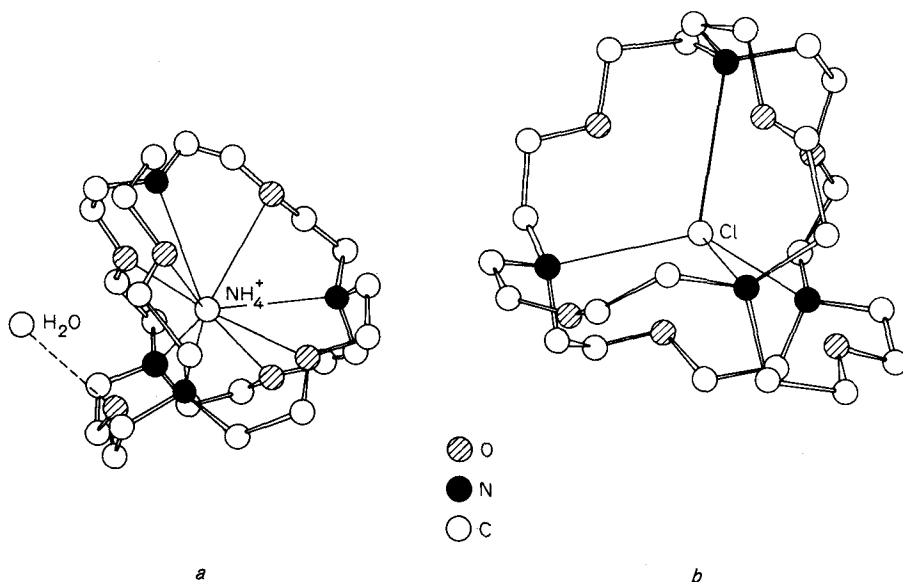


Fig. 71. X-ray resolved structures of two complexes of the macrotricyclic ligand 2 (Fig. 70).
 a, the $[\text{LNH}_4]^+$ complex; b, the $[\text{ClH}_4]^{3+}$ complex (L = ligand)
 [Reproduced from Metz, B., *et al.*: J. C. S. Chem. Comm. 1976, 533.]

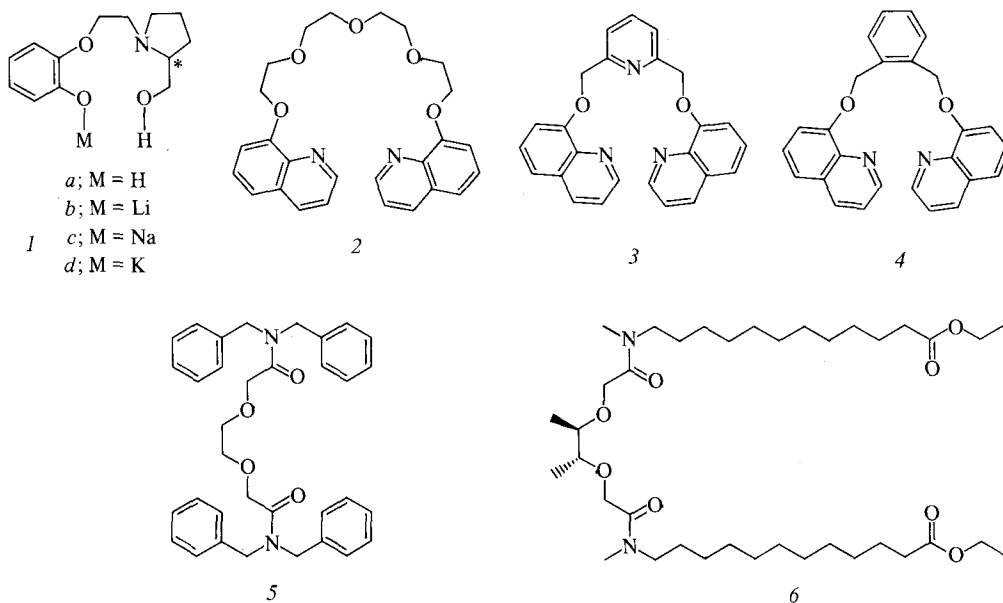


Fig. 72. Structures of some synthetic non-cyclic ligands
 [Reproduced from Wudl, F.: J. C. S. Chem. Comm. 1972, 1229 and Weber, E., Vögtle, F.: Tetrahedron Letters 1975, 2415 and Ammann, D., *et al.*: Analyt. Letters 7, 23 (1974) and Kirsch N., Simon, W.: Helv. Chim. Acta 59, 235 (1976).]

5.7. Synthetic Non-Cyclic Ligands

Certain non-cyclic compounds which were synthesized in the last years have interesting complex formation properties (Fig. 72). Compound 1 exhibits an ion selectivity of $\text{Li}^+ < \text{Na}^+ > \text{K}^+$. From ORD spectra of the complexes it was concluded that Li^+ and Na^+ are encapsulated and that K^+ is not³¹³. Compounds 2, 3, and 4 combine the structural concepts of crown polyethers and the chelate forming 8-hydroxyquinoline. Crystalline 1:1 complexes²⁹⁵ of these ligands could be obtained with K^+ and several other cations, however, not with Na^+ . Compounds 5 and 6 are examples from a large number of substances, designed and synthesized by Simon and coworkers in order to obtain ion carriers for ion specific membrane electrodes^{6,9}. These ligands form 1:1 and 2:1 ligand-cation complexes with alkali and alkaline earth cations^{34, 150, 151} and induce ion transport in bulk membranes³¹⁴. The dependence of their monovalent/divalent cation selectivity on structural features has been studied⁹. If incorporated in liquid membrane electrodes, compound 5 shows a potentiometric selectivity⁷ of $\text{Na}^+ > \text{Ca}^{++}$ while compound 6 shows $\text{Ca}^{++} > \text{Na}^+$ selectivity¹⁵¹.

6. Applications of Alkali Cation Selective Ligands

Theoretical studies with the compounds discussed in this article have provided much important information on the mechanisms of cation complex formation and transmembrane ion transport. The unique molecular properties of these ligands have also led to a number of practical applications in organic synthesis, analytical chemistry, and biochemistry which are briefly represented in this chapter.

6.1. Use of Crown Polyethers as Lipophilizers

Complex formation of a cation with a lipophilic ligand involves an effective shielding of the cation from its environment. As a consequence, dissociation of the anion is promoted resulting in ion-paired or more or less solubilized anions. Lipophilic ligands can therefore enhance the solubility of a substance in non-polar organic solvents. As was pointed out by Lehn, separation of cation and anion should be highest for the ligands with thick organic layers¹⁶⁷. In case of small "hard" anions, complete cation-anion separation does not favour solubilization of a salt in organic media of low polarity. Thus a compromise between cation-anion separation and solubility of the complex has to be found. Highly lipophilic ligands are expected to be particularly well suited in this respect¹⁶⁷.

Impressive applications of the solubilizing effects of crown polyethers and cryptands have been described. For example, the dissolution of sodium, potassium, and cesium metal in tetrahydrofuran and diethylether is mediated by certain ligands of this type^{57, 78, 171}. Such solutions have provided new systems for the study of solvated electrons and alkali metal anions. Substances like KMnO_4 , *tert*- $\text{C}_4\text{H}_9\text{OK}$, or

K_2PtCl_4 can be dissolved in aromatic hydrocarbons merely by addition of perhydrodibenzo-18-crown-6²³¹⁾. Reactions involving the anions can thus be carried out in non-polar solvents, for example, saponifications by KOH in benzene²²⁷⁾, KOH-catalyzed rearrangements in methylene chloride¹⁵³⁾, and oxidations with $KMnO_4$ in benzene²⁵⁶⁾. Crown polyethers and cryptands have also been used as phase-transfer catalysts for anion-promoted reactions in two phase water-organic solvent systems, such as nucleophilic substitutions, C-alkylations, cyclopropanations, and borohydride reductions^{54, 161)}.

It has been demonstrated that crown polyethers affect greatly the ion-pair structure of alkali carbanion salts³¹¹⁾ and the rate and stereospecific course of reactions involving ion pairs⁵⁾. A number of individual reactions are discussed in Ref.²¹⁷⁾.

Covalent attachment of ligands to polymer supports retains their complexing properties¹⁵⁶⁾ and widens their applications. For instance, immobilized crown polyethers and cryptands used as phase-transfer catalysts can be recycled⁵⁵⁾. Chiral ligands have been used for a chromatographical separation of D- and L-amino acids⁷⁵⁾.

6.2. Carriers as Elements of Ion Selective Electrodes

Analytical applications of the ligands have also been developed utilizing their ion discrimination and/or carrier properties. For example, the ORD spectral changes due to complex formation of ligand 1 (Fig. 72) could be used for an analytical determination³¹³⁾ of Na^+ in presence of Li^+ and K^+ . Probably the most important analytical application of alkali and alkaline earth cation ligands has been their incorporation in cation-selective electrodes. Already 1967, Simon and coworkers constructed K^+ -selective electrodes containing a membrane with macrotetrolides dissolved in organic solvents²⁷²⁾. Then a membrane electrode containing valinomycin dissolved in diphenylether was constructed which responded to K^+ concentrations between 10^{-5} and 10^{-1} M with an approximately Nernstian potential dependence. The high potentiometric selectivity of $K^+ > Na^+$, Li^+ made this electrode superior to glass electrodes²³⁷⁾. A theoretical treatment of the ion selectivity of membrane electrodes was given by Simon and coworkers²⁶⁹⁾. During the last years, more membrane electrodes have been developed, including an NH_4^+ -selective electrode based on nonactin²⁶⁰⁾. Na^+ -, Ca^{++} -, and Ba^{++} -selective liquid membrane electrodes have been constructed containing synthetic non-cyclic ligands as ion carriers^{7, 245)}. Valinomycin has also been used for the construction of a K^+ -selective coated wire electrode⁴⁴⁾. Electrodes containing valinomycin and other carriers have become commercially available and are routinely used, e.g. for alkali ion determinations in whole blood¹⁹⁴⁾. A new review on the electrodes is available⁸⁾.

6.3. Biomedical Applications

In biochemistry and medicine, the membrane active ligands have been valuable tools for studying ion transport and related cell membrane phenomena. Valinomycin has been most widely used and has been applied to a variety of biological systems. For

the interested reader, a list of recent publications dealing with biomedical applications of valinomycin is included as appendix. Antibiotic X-537 A has also found wide application especially for studies in relation to its effects on Ca^{++} ion transport and on cardiac contractility. A recent survey on biological applications of X-537 A was given by Pressman and de Guzman²⁴²⁾.

Finally one particular problem of alkali ion complex specificity of enormous medical relevance should be mentioned, *i.e.* the finding that lithium is very effective as a psychoactive agent in the treatment of manic-depressive disorders. This finding, first made by Cade³²⁰⁾ in 1949, and systematically investigated by Schou and his coworkers³²¹⁾, has stimulated many studies of biological effects of lithium.

Experiments with various lithium salts clearly revealed that it was the lithium ion itself that was responsible for the therapeutic effect. Lithium is found in many minerals in the earth's crust, in seawater with a concentration of about 0.014 mM and in some springs at concentrations as high as 0.8 mM. Although very small amounts are also found in animal tissues and plants no obvious physiologic function could be ascribed to this alkali metal ion so far.

In order to explain the unique antipsychotic phenomenon one may reasonably postulate that the lithium ion must interact with specific "receptors". Such an assumption requires that (i) specific receptors exist, (ii) the receptors selectively bind lithium in the presence of other cations known to exist in biological tissue in appreciable higher concentrations, and (iii) binding of lithium to the receptor triggers some mechanism responsible for the suppression of the psychotic effect.

If this hypothesis^{322, 323)} is correct, all the prerequisites for specific ligand architecture and selective complexing mechanisms as discussed in Sections 2.1 and 3.1 must be fulfilled by the receptor. In particular the receptor should be able to discriminate against sodium ions, present in extracellular media, and against potassium ions more abundant in intracellular media, both at concentrations as high as 100 mM. In this connection it might be of interest that recently Pert and Snyder have demonstrated a specific interaction of Na^+ ions with the opiate receptor from rat brain³²⁷⁾. In presence of Na^+ the binding of opiate antagonists to the receptor is enhanced while the binding of agonists is diminished. It was therefore proposed that the opiate receptor might exist in two interconvertible conformational states, an "antagonist form" in the presence of Na^+ and an "agonist form" in the absence of Na^+ .

The ideas regarding the possible actions of lithium have been discussed recently in a work session of the Neuroscience Research Program, and are reviewed in Ref. 324. The unique therapeutical effect of lithium demonstrates clearly the relevance of the subject discussed here, which will have many further implications of a similar interdisciplinary nature.

Acknowledgement. We are most grateful to Manfred Eigen for stimulating and encouraging discussions as well as many valuable suggestions for the preparation of the manuscript. We also want to thank Christopher Holloway for his advices with respect to the English text.

7. Appendix

Compilation of recent publications on biomedical applications of valinomycin

- Akerman, K. E., Saris, N. E.: *Biochim. Biophys. Acta.* 426 (4), 624 (1976). Stacking of safranine in liposomes during valinomycin-induced efflux of potassium ions
- Besette, F., Seufert, W. D.: *Biochim. Biophys. Acta.* 375 (1), 10 (1975). Increase in fluorescence energy transfer across lipid bilayers induced by valinomycin
- Bielawski, J., Kwinto, B.: *Acta. Biochim. Pol.* 22 (4), 269 (1975). The influence of gramicidin A and valinomycin of the permeability of mammalian erythrocytes
- Blok, M. C., De Gier, J., Van Deenen, L. L.: *Biochim. Biophys. Acta.* 367 (2), 210 (1974). Kinetics of the valinomycin-induced potassium ion leak from liposomes with potassium thiocyanate enclosed
- Breitbart, H., Atlan, H., Eltes, F., Herzberg, M.: *Mol. Biol. Rep.* 2 (2), 167 (1975). Interaction between membrane properties and proteins synthesis in reticulocytes — a two step inhibition of protein synthesis by valinomycin
- Briand, Y., Debise, R., Durand, R.: *Biochimie* 57 (6–7), 787 (1975). Effect of phosphate and ionophores on (14C)-NEM incorporation in mitochondrial membranes and relationships with phosphate carrier system
- Carmeliet, E. E., Lieberman, M.: *Pflueger's Arch.* 358 (3), 243 (1975). Increase of potassium flux by valinomycin in embryonic chick heart
- De Cespedes, C., Christensen, H. N.: *Biochim. Biophys. Acta.* 339 (1), 139 (1974). Complexity in valinomycin effects on amino acid transport
- Dolais-Kitabgi, J., Perlman, R. L.: *Mol. Pharmacol.* 11 (6), 745 (1975). The stimulation of catecholamine release from chromaffin granules by valinomycin
- Harold, F. M., Altendorf, K. H., Hirata, H.: *Ann. N.Y. Acad. Sci.* 235 (0), 149 (1974). Probing membrane transport mechanisms with ionophores
- Haynes, Jr. R. C., Garrison, J. C., Yamazaki, R. K.: *Mol. Pharmacol* 10 (3), 381 (1974). Comparison of effects of glucagon and valinomycin on rat liver mitochondria and cells
- Herzberg, M., Breitbart, H., Atlan, H.: *Eur. J. Biochem.* 45 (1), 161 (1974). Interactions between membrane functions and protein synthesis in reticulocytes. Effects of valinomycin and dicyclohexyl-18-crown-6
- Hinkle, M., Van der Kloot, W.: *Comp. Biochem. Physiol. [A]* 46 (2), 269 (1973). The effects of valinomycin on striated muscles of the frog and the crayfish
- Järvisalo, J., Saris, N. E.: *Biochem. Pharmacol.* 24 (18), 1701 (1975). Action of propranolol on mitochondrial functions effects on energized ion fluxes in the presence of valinomycin
- Kaplan, J. H., Passow, H.: *Hoppe Seyler's Z. Physiol. Chem.* 355 (10), 1215 (1974). Proceedings: Asymmetric effects of phlorizin on valinomycin-mediated ion movements across the human erythrocyte membrane
- Kaplan, J. H., Passow, H.: *J. Membr. Biol.* 19 (1), 179 (1974). Effects of phlorizin on net chloride movements across the valinomycin-treated erythrocyte membrane
- Kresca, L., Cotlier, E.: *Invest. Ophthalmol.* 13 (4), 310 (1974). Valinomycin-stimulated 86 — rubidium transport and efflux from lens
- Larkum, A. W., Boardman, N. K.: *FEBS Letters* 40 (1), 229 (1974). The effect of nigericin and valinomycin on CO₂ fixation electron transport and P518 in intact spinach chloroplasts

- Manteifel, V. M., Sorokina, I. B.: Antibiotiki (9), 834 (1975). Action of valinomycin in vivo on Ehrlich ascites tumor cells. A change in the ultrastructure of the tumor cells under the influence of valinomycin
- Murav'eva, T. I., Riabova, I. D., Oreshnikova, N. A., Novikova, M. A.: Mikrobiologiya 42 (1), 83 (1973). Study of the action of valinomycin on yeasts
- Murav'eva, T. I., Riabova, I. D., Oreshnikova, N. A., Novikova, M. A.: Biokhimiya 38 (4), 845 (1973). Effect of valinomycin on the respiration and transport of potassium ions in the mitochondria of yeast fungi
- Niven, D. F., Hamilton, W. A.: FEBS Letters 37 (2), 244 (1973). Valinomycin-induced amino acid uptake by *Staphylococcus aureus*
- Prince, R. C., Crofts, A. R., Steinrauf, L. K.: Biochem. Biophys. Res. Comm. 59 (2), 697 (1974). A comparison of beauvericin, enniatin and valinomycin as calcium transporting agents in liposomes and chromatophores
- Reid, M., Gibb, L. E., Eddy, A. A.: Biochem. J. 140 (3), 383 (1974). Ionophore-mediated coupling between ion fluxes and amino acid absorption in mouse ascites-tumour cells. Restoration of the physiological gradients of methionine by valinomycin in the absence of adenosine triphosphate
- Reijngoud, D., Tager, J. M.: FEBS Letters 54 (1), 76 (1975). Effect of ionophores and temperature on intralysosomal pH
- Ryabova, I. D., Gorneva, G. A., Ovchinnikov, Y. A.: Biochim. Biophys. Acta 401 (1), 109 (1975). Effect of valinomycin on ion transport in bacterial cells and on bacterial growth
- Schneider, J. A., Shigenobu, K., Sperelakis, N.: Recent. Adv. Stud. Cardiac. Struct. Metab. 9, 33 (1976). Valinomycin inhibition of the inward slow current of cardiac muscle
- Schneider, J. A., Sperelakis, N.: Eur. J. Pharmacol. 27 (3), 349 (1974). Valinomycin blockade of slow channels in guinea pig hearts perfused with elevated D plus and isoproterenol
- Seshachalam, D., Frahm, D. H., Ferraro, F. M.: Antimicrob. Agents Chemother. 3 (1), 63 (1973). Cation reversal of inhibition of growth by valinomycin in *Streptococcus pyogenes* and *Clostridium sporogenes*
- Shigenobu, K., Sperelakis, N.: Am. J. Physiol. 228 (4), 1113 (1975). Valinomycin shortening of action potential of embryonic chick hearts
- Spector, I., Palfrey, C., Littauer, U. Z.: Nature, 254 (5496), 121 (1975). Enhancement of the electrical excitability of neuroblastoma cells by valinomycin
- Uribe, E. G.: FEBS Letters 36 (2), 143 (1973). ATP synthesis driven by a K^+ -valinomycin-induced charge imbalance across chloroplast grana membranes
- Wigglesworth, J. M., Nicholls, P.: Biochem. Soc. Trans. 3 (1), 168 (1975). Valinomycin sensitivity of cytochrome c oxidase vesicles

8. References

- 1) Agtarap, A., Chamberlin, J. W., Pinkerton, M., Steinrauf, L. K.: *J. Am. Chem. Soc.* **89**, 5737 (1967).
- 2) Alleaume, M., Hickel, D.: *J. C. S. Chem. Comm.* **1970**, 1422.
- 3) Alleaume, M., Hickel, D.: *Chem. Commun.* **1972**, 175.
- 4) Alleaume, M., Busetta, B., Farges, C., Gachon, P., Kergomard, A., Staron, T.: *J. C. S. Chem. Comm.* **1975**, 411.
- 5) Almy, J., Garwood, D. C., Cram, D. J.: *J. Am. Chem. Soc.* **92**, 4321 (1970).
- 6) Ammann, D., Pretsch, E., Simon, W.: *Helv. Chim. Acta* **56**, 1780 (1973).
- 7) Ammann, D., Pretsch, E., Simon, W.: *Analyt. Letters* **7**, 23 (1974).
- 8) Ammann, D., Bissig, R., Cimerman, Z., Fiedler, U., Guggi, M., Morf, W. E., Ohme, M., Osswald, H., Pretsch, E., Simon, W.: Synthetic neutral carriers for cations. In: *Proceedings of the international workshop on ion selective electrodes and on enzyme electrodes in biology and in medicine*. München – Berlin – Wien: Urban & Schwarzenberg 1975.
- 9) Ammann, D., Bissig, R., Guggi, M., Pretsch, E., Simon, W., Borowitz, J., Weiss, L.: *Helv. Chim. Acta* **58**, 1535 (1975).
- 10) Ando, K., Oishi, H., Hirano, S., Okutani, T., Suzuki, K., Okazaki, H., Sawada, M., Sagawa, T.: *J. Antibiot.* **24**, 347 (1971).
- 11) Andreev, I. M., Malenkov, G. G., Shkrob, A. M., Shemyakin, M. M.: *Mol. Biol.* **5** (4), 488 (1972).
- 12) Arnett, E. M., Moriaity, T. C.: *J. Am. Chem. Soc.* **93**, 4908 (1971).
- 13) Asher, I. M., Rothschild, K. J., Stanley, H. E.: *J. Mol. Biol.* **89**, 205 (1974).
- 14) Ashton, R., Steinrauf, L. K.: *J. Mol. Biol.* **49**, 547 (1970).
- 15) Bamberg, E., Läuger, P.: *J. Membr. Biol.* **11**, 177 (1973).
- 16) Bamberg, E., Läuger, P.: *Biochim. Biophys. Acta* **367**, 127 (1974).
- 17) Bamberg, E., Benz, R.: *Biochim. Biophys. Acta* **426**, 570 (1976).
- 18) Bamberg, E., Janko, K.: *Biochim. Biophys. Acta* **426**, 447 (1976).
- 19) Basolo, F., Pearson, R. G., in: *Mechanisms of inorganic reactions*. 2nd edit. New York: John Wiley and Sons 1967, p. 62.
- 20) Baumann, G., Mueller, P.: *J. Supramol. Structure* **2**, 538 (1974).
- 21) Behr, J.-P., Lehn, J.-M., Vierling, P.: *J.C.S. Chem. Comm.* **1976**, 621.
- 22) Benesi, H. A., Hildebrand, J. H.: *J. Am. Chem. Soc.* **71**, 2703 (1949).
- 23) Benz, R., Stark, G.: *Biochim. Biophys. Acta* **382**, 27 (1975).
- 24) Benz, R., Läuger, P.: *J. Membr. Biol.* **27**, 171 (1976).
- 25) Bissell, E. C., Paul, I. C.: *J.C.S. Chem. Comm.* **1972**, 967.
- 26) Blount, J. F., Westley, J. W.: *J.C.S. Chem. Comm.* **1971**, 927.
- 27) Blout, E. R., Deber, C. M., Pease, L. G.: in: *Peptides, polypeptides and proteins*. Blout, E. R. *et al.* (eds.). New York: John Wiley and Sons 1974, pp. 266–281.
- 28) Boheim, G., Hall, J. E.: *Biochim. Biophys. Acta* **389**, 436 (1975).
- 29) Boheim, G., Janko, K., Leibfritz, D., Ooka, T., König, W. A., Jung, G.: *Biochim. Biophys. Acta* **433**, 182 (1976).
- 30) Boone, D. J., Kowalsky, A.: *Biochemistry* **13**, 731 (1974).
- 31) Born, M.: *Z. Phys.* **1**, 45 (1920).
- 32) Bradshaw, J. S., Hansen, L. D., Nielsen, S. F., Thompson, M. D., Reeder, R. A., Izatt, R. M., Christensen, J. J.: *J.C.S. Chem. Comm.* **1975**, 874.
- 33) Brockmann, H., Schmidt-Kastner, G.: *Chem. Ber.* **88**, 57 (1955).
- 34) Büchi, R., Pretsch, E.: *Helv. Chim. Acta* **58**, 1573 (1975).
- 35a) Burgermeister, W.: *Doctoral Thesis, Heidelberg* (1972).
- 35b) Burgermeister, W., Wieland, T., Winkler, R.: *Eur. J. Biochem.* **44**, 305 (1974).
- 36) Burgermeister, W., Wieland, Th., Winkler, R.: *Eur. J. Biochem.* **44**, 311 (1974).
- 37) Burgess, A. W., Leach, S. J.: *Biopolymers* **12**, 2691 (1973).
- 38) Bush, M. A., Truter, M. R.: *J.C.S. Chem. Comm.* **1970**, 1439.
- 39) Bush, M. A., Truter, M. R.: *J. Chem. Soc. (B)* **1971**, 1440.

- 40) Bush, M. A., Truter, M. R.: *J.C.S. Perkin II*, 1972, 341.
- 41) Bush, M. A., Truter, M. R.: *J.C.S. Perkin II*, 1972, 345.
- 42) Byrn, S. R.: *Biochemistry* 13, 5186 (1974).
- 43) Cass, A., Finkelstein, A., Krespi, V.: *J. Gen. Physiol.* 56, 100 (1970).
- 44) Cattrall, R. W., Tribuzio, S., Freiser, H.: *Anal. Chem.* 46, 2223 (1974).
- 45) Célis, H., Estrada, S., Montal, M.: *J. Membr. Biol.* 18, 187 (1974).
- 46) Chance, B., in *Technique of chemistry*. 2nd edit., Vol. VI, part II. Weissberger, A., and Hammes, G. G.(eds.) New York: Wiley-Interscience 1974, p. 5.
- 47) Cheney, J., Lehn, J.-M., Sauvage, J. P., Stubbs, M. E.: *J.C.S. Chem. Comm.* 1972, 1100.
- 48) Chock, P. B.: *Proc. Nat. Acad. Sci. USA* 69, 1939 (1972).
- 49) Chock, P. B., Titus, E. O.: in: *Current research topics in bioinorganic chemistry*. New York: John Wiley and Sons 1973, p. 287.
- 50) Chock, P. B., Eggers, F., Eigen, M., Winkler, R.: *J. Biophys. Chem.*: in press (1977).
- 51) Christensen, J. J., Hill, J. O., Izatt, R. M.: *Science* 74, 459 (1971).
- 52) Christensen, J. J., Eatough, D. J., Izatt, R. M.: *Chem. Rev.* 74, 351 (1974).
- 53) Ciani, S. M., Eisenman, G., Laprade, R., Szabo, G., in: *Membranes — a series of advances*. Vol. 2. Eisenman, G. (ed.) Dekker New York: p. 61 (1973).
- 54) Cinquini, M., Montanari, F., Tundo, P.: *J.C.S. Chem. Comm.* 1975, 393.
- 55) Cinquini, M., Colonna, S., Molinari, H., Montanari, F., Tundo, P.: *J.C.S. Chem. Comm.* 1976, 394.
- 56) Cornelius, G., Gärtner, W., Haynes, D. H.: *Biochemistry* 13, 3052 (1974).
- 57) Cram, D. J., Cram, J. M.: *Science* 183, 803 (1974).
- 58) Curtis, W. D., King, R. M., Stoddart, J. F., Jones, G. H.: *J.C.S. Chem. Comm.* 1976, 284.
- 59) Czerwinski, E. W., Steinrauf, L. K.: *Biochem. Biophys. Res. Comm.* 45, 1284 (1971).
- 60) Davis, D. G.: *Biochem. Biophys. Res. Comm.* 63, 786 (1975).
- 61) Davis, D. G., Gisin, B. F., and Tosteson, D. C.: *Biochemistry* 15, 768 (1976).
- 62) Deber, C. M., Madison, V., Blout, E. R.: *Accounts Chem. Res.* 9, 106 (1976).
- 63) Deber, C. M., Pfeiffer, D. R.: *Biochemistry* 15, 132 (1976)
- 64) Debye, P.: *Trans. Electrochem. Soc.* 82, 265 (1942).
- 65) Degani, H., Friedman, H. L.: *Biochemistry* 13, 5022 (1974).
- 66) Diebler, H., Eigen, M., Ilgenfritz, G., Maass, G., Winkler, R.: *Pure and Appl. Chem.* 20, 93 (1969)
- 67) Diercksen, G. H. F., Kraemer, W. P.: *Theoret. Chim. Acta* 23, 389 (1972).
- 68) Dietrich, B., Lehn, J.-M., Sauvage, J. P.: *Tetrahedron Letters* 1969, 2889.
- 69) Dietrich, B., Lehn, J.-M., Sauvage, J. P.: *J.C.S. Chem. Comm.* 1970, 1055.
- 70) Dietrich, B., Lehn, J.-M., Sauvage, J. P.: *J.C.S. Chem. Comm.* 1973, 15.
- 71) Dobler, M., Dunitz, J. D., Kilbourn, B. T.: *Helv. Chim. Acta* 52, 2573 (1969).
- 72) Dobler, M., Dunitz, J. D., Kraewski, J.: *J. Mol. Biol.* 42, 603 (1969).
- 73) Dobler, M.: *Helv. Chim. Acta* 55, 1371 (1972).
- 74) Dobler, M., Phizackerley, R. P.: *Helv. Chim. Acta* 57, 664 (1974).
- 75) Dotsevi, G., Sogah, Y., Cram, D. J.: *J. Amer. Chem. Soc.* 98, 3038 (1976).
- 76) Duax, W. L.: *Acta Crystallogr. A* 28, 2912 (1972).
- 77) Duax, W. L., Hauptmann, H., Weeks, C. M., Norton, D. A.: *Science* 176, 911 (1972).
- 78) Dye, J. L., De Backer, M. G., Nicely, V. A.: *J. Amer. Chem. Soc.* 92, 5226 (1970).
- 79) Ebata, E., Kasahara, H., Sekine, K., Inoue, Y.: *J. Antibiot.* 28, 118 (1975).
- 80) Eggers, F.: *Acustica* 19, 323 (1967/68).
- 81a) Eigen, M.: *Z. Physik. Chem. N. F.* 1, 176 (1954).
- 81b) Eigen, M.: *Ber. Bunsenges. Phys. Chem.* 67, 753 (1963).
- 82) Eigen, M.: *Pure and Appl. Chem.* 6, 97 (1963).
- 83) Eigen, M., Geier, G., Kruse, W.: *Essays in Coord. Chem. Exper. Suppl. IX* (1964), p. 164.
- 84) Eigen, M., Wilkins, R. G.: in: *Mechanism of inorganic reactions*. *Advan. Chem. Ser.* 49, 55 (1965).
- 85) Eigen, M., Winkler, R., in: *The Neurosciences*, 2nd Study Program. Schmitt, F. O. (ed.), New York: The Rockefeller University Press 1970, p. 685.
- 86) Eigen, M., in: *Quantum statistical mechanics in the natural sciences*. Kursunoglu, B, *et al* (eds.). New York: Plenum Publ. Comp. 1974, p. 37.

- 87) Eigen, M., De Maeyer, L., in: *Technique of chemistry*. 3rd edit., Vol. VI, Part II. Weissberger, A., and G. G. Hammes (eds.). New York: Wiley-Interscience 1974, p. 63.
- 88) Eigen, M., Winkler, R.: *Angew. Chem. (German and Internat. Edit.)*: in press (1977).
- 89) Eisenman, G., Radin, D. O., Casby, J. U.: *Science* 126, 831 (1957).
- 90) Eisenman, G.: *Adv. Anal. Chem. Instr.* 4, 213 (1965).
- 91) Eisenman, G., Ciani, S., Szabo, G.: *J. Membr. Biol.* 1, 294 (1969).
- 92) Eisenman, G., Krasne, S., Ciani, S.: *Ann. NY. Acad. Sci.* 264, 34 (1975).
- 93) Faulstich, H., Wieland, T., Walli, A., Birkmann, K.: *Hoppe-Seyler's Z. Physiol. Chem.* 355, 1162 (1974).
- 94) Feinstein, M. B., Felsenfeld, H.: *Proc. Nat. Acad. Sci. USA* 68, 2037 (1971).
- 95) Feldberg, S. W., Kissel, G.: *J. Membr. Biol.* 20, 269 (1975).
- 96) Fenton, D. E., Mercer, M., Poonia, N. S., Truter, M. R.: *J.C.S. Chem. Comm.* 1972, 66.
- 97) Fischer, J., Ricard, L., Weiss, R.: *J. Amer. Chem. Soc.* 98, 3050 (1976).
- 98) Fossel, E. T., Veatch, W. R., Ovchinnikov, Y. A., Blout, E. R.: *Biochemistry* 13, 5264 (1974).
- 99) Frensdorff, H. K.: *J. Amer. Chem. Soc.* 93, 600 (1971).
- 100) Frensdorff, H. K.: *J. Am. Chem. Soc.* 93, 4684 (1971).
- 101) Fröh, P. U., Clerc, J. J., Simon, W.: *Helv. Chim. Acta* 54, 1445 (1971).
- 102) Funck, Th., Eggers, F., Grell, E.: *Chimia* 26, 632 (1972).
- 103) Funck, Th., Eggers, F., Grell, E.: *Chimia* 26, 637 (1972).
- 104) Gachon, P., Kergomard, A.: *J. Antibiot.* 28, 351 (1975).
- 105) Geier, G.: *Helv. Chim. Acta* 50, 1879 (1967).
- 106) Gerlach, H., Prelog, V.: *Liebigs Ann. Chem.* 669, 121 (1963).
- 107) Gerlach, H., Oertle, K., Thalmann, A., Servi, S.: *Helv. Chim. Acta* 58, 2036 (1975).
- 108) Goodall, M. C.: *Biochim. Biophys. Acta* 219, 471 (1970).
- 109) Gordon, L. G., Haydon, D. A.: *Philos. Trans. R. Soc. Lond.* 270, 433 (1975).
- 110) Graf, E., Lehn, J.-M.: *J. Amer. Chem. Soc.* 97, 5022 (1975).
- 111) Grell, E., Eggers, F., Funck, Th.: *Chimia* 26, 632 (1972).
- 112) Grell, E., Funck, Th., Eggers, F., in: *Molecular mechanisms on antibiotic action on protein biosynthesis and membranes*. Munoz, E., Garcia-Ferrandiz, F., and Vazquez, D. (eds.). Amsterdam: Elsevier 1972, p. 646.
- 113) Grell, E., Funck, Th.: *J. Supramol. Structure* 1973, 307.
- 114) Grell, E., Funck, Th., Sauter, H.: *Eur. J. Biochem.* 34, 415 (1973).
- 115a) Grell, E., Funck, Th., Eggers, F., in: *Membranes — a series of advances*. Vol. 3. Eisenman, G. (ed.). New York: Dekker 1975.
- 115b) Grell, E., Oberbäumer, I., in: *Chemical relaxation in molecular biology*. Rigler, R. and Pecht, I. (eds.). Berlin — Heidelberg — New York: Springer 1976.
- 116) Hall, J. E.: *Biophys. J.* 15, 934 (1975).
- 117) Hamill, R. L., Higgins, C. E., Boaz, N. E., Gorman, M.: *Tetrahedron Letters* 1969, 4255.
- 118) Hamilton, J. A., Steinrauf, L. K., Braden, B.: *Biochem. Biophys. Res. Comm.* 64, 151 (1975).
- 119) Harned, R. L., Hidy, P. H., Corum, C. J., Jones, K. L.: *Antibiot. Chemotherap.* 1, 594 (1951).
- 120) Hauser, H., Finer, E. G., Chapman, D.: *J. Mol. Biol.* 53, 419 (1970).
- 121a) Haynes, D.: *FEBS Lett.* 20, 221 (1972).
- 121b) Haynes, D., Pressman, B. C.: *J. Membr. Biol.* 18, 1 (1974).
- 122) Haynes, D. H., Wiens, T., Pressman, B. C.: *J. Membr. Biol.* 18, 23 (1974).
- 123) Hladky, S. B., Haydon, D. A.: *Biochem. Biophys. Acta* 274, 294 (1972).
- 124) Hladky, S. B., Gordon, L. G. M., Haydon, D. A.: *Annu. Rev. Phys. Chem.* 1974, 11.
- 125) Hladky, S. B.: *Biochim. Biophys. Acta* 375, 327 (1975).
- 126) Hladky, S. B.: *Biochim. Biophys. Acta* 375, 350 (1975).
- 127) Hodgkinson, L. C., Leigh, S. J., Sutherland, I. O.: *J.C.S. Chem. Comm.*, 1976, 640.
- 128) Hotchkiss, R. D.: *J. Biol. Chem.* 141, 171 (1941).
- 129) Iitaka, Y., Sakamaki, T., and Nawata, Y.: *Chem. Letters (Japan)* 1972, 1225.
- 130) Ivanov, V. T., Laine, I. A., Abdullaev, N. D., Senyavina, L. B., Popov, E. M., Ovchinnikov, Y. A., Shemyakin, M. M.: *Biochem. Biophys. Res. Comm.* 34, 803 (1969).

- 131) Ivanov, V. T., Miroshnikov, A. I., Abdullaev, N. D., Senyavina, L. B., Arkhipova, S. F., Uvarova, N. N., Khalilulina, K. K., Bystrov, V. F., Ovchinnikov, Y. A.: *Biochim. Biophys. Res. Comm.* **42**, 654 (1971).
- 132) Ivanov, V. T., Ovchinnikov, Y. A., in: *Conformational analysis*. Chiurdoglu, G. (ed.). New York: Academic Press 1971, p. 111.
- 133) Ivanov, V. T., Evstratov, A. V., Sumskeya, L. V., Melnik, E. I., Chumburidze, T. S., Portnova, S. L., Balashova, T. A., Ovchinnikov, Y. A.: *FEBS Letters* **36**, 65 (1973).
- 134) Ivanov, V. T.: *Ann. N. Y. Acad. Sci.* **264**, 221 (1975).
- 135) Izatt, R. M., Nelson, D. P., Rytting, J. H., Haymore, B. L., Christensen, J. F.: *J. Am. Chem. Soc.* **93**, 1619 (1971).
- 136) Johnson, S. M., Herrin, J., Liu, S. J., Paul, I. C.: *J.C.S. Chem. Comm.* **1970**, 72.
- 137) Jovin, T., in: *Trends in biochemical fluorescence spectroscopy*. Chen, R. *et al.* (eds.). New York: Dekker (1974).
- 138) Jung, G., Leibfritz, D., Ottend, M., Dubischar, N., Probst, H.: *Hoppe Seyler's Z. Physiol. Chem.* **355**, 1213 (1974).
- 139) Jung, G., Dubischar, N.: *Eur. J. Biochem.* **54**, 395 (1975).
- 140) Jung, G., König, W. A., Leibfritz, D., Ooka, T., Janko, K., Boheim, G.: *Biochim. Biophys. Acta* **433**, 164 (1976).
- 141) Karle, I. L., Karle, J., Wieland, T., Burgermeister, W., Faulstich, H., Witkop, B.: *Proc. Nat. Acad. Sci. USA* **70**, 1836 (1973).
- 142) Karle, I. L.: *J. Amer. Chem. Soc.* **96**, 4000 (1974).
- 143) Karle, I. L.: *Biochemistry* **13**, 2155 (1974).
- 144) Karle, I. L.: *J. Amer. Chem. Soc.* **97**, 4379 (1975).
- 145) Karle, I. L., Karle, J., Wieland, T., Burgermeister, W., Witkop, B.: *Proc. Nat. Acad. Sci. USA* **73**, 1782 (1976).
- 146) Keller-Juslén, C., King, H. D., Kis, Z. L., von Wartburg, A.: *J. Antibiot.* **28**, 854 (1975).
- 147) Kilbourn, B. T., Dunitz, J. D., Pioda, L. A. R., Simon, W.: *J. Mol. Biol.* **30**, 559 (1967).
- 148) Kinashi, H., Otake, N., Yonehara, H.: *Tetrahedron Letters* **49**, 4955 (1973).
- 149) Kirch, M., Lehn, J.-M.: *Angew. Chem., Internat. Edit.* **14**, 555 (1975).
- 150) Kirsch, N. N. L., Simon, W.: *Helv. Chim. Acta* **59**, 235 (1976).
- 151) Kirsch, N. N. L., Simon, W.: *Helv. Chim. Acta* **59**, 357 (1976).
- 152) Kitame, F., Utsushikawa, K., Koama, T., Saito, T., Kiduchi, M.: *J. Antibiot.* **27**, 884 (1974).
- 153) Knipe, A. C., Sridhar, N., Loughran, A.: *J.C.S. Chem. Comm.* **1976**, 630.
- 154) Knoll, W., Stark, G.: *J. Membr. Biol.* **25**, 249 (1975/76).
- 155) Kolb, H. A., Läuger, P., Bamberg, E.: *J. Membr. Biol.* **20**, 133 (1975).
- 156) Kopolow, S., Hogen Esch, T. E., Smid, J.: *Macromolecules* **4**, 359 (1971).
- 157) Kraemer, W. P., Diercksen, G. H. F.: *Theoret. Chim. Acta* **23**, 393 (1972).
- 158) Krasne, S., Eisenman, G., Szabo, G.: *Science* **174**, 412 (1971).
- 159) Läuger, P.: *Science* **178**, 24 (1972).
- 160) Läuger, P.: *Chemie in unserer Zeit* **2**, 33 (1974).
- 161) Landini, D., Montanari, F., Pirisi, F. M.: *J.C.S. Chem. Comm.* **1974**, 879.
- 162) Laprade, R., Ciani, S., Eisenman, G., Szabo, G., in: *Membranes — a series of advances*. Vol. 3. Eisenman, G. (ed.). New York: Dekker 1975, p. 127.
- 163) Lardy, H. A., Grawen, S. N., Estrada-O, S.: *Fed. Proc.* **26**, 1355 (1967).
- 164) Latimer, W. M., Pitzer, K. S., Slansky, C. M.: *J. Chem. Phys.* **7**, 108 (1939).
- 165) Lehn, J.-M., Sauvage, J. P., Dietrich, B.: *J. Amer. Chem. Soc.* **92**, 2916 (1970).
- 166) Lehn, J.-M., Montavon, F.: *Tetrahedron Letters* **44**, 4557 (1972).
- 167) Lehn, J.-M.: *Structure and Bonding* **16**, 1 (1973).
- 168) Lehn, J.-M.: *J. Amer. Chem. Soc.* **97**, 6700 (1975).
- 169) Lehn, J.-M., Sauvage, J. P.: *J. Amer. Chem. Soc.* **97**, 6700 (1975).
- 170) Lehn, J.-M., Montavon, F.: *Helv. Chim. Acta* **59**, 1566 (1976).
- 171) Lok, J. L., Tehan, F., Coolen, R. B., Papadakis, N., Ceraso, J. M., De Backer, M. G.: *Ber. Bunsenges. Physik. Chem.* **75**, 659 (1971).
- 172) Lutz, W. K., Wipf, H.-K., Simon, W.: *Helv. Chim. Acta* **53**, 1741 (1970).
- 173) Lutz, W. K., Früh, P. U., Simon, W.: *Helv. Chim. Acta* **54**, 2767 (1971).

- 174) Lutz, W. K., Winkler, F. K., Dunitz, J. D.: *Helv. Chim. Acta* 54, 1103 (1971).
- 175) Madison, V., Atreyi, M., Deber, C. M., Blout, E. R.: *J. Am. Chem. Soc.* 96, 6725 (1974).
- 176) Maier, C. A., Paul, I. C.: *J.C.S. Chem. Comm.* 1971, 181.
- 177) Maigret, B., Pullman, B.: *Biochem. Biophys. Res. Comm.* 50, 908 (1973).
- 178) Mallinson, P. R., Truter, M. R.: *J. Chem. Soc.* 1972, 1818.
- 179) Markin, V. S., Sokolov, V. S., Bogulavsky, L. I., Jaguzhinsky, L. S.: *J. Membr. Biol.* 25, 23 (1975).
- 180) Martin, D. R., Williams, R. J.: *Biochem. J.* 153, 181 (1976).
- 181) Max, N. L.: *Biopolymers* 12, 1565 (1973).
- 182) Mayers, D. F., Urry, D. W.: *J. Amer. Chem. Soc.* 94, 77 (1972).
- 183) McMullen, A. I., Marlborough, D. I., Bayley, P. M.: *FEBS Letters* 16, 278 (1971).
- 184) McMurray, W., Begg, R. W.: *Arch. Biochem. Biophys.* 84, 546 (1959).
- 185) Metz, B., Moras, D., Weiss, R.: *J.C.S. Chem. Comm.* 1970, 217.
- 186) Metz, B., Rosalky, J. M., and Weiss, R.: *J.C.S. Chem. Comm.* 1976, 533.
- 187) Meyer, C. E., Reusser, F.: *Experientia* 23, 85 (1967).
- 188) Miscenko, K., *Acta physicochem. (russ.)* 3, 693 (1935).
- 189) Mitani, M., Yamanishi, T., Miyazaki, Y.: *Biochem. Biophys. Res. Comm.* 66, 1231 (1975).
- 190) Moelwyn-Hughes, E. A., in: *Kinetics of reactions in solution*. Oxford: Clarendon Press 1942.
- 191) Moody, G. J., Thomas, J. D. R. in: *Selective ion sensitive electrodes*. Watford, England: Merrow Publ. Co. 1971.
- 192) Moore, C., Pressman, B. C.: *Biochem. Biophys. Res. Comm.* 15, 562 (1964).
- 193) Moore, L. E., Neher, E.: *J. Membr. Biol.* 27, 347 (1976).
- 194) Morel, F. M.: *J. Membr. Biol.* 12, 69 (1973).
- 195) Morf, W. E., Simon, W.: *Helv. Chim. Acta* 54, 794 (1971).
- 196) Mueller, P., Rudin, D. O., Tien, H. T., Wescott, W. C.: *J. Phys. Chem.* 67, 534 (1963).
- 197) Mueller, P., Rudin, D. O.: *Biochem. Biophys. Res. Comm.* 26, 398 (1967).
- 198) Mueller, P., Rudin, D. O.: *Curr. Top. Bioenerg.* 3, 157 (1969).
- 199) Mueller, P.: *Ann. N. Y. Acad. Sci.* 264, 247 (1975).
- 200) Nawata, Y., Sakamaki, T., Iitaka, Y.: *Chem. Letters (Japan)* 1975, 151.
- 201) Neupert-Laves, K., Dobler, M.: *Helv. Chim. Acta* 58, 432 (1975).
- 202) Neupert-Laves, K., Dobler, M.: *Helv. Chim. Acta* 59, 614 (1976).
- 203) Newkome, G. R., McClure, G. L., Broussard Simpson, J., Danesh-Khoshboo, F.: *J. Amer. Chem. Soc.* 97, 3232 (1975).
- 204) Ninet, L., Benazet, F., Depaire, H., Florent, J., Lunel, J., Mancy, D., Abraham, A., Cartier, J. R., des Chezelles, N., Godard, C., Moreau, M., Tissier, R., Lallemand, J. Y.: *Experientia* 32, 319 (1976).
- 205) Nishimura, H., Mayama, N., Kimura, T., Kimura, A., Kawamura, Y., Tawara, K., Tanaka, Y., Okamoto, S., Kyotani, H.: *J. Antibiot. Ser. A* 17, 11 (1964).
- 206) Ochrymowycz, L. A., Ching-Pong Mak, Michna, J. D.: *J. Org. Chem.* 39, 2079 (1974).
- 207) Ohnishi, M., Urry, D. W.: *Biochem. Biophys. Res. Comm.* 36, 194 (1969).
- 208) Ohnishi, M., Urry, D. W.: *Science* 168, 1091 (1970).
- 209) Ohnishi, M., Fedarko, M.-C., Baldeschwieler, J. D.: *Biochem. Biophys. Res. Comm.* 46, 312 (1972).
- 210) Ooka, T., Shimojima, Y., Akimoto, T., Takeda, I., Senoh, S., Abe, J.: *Agric. Biol. Chem.* 30, 700 (1966).
- 211) Ovchinnikov, Y. A., Ivanov, V. T., Evstratov, A. V., Bystrov, V. F., Abdullaev, N. D., Popov, E. M., Lipkind, G. M., Arkhipova, S. F., Efremov, E. S., Shemyakin, M. M.: *Biochem. Biophys. Res. Comm.* 37, 668 (1969).
- 212) Ovchinnikov, Y. A., Ivanov, V. T., Mikhaleva, I. I.: *Tetrahedron Letters* 1971, 159.
- 213) Ovchinnikov, Y. A., Kiryushkin, A. A., Kozhevnikova, I. V.: *Gen. Chem. USSR* 41, 2105 (1971).
- 214) Ovchinnikov, Y. A., Ivanov, V. T., Barsukov, L. I., Melnik, E. I., Oreshnikova, N. A., Bogolyubova, N. D., Ryabova, I. D., Miroshnikov, A. I., Rimskaya, V. A.: *Experientia* 28, 399 (1972).

- 215) Ovchinnikov, Y. A., Ivanov, V. T., Bystrov, V. F., Miroshnikov, A. I., in: Chemistry and biology of peptides. Meienhofer, J. (ed.). Ann Arbor: Ann Arbor Science 1972, p. 111.
- 216) Ovchinnikov, Y. A.: FEBS Letters **44**, 1 (1974).
- 217) Ovchinnikov, Y. A., Ivanov, V. T., Shkrob, A. M. in: Membrane-active complexones. BBA Library, Vol. 12. Amsterdam: Elsevier 1974.
- 218) Ovchinnikov, Y. A., Ivanov, V. T.: Tetrahedron **31**, 2177 (1975).
- 219) Owen, J. D., Wingfield, J. N.: J.C.S. Chem. Comm. **1976**, 318.
- 220) Patel, D. J., Tonelli, A. E.: Biochemistry **12**, 486 (1973).
- 221) Patel, D. J.: Biochemistry **12**, 496 (1973).
- 222) Patel, D. J.: Biochemistry **12**, 667 (1973).
- 223) Patel, D. J.: Biochemistry **12**, 677 (1973).
- 224) Patel, D. J., Tonelli, A. E.: Biochemistry **13**, 788 (1974).
- 225) Payne, J. W., Jakes, R., Hartley, B. S.: Biochem. J. **117**, 757 (1970).
- 226) Peacock, S. C., Cram, D. C.: J.C.S. Chem. Comm. **1976**, 282.
- 227) Pedersen, C. J.: J. Amer. Chem. Soc. **89**, 7017 (1967).
- 228) Pedersen, C. J.: Fed. Proc. **27**, 1305 (1968).
- 229) Pedersen, C. J.: J. Amer. Chem. Soc. **92**, 391 (1970).
- 230) Pedersen, C. J.: J. Amer. Chem. Soc. **92**, 386 (1970).
- 231) Pedersen, C. J., Frensdorff, H. K.: Angew. Chem. Internat. Edit. **11**, 16 (1972).
- 232) Pfeiffer, D. R., Lardy, H. A.: Biochemistry **15**, 935 (1976).
- 233) Pinkerton, M., Steinrauf, L. K., Dawkins, P.: Biochem. Biophys. Res. Comm. **35**, 512 (1969).
- 234) Pinkerton, M., Steinrauf, L. K.: J. Mol. Biol. **49**, 533 (1970).
- 235) Pioda, L. A. R., Wachter, H. A., Dohner, R. E., Simon, W.: Helv. Chim. Acta **50**, 1373 (1967).
- 236) Pioda, L. A. R., Wipf, H.-K., Simon, W.: Chimia **22**, 189 (1968).
- 237) Pioda, L. A. R., Simon, W.: Chimia **23**, 72 (1969).
- 238) Plattner, P., Nager, U.: Experientia **3**, 325 (1947).
- 239) Plattner, P. A., Vogler, K., Studer, R. O., Quitt, P., Keller-Schierlein, W.: Helv. Chim. Acta **46**, 927 (1963).
- 240) Pressman, B. C.: Fed. Proc. **27**, 1283 (1968).
- 241) Pressman, B. C., Haynes, D. H. in: The molecular basis of membrane function. Tosteson, D. C. (ed.). New Jersey: Prentice Hall Englewood Cliffs 1970.
- 242) Pressman, B. C., de Guzman, N. T.: Ann. N.Y. Acad. Sci. **264**, 373 (1975).
- 243) Prestegard, J. H., Chan, S. I.: Biochemistry **8**, 3921 (1969).
- 244) Prestegard, J. H., Chan, S. I.: J. Amer. Chem. Soc. **92**, 4440 (1970).
- 245) Pretsch, E., Ammann, D., Simon, W.: Research/Development **25**, 20 (1974).
- 246) Quitt, P., Studer, R. O., Vogler, K.: Helv. Chim. Acta **46**, 1715 (1963).
- 247) Reinhoudt, D. N., Gray, R. T.: Tetrahedron Letters. **1975**, 2105.
- 248) Ristow, H., Schazschneider, B., Bauer, K., Kleinkauf, H.: Biochim. Biophys. Acta **390**, 246 (1975).
- 249) Ristow, H., Schazschneider, B., Kleinkauf, H.: Biochem. Biophys. Res. Commun. **63**, 1085 (1975).
- 250) Ristow, H., Schazschneider, B., Vater, J., Kleinkauf, H.: Biochim. Biophys. Acta **414**, 1 (1975).
- 251) Robinson, R. A., Stokes, R. H., in: Electrolyte solutions. London: Butterworths Scientific Publications 1959.
- 252) Rothschild, K. J., Asher, I. M., Anastassakis, E., Stanley, H. E.: Science **182**, 384 (1973).
- 253) Rothschild, K. J., Stanley, H. E.: Science **185**, 616 (1974).
- 254) Rothschild, K. J., Stanley, H. E.: Am. J. Clin. Pathol. **63**, 695 (1975).
- 255) Roy, G.: J. Membr. Biol. **24**, 71 (1975).
- 256) Sam, D. J., Simmons, H. E.: J. Amer. Chem. Soc. **94**, 4024 (1972).
- 257) Sarges, R., Witkop, B.: Biochemistry **4**, 2491 (1965).
- 258) Schmid, R., Junge, W.: Biochim. Biophys. Acta **394**, 76 (1975).
- 259) Schmidt, P. G., Wang, A. H.-J., Paul, I. C.: J. Amer. Chem. Soc. **96**, 6189 (1974).

- 260) Scholer, R. P., Simon, W.: *Chimia* 24, 372 (1970).
- 261) Schuster, P., Preuss, H. W.: *Chem. Phys. Letters* 11, 35 (1971).
- 262) Schwarzenbach, G., Gysling, H.: *Helv. Chim. Acta* 32, 1314 (1949).
- 263) Schwarzenbach, G., Flaschka, H.: in: *Die komplexometrische Titration*. Stuttgart: Ferdinand Enke Verlag 1965.
- 264) Schwyzer, R., Tun-Kyi, A., Caviezel, M., Moser, P.: *Helv. Chim. Acta* 53, 15 (1970).
- 265) Shchori, E., Jagur-Grodzinski, Luz, Z., Shporer, M.: *J. Amer. Chem. Soc.* 93, 7133 (1971).
- 266) Shemyakin, M. M., Aldanova, N. A., Vinogradova, E. I., Feigina, M. Y.: *Tetrahedron Letters* 1963, 1921.
- 267) Shemyakin, M. M., Ovchinnikov, Y. A., Ivanov, V. T., Antonov, V. K., Shkrob, A. M., Mikhaleva, I. I., Evstratov, A. V., Malenkov, G. G.: *Biochem. Biophys. Res. Comm.* 29, 834 (1967).
- 268) Shemyakin, M. M., Ovchinnikov, Y. A., Ivanov, V. T., Antonov, V. K., Vinogradova, E. I., Shkrob, A. M., Malenkov, G. G., Evstratov, A. V., Ryabova, I. D., Laine, I. A., Melnik, E. I.: *J. Membr. Biol.* 1, 402 (1969).
- 269) Simon, W., Morf, W. E., Meier, P. Ch.: *Structure and Bonding* 16, 113 (1973).
- 270) Smith, G. D., Duax, W. L., Langs, D. A., De Titta, G. T., Edmonds, J. W., Rohrer, D. C., Weeks, C. M.: *J. Amer. Chem. Soc.* 97, 7242 (1975).
- 271) Stark, G., Ketterer, B., Benz, R., Luger, P.: *Biophys. J.* 11, 981 (1971).
- 272) Stefanac, Z., Simon, W.: *Microchem. J.* 12, 125 (1967).
- 273) Steinrauf, L. K., Pinkerton, M., Chamberlin, J. W.: *Biochem. Biophys. Res. Comm.* 33, 29 (1968).
- 274) Steinrauf, L. K., Czerwinski, E. W., Pinkerton, M.: *Biochem. Biophys. Res. Comm.* 45, 1279 (1971).
- 275) Strehlow, H.: *Z. Elektrochem.* 56, 119 (1952).
- 276) Strehlow, H.: *Ber. Bunsenges. Phys. Chem.* 56, 119 (1952); and in: *Chemistry in non-aqueous solvents*. Vol. 1. New York: Academic Press 1966.
- 277) *Structure and Bonding* 16 (1973) with articles by Lehn, J.-M., Truter, M. R., Simon, W., Morf, W. E., Meier, P. Ch., Izatt, R. M., Eatough, D. J., Christensen, J. J.
- 278) Szabo, G., Eisenman, G., and Ciani, S.: *J. Membr. Biol.* 1, 346 (1969).
- 279) Szabo, G., Eisenman, G., Laprade, R., Ciani, S. M., Krasne, S., in: *Membranes – a series of advances*. Vol. 2. Eisenman, G. (ed.). New York: Dekker 1973, p. 179.
- 280) Thusius, D., in: *Dynamic aspects of conformation changes in biological macromolecules*. Sadron, C. (ed.) Holland: Reidel Publishing Company 1973, p. 271.
- 281) Timko, J. M., Cram, D. J.: *J. Amer. Chem. Soc.* 96, 7159 (1974).
- 282) Ting-Beall, H. P., Tosteson, M. T., Gisin, B. F., Tosteson, D. C.: *J. Gen. Physiol.* 63, 492 (1974).
- 283) Tonelli, A. E., Patel, D. J., Goodman, M., Naider, F., Faulstich, H., Wieland, T.: *Biochemistry* 10, 3211 (1971).
- 284) Tonelli, A. E.: *Biochemistry* 12, 689 (1973).
- 285) Tosteson, D. C.: *Fed. Proc.* 27, 1269 (1968).
- 286) Truter, M. R.: *Structure and Bonding* 16, 71 (1973).
- 287) Urry, D. W.: *Proc. Nat. Acad. Sci. USA* 68, 672 (1971).
- 288) Urry, D. W., Goodall, M. C., Glickson, J. S., Mayers, D. F.: *Proc. Nat. Acad. Sci. USA* 68, 1907 (1971).
- 289) Urry, D. W.: *Proc. Nat. Acad. Sci. USA* 69, 1610 (1972).
- 290) Urry, D. W., Kumar, N. G.: *Biochemistry* 13, 1829 (1974).
- 291) Urry, D. W., Long, M. M., Jacobs, M., Harris, R. D.: *Ann. N.Y. Acad. Sci.* 264, 203 (1975).
- 292) Veatch, W. R., Blout, E. R.: *Biochemistry* 13, 5257 (1974).
- 293) Veatch, W. R., Fossel, E. T., Blout, E. R.: *Biochemistry* 13, 5249 (1974).
- 294) Veatch, W. R., Mathies, R., Eisenberg, M., Stryer, L.: *J. Mol. Biol.* 99, 75 (1975).
- 295) Weber, E., Vogtle, F.: *Tetrahedron Letters* 1975, 2415.
- 296) Weber, E., Vogtle, F.: *Chem. Ber.* 10, 1803 (1976).
- 297) Weber, E., Wiedler, W., Vogtle, F.: *Chem. Ber.* 109, 1002 (1976).
- 298) Wieland, T., Luben, G., Ottenheym, H., Faesel, J., de Vries, J. X., Konz, W., Prox, A., Schmid, J.: *Angew. Chem.* 80, 209 (1968); *Angew. Chem. Internat. Edit.* 7, 204 (1968).

- 299) Wieland, T., Birr, C., Flor, F.: *Liebigs Ann. Chem.* 727, 130 (1969).
- 300) Wieland, T., Faulstich, H., Burgermeister, W., Otting, W., Möhle, W., Shemyakin, M. M., Ovchinnikov, Y. A., Ivanov, V. T., Malenkov, G. G.: *FEBS Letters* 9, 89 (1970).
- 301) Wieland, T., Faulstich, H., Burgermeister, W.: *Biochem. Biophys. Res. Comm.* 47, 984 (1972).
- 302) Wieland, T., Faulstich, H., Jahn, W., Govindan, M. V., Puchinger, H., Kopitar, Z., Schmaus, H., Schmitz, A.: *Hoppe-Seyler's Z. Physiol. Chem.* 353, 1337 (1972).
- 303) Wieland, T., Birr, C., Burgermeister, W., Trietsch, P., Rohr, G.: *Liebigs Ann. Chem.* 1974, 24.
- 304) Wiest, R., Weiss, R.: *J.C.S. Chem. Comm.* 1973, 678.
- 305) Winkler, R.: Doctoral Thesis, Göttingen – Wien 1969.
- 306) Winkler, R.: *Structure and Bonding* 10, 1, (1972).
- 307) Wipf, H.-K., Pioda, L. A. R., Stefanac, Z., Simon, W.: *Helv. Chim. Acta* 51, 377 (1968).
- 308) Wipf, H. K., Pache, W., Jordan, P., Zähler, H., Keller-Schierlein, W., Simon, W.: *Biochem. Biophys. Res. Comm.* 36, 387 (1969).
- 309) Wipf, H. K., Olivier, A., Simon, W.: *Helv. Chim. Acta* 53, 1605 (1970).
- 310) Wipf, H. K., Simon, W.: *Helv. Chim. Acta* 53, 1732 (1970).
- 311) Wong, K. H., Konizer, G., Smid, J.: *J. Amer. Chem. Soc.* 92, 666 (1970).
- 312) Wong, K. H., Konizer, G., Smid, J.: *J. Amer. Chem. Soc.* 93, 7133 (1971).
- 313) Wudl, F.: *J.C.S. Chem. Comm.* 1972, 1229.
- 314) Wuhrmann, P., Thoma, A. P., Simon, W.: *Chimia* 27, 637 (1973).
- 315) Züst, Ch. U., Früh, P. U., Simon, W.: *Helv. Chim. Acta*, 56, 495 (1973).
- 316) Sillén, L. G., Martell, A. E., in: *Stability constants of metal ion complexes. Special publication Nr. 17 (1964) and Nr. 25 (1971)* London: Chemical Society.
- 317) Rechnitz, G. A., Eyal, E.: *Anal. Chem.*, 44, 370 (1972).
- 318) Petránek, J., Ryba, O.: *Coll. Czech. Chem. Comm.* 39, 2033 (1974).
- 319) McLaughlin, S. G. A., Szabo, G., Eisenman, G., Ciani, S.: *Abstracts, 14th Annual Meeting of the Biophysical Society, Baltimore, Md., (1970), p 96a.*
- 320) Cade, J. F. J.: *Med. J. Aust.* 2, 349 (1949).
- 321) Schou, M., in: *Lithium: Its role in psychiatric research and treatment*, Gershon, S. and Shopsin, B. (eds). New York: Plenum Press 1973, 269.
- 322) Winkler, R., in: *Neurosciences res. prog. bull.*, Vol. 14, Nr. 2, 1976, p. 139.
- 323) Eigen, M., in: *Neurosciences res. prog. bull.*, Vol. 14, Nr. 2, 1976, p. 142.
- 324) The neurobiology of lithium. *Neurosciences res. prog. bull.*, Vol. 14, Nr. 2, 1976.
- 325) Noyes, R. M., *J. Amer. Chem. Soc.* 84, 513 (1962).
- 326) Karle, I. L., Duesler, E.: *Proc. Nat. Acad. Sci. USA*, in press (July–August, 1977).
- 327) Pert, C. B., Snyder, S. H.: *Mol. Pharmacol.* 10, 868 (1974).

Received December 15, 1976

Author Index Volumes 26 - 69

The volume numbers are printed in italics

- Albini, A., and Kisch, H.: Complexation and Activation of Diazenes and Diazo Compounds by Transition Metals. *65*, 105–145 (1976).
- Altona, C., and Faber, D. H.: Empirical Force Field Calculations. A Tool in Structural Organic Chemistry. *45*, 1–38 (1974).
- Anderson, J. E.: Chair-Chair Interconversion of Six-Membered Rings. *45*, 139–167 (1974).
- Anet, F. A. L.: Dynamics of Eight-Membered Rings in Cyclooctane Class. *45*, 169–220 (1974).
- Ariëns, E. J., and Simonis, A.-M.: Design of Bioactive Compounds. *52*, 1–61 (1974).
- Aurich, H. G., and Weiss, W.: Formation and Reactions of Aminyloxides. *59*, 65–111 (1975).
- Bardos, T. J.: Antimetabolites: Molecular Design and Mode of Action. *52*, 63–98 (1974).
- Barnes, D. S., see Pettit, L. D.: *28*, 85–139 (1972).
- Bauer, S. H., and Yokozeki, A.: The Geometric and Dynamic Structures of Fluorocarbons and Related Compounds. *53*, 71–119 (1974).
- Baumgärtner, F., and Wiles, D. R.: Radiochemical Transformations and Rearrangements in Organometallic Compounds. *32*, 63–108 (1972).
- Bernauer, K.: Diastereoisomerism and Diastereoselectivity in Metal Complexes. *65*, 1–35 (1976).
- Boettcher, R. J., see Mislow, K.: *47*, 1–22 (1974).
- Brandmüller, J., and Schrötter, H. W.: Laser Raman Spectroscopy of the Solid State. *36*, 85–127 (1973).
- Bremser, W.: X-Ray Photoelectron Spectroscopy. *36*, 1–37 (1973).
- Breuer, H.-D., see Winnewisser, G.: *44*, 1–81 (1974).
- Brewster, J. H.: On the Helicity of Various Twisted Chains of Atoms. *47*, 29–71 (1974).
- Brocas, J.: Some Formal Properties of the Kinetics of Pentacoordinate Stereoisomerizations. *32*, 43–61 (1972).
- Brunner, H.: Stereochemistry of the Reactions of Optically Active Organometallic Transition Metal Compounds. *56*, 67–90 (1975).
- Buchs, A., see Delfino, A. B.: *39*, 109–137 (1973).
- Bürger, H., and Eujen, R.: Low-Valent Silicon. *50*, 1–41 (1974).
- Burgermeister, W., and Winkler-Oswatitsch, R.: Complex Formation of Monovalent Cations with Biofunctional Ligands. *69*, 91–196 (1977).

- Butler, R. S., and deMaine, A. D.: CRAMS – An Automatic Chemical Reaction Analysis and Modeling System. *58*, 39–72 (1975).
- Caesar, F.: Computer-Gas Chromatography. *39*, 139–167 (1973).
- Čásky, P., and Zahradník, R.: MO Approach to Electronic Spectra of Radicals. *43*, 1–55 (1973).
- Chandra, P.: Molecular Approaches for Designing Antiviral and Antitumor Compounds. *52*, 99–139 (1974).
- Chapuisat, X., and Jean, Y.: Theoretical Chemical Dynamics: A Tool in Organic Chemistry. *68*, 1–57 (1976).
- Christian, G. D.: Atomic Absorption Spectroscopy for the Determination of Elements in Medical Biological Samples. *26*, 77–112 (1972).
- Clark, G. C., see Wasserman, H. H.: *47*, 73–156 (1974).
- Clerc, T., and Erni, F.: Identification of Organic Compounds by Computer-Aided Interpretation of Spectra. *39*, 91–107 (1973).
- Clever, H.: Der Analysenautomat DSA-560. *29*, 29–43 (1972).
- Connors, T. A.: Alkylating Agents. *52*, 141–171 (1974).
- Craig, D. P., and Mellor, D. P.: Discriminating Interactions Between Chiral Molecules. *63*, 1–48 (1976).
- Cram, D. J., and Cram, J. M.: Stereochemical Reaction Cycles. *31*, 1–43 (1972).
- Gresp, T. M., see Sargent, M. V.: *57*, 111–143 (1975).
- Dauben, W. G., Lodder, G., and Ipaktschi, J.: Photochemistry of β , γ -Unsaturated Ketones. *54*, 73–114 (1974).
- DeClercq, E.: Synthetic Interferon Inducers. *52*, 173–198 (1974).
- Degens, E. T.: Molecular Mechanisms on Carbonate, Phosphate, and Silica Deposition in the Living Cell. *64*, 1–112 (1976).
- Delfino, A. B., and Buchs, A.: Mass Spectra and Computers. *39*, 109–137 (1973).
- deMaine, A. D., see Butler, R. S.: *58*, 39–72 (1975).
- DePuy, C. H.: Stereochemistry and Reactivity in Cyclopropane Ring-Cleavage by Electrophiles. *40*, 73–101 (1973).
- Devaquet, A.: Quantum-Mechanical Calculations of the Potential Energy Surface of Triplet States. *54*, 1–71 (1974).
- Dimroth, K.: Delocalized Phosphorus-Carbon Double Bonds. Phosphamethincyanines, λ^3 -Phosphorins and λ^5 -Phosphorins. *38*, 1–150 (1973).
- Döpp, D.: Reactions of Aromatic Nitro Compounds *via* Excited Triplet States. *55*, 49–85 (1975).
- Dougherty, R. C.: The Relationship Between Mass Spectrometric, Thermolytic and Photolytic Reactivity. *45*, 93–138 (1974).
- Dryhurst, G.: Electrochemical Oxidation of Biologically-Important Purines at the Pyrolytic Graphite Electrode. Relationship to the Biological Oxidation of Purines. *34*, 47–85 (1972).
- Dürr, H.: Reactivity of Cycloalkene-carbenes. *40*, 103–142 (1973).
- Dürr, H.: Triplet-Intermediates from Diazo-Compounds (Carbenes). *55*, 87–135 (1975).

- Dürr, H., and Kober, H.: Triplet States from Azides. *66*, 89–114 (1976).
- Dürr, H., and Ruge, B.: Triplet States from Azo Compounds. *66*, 53–87 (1976).
- Dugundji, J., and Ugi, I.: An Algebraic Model of Constitutional Chemistry as a Basis for Chemical Computer Programs. *39*, 19–64 (1973).
- Eglinton, G., Maxwell, J. R., and Pillinger, C. T.: Carbon Chemistry of the Apollo Lunar Samples. *44*, 83–113 (1974).
- Eicher, T., and Weber, J. L.: Structure and Reactivity of Cyclopropanones and Triafulvenes. *57*, 1–109 (1975).
- Erni, F., see Clerc, T.: *39*, 139–167 (1973).
- Eujen, R., see Bürger, H.: *50*, 1–41 (1974).
- Faber, D. H., see Altona, C.: *45*, 1–38 (1974).
- Fietzek, P. P., and Kühn, K.: Automation of the Sequence Analysis by Edman Degradation of Proteins and Peptides. *29*, 1–28 (1972).
- Finocchiaro, P., see Mislow, K.: *47*, 1–22 (1974).
- Fischer, G.: Spectroscopic Implications of Line Broadening in Large Molecules. *66*, 115–147 (1976).
- Fluck, E.: The Chemistry of Phosphine. *35*, 1–64 (1973).
- Flygare, W. H., see Sutter, D. H.: *63*, 89–196 (1976).
- Fowler, F. W., see Gelernter, H.: *41*, 113–150 (1973).
- Freed, K. F.: The Theory of Radiationless Processes in Polyatomic Molecules. *31*, 105–139 (1972).
- Fritz, G.: Organometallic Synthesis of Carbosilanes. *50*, 43–127 (1974).
- Fry, A. J.: Stereochemistry of Electrochemical Reductions. *34*, 1–46 (1972).
- Ganter, C.: Dihetero-tricycloadecanes. *67*, 15–106 (1976).
- Gasteiger, J., Gillespie, P., Marquarding, D., and Ugi, I.: From van't Hoff to Unified Perspectives in Molecular Structure and Computer-Oriented Representation. *48*, 1–37 (1974).
- Geick, R.: IR Fourier Transform Spectroscopy. *58*, 73–186 (1975).
- Geist, W., and Ripota, P.: Computer-Assisted Instruction in Chemistry. *39*, 169–195 (1973).
- Gelernter, H., Sridharan, N. S., Hart, A. J., Yen, S. C., Fowler, F. W., and Shue, H.-J.: The Discovery of Organic Synthetic Routes by Computer. *41*, 113–150 (1973).
- Gerischer, H., and Willig, F.: Reaction of Excited Dye Molecules at Electrodes. *61*, 31–84 (1976).
- Gillespie, P., see Gasteiger, J.: *48*, 1–37 (1974).
- Gleiter, R., and Gygax, R.: No-Bond-Resonance Compounds, Structure, Bonding and Properties. *63*, 49–88 (1976).
- Guibé, L.: Nitrogen Quadrupole Resonance Spectroscopy. *30*, 77–102 (1972).
- Gundermann, K.-D.: Recent Advances in Research on the Chemiluminescence of Organic Compounds. *46*, 61–139 (1974).
- Gust, D., see Mislow, K.: *47*, 1–22 (1974).
- Gutman, I., and Trinajstić, N.: Graph Theory and Molecular Orbitals. *42*, 49–93 (1973).

- Gutmann, V.: Ionic and Redox Equilibria in Donor Solvents. 27, 59–115 (1972).
Gygax, R., see Gleiter, R.: 63, 49–88 (1976).
- Haaland, A.: Organometallic Compounds Studied by Gas-Phase Electron Diffraction. 53, 1–23 (1974).
Häfelinger, G.: Theoretical Considerations for Cyclic (pd) π Systems. 28, 1–39 (1972).
Hariharan, P. C., see Lathan, W. A.: 40, 1–45 (1973).
Hart, A. J., see Gelernter, H.: 41, 113–150 (1973).
Hartmann, H., Lebert, K.-H., and Wanczek, K.-P.: Ion Cyclotron Resonance Spectroscopy. 43, 57–115 (1973).
Hehre, W. J., see Lathan, W. A.: 40, 1–45 (1973).
Hendrickson, J. B.: A General Protocol for Systematic Synthesis Design. 62, 49–172 (1976).
Hengge, E.: Properties and Preparations of Si-Si Linkages. 51, 1–127 (1974).
Henrici-Olivé, G., and Olivé, S.: Olefin Insertion in Transition Metal Catalysis. 67, 107–127 (1976).
Herndon, W. C.: Substituent Effects in Photochemical Cycloaddition Reactions. 46, 141–179 (1974).
Höfler, F.: The Chemistry of Silicon-Transition-Metal Compounds. 50, 129–165 (1974).
- Ipaktschi, J., see Dauben, W. G.: 54, 73–114 (1974).
- Jacobs, P., see Stohrer, W.-D.: 46, 181–236 (1974).
Jahnke, H., Schönborn, M., and Zimmermann, G.: Organic Dyestuffs as Catalysts for Fuel Cells. 61, 131–181 (1976).
Jakubetz, W., see Schuster, P.: 60, 1–107 (1975).
Jean, Y., see Chapuisat, X.: 68, 1–57 (1976).
Jørgensen, C. K.: Continuum Effects Indicated by Hard and Soft Antibases (Lewis Acids) and Bases. 56, 1–66 (1975).
Julg, A.: On the Description of Molecules Using Point Charges and Electric Moments. 58, 1–37 (1975).
- Kaiser, K. H., see Stohrer, W.-D.: 46, 181–236 (1974).
Khaikin, L. S., see Vilkow, L.: 53, 25–70 (1974).
Kisch, H., see Albini, A.: 65, 105–145 (1976).
Kober, H., see Dürr, H.: 66, 89–114 (1976).
Kompa, K. L.: Chemical Lasers. 37, 1–92 (1973).
Kratochvil, B., and Yeager, H. L.: Conductance of Electrolytes in Organic Solvents. 27, 1–58 (1972).
Krech, H.: Ein Analysenautomat aus Bausteinen, die Braun-Systematic. 29, 45–54 (1972).
Kühn, K., see Fietzek, P. P.: 29, 1–28 (1972).
Kustin, K., and McLeod, G. C.: Interactions Between Metal Ions and Living Organisms in Sea Water. 69, 1–37 (1977).

- Kutzelnigg, W.: Electron Correlation and Electron Pair Theories. *40*, 31–73 (1973).
- Lathan, W. A., Radom, L., Hariharan, P. C., Hehre, W. J., and Pople, J. A.: Structures and Stabilities of Three-Membered Rings from *ab initio* Molecular Orbital Theory. *40*, 1–45 (1973).
- Lebert, K.-H., see Hartmann, H.: *43*, 57–115 (1973).
- Lodder, G., see Dauben, W. G.: *54*, 73–114 (1974).
- Luck, W. A. P.: Water in Biologic Systems. *64*, 113–179 (1976).
- Lucken, E. A. C.: Nuclear Quadrupole Resonance. Theoretical Interpretation. *30*, 155–171 (1972).
- Mango, F. D.: The Removal of Orbital Symmetry Restrictions to Organic Reactions. *45*, 39–91 (1974).
- Maki, A. H., and Zuclich, J. A.: Protein Triplet States. *54*, 115–163 (1974).
- Margrave, J. L., Sharp, K. G., and Wilson, P. W.: The Dihalides of Group IVB Elements. *26*, 1–35 (1972).
- Marius, W., see Schuster, P.: *60*, 1–107 (1975).
- Marks, W.: Der Technicon Autoanalyzer. *29*, 55–71 (1972).
- Marquarding, D., see Gasteiger, J.: *48*, 1–37 (1974).
- Maxwell, J. R., see Eglinton, G.: *44*, 83–113 (1974).
- McLeod, G. C., see Kustin, K.: *69*, 1–37 (1977).
- Mead, C. A.: Permutation Group Symmetry and Chirality in Molecules. *49*, 1–86. (1974).
- Meier, H.: Application of the Semiconductor Properties of Dyes Possibilities and Problems. *61*, 85–131 (1976).
- Meller, A.: The Chemistry of Iminoboranes. *26*, 37–76 (1972).
- Mellor, D. P., see Craig, D. P.: *63*, 1–48 (1976).
- Michl, J.: Physical Basis of Qualitative MO Arguments in Organic Photochemistry. *46*, 1–59 (1974).
- Minisci, F.: Recent Aspects of Homolytic Aromatic Substitutions. *62*, 1–48 (1976).
- Mislow, K., Gust, D., Finocchiaro, P., and Boettcher, R. J.: Stereochemical Correspondence Among Molecular Propellers. *47*, 1–22 (1974).
- Nakajima, T.: Quantum Chemistry of Nonbenzenoid Cyclic Conjugated Hydrocarbons. *32*, 1–42 (1972).
- Nakajima, T.: Errata. *45*, 221 (1974).
- Neumann, P., see Vögtle, F.: *48*, 67–129 (1974).
- Oehme, F.: Titrierautomaten zur Betriebskontrolle. *29*, 73–103 (1972).
- Olivé, S., see Henrici-Olivé, G.: *67*, 107–127 (1976).
- Papoušek, D., and Špirko, V.: A New Theoretical Look at the Inversion Problem in Molecules. *68*, 59–102 (1976).
- Pearson, R. G.: Orbital Symmetry Rules for Inorganic Reactions from Perturbation Theory. *41*, 75–112 (1973).
- Perrin, D. D.: Inorganic Medicinal Chemistry. *64*, 181–216 (1976).

- Pettit, L. D., and Barnes, D. S.: The Stability and Structure of Olefin and Acetylene Complexes of Transition Metals. 28, 85–139 (1972).
- Pignolet, L. H.: Dynamics of Intramolecular Metal-Centered Rearrangement Reactions of Tris-Chelate Complexes. 56, 91–137 (1975).
- Pillinger, C. T., see Eglinton, G.: 44, 83–113 (1974).
- Pople, J. A., see Lathan, W. A.: 40, 1–45 (1973).
- Puchelt, H.: Advances in Inorganic Geochemistry. 44, 155–176 (1974).
- Pullman, A.: Quantum Biochemistry at the All- or Quasi-All-Electrons Level. 31, 45–103 (1972).
- Quinkert, G., see Stohrer, W.-D.: 46, 181–236 (1974).
- Radom, L., see Lathan, W. A.: 40, 1–45 (1973).
- Renger, G.: Inorganic Metabolic Gas Exchange in Biochemistry. 69, 39–90 (1977).
- Rice, S. A.: Conjectures on the Structure of Amorphous Solid and Liquid Water. 60, 109–200. (1975).
- Rieke, R. D.: Use of Activated Metals in Organic and Organometallic Synthesis. 59, 1–31 (1975).
- Ripota, P., see Geist, W.: 39, 169–195 (1973).
- Rüssel, H. and Tölg, G.: Anwendung der Gaschromatographie zur Trennung und Bestimmung anorganischer Stoffe/Gas Chromatography of Inorganic Compounds. 33, 1–74 (1972).
- Ruge, B., see Dürr, H.: 66, 53–87 (1976).
- Sargent, M. V., and Cresp, T. M.: The Higher Annulenones. 57, 111–143 (1975).
- Schäfer, F. P.: Organic Dyes in Laser Technology. 61, 1–30 (1976).
- Schneider, H.: Ion Solvation in Mixed Solvents. 68, 103–148 (1976).
- Schönborn, M., see Jahnke, H.: 61, 133–181 (1976).
- Schrötter, H. W., see Brandmüller, J.: 36, 85–127 (1973).
- Schuster, P., Jakubetz, W., and Marius, W.: Molecular Models for the Solvation of Small Ions and Polar Molecules. 60, 1–107 (1975).
- Schutte, C. J. H.: The Infra-Red Spectra of Crystalline Solids. 36, 57–84 (1973).
- Scrocco, E., and Tomasi, J.: The Electrostatic Molecular Potential as a Tool for the Interpretation of Molecular Properties. 42, 95–170 (1973).
- Sharp, K. G., see Margrave, J. L.: 26, 1–35 (1972).
- Shue, H.-J., see Gelernter, H.: 41, 113–150 (1973).
- Simonetta, M.: Qualitative and Semiquantitative Evaluation of Reaction Paths. 42, 1–47 (1973).
- Simonis, A.-M., see Ariëns, E. J.: 52, 1–61 (1974).
- Smith, S. L.: Solvent Effects and NMR Coupling Constants. 27, 117–187 (1972).
- Špirko, V., see Papoušek, D.: 68, 59–102 (1976).
- Sridharan, N. S., see Gelernter, H.: 41, 113–150 (1973).
- Stohrer, W.-D., Jacobs, P., Kaiser, K. H., Wiech, G., and Quinkert, G.: Das sonderbare Verhalten elektronen-angeregter 4-Ringe-Ketone. — The Peculiar Behavior of Electronically Excited 4-Membered Ring Ketones. 46, 181–236 (1974).

- Stoklosa, H. J., see Wasson, J. R.: 35, 65-129 (1973).
- Suhr, H.: Synthesis of Organic Compounds in Glow and Corona Discharges. 36, 39-56 (1973).
- Sutter, D. H., and Flygare, W. H.: The Molecular Zeeman Effect. 63, 89-196 (1976).
- Thakkar, A. J.: The Coming of the Computer Age to Organic Chemistry. Recent Approaches to Systematic Synthesis Analysis. 39, 3-18 (1973).
- Tölg, G., see Rüssel, H.: 33, 1-74 (1972).
- Tomasi, J., see Scrocco, E.: 42, 95-170 (1973).
- Trinajstić, N., see Gutman, I.: 42, 49-93 (1973).
- Trost, B. M.: Sulfuranes in Organic Reactions and Synthesis. 41, 1-29 (1973).
- Tsuji, J.: Organic Synthesis by Means of Transition Metal Complexes: Some General Patterns. 28, 41-84 (1972).
- Turley, P. C., see Wasserman, H. H.: 47, 73-156 (1974).
- Ugi, I., see Dugundji, J.: 39, 19-64 (1973).
- Ugi, I., see Gasteiger, J.: 48, 1-37 (1974).
- Veal, D. C.: Computer Techniques for Retrieval of Information from the Chemical Literature. 39, 65-89 (1973).
- Vennesland, B.: Stereospecificity in Biology. 48, 39-65 (1974).
- Vepřek, S.: A Theoretical Approach to Heterogeneous Reactions in Non-Isothermal Low Pressure Plasma. 56, 139-159 (1975).
- Vilkov, L., and Khaikin, L. S.: Stereochemistry of Compounds Containing Bonds Between Si, P, S, Cl, and N or O. 53, 25-70 (1974).
- Vögtle, F., and Neumann, P.: [2.2] Paracyclophanes, Structure and Dynamics. 48, 67-129 (1974).
- Vollhardt, P.: Cyclobutadienoids. 59, 113-135 (1975).
- Wänke, H.: Chemistry of the Moon. 44, 1-81 (1974).
- Wagner, P. J.: Chemistry of Excited Triplet Organic Carbonyl Compounds. 66, 1-52 (1976).
- Wanczek, K.-P., see Hartmann, K.: 43, 57-115 (1973).
- Wasserman, H. H., Clark, G. C., and Turley, P. C.: Recent Aspects of Cyclopropanone Chemistry. 47, 73-156 (1974).
- Wasson, J. R., Woltermann, G. M., and Stoklosa, H. J.: Transition Metal Dithio- and Diselenophosphate Complexes. 35, 65-129 (1973).
- Weber, J. L., see Eicher, T.: 57, 1-109 (1975).
- Weiss, A.: Crystal Field Effects in Nuclear Quadrupole Resonance. 30, 1-76 (1972).
- Weiss, W., see Aurich, H. G.: 59, 65-111 (1975).
- Wentrup, C.: Rearrangements and Interconversion of Carbenes and Nitrenes. 62, 173-251 (1976).
- Werner, H.: Ringliganden-Verdrängungsreaktionen von Aromaten-Metall-Komplexen. 28, 141-181 (1972).
- Wiech, G., see Stohrer, W.-D.: 46, 181-236 (1974).

- Wild, U. P.: Characterization of Triplet States by Optical Spectroscopy. 55, 1–47 (1975).
- Wiles, D. R., see Baumgärtner, F.: 32, 63–108 (1972).
- Willig, F., see Gerischer, H.: 61, 31–84 (1976).
- Wilson, P. W., see Margrave, J. L.: 26, 1–35 (1972).
- Winkler-Oswatitsch, R., see Burgermeister, W.: 69, 91–196 (1977).
- Winnewisser, G., Mezger, P. G., and Breuer, H. D.: Interstellar Molecules. 44, 1–81 (1974).
- Wittig, G.: Old and New in the Field of Directed Aldol Condensations. 67, 1–14 (1976).
- Woenckhaus, C.: Synthesis and Properties of Some New NAD[®] Analogues. 52, 199–223 (1974).
- Woltermann, G. M., see Wasson, J. R.: 35, 65–129 (1973).
- Wrighton, M. S.: Mechanistic Aspects of the Photochemical Reactions of Coordination Compounds. 65, 37–102 (1976).
- Yeager, H. L., see Kratochvil, B.: 27, 1–58 (1972).
- Yen, S. C., see Gelernter, H.: 41, 113–150 (1973).
- Yokozeki, A., see Bauer, S. H.: 53, 71–119 (1974).
- Yoshida, Z.: Heteroatom-Substituted Cyclopropenium Compounds. 40, 47–72 (1973).
- Zahradník, R., see Čársky, P.: 43, 1–55 (1973).
- Zeil, W.: Bestimmung der Kernquadrupolkopplungskonstanten aus Mikrowellenspektren. 30, 103–153 (1972).
- Zimmermann, G., see Jahnke, H.: 61, 133–181 (1976).
- Zoltewicz, J. A.: New Directions in Aromatic Nucleophilic Substitution. 59, 33–64 (1975).
- Zuclich, J. A., see Maki, A. H.: 54, 115–163 (1974).